WHP Cruise Summary Information

WOCE section designation	A08
Expedition designation (EXPOCODE)	06MT28_1
Chief Scientist(s) and their affiliation	Thomas Müller, IfMK
Dates	1994.03.29 – 1994.05.11
Ship	METEOR
Ports of call	Recife, Brazil to Walvisbay, Namibia
Number of stations	126
Geographic boundaries of the stations	08º16.31''S 05º45.08''W 13º32.42''E 11º40.50''S
Floats and drifters deployed	see 4.1
Moorings deployed or recovered	none

Contributing Authors (in order of appearance)	
U. Beckmann	C. Schmid
P. Beining	W. Zenk
C. Dieterich	J. Pätzold
U. Koy	W. Krauß
P. Meyer	T. Knutz
W.H. Pinaya	C. Zelck
D.J. Hydes	H.-Ch. John
S. Kohrs	J. Brinkmann
R. Meyer	G. Schebeske
S. Müller	W. Emery
A. Putzka	M. Suarez
K. Bulsiewicz	R. Cordes
H. Düßmann	J. Funk
W. Plep	R. Rieger
J. Sültenfuß	M. Schneider
K. Johnson	K. Ballschmiter
K. Wills	K. Flechsenhar
D. Hydes	W. Roether
G. Siedler	J.C. Jennings
O. Boebel	L.I. Gordon

WHP Cruise and Data Information

Instructions: Click on items below to locate primary reference(s) or use navigation tools above.

Table of Contents:

Station locations for a08

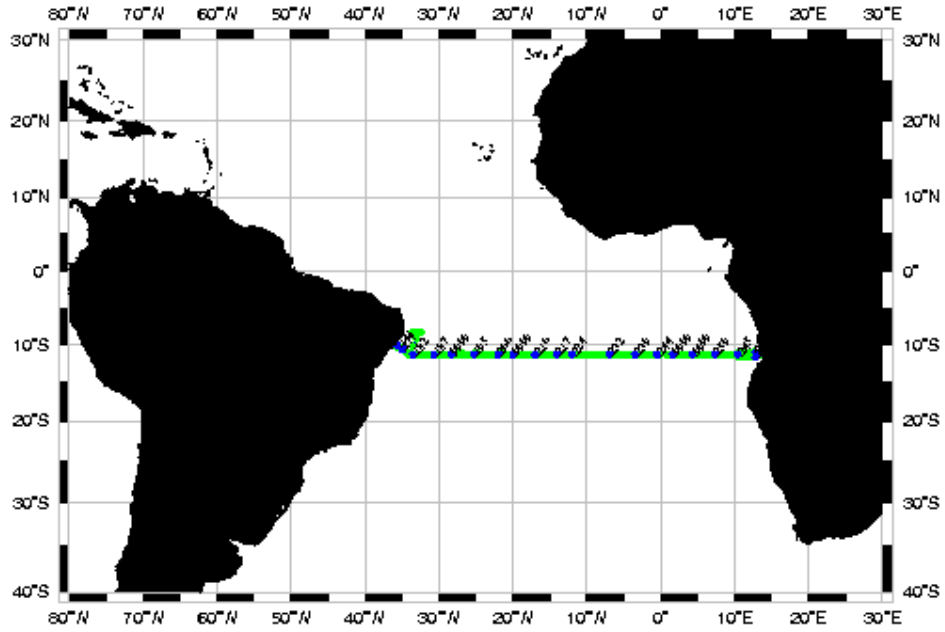

(Produced from .SUM files by WHPO)

Abstract

From 29 March to 14 June 1994 the German research vessel METEOR performed its 28th cruise, a journey in the subtropical South Atlantic divided into two legs. The main objectives were hydrographical and tracer observations in the frame work of the internationally coordinated World Ocean Circulation Experiment (WOCE). The cruise contributed to the WOCE Hydrographic Programme (WHP) and to the Deep Basin Experiment (DBE) in the Brazil Basin. Physical observations were supplemented by biological, air and environmental chemical and geological components, including a contribution to the Joint Global Ocean Flux Studies (JGOFS).

The present cruise report contains a summary of the research objectives and comprises the research programme, a cruise narrative and preliminary observational results. The report was funded by the Deutsche Forschungsgemeinschaft (DFG) and the Bundesministerium für Bildung, Wissenschaft, Forschung and Technologie (BMBF).

Zusammenfassung

Vom 29. März bis 14. Juni 1994 fand die 28. Reise des deutschen Forschungsschiffes METEOR statt. Die Reise führte in den subtropischen S0datlantik, und sie war in zwei Abschnitte unterteilt. Der Schwerpunkt lag bei hydrographischen und Spurenstoffbeobachtungen. Sie wurden im Rahmen des international koordinierten Programms "World Ocean Circulation Experiment" (WOCE) durchgeführt. Die Expedition lieferte Beiträge zum "WOCE Hydrographic Programme" (WHP) und zum "Deep Basin Experiment" (DBE), einer Studie im Brasilianischen Becken. Die physikalischen Untersuchungen wurden ergänzt durch biologische, luft- und umweltchemische sowie geologische Beobachtungen, zu denen auch Beiträge zur "Joint Global Ocean Flux Study" (JGOFS) gehören.

Der vorliegende Expeditionsbericht enthält eine Zusammenfassung der wissenschaftlichen Ziele und des Programms. Außerdem enthält er die Fahrtbeschreibung sowie vorläufige Beobachtungsergebnisse. Der Bericht umfaßt ferner ausführliche Tabellen zu allen Stationsarbeiten. Die Reise wurde von der Deutschen Forschungsgemeinschaft (DFG), sowie vom Bundesministerium für Bildung, Wissenschaft, Forschung und Technologie (BMBF) gefördert.

1 Research Objectives

The German research vessel METEOR operated under the auspices of the World Ocean Experiment (WOCE) from March 29 - June 14, 1994 in the subtropical South Atlantic (Fig. 1, Tab. 1). WOCE is a major component of the World Climate Research Programme, which was established in 1979 by the World Meteorological Organisation (WMO) and the International Council of Scientific Unions (ICSU) in cooperation with the UNESCO and the Scientific Committee in Oceanic Research (SCOR). WOCE encompasses planning, implementing and coordinating the global fieldwork and extensive modeling studies. The information gained will allow to better understand the ocean's role in climate and its changes resulting from both natural and anthropogenic causes.

The WOCE Hydrographic Programme (WHP) includes a large set of sections in all oceans, with measurements of temperature, salinity, oxygen, nutrients and anthropogenic tracers. Its aim is the determination of global water mass distribution and geostrophic mass and heat transports. The zonal WHP section A8 on 11˚S was selected for leg 1, Recife - Walvis Bay. In the beginning and at the end of this transatlantic CTD-section additional measurements were conducted in the source region of the Brazil Current and in the Angola Dome. The hydrographic investigations were supplemented by observations of the carbonate system as a contribution to the Joint Global Flux Study (JGOFS), by the biological sampling for the determination of near-surface plankton, and by measurements of aerosols and precipitation analyses.

During leg 2 studies of the Deep Basin Experiment (DBE), a subprogramme of WOCE was continued between Walvis Bay and Buenos Aires. The main subject dealt with water mass distribution and spreading within the Brazil Basin. The advection of Antarctic Intermediate Water on its west- and northward paths was investigated in combination with the southward transport of North Atlantic Deep Water and Antarctic Bottom Water. Special attention was given to the overflow phenomenon across the Rio Grande Rise at the Hunter Channel. Direct current observations by moored instruments and drifting buoys near the surface and at 1000 m depth were initiated. Seven deep-sea current meter and thermistor chain moorings had been deployed by METEOR in December 1992. The programme included the recovery of this instrument array in the Hunter Channel region.

The investigation further included radiative measurements at the sea surface, an environmental chemistry component and sediment sampling in combination with CTD.

Tab. 1: Legs and Chief Scientists of METEOR cruise no. 28

Leg M 28/1
29 March - 12 May 1994,
Recife/Brazil - Walvis Bay/South Africa
Chief scientist: Dr. T.J. Müller

Leg M 28/2
15 May - 14 June 1994,
Walvis Bay/South Africa - Buenos Aires/Argentina
Chief scientist: Dr. W. Zenk

Coordination:
Dr. W. Zenk

Master:
Leg M 28/1: Captain H. Andresen
Leg M 28/2: Captain H. Papenhagen

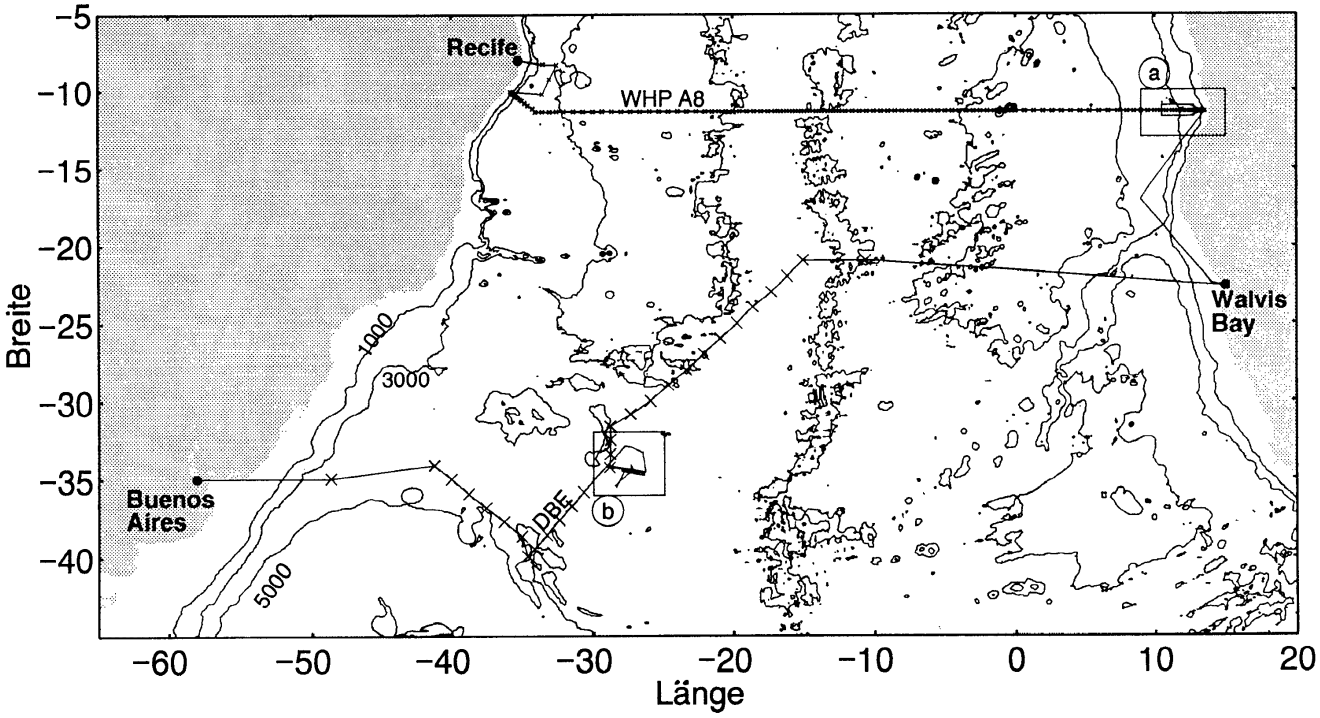

Fig. 1a: Track and working area of METEOR cruise no. 28

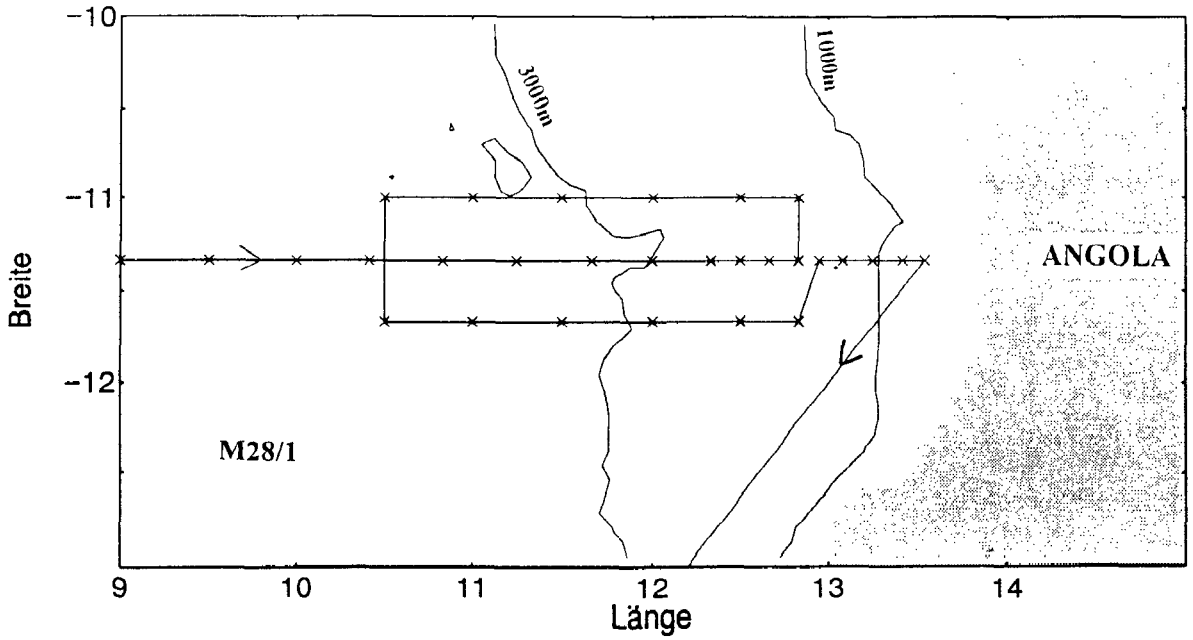

Fig. 1b: Detailed cruise track

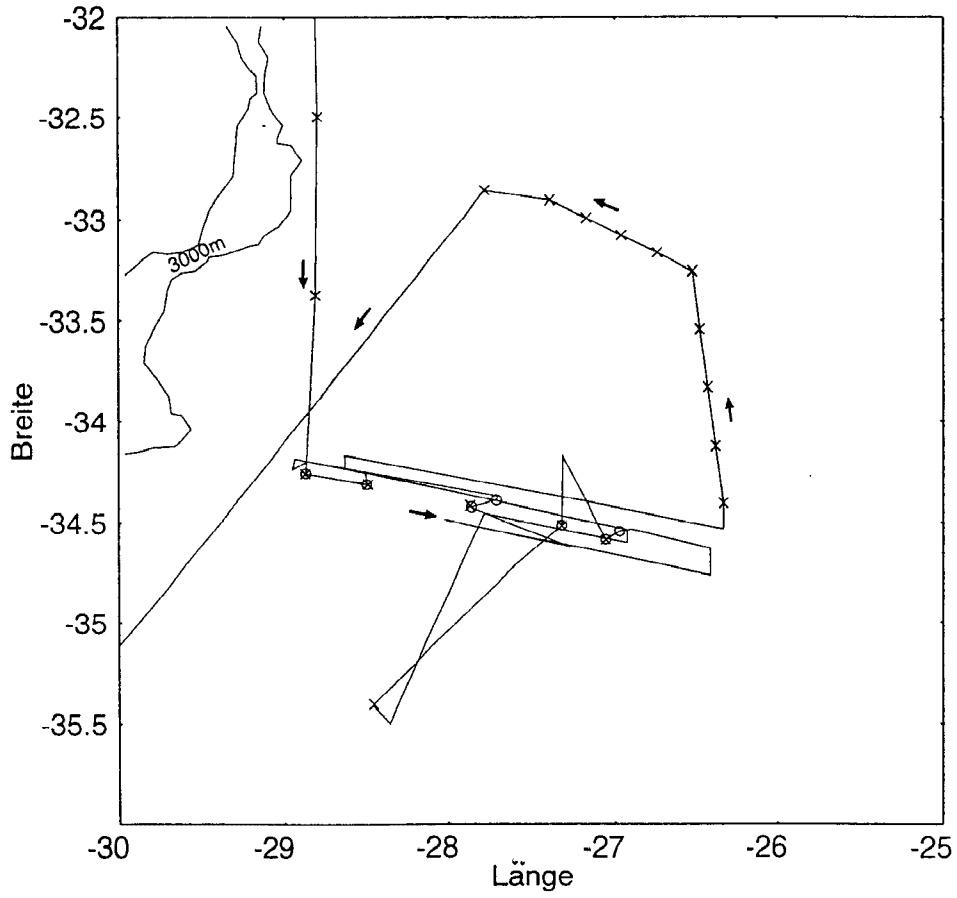

Fig. 1c: Detailed cruise track

2 Participants

Tab. 2: Participants of METEOR cruise no. 28

Leg M 28/1

Name	Speciality	Institut
Müller, Thomas J., Dr. (Chief scientist)	Marine Physics	IfMK
Bassek, Dieter, T.A.	Meteorology	SWA
Beckmann, Uwe, T.A.	Marine Physics	IfMK
Beining, Peter, Dr.	Marine Physics	IfMK
Brinkmann, Jutta, Dipl.-Met.	Atmospheric Physics	UMZ
Bulsiewicz, Klaus, Dipl.-Phys.	Tracer Physics	IUOB
Campos, Ricardo, Cap. Ten.	Observer Brazil	DHN
Dieterich, Christian, student	Marine Physics	IfMK
Düßmann, Heiko, student	Tracer Physics	IUOB
Flechsenhar, Kurt, Dipl.-Met.	Meteorology	SWA
Hydes, David, Dr.	Marine Chemistry	IOS
John, Hans-Chr., Dr.	Marine Taxonomy	BAH
Johnson, Kenneth M., M.Sc.	CO_2-Group	BNL
Kohrs, Stephan, B.Sc.	Marine Chemistry	IfMK
Koy, Uwe, T.A.	Marine Physics	IfMK
Meyer, Peter, Dipl.-Ing.	Marine Physics	IfMK
Meyer, Ralf, student	Marine Chemistry	IfMK
Müller, Sabine, student	Marine Chemistry	IfMK
Neill, Craig, B.Sc.	CO_2-Group	BNL
Pinaya, Walter H., student	Marine Physics	IOUSP
Plep, Wilfried, T.A.	Tracer Physics	IUOB
Putzka, Alfred, Dr.	Tracer Physics	IUOB
Schebeske, Günther, Dipl.-Ing.	Atmospheric Physics	MPI
Schneider, Wilhelm, T.A.	Atmospheric Physics	UMZ
Sültenfuß, Jürgen, Dipl.-Phys.	Tracer Physics	IUOB
Thomas, Rüdiger, Dipl.-Ing.	Marine Physics	IAPK
Welter, Alexander, student	Marine Physics	IfMK
Wills, Kevin, B.Sc.	CO_2-Group	BNL
Zelck, Clementine, Dipl.-Biol.	Marine Taxonomy	BAH

Leg M 28/2

Name	Speciality	Institut
Zenk, Walter, Dr. (Chief scientist)	Marine Physics	IfMK
Bassek, Dieter, T.A.	Meteorologie	SWA
Berger, Ralf, T.A.	Marine Physics	IfMK
Boebel, Olaf, Dr.	Marine Physics	IfMK
Carlsen, Dieter, T.A.	Marine Physics	IfMK
Cordes, Rainer, student	Sedimentology	UBG
Emery, William, Prof.	Radiation Physics	CCAR
Flechsenhar, Kurt, Dipl.-Met.	Meteorology	SWA
Funk, Jens, student	Sedimentology	UBG
Hauser, Janko, student	Marine Physics	IfMK
Kipping, Antonius, T.A.	Marine Physics	IfMK
Möller, Karsten, student	Applied Physics	IAPK
Onken, Rainer, Dr.	Marine Physics	IfMK
Riger, Roland, Dipl.-Chem.	Environm. Chem.	UUM
Roese, Martin, B.Sc.	Marine Physics	IAA
Romaneeßen, Ezard, Dipl.-Oz.	Marine Physics	IfMK
Schmid, Claudia, Dipl.-Oz.	Marine Physics	IfMK
Schneider, Manfred, Dipl.-Chem.	Environm. Chem.	UUM
Snarez, Manuel, B.Sc.	Radiation Physics	CCAR
Wehrend, Dirk, T.A.	Marine Physics	IfMK

Tab. 3: Participating Institutions

BAH Taxonomische Arbeitsgruppe der
Biologischen Anstalt Helgoland (TAG)
c/o Zoologisches Institut und Museum
Martin-Luther-King-Platz 3
20146 Hamburg
Germany

BNL Brookhaven National Laboratory
Associated Universities, Inc.
Upton, NY, 11973
U.S.A.

CCAR University of Colorado
Box 431
Boulder, CO, 80309
U.S.A.

DHN Diretoria Hidrografia e Navegacao
Niteroi, RJ
Brazil

IAA Instituto Antarctico Argentino
Cerrito 1248
1010 Capital Federal
Argentina

IAPK Institut für Angewandte Physik
der Universität Kiel
Leibnitzstr. 11
24118 Kiel
Germany

IfMK Institut für Meereskunde
an der Universität Kiel
Düsternbrooker Weg 20
24105 Kiel
Germany

IOS Institute of Oceanographic Sciences
Deacon Laboratory
Wormley, Godalming
Surrey, GU8 5UB
UK

IOUSP Universidade de Sao Paulo
Instituto de Oceanográfico
Cidade Universitária
CEP 055 08
P.O. Box 9075
Sao Paulo
Brazil

IUOB Universität Bremen
Institut für Umweltphysik und Ozeanographie
Postfach 33 04 40
28334 Bremen
Germany

MPI Max-Planck-Institut für Chemie
Abt. Biogeochemie
B.-B.-Becherweg 27
55099 Mainz
Germany

SWA Deutscher Wetterdienst
- Seewetteramt -
Bernhard-Nocht-.Str. 76
20359 Hamburg
Germany

UBG Universität Bremen
Fachbereich 5 - Geowissenschaften
Postfach 33 04 40
28334 Bremen
Germany

UMZ Institut für Physik der Atmosphäre
Johannes -Gutenberg-Universität
Saarstr. 21
55122 Mainz
Germany

UUM Universität Ulm
Abt. Analytische Chemie und Umweltchemie
Albert-Einstein-Allee 11
89069 Ulm
Germany

3 Research Programme

3.1 WOCE Hydrographic Programme (WHP): Section A8

The main programme of leg M 28/1 was devoted to the World Ocean Circulation Experiment (WOCE) which is internationally coordinated by the World Meteorological Organisation (WMO) and the International Council of Scientific Unions (ICSU). Within the fieldwork of WOCE, for the first time in history the present state and dynamics of the ocean will be observed world wide within less than ten years. Closely related to WOCE is the Joint Ocean Global Flux Studies (JGOFS) within which sampling of CO_2 components is requested on WOCE hydrographic sections.

One major component of WOCE is the Hydrographic Programme (WHP). German institutes took responsibility to occupy three zonal transatlantic hydrographic sections in the South Atlantic: Sections A9 along 19˚S and A10 along 30˚S were obtained during METEOR cruises no. 15/3 in 1991 and no. 22/5 in 1993, respectively. During the present METEOR cruise no. 28/1, section A8 along nominal 11˚20 S was occupied with a total of 110 hydrographic stations with CTD and up to 40 small (10 l) volume rosette samples per station. The nominal station spacing was decreased down to 10 p.m. and 5 n.m. over the shelf and continental breaks, to 24 n.m. over the Mid-Atlantic Ridge, and increased to 38 n.m. over the deep Pernambuco Basin and

Angola Basin. Bottle samples to analyze for oxygen, nutrients and salinity were taken on each station, samples for anthropogenic tracers and CO_2 on every other station.

In addition, four test stations and a survey with ADCP were performed off the Brazilian shelf before the WHP section began, and a box around the eastern tail of the section was occupied.

Underway measurements of currents down to 200 m with a ship borne Acoustic Doppler Current Profiler (ADCP) and with a Geomagnetic Electro Kinetograph (GEK), satellite tracked drifting buoys and expendable current profilers as well as near-surface temperature and salinity and meteorological parameters supplemented the station work.

As part of a long-term Atlantic wide survey on the distribution and ecology of fish larvae, biological stations with 69 plankton hauls from the surface and in 5 levels between the surface and 200 m depth were performed.

Aerosols determine the formation of clouds. Over the South Atlantic several sources may be expected: Aerosols of sea salt and remainders of continental aerosols of mostly desertal origin as well as particles which result from decomposition of dimethylsulfide (DMS) formed by chlorophyll in the sea. All types of these aerosols were filtered from air and are to be correlated to DMS concentrations in seawater and air.

3.2 WOCE Deep Basin Experiment (DBE)

During leg M 28/2 earlier work, performed in the Brazil Basin by METEOR in 1991 and 1992, was continued and extended towards a larger area. These activities contributed to the Deep Basin Experiment of WOCE implemented by scientists from Brazil, France, Germany and the USA. Certified knowledge of the regional water mass circulation as well as the distribution of horizontal divergence and convergence zones are essential for appropriate modelling, one of the research targets of WOCE.

Besides XBT, CTD and GEK measurements (chap. 3.4) circulation studies of the near-surface Central Water were conducted on a quasi-meridional section through the Brazil Basin across the Rio Grande Rise towards the northern Argentine Basin. Among other instrumentation satellite tracked drift buoys from Kiel were used for these observations (chapter 3.3).

Within the deeper levels (800 - 1000 m) of the Antarctic Intermediate Water Lagrangian current observation with RAFOS floats were performed. Results from the previous METEOR cruise No. 22 have impressively confirmed the westward circulation pattern above the Rio Grande Rise. However, we definitely still need more observations of the Intermediate Water in the central part of the Brazil Basin and near the Subtropical Convergence in the Argentine Basin.

The RAFOS sound array has been enlarged by two more sound sources moored at the northern rim of the Argentine Basin. In fact, the whole array in the South Atlantic consists of nine American and six German sound sources (status: Nov. 1994). We deployed 27 floats, built and ballasted by the Institut für Meereskunde at Kiel. The recovery of seven current meter and thermistor chain moorings in the Hunter Channel was another research topic. These Eulerian long-term observations began during METEOR cruise No. 22 in December 1992. The obtained data supplement an existing set of observations monitoring the more westerly part of the water exchange between the Argentine and the Brazil Basin.

Near-bottom CTD casts were utilized for taking bottom samples by means of a minicorer of the University of Bremen (chapter 3.8). Results are analyzed in terms of paleoceanographic objectives.

3.3 Near-Surface Circulation from Drifters

Within the framework of WOCE about 135 satellite tracked drifting buoys (drogue depth 100 m) have been deployed in the South Atlantic by the Institut für Meereskunde at Kiel since 1990. The objective is to deduce near-surface circulation properties in the South Atlantic. Analysis of the eddy statistics was already started in selected areas. But up to now the data density is insufficient for a basin-wide determination of physical parameters like mean velocity and eddy kinetic energy. Therefore the data set has been supplemented by deploying 80 new buoys - 30 of them during M 28.

3.4 GEK Observations

During both legs GEK (Geomagnetic Electro Kinetograph) observations were taken (Fig. 2). Motion induced electrical potential difference is recorded, representing ocean currents perpendicular to the cruising ship. Developments over the past five years have made the GEK set an easy to use instrument. The new measurements supplement earlier records from RV RESEARCHER and RV POLARSTERN obtained in 1987. Due to its simple handling the GEK set could be used without additional ship time.

GEK current registrations will be correlated with meteorological and hydrographical data sets. We aimed the question, in how far it is possible to use a GEK system as an online aid for advanced planning of XBT drops and CTD stations. The post-cruise analysis is expected to evaluate the effectiveness of a low cost and easy to handle GEK in terms of future XBT operations.

3.5 Taxonomy and Distribution of Fish Larvae in the Tropical South Atlantic

3.5.1 Introduction

The zonal transect surveyed during the M 28/1 is part of a long-term programme to describe fish larvae (taxonomy), investigate their distribution (ichthyogeography) and their environmental requirements (ecology) in the entire Atlantic Ocean.

Ichthyogeography can be studied more easily and more economically by larval catches (ichthyoplankton) than by fisheries on adult fish. Larvae cover a vertically more restricted space, are much more abundant, are less capable of escape movements and can be stored more easily (e.g. LASKER, 1981). Some potential disadvantages may be seasonality in occurrence (JOHN, 1979) and the still limited knowledge of larvae taxonomy. World wide the knowledge is most restricted in tropical seas (AHLSTROM and MOSER, 1981).

Quantitative plankton samples can, even after coarse taxonomic analysis only, reveal large scale regional differences in biogeography (JOHN, 1976/77). The spatial resolution increases with taxonomic precision. Additionally such quantitative studies can indicate those environmental parameters limiting the specific distributions (JOHN, 1985). The ranges of most vulnerable youngest stages generally conform with optimum conditions for reproduction, whilst gradients of abundance and age indicate the paths of dispersal and areas of decay (JOHN, 1984). Combining results of other marine sciences, parameters of relevance can be revealed and quantified (e.g. HAMANN et al., 1981). In spite of many uncertainties, fish are among the best investigated marine organisms and provide some regional comparative data covering decades. Comparison of such data can allow an assessment of the effects of climatic changes (e.g. EHRICH et al., 1987). Therefore, in light of the recent discussion concerning Global Change, such quantitative studies should be continued and intensified.

3.5.2 Plankton Sampling

Samples were taken on a total of 69 biological stations, strictly following the box or lines of the CTD stations shown in the reports above, which made the hydrographical parameters available. However, distances between plankton tows in the biologically somewhat more uniform oceanic realm were wider than for CTD stations. Nevertheless, at the continental slopes off Brazil and Angola smaller scale hydrographical features, particularly bottom depths and bottom types, were anticipated to cause small scale heterogeneities in species composition and abundance. There a finer resolution of sometimes only 3 n.m. between stations could be achieved, neglecting likely diurnal differences in light-sensitive neustonic organisms. In the open ocean daylight and nighttime stations were taken in similar numbers.

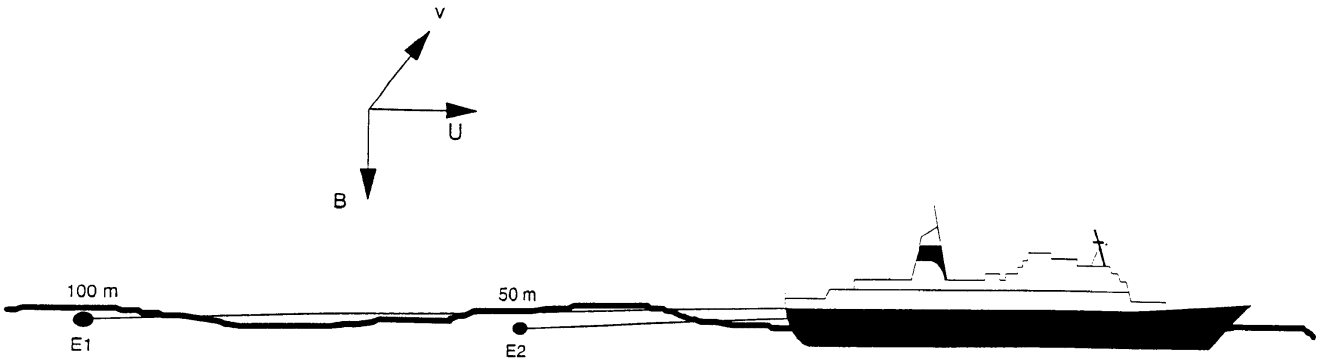

Fig. 2: GEK current measurements by a cruising ship. E1, E2 are electrodes.
- E1, E2: electrodes - B: earth magnetic field, vertical component
- U: induced potential- v: velocity

Samplers deployed were a David Neuston net NEU (modified, see HEMPEL and WEIKERT, 1972) and a Multiple-opening-Closing Net (MCN) after BÉ (for modifications see KLOPPMANN, 1990). Both samplers had an identical mesh size of 300 µm and were towed simultaneously at net speeds of 1.1 - 1.5 m/s for about 30 minutes. While the NEU provided strictly two-dimensional samples 0 - 8 cm, the MCN yielded 5 strata 200 m - 150 m (net no. 1), 150 - 100; 100 - 50; 50 - 25, and 25 - 0 m (net no. 5). The entire catch was transferred to the laboratory immediately after the catch and preserved in buffered 4% formaldehyde seawater solution.

Technical problems early in the cruise caused a delayed availability of the MCN and a few malfunctions, resulting in inconsecutive haul numbers for both gears. Chapter 7.2.6 provides the respective station data and indicates MCN-haul quality. The sample statistics are given in Table 4.

Tab. 4: Volumes or areas filtered by NEU and MCN (successful tows only).

Sampler	**NEU**	**MCN**					**MCN**
		-net 1	net 2	net 3	net 4	net 5	total
Mean Vol. (m^3)		226.9	208.8	207.9	128.2	90.5	173.0
SD (m^3)		67.6	49.5	53.7	40.1	34.8	73.4
Mean Area (m^2)	830.3	4.5	4.2	4.2	5.1	3.6	4.3
SD (m^2)	58.6	1.4	1.0	1.0	1.6	1.4	1.4
N	68	61	59	59	58	59	296

SD - standard deviation
N - Numbers of samples

3.6 Atmospheric Physics and Chemistry

Aerosol particles over the subtropical South Atlantic are mainly influenced by two sources: The sea salt aerosol and aged continental background aerosol with a contribution of the Sahara or Namib desert.

During M 28/1 the size distribution of the marine aerosol particles ranged from 0.005 μm to about 50 ~m radius.

The ocean is an important source of biological aerosol particles. These are able to contribute to cloud forming processes. Thus particles of this type were determined in the radius range > 0.2 ~m. Measurements during METEOR cruise no. 9/2-4 and 22/5 showed discrepancies in the biological content. Therefore dimethylsulfide (DMS) was measured additionally during M 28/1.

In presence of sun light marine phytoplancton is able to produce a compound which decomposes in seawater and enters the atmosphere as DMS. This component in turn is unstable in the atmosphere and oxidizes to sulfate which forms particles and thus influences the cloud condensation nuclei density.

The DMS concentration will be correlated with the concentration of the biological aerosol particles on one hand and with the concentration of the aerosol particles on the other hand. The latter were measured continuously during leg 1.

Additional information will be given by filter samples that were done simultaneously. The filters will be analyzed in order to determine the carbonaceous part of the aerosol.

3.7 Radiative Physics - Skin Sea Surface Temperature Investigation

The purpose of the measurements collected during M 28/2 in the South Atlantic ocean is to examine the radiative skin sea surface temperature (SST) and its relationship to simultaneous measurement of bulk SST. It is the radiative skin SST that is viewed by satellite infrared radiometers and we wish to develop new calibration procedures for the satellite sensors. We have used systems similar to that to be installed on METEOR for cruises in the North Atlantic (on the old METEOR in the fall of 1984), in the Arctic (from VALDIVIA in 1988) in the South Pacific (RV M BALDRIGE in 1990) and in the tropical Pacific (RV VICKERS in spring 1993). Thus measurements from the South Atlantic compliment some of our other measurements of skin and bulk temperature. We have yet to collect a set of skin, bulk SST measurements in the North Pacific.

The new radiometer (Fig. 3) has only been used once before in the tropical Pacific last year. It is a unique system designed for this measurement and the radiometer has 6 different infrared channels for the measurement of skin SST. Four of these 6 channels are the same channels that are available from the satellite radiometer. The

housing is cooled with seawater and there is a reference bucket system to continuously calibrate the radiometer every 2.3 minutes. As the goal was to collect as many contributing measurements as possible we had also installed a pair of upward looking Eppley radiometers measuring solar input in the long and short wave lengths. We used the ship's systems to collect data on wind (speed and direction), air temperature, bulk temperature (at 2 m depth), and position. In addition the meteorological data set is also very useful as it includes not only subjective observations of clouds it also has twice daily radiosonde profiles useful for our studies of the air-sea heat flux associated with the skin-bulk SST difference. Finally the shallow (upper 20 m) CTD profiles will be used to initialize our numerical model of the skin-bulk temperature differences.

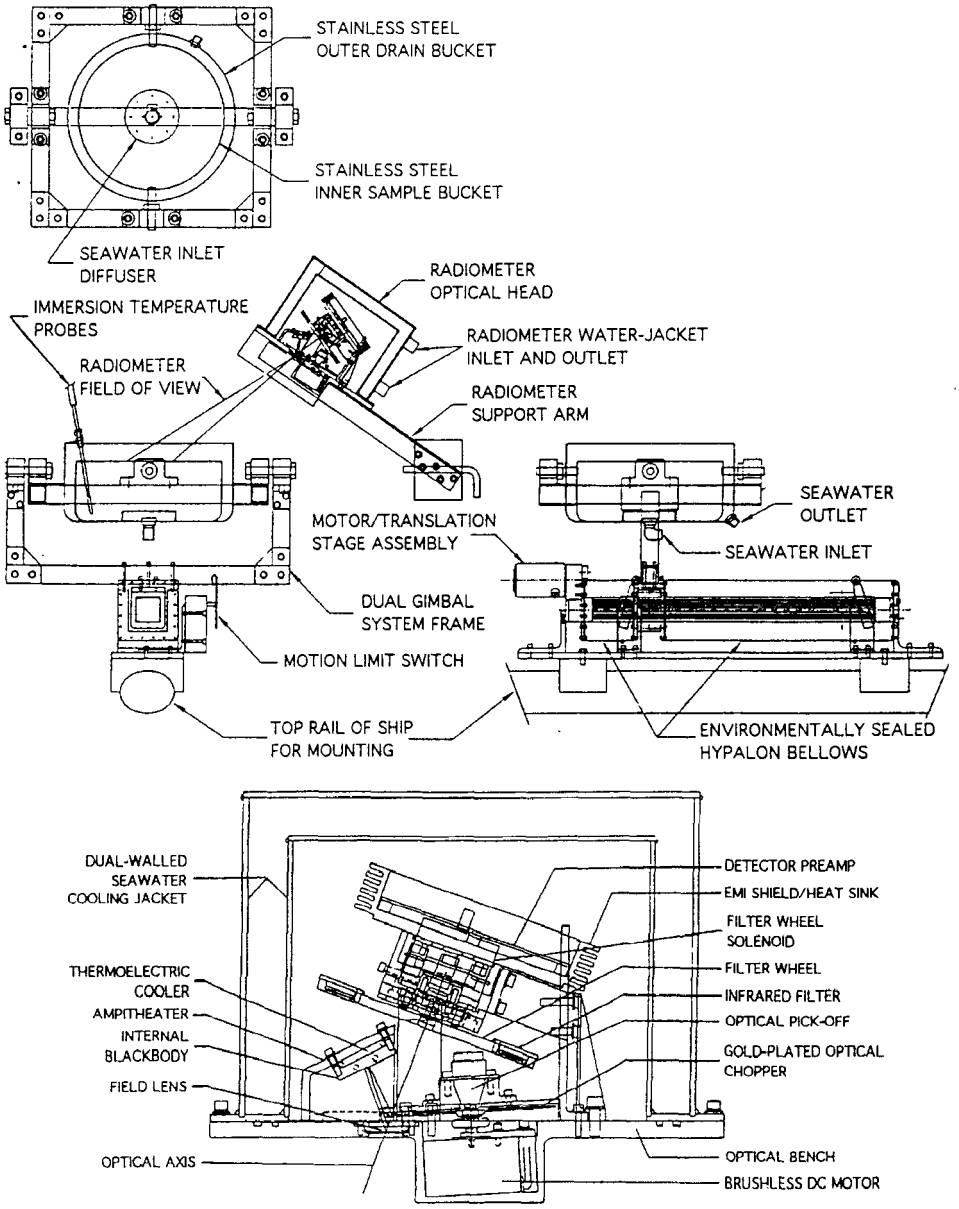

Fig. 3: Apparatus for the continuous registration of the skin sea surface temperature (a) and details of the new radiometer (b).

Using previous data we have been able to parameterize the night relationship between skin and bulk SSTs which at that time are strictly a function of the local wind speed driving the ocean turbulence. During the day a more complex numerical model must be coupled to our paratermization to model conditions when solar insolation occurs along with the local wind stress.

3.8 Marine Geology

During leg 2 sediment samples up to 20 cm depth as well as water samples were taken on the whole profile across the Atlantic. A minicorer with four sampling tubes has been used to sample the sediment.

The aim of the geological sampling during the second leg is to obtain core material for paleoceanographic studies of the time span from the last glacial to recent times. Furthermore the expressiveness of the proxy parameter should be improved.

On the water samples measurements of the stable oxygene-isotopes $^{18}O/^{16}O$ and of nutrients as well as measurements of the $^{13}C/^{12}C$ compositions of $\sum CO_2$ have been carried out. These measurements will enlarge the Geochemical Ocean Section Study (GEOSECS) data set of the Atlantic.

3.9 Environmental Chemistry

The Department of Analytical and Environmental Chemistry joined M 28/2 to investigate the global occurrence and distribution of organic xenobiotics. These persistent compounds are mainly produced in the northern hemisphere and reach the environment, where they are transported and distributed in the atmosphere, hydrosphere and biosphere by the global mass flow of these compartments. The inter-hemispheric exchange however occurs very slowly resulting in very low concentrations of xenobiotics in the southern hemisphere. Thus data of persistent organic compounds in the southern hemisphere reflect the global distribution of these compounds. Level and pattern of multi-component mixtures of xenobiotics indicate formation or global translocation.

During M 28/2 samples from the surface seawater, micro layer and air from the lower troposphere were sampled for analysis of organic xenobiotics, namely chlorinated paraffins (PC) and alkyl nitrates. Chlorinated paraffins were detected in all seawater samples and surface micro layer samples in ng/l concentrations, whereas in air samples CP were not detectable. These data confirm the global occurrence and distribution of chlorinated paraffins. High volatile as well as long-chain alkyl nitrates were detected in air samples of the lower troposphere. Levels and patterns can be discussed in order to investigate the origin of these xenobiotics.

4 Narrative of the Cruise

4.1 Leg M 28/1 (T.J. Müller)

METEOR sailed from Recife on March 29, at 14:15 lt (19:15 UTC), T.J. Müller being chief scientist. Heading eastwards (see Fig. 1), outside the 12 n.m. zone of Brazil at position 8˚17 S/34˚30 W the continuously re-coding systems were switched on: The integrated system DVS to acquire navigational data, the ship borne 150 KHz ADCP, and the towed GEK. The first two days were designed to test both CTD systems, each equipped with a 24x10 l rosette sampler, on four deep water stations (Sta. 165 to 168). Also, the analyzing systems for oxygen, nutrients, freons and CO_2 were set up. At 11˚20 S/34˚W we began a section along A8 shore-wards with XBT and XCP thereby achieving a box with ADCP and GEK in the divergence zone of the western branch of the South Equatorial Current.

On April 1, WHP section A8 started on position 10˚03 S/35˚46 W on the 200 in depth contour outside the 12 n.m. zone of Brazil normal to the continental break with Sta. 169. On each of the following stations, together with the first CTD rosette, a 150 kHz self-containing ADCP was lowered (LADCP) to maximal 1000 in depth. The bottles were used to increase the number of samples up to 40, where the bulk came from the main CTD which always went down until 10 m above the bottom. At 34˚W the nominal latitude 11˚20 S was reached again (Sta. 181), 13 stations at 5 n.m. to 20 n.m. spacing were obtained. Station spacing now was increased to 30 n.m. until 32˚W (Sta. 185).

Here, outside the 200 n.m. economic zone of Brazil, measurements with the multi-beam echo-sounding system Hydrosweep, surface meteorological data, and sampling of aerosols began. Over the Pernambuco Basin, station spacing was increased to 38 n.m. with XBTs of type T5 (nominal depth 1800 m at 6 kn) launched halfway in between. Until Sta. 190 at 25˚20 W, all stations were biological, too. From then on, spacing for biological hauls was 70 to 90 n.m. Four satellite tracked surface drifters which are drogued at 100 m depth were launched between 20˚W and 15˚45 W. Approaching the Mid-Atlantic Ridge, from 22˚W on (Sta. 200) spacing was decreased to 30 n.m. until 17˚W (Sta. 210) and down to 24 n.m. over the ridge until 12˚W (Sta. 222).

Spacing was increased again towards the Angola Basin to 28 n.m. until 1˚W where the section ran close to the Dampier Seamount. Expecting higher hydrographic variability and different species of fish larvae, two extra CTD stations (Sta. 245, Sta. 247, no bottles) and plankton hauls were obtained.

From 0˚E on station spacing increased over the Angola Basin to 38 n.m. until we reached the African continental break at 8˚E (Sta. 260). Again, on this wider spaced part of the section XBT T5 probes were launched halfway between stations. Also, four more satellite drifting buoys were launched between 1˚20 E and 5˚20 E.

With 28 n.m. station spacing we reached 10˚E (Sta. 264) where we entered the 200 n.m. economic zone of Angola. Since no clearance had been applied for plankton hauls, XBT, XCP, and GEK, we had to continue with CTD measurements only. Station spacing was reduced first to 25 n.m. and then to 10 n.m. until we reached the 50 n.m. zone at 12˚57 E (Sta. 274). Waiting for an extension of the clearance to 12 n.m. and plankton hauls within 200 n.m. which was to be arranged by the German Embassy in Luanda, Angola, we surveyed the northern part of a box around the eastern tail of A8 using the CTD/LADCP system down to 1000 in depth (Sta. 275 to 281 along 11˚S). We completed this box in the south (Sta. 282 to Sta. 286 along 11˚40 S) after the extension of the clearance came with plankton hauls as well. We joined A8 again after two days interruption on 11˚20 S at 13˚05 E (Sta. 287) and completed it on the 200 m depth contour at 13˚33 E with Sta. 290 on May 07, 1994.

4.2 Leg M 28/2 (W. Zenk)

In Walfish Bay, Namibia, W. Zenk took over as chief scientist at midday of May 13, 1994. Previously Captain H. Papenhagen and both chief scientists had briefed the press on board the ship. This meeting had been carefully arranged by H. Hoffmann from the German Embassy in Windhoek. In addition to the Regional Governor of the Erongo Region, Mr. A. Kapere, we enjoyed the company of Mayor B. Edwards and Mayor D. Kambo, representing the cities of Walfish Bay and Swakopmund, respectively.

In his introductory remarks H. Hofmann remembered the days 68 years ago, when METEOR's predecessor, the old METEOR, made a port call in Walfish Bay during her famous cruise, the "Deutsche Atlantische Expedition". W. Zenk welcomed the guests on behalf of the Deutsche Forschungsgemeinschaft and T.J. Müller introduced some of the very first results of the WOCE section A8 that the METEOR had just completed.

Initiated by a press release issued by the coordinator's office in Kiel and the German Embassy in Windhoek, the arrival of the METEOR was well received in Namibia. The city and habour of Walfish Bay had been peacefully incorporated by the Republic of Namibia only 74 days earlier. A respectable number of German speaking inhabitants visited METEOR informally. Among them were a few elderly guests who enthusiastically reported their unforgotten impressions of the old METEOR they had visited as school kids. Our port call at Walfish Bay exceeded everybody's expectation. We highly recommend this efficient port for future needs of the German research fleet.

Early Sunday morning on May 15, METEOR left Namibia and sailed directly towards target point "A" at 21˚S/10˚W, situated on the eastern flank of the Mid-Atlantic Ridge. Until early February 1994, we had planned to reach "A" coming from Pointe Noire, Republic of Congo, passing the island of St. Helena. However, due to official travel warnings from the American Secretary of State and the German Foreign Ministry we were forced to reorganize the cruise track on short notice.

On May 21, METEOR crossed the Mid-Atlantic Ridge and occupied the first stations in the eastern Brazil Basin. Until then, all continuously recording systems, i.e. Geomagnetic Electro Kinetograph (GEK), ADCP, radiation and environmental chemistry loggers, had become and remained fully operational for most of the expedition time. The first surface drifters and RAFOS floats were launched at the corner Sta. 295. All drifters were equipped with drogues at a depth of 100 m. The course then changed to 223˚.

Further CTD/RO stations partly in combination with minicorer deployments, more float and drifter deployments and zodiac based chemical sampling followed till we reached mooring "R", at Sta. 305 on the eastern flank of the Rio Grande Rise on May 25. This as all other mooring had been deployed by METEOR in mid December 1992 as a component of the 'Deep Basin Experiment', a subprogramme of WOCE.

On May 27, we reached the western side of the 200 km wide zonal cross Hunter Channel array at moorings "H1-6", being 200 km wide. Favoured by excellent weather conditions all moorings were recovered (Sta. 309-319, 27-30 May) after a 17 month deployment duration. The remaining time in the region was utilized for Hydrosweep surveys and GEK tracks at night. The systematic survey of the bottom topography of the Hunter Channel is a long-term project of the Alfred -Wegener-Institut, Bremerhaven, the University of Bremen and the Institut für Meereskunde at Kiel. Selected CTD stations with minicorer deployments will allow more precise hydrographic and sedimentological descriptions of this important passage for Antarctic Bottom Water on its equatorward drift.

We expected serious problems with mooring "K0". This sound source rig broke loose in mid February 1994, when signals from the watch dog top buoy were reported by Service ARGOS. Upon several release commands no remainders showed up at the mooring site of "K0" in the Hunter Channel. However, to our greatest surprise we were able to locate the sound source's shifted position at approximately 35˚22 S/28˚28 W by listening with two MAFOS monitors on the hydrographic wire. The listening procedure was repeated five nights from different spots resulting in a search radius of < 8 n.m. Despite of a 36 hour intensive search METEOR was unable to find the lost mooring on the sea surface.

On June 1, the search was discontinued. The ship returned to the Hunter Channel and set the replacement sound source mooring "K0 2" (Sta. 322). After a final hydrosweep leg across the Hunter Channel a narrowly spaced deep CTD-section was occupied at the eastern and northern exits of the channel area (Sta. 323-332). Because of rough weather conditions we had to skip further minicorer deployments, which were otherwise performed regularly under the CTD probe on deep stations. Chemical samples from the surface (University of Ulm) were taken regularly from the zodiac during CTD operations whenever the weather conditions allowed.

On June 4, METEOR left the well measured Hunter region and headed for its southernmost position at 40˚S/35˚W. Here sound source mooring "K4" was launched at Sta. 338. Sound sources are an integral component of the RAFOS system. Their signals are sensed by drifting floats. Arrival times of the coded transmissions are recorded in the floats. After the floats surface, typically after 10-15 months, the stored information is transmitted by a satellite link and converted in Kiel into a series of float positions.

The sound source "K4" was a brand-new instrument that had been shipped from the manufacturer WRC directly to METEOR in Hamburg. It was only the qualified assistance of the ship's electronic technician B. James that we were able to solve a problem that remained undiscovered until we unpacked the instrument on board of METEOR. The passage towards "K4" was combined with more float and drifter launches and GEK observations, resulting in a quasi -continuous section from the centre (21˚S) of the subtropical gyre to its southern extend north of the confluence region (35˚S).

On station 338 an extended CTD cast was taken. Samples include, as in other selected cases, probes of helium, tritium, nutrients (University of Bremen) and sulfurhaxaflouride (Woods Hole Oceanographic Institution). After METEOR had occupied this southern corner station she cruised northwestward towards the outer Vema Channel. Additional drifters and floats were launched between shallow CTD station 338 and 344.

After the last drifter and float were deployed on Sta. 342 and 343, respectively, the ship cruised to the final position at the 200 n.m.-zone off the Brazilian coast line. Here, at Sta. 34S more water samples were taken in the western boundary current system before METEOR called at Buenos Aires on 14 June 1994.

When approaching the South American shelf METEOR had occupied 44 CTD stations, 23 of them included joint minicorer deployments. 89 XBT probes were dropped. Seven moorings had been recovered, two were deployed. 27 RAFOS floats, two MAFOS monitors and 20 satellite tracked surface drifters with drogues at 100 m depth could be launched. Quasi-continuous measurements of solar radiation and skin sea surface temperature as well as nearly uninterrupted GEK records were collected.

Fig. 4a: Participants of M 28/1

Fig. 4b: Participants of M 28/2

5 Preliminary Results

In this chapter, methods of sampling and calibration, and preliminary results are discussed from the WOCE Hydrographic Programme (WHP) section A8 along 11˚20 S, from the Deep Basin Experiment (DBE), and other projects of the cruise.

5.1 The WHP Section A8 along 11˚20'S

The backbone of the station work were two MKIIIB CTDs to measure continuous profiles of pressure, temperature, salinity and dissolved oxygen. Attached to the main CTD was a General Oceanic rosette sampler with 24x10 l Niskin bottles. With this main CTD, all stations were profiled down to 5 m to 10 m above the bottom to achieve a consistent set of high resolution hydrographic data along the section.

To take samples for chemical analysis, during the all upcasts the first two bottles were closed at nominally 10 m above the bottom, and the last two bottles were closed in the mixed layer at nominally 10 m depth. This, together with the remaining bottles closed in between assured full depth calibration values for the CTD. The remaining bottles in between were closed according to a sampling scheme that took into account that zonal variations along this zonal section were expected to be small: During two successive stations, bottles were closed at fixed depths, during the next two stations the closing depths were set midth between those of the preceeding two profiles. Then the scheme was repeated. In order to fulfill the WHP requirements for high resolution sampling in the vertical, over the deep basins bottles from a second CTD/Rosette with up to 18x10 l bottles were added.

When on deck after a profile, samples were drawn in the following order: CFCs, helium, oxygen, CO_2, nutrients, tritium, salinity.

The second CTD/Rosette system carried a self contained 150 kHz Acoustic Doppler Current Profiler (ADCP) that was lowered (LADCP) down to 1000 m on all but two stations to measure currents in the upper ocean. These LADCP data together with data from a ship borne 150 kHz ADCP and 8 profiles taken with Expandable Current Profilers (XCP) in the western boundary, will provide estimates of absolute currents.

Due to reasons mentioned in chapter 4, underway measurements of near-surface temperature and salinity, the multibeam echo sounding system Hydrosweep, and continuously recorded meteorological parameters are available only outside the 200 n.m. economic zone of Brazil.

Table 5 summarizes the most important events of the WHP section A8. Chapters 5.1.1 to 5.1.4 describe methods, calibrations and instruments used for analysis on board in more detail while in chapter 5.1.5 we present sections of hydrographic and tracer parameters as measured along A8.

Table 5: Events on WHP section A8

Date	Time	Station	Latitude	Longitude	Remarks
1994	**UTC-3**				
29.03.	13.18				sail Recife, local time UTC-3
	17.30	164	08˚07.5S	34˚16.6W	start test stations with N132, NB3
					start GEK
					start ADCP
					start DVS (no Hydrosweep)
	23.00	165	08˚16.4S	33˚27.4W	start tests N132, NB3, MSN, NEU
30.03.	22.28		11˚14.1S	34˚08.3W	start XBT/XCP section normal to Brazilian coast
01.04.	14.22	169	10˚03.6S	35˚45.1W	start WHP section A8
05.04.	22.45	185	11˚20.0S	32˚00.0W	leave 200 nm economic zone of Brazil
					start Hydrosweep
	UTC-2				
08.04.94	01.05	190	11˚19.9S	28˚39.9W	local time UTC-2
	19.50	192	11˚20.0S	27˚20.0W	W03 broke, NB2 and NB3 on W02
09.04.	16.22	194	11˚20.0S	26˚00.0W	NB3 on W10/12, NB2 on W02
13.04.	14.53	204	11˚19.9S	20˚00.0W	W03 repaired, NB3 on W03
	UTC-1				
15.04.	01.31	208	11˚18.6S	17˚57.6W	local time UTC-1
	UTC 0				
22.04.	03.15	233	11˚20.0S	06˚30.0W	local time UTC 0
25.04.	20.18	245	11˚20.0S	00˚45.0W	extra station DAMPIER Seamount
26.04	08.59	247	11˚20.0S	00˚15.0W	extra station DAMPIER Seamount
	UTC+1				
29.04.	01.00	254	11˚20.0S	04˚00.0E	local time UTC+1
30.04.	10.55	258	11˚20.0S	06˚40.0E	test ICTD
02.05.	18.48	265	11˚20.0S	10˚25.0E	stop GEK, MSN, NEU
					enter 200 nm Angolan economic zone
04.05.	12.36	274	11˚20.0S	12˚57.0E	break WHP A8 at 50 nm Angolan zone, wait for extension of Angolan clearance, start eastern box with NB2
05.05.	19.50	282	11˚40.0S	11˚00.0E	continue with MSN and NEU, continue eastern box
06.05.	17.40	287	11˚20.0S	13˚05.0E	continue WHP A8
07.05.	05.49	290	11˚20.0S	13˚32.4E	last station on WHP A8, calibration course for ADCP
10.05	08.00				Walvis Bay

Notations:

ADCP shipmounted 150 KHz acoustic Doppler Current Profiler, RDI
DVS ship's online data acquiring system
GEK towed Geomagnetic Electro Kinetograph
NB3 combined CTD˚O2, 24 x 10 l rosette
NB2 combined CTD˚O2, 20 x 10 l rosette, 150 KHz ADCP
MSN towed multiple opening and closing net, maximum depth 200 m
NEU Neuston plankton surface net
DR satellite tracked surface drifter
W02/03 CTD winches 2 and 3
W10/12 winches 10 and 12

5.1.1 Hydrography and Currents

(T.J. Müller, U. Beckmann, P. Beining, C. Dieterich, U. Koy, P. Meyer, W.H. Pinaya)

The measurements to be made and controlled were: Two CTD/Rosette systems and two salinometers; XBT and XCP drops; Lowered Acoustic Doppler Profiling (LADCP) for vertical profiling of currents deeper than 300 in. Support came from the crew's electronic group running the ship borne ADCP and other underway measurements: Near-surface temperature (T_0) and salinity (S_0) which were distributed by the ship's data collection and distribution system DVS along with data from the ship's navigation and echo sounding system and from the automatic weather station.

CTD/Rosette

Two MKIIIB CTDO_2/Rosette systems were used with the sampling scheme described in chapter 5.1 above. Both CTDs were made by Neil Brown Instruments (NBIS) (BROWN and MORRISON, 1978). No technical changes were made, because the instruments were known to have relative smooth outputs. Thus, precision and fast temperature have a combined output resulting in a priori weak salinity spiking, pressure is measured with a strain gauge sensor which is capsulated in steel and which is temperature compensated. Attached to both CTDs were Clark type oxygen sensors.

The main CTD (IfMK code NB3) was used on all stations along with a 24x10 l bottle General Oceanics rosette down to the bottom. The second CTD (IfMK code NB2) went down to 1000 in on almost each station to increase bottle samplings depths to WHP requirements. Attached to this second system was a 150 kHz LADCP to measure vertical current profiles.

Pre-cruise calibrations of both CTDs were performed in November 1993 at IfMK's calibration laboratory before shipping the instruments (SAUNDERS et al., 1991; MOLLER et al., 1994, for details in the procedure). First, the correction of the CTD's temperature output to the international temperature scale of 1990 (ITS90) was determined with a Rosemount Pt25 resistance as part of a high precision bridge made by 'Sensoren Instrumente Systeme' SIS in Kiel. Two triple point cells of water

and two melting point cells of gallium defined the fix-points of the reference bridge at 0.01˚C and close to 28˚C. The quadratic term for the Pt25 was taken from the original calibration certificate. The drift between the two calibrations of the main CTD (N133) was less 1 mK (Fig. 5). Comparisons made during the cruise with the main CTD (NB3) and three electronic reversing thermometers which have 1 mK resolution and were turned on the same frame (depth) on almost each station also showed no drift or jump. Thus, the accuracy for A8 over the whole range is better than 2 mK.

For both CTDs, the pressure sensors static correction at three different temperatures (ca. 0.5˚C, 10˚C, and 25˚C) were determined over the whole range, 0 dbar to 6000 dbar, in loading mode, and in unloading mode with three maximum pressures at 6000 dbar, 4000 dbar and 2000 dbar. A Budenberg dead weight tester with certified masses corresponding to 500 dbar increments served as reference. The drift for both sensors is less 1 dbar (Fig. 6), the accuracy for the static calibration is better than 1.5 dbar over the whole range. For both sensors, fast temperature changes at fixed pressure result in sensor responses of order 0.3 dbar/K with time constants of the order of 1.5 h. A simple model can reduce this error to less than 30% (MÜLLER et al., 1994). Observing static and dynamic corrections, the overall accuracy of pressure measurements during A8 is better 2 dbar.

Conductivity is calibrated using the salinity of water samples taken during each cast and analyzed on an Guildline Autosal salinometer along with calibrated CTD temperature and pressure. The salinometer was calibrated with standard seawater batch P120. Double samples from two rosette bottles were taken 10 in above the bottom and within the mixed layer. All other samples for calibration stem from weak gradient layers at 2000 m, 3000 m, 4000 m and 5000 in depth giving a total of 1000 samples for CTD calibration. At stations 165 and 166, the bottles of the main rosette were closed at same depths to achieve an estimate of 0.0005 as mean precision of reference salinities. The drift of the Autosal was less 0.0005 over the whole cruise, if some obvious instabilities due to noise in the power supply and radio operations are ignored. After full evaluation we expect an accuracy of better 0.0015 in salinometer salinity and better 0.002 in CTD salinity.

Since the response of the oxygen sensor is known to be sensitive to uniform flow conditions, the calibration procedure at IfMK uses oxygen sensor and CTD values from the down cast and compares them to titrated values from the upcast on potential density surfaces in high gradient levels up to a pressure of 2000 dbar, and on pressure surface for higher pressures where oxygen gradients are weak. The formula for conversion of the sensor output to physical units is essentially that of OWENS and MILLARD (1985).

Lowered ADCP

A 150 kHz self-contained ADCP made by RD Instruments was attached to the second CTD/Rosette system to measure the vertical distribution of currents down to 1000 m depth on stations. The instrument worked on all stations except stations 181, 209, and 270. Data processing follows the method described by FISCHER and

VISBEK (1993). As a result, we hope to be able to adjust geostrophically calculated currents to directly measured currents below the Ekman layer.

Ship borne ADCP
Like the LADCP, the 150 kHz ship borne ADCP may serve to adjust geostrophically calculated currents to directly measured, at least in its deeper part. After station 208 the transducer mounted on the ship's hull broke and had to be replaced by a spare transducer mounted in the moon poole.

Major problems to be solved with data processing, are to compensate for misalignment and scaling error of the transducers with respect to the ship's main axis (course) and to remove high frequency fluctuations from the measurements like semidiurnal and diurnal tides. To determine the engineering constants, two calibration courses during the proceeding leg M 27/3 and at the end of M 28/1 were performed in bottom track mode over the shelves of Brazil and Angola (JOYCE, 1989; POLLARD and READ, 1989).

XBT and XCP measurements
Both, 16 XBT probes T5 and Deep Blue (T7), and 8 XCP probes were used to measure the thermal and velocity structure on the continental break off Brazil westward along the western most part of WHP section AS before the section started on the shelf. While XBTs were dropped at full speed of the ship, during XCP measurements the ship's speed 30 s after dropping an XCP probe was dropped to 2 kn, in order to receive properly the radio transmitter's signal. The XCP measurements will be merged with the hydrographic measurements.

Underway measurements (DVS)
Underway measurements consisted of several parts. Common is that all these data are merged and distributed by the vessel's data distribution system DVS. Sampled were in 2 minute recording intervals information on navigation (mostly GPS), the ship's echo sounding systems Hydrosweep and Parasound (outside the 200 n.m. economic zone of Brazil from station 185 on only, see section 3), near-surface (4 m depth) temperature at the ship's hull (T_0), nearsurface salinity (4 m depth inlet, S_0), and meteorological parameters from the ship's automatic meteorological station as measured on both sides of the ship, leeward and windward (also outside the Brazilian economic zone).

T_0 and S_0 are calibrated on CTD stations to better 0.05 K and 0.05 in salinity, respectively. The multibeam echo-sounding system Hydrosweep which is mostly to record depth, is a self-calibrating system, and on METEOR provides water depths, and no soundings. The meteorological station is operated during the cruise and checked on a pre-cruise basis by the German Maritime Weather Service (SWA). No in-cruise calibrations are available.

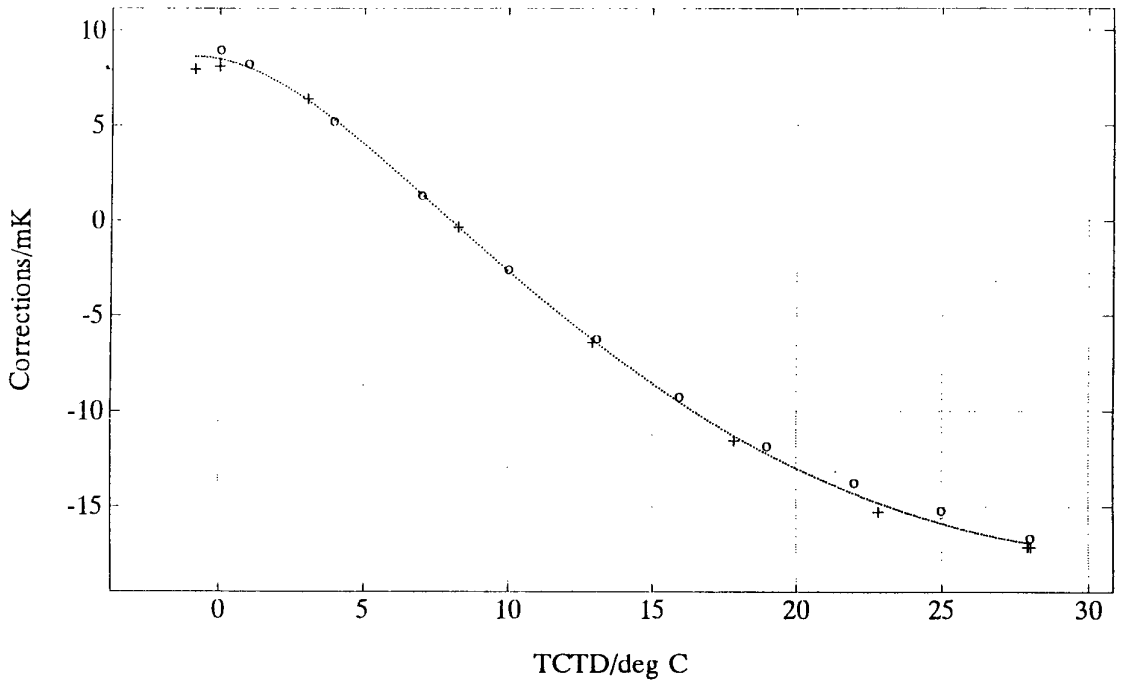

Fig. 5: Pre-, post-cruise temperature calibrations of the main CTD (NB3). The drift between pre- and post-cruise calibration is less 1 mK.

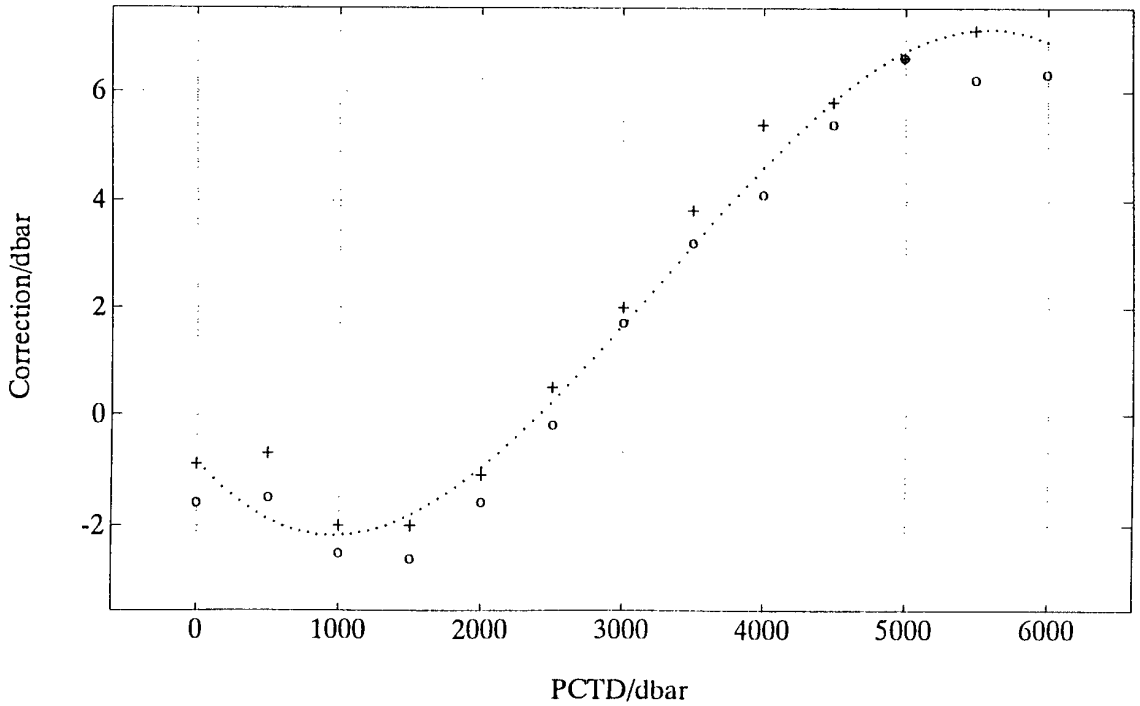

Fig. 6: Pre-, post-cruise and cruise static calibrations at low temperatures of the main CTD (NB3) pressure sensor. The drift between pre- and post-cruise calibration is less 1 dbar.

5.1.2 **Dissolved Oxygen and Nutrients** (D.J. Hydes, S. Kohrs, R. Meyer, S. Müller)

Samples to measure dissolved oxygen and the nutrients phosphate, nitrate and silicate were taken from each bottle closed on A8, and amount to more than analyzed 3700 probes not including double probes to determine precision. Whereas the measurements of oxygen, nitrate and silicate are of high quality, it was not possible to measure phosphate because of irreparable malfunction of the apparatus.

Dissolved oxygen
Bottle oxygen sub-samples were taken in calibrated clear glass bottles with ground glass stoppers from all WOCE section water samples collected on the cruise. Samples were taken immediately after the rosette was on deck or following the drawing of tracer samples of CFCs and helium. At the time of chemical fixation the temperature of the water was measured on a separate sample collected in the same manner as the oxygen samples themselves. This information was used to correct the change in density of the sample between the closure of the rosette bottle and the fixing of the dissolved oxygen. Duplicate samples were taken on every cast. These were the first four bottles on the deep rosette, and the first two bottles on the shallow rosette.

Analysis followed the Winkler whole bottle method. The thiosulphate titrations were carried out in an air conditioned laboratory, the temperature varied between 25˚C and 21˚C over the period of the cruise. Potassium Iodate standards were determined in conjunction with most of the analytical runs. A mean value of the standard measurement was used to calibrate the titration of oxygen. The titration was controlled at the end point using a Metrohm Titrino (a combined automated burette and micro-processor unit). The end point was determined amperometrically titrating to a dead stop (CULBERSON and HUANG, 1987). The concentration of the thiosulphate was 25 g/l this gives a titration volume close to 1 ml for oxygen saturated water. The thiosulphate solution is dispensed from a 5 ml exchange unit on the Titrino. The calculation of oxygen concentration in the solutions followed the procedure outlined in the WOCE Manual of Operations and Methods (CULBERSON, 1991) committing the unnecessary intermediate conversion to volumetric units. Appropriate corrections for density of samples and reagents and volumes of glass-ware were applied as well as for impurities in the reagents (as outlined in CULBERSON, 1991).

Bottle oxygen titrations are calibrated against a Potassium Iodate standard solution. These were prepared on board by dissolving amounts of the dried salt weighed to a precision of 0.0001 g, in a calibrated volumetric flask. Before weighing the salt was dried over night in an oven at 110˚C. The dried salt was cooled over silica gel before weighing. The accuracy of these solutions was checked against a Sagami Potassium Iodate standard which is certified to be a 0.0100 normal solution. These comparisons agreed within the precision of the titrations. The precision of the measurements as indicated by the determination of the difference between duplicate samples taken from the same Niskin bottle were calculated as the mean of the absolute difference

between duplicate measurements for groups of ten stations. The results are presented in Table 6, which includes the number of observations in each group of stations and the number and percent of the duplicate differences greater than 1 μmol and greater than 2 μmol.

Nutrients

Nutrient samples were drawn from all the Niskin bottles closed on the WOCE section stations. Sampling followed that for oxygen and CO_2 on those stations where CO_2 samples were taken. Samples were collected into virgin polystyrene 30 ml Vials (Coulter Counter type). These were rinsed three times before filling. The samples were then stored in a refrigerator at 4˚C, until they were analyzed. The tests carried out on WOCE leg A11 showed that samples from all depths stored for a week in a refrigerator at 4˚C were not detectably effected by storage. Actual storage times on M 28/1 were up to 12 hours before being analyzed.

The nutrient analyses were performed on a Chemlab AAII type Auto Analyser, coupled to a Digital -Analysis Microstream data capture and reduction system. Due to problems with noise in the ship's electricity, supply the Chemlab Colorimeter was modified at the start of the cruise so that the detectors and light source were driven from stabilized DC supplies. For silicate, the standard AAII molybdate-ascorbic acid method with the addition of a 37˚C heating bath was used (HYDES, 1984), and for nitrate the standard AAII method using sulphanilamide and naphtylethylenediamine-dihydrochloride was applied (GRASSHOFF, 1976), with a Cadmium-Copper alloy reduction column (HYDES and HELL, 1985).

As for phosphate it was intended to use the standard AAII phosphate method (HYDES, 1984) which follows the method of MURPHY and RILEY (1962). However, when the apparatus was set up the sensitivity of the method was so low as to make measurements meaningless.

The calibration of all the volumetric flasks and pipettes used on the cruise were checked before packing and were rechecked on return to the laboratory.

Nutrient primary standards were prepared on board from weighed dry salts. The salts were dried at 110˚C for two hours and cooled over silica gel in a desiccator before weighing. Precision of the weighings was better than 1 part per thousand. For nitrate 0.510 g of potassium nitrate was dissolved in 500 ml of distilled water in a calibrated glass volumetric flask. Four different solutions were prepared in three different flasks. No detectable difference could be found between these solutions. For silicate 0.960 g of sodium silica fluoride was dissolved in 500 ml of distilled water in a calibrated plastic (PMP) volumetric flask. No detectable difference could be found between this solution and a standard solution which had been prepared on shore.

Table 6: Precision of oxygen measurements on WHP section A8 from duplicate samples within groups of 10 stations. N is the number of double samples within batches of 10 stations. D1 and D2 denote the number of pairs with differences greater 1 μmol and greater 2 μmol, respectively.

Station	mean	mean dif.	D1	differences D1/%	differences D2	D2/%	N
169-175	4.33	1.90	21	88	16	67	24
176-180	2	0.90	16	50	13	41	32
181-190	0.89	0.43	18	32	13	23	56
191-200	0.66	0.32	13	22	2	3	59
201-210	0.88	0.47	12	24	7	14	51
211-220	0.62	3.00	11	19	3	5	59
221-230	0.71	0.35	14	25	2	4	57
231-240	0.44	0.22	6	11	0	0	54
241-250	0.58	0.29	8	19	1	2	42
251-260	0.84	0.41	14	25	6	11	57
261-270	0.94	0.52	13	25	5	10	52
271-274	0.6	0.30	3	19	0	0	16

All analytical runs were calibrated on the basis of four mixed secondary standards measured in duplicate at the start of the run. Drift samples and blanks were measured after the standards, halfway though the run and at the end of the run. The concentrations of the standards were for silicate 125, 100, 50, 25 μmol in the western basin, and 100, 75, 50, and 25 μmol in the eastern basin; for nitrate the concentrations were 40, 30, 20, and 10 μmol in both basins. Calibration was on the basis of a linear fit by the least squares method forced though the origin. The gains on the colorimeter channels were not altered after being established at the start of the cruise. The apparent sensitivity of each run was recorded along with the standard error estimated from the least squares fit. The secondary standards were prepared in 40 g/l Analar Sodium Chloride solution. The blank in this solution was checked daily against OSI-Low Nutrient Seawater, and was undetectable throughout the cruise (less than 0.05 μmol nitrate and less than 0.1 μmol for silicate). The apparent sensitivity of the methods used in Sodium Chloride solution were checked against standards prepared in OSILow Nutrient Seawater at the start of the cruise. There were no detectable differences.

Duplicate samples were collected from the first four bottles on the deep CTD-3 rosette and the first two bottles on the shallow CTD-2 rosette. All samples were then measured once by the analyzer. e results for the reproducabilty of measurements of the duplicates were assessed on the basis of the variation over groups of ten stations (see Table 7).

Table 7: Precision of nutrient measurements on WHP section A8

Station	Silicate			Nitrate		
	mean µmol	mean dif.	mean dif. %	mean µmol	mean dif.	mean dif.%
171-180	52.4	0.13	0.25	24.7	0.06	0.25
181-190	87.2	0.27	0.30	32.3	0.10	0.32
191-200	86.5	0.24	0.28	31.9	0.08	0.24
201-210	65.1	0.32	0.49	28.8	0.11	0.38
211-220	35.7	0.12	0.34	21.3	0.07	0.31
221-230	37.1	0.11	0.30	24.4	0.07	0.31
231-240	41.0	0.09	0.22	27.7	0.05	0.17
241-250	46.3	0.12	0.26	27.5	0.07	0.27
251-260	45.5	0.12	0.25	27.9	0.09	0.33
261-270	41.4	0.11	0.27	26.9	0.11	0.41
271-274	28.4	0.11	0.37	26.1	0.13	0.48
287-290	25.1	0.11	0.45	35.4	0.06	0.18

Overall the mean difference for silicate was 0.2 µmol with a standard deviation of 0.3 µmol (N=594 duplicate samples) and for nitrate the mean difference was 0.1 µmol (stdev 0.1 µmol, N=594). The standard deviations on the differences are similar to the means of the standard errors of the least squares calculation of the calibration equations Si-0.28 µmol and NO_3-0.097 µmol.

The accuracy of measurements was monitored through the cruise by measurements of Sagami Chemical Co. Nutrient Standard Solutions. New bottles of these solutions were opened each week. The results were for: Nitrate in a nominally 10.0 µmol Sagami Standard Solution, the mean value determined was 9.76 µmol stdev 0.14 µmol (N=36). Silicate in a nominally 50.0 µmol Sagami Standard Solution, the mean value determined was 49.70 µmol stdev 0.40 µmol (N=27).

5.1.3 Tracers (A. Putzka, K. Bulsiewicz, H. Düßmann, W. Plep, J. Sültenfuß)

The investigated tracers are helium, tritium and the chlorofluorocarbons (CFC) F-11, F-12, F-113 and carbon tetrachloride CCl_4. The main part of tritium, the unstable hydrogen isotope which decays to ^{3}He, and the CFCs are anthropogenic. Their time dependent input at the ocean surface is known. The tracer concentration is altered by mixing processes and as for tritium by radioactive decay while the water descends to deeper levels of the ocean. Measuring the concentration of the tracers provides information about time scales of ventilation processes of subsurface water.

The atmospheric F-11 and F-12 contents increase monotonously with different rates since 1940, CCl_4 increases since 1920 while F-113 began to increase 1970. Hence the concentration ratios of different tracers vary over wide ranges and can be used to indicate the 'age' of water masses, i.e. the time since they had their last contact with

the surface. 'Younger' water is tagged with higher CFC concentration compared with 'older' water. Combining concentrations and concentration ratios in the ocean with corresponding input functions at the sea surface provides information about mixing processes in the ocean.

Sampling
Samples were taken according to the WOCE scheme. About 1700 samples for CFC analysis were taken from all bottle depths of each other station over the deep ocean and of each station close to the continental margins. Samples were stored in glass syringes and measured on board.

Helium samples were extracted on board from 630 glass pipets. Another 520 helium samples in copper tubes and 645 tritium samples in glass tubes were taken for later shore based analysis. Therefore, in chapter 5.1.5, only the CFC and CCl_4 measurements are discussed.

Onboard measurements of CFCs
The Bremen system measures the CFCs F-11, F-12, F-113 and carbon tetrachloride CCl_4 concentrations of seawater samples. It consists of a gas chromatograph made by Hewlett Packard which is equipped with a capillary column and a special non commercial sample preparation unit. The latter is to prepare gas aliquots for calibration purposes and to handle water samples, especially the stripping of essentially all gases from water samples of about 30 cc.

The gases are transferred to a trap which is cooled with liquid CO_2 down to -40˚C. The trap is filled with a special packing material to accumulate the compounds we are interested in. During the next step these compounds are released by heating the trap to about (100˚C) and transferred through the capillary column by a steady carrier gas flow to separate the compounds.

The gases are detected using an electron capture detector (ECD). Temperature programming facilities of the gas chromatograph is applied to accelerate the whole analytic procedure. All main parts of the system are controlled by a standard PC driven by self developed software while the acquisition and integration of the chromatograms is done using commercial software on the same PC. The preparation unit is equipped with a multi sampler device which allows to analyze 7 water samples without further attendance together with one gas standard and two blanks within about 3 hour. Within 24 hours, 50 water samples can be processed. Every other day a calibration curve has to be measured, since the detector is non-linear and its sensitivity might change with time. This has to be taken into account for the evaluation of the raw data.

The measurements for F-11, F-12 and CCl_4 cover the range from the detection limit of 0.002 pmol/kg to about 2 pmol/kg. While the reproducibility of gas standards is below 0.5% standard deviation the values for the water measurements is slightly greater of about 0.8% or 0.003 pmol/kg whichever is greater. The analytic resolution

for F-113 was not as sufficient as for the other compounds, but further evaluation of the chromatograms will recover some reasonable figures for this parameter.

5.1.4 CO_2-Measurements (K. Johnson, K. Wills)

Research cruise M 28/1 (WOCE section A8) continues a tradition whereby personnel from the Brookhaven National Laboratory, Upton, N.Y., U.S.A., have made CO_2 measurements aboard METEOR. This cruise is the fourth WOCE line involving the Brookhaven group and the Institut für Meereskunde at Kiel. The A8 section data join the results for WOCE sections A9 (M 15) and A10 (M 22) completed by the CO_2 group, and with its completion Brookhaven is now in possession of data from three contiguous latitude lines 11˚S, 19˚S, and 30˚S, respectively. This gives Brookhaven chemical oceanographers and oceanographic co-workers from Kiel, Warnemünde, and Wormley a unique opportunity to validate the calculation of CO_2 transport in a manner analogous to that done for heat transport.

During M 28/1 two parameters of the carbonate system were measured. The first, total carbon dioxide (CT), was measured by continuous gas extraction of acidified seawater with the resultant CO_2 determined by coulometric titration. The second, the discrete partial pressure of CO_2 (pCO_2), was measured by equilibrating known volumes of a liquid phase (seawater) and a gas phase (air of known CO_2 concentration) by shaking for three hours at constant temperature. Following equilibration, the CO_2 in the gas phase was determined on a gas chromatograph equipped with a flame ionization detector (FID) after the catalytic conversion of CO_2 to CH_4. The pCO_2, at the in situ temperature and the sample alkalinity were calculated from the ancillary nutrient and oxygen data and from the thermodynamic considerations and constants of the carbonate system. Unlike previous cruises where continuous underway pCO_2, was determined in the surface waters, the discrete method above was used to measure the pCO_2 throughout the water column, and to our knowledge this is the first WOCE section for which a complete set of pCO_2 data exits.

The precision of the total carbon dioxide duplicate analyses during the cruise was 0.80 mol/kg (0.04%), while preliminary calculations indicate that the precision of the pCO_2 determinations was 1.0%. In addition, 76 samples of 'Certified Reference Materials' (CRM) were analyzed for total carbon dioxide as a check on accuracy. The CRM, seawater samples spiked with sodium bicarbonate, were analyzed before the cruise for CT in the laboratory of Dr. C.D. Keeling at the Scripps Institution of Oceanography (SIO) by vacuum extraction and manometry. The certified mean of 9 samples was 1991.94 mol/kg. For the 76 samples CRM analyzed by coulometry during M 28/1, the mean was 1991.37 mol/kg with standard deviation 1.27 mol/kg. As a further precaution, forty (40) samples were collected during the cruise and preserved for later analysis in the laboratory of Dr. Keeling at SIO.

During M 28/1 some 51 stations (nearly 50% of the WOCE stations) were sampled for the CO_2 parameters. Approximately, 1,588 individual total carbon dioxide samples and 1,549 individual pCO_2 samples (duplicates not included) were drawn and analyzed. Counting

the duplicates adds another 200 samples and analyses. Because the data set is very large and there are still some uncertainties in the final depths and associated nutrient values, analysis of the data set in chapter 5.1.5 still is preliminary.

5.1.5 First Results from WHP A8

(T.J. Müller, P. Beining, D. Hydes, K. Johnson, A. Putzka, G. Siedler)

We show zonal sections along 11˚20 S of preliminary WHP standard parameters: Potential temperature, salinity, dissolved oxygen, nitrate, silicate, the CFCs F-11, F-12, and CCl_4, and potential density (Figures 7 to 15, respectively). Potential density is referred to the surface for the depth range 0 dbar to 1000 m, to 2000 dbar for the 1000 m to 3000 in range, and to 4000 dbar for depths greater 3000 m.

Some parameters will not be or are not yet available: Phosphate was not measured because of the insensitivity of the apparatus used on board (see chapter 5.1.2). The measurements of the CFC F-113 did not provide high enough resolution and need special post cruise analysis of spectograms (see chapter 5.1.3). Samples of the tracers tritium and helium are still to be analyzed ashore. Also, the carbon measurements still need final adjustment.

The sections in figures 7 to 15 are based on preliminary data from the more than 3700 depths where bottles were closed (dots in the density section, Fig. 15). Temperature, salinity and density are from upcast CTD values at depths where bottles were closed. For tracers and CO_2 over deep ocean basins, each second station is sampled only. Samples from some 10% of all bottles showed obvious misalignment to water mass structures due to malfunctions of the rosette. They were rearranged subjectively to appropriate depths. The contouring procedure uses a Kriging algorithm for smoothing, and the colours for contouring are chosen to appropriately resolve the main structures of water masses.

The different water masses below the warm and high saline surface water and the low oxygen South Atlantic Central Water (SACW) show up in minima and maxima of characteristic parameters. These extrema usually are most pronounced at the western boundary current regime and they gradually decay and eventually vanish eastward. Especially the anthropogenic tracers show a sharp frontal structure over the Mid-Atlantic Ridge with low values down to the detection limits in the eastern Angola Basin denoting weak ventilation in that basin.

Near the surface, both, temperature and salinity decrease in the well-known manner from west to east. At 9˚E, we find the isohalines doming to the surface and bowling down to 250 m. The SACW is characterized by low oxygen with lowest values in the east. In the eastern basin this minimum also is reflected in the highest pCO_2 and CT values (not shown here) we have observed in the Atlantic. Commencing at 3˚E to 4˚E in the Angolan Basin, pCO_2 and CT reached 2000 µatm and 2263 µmol/kg, respectively, at depths of 400 m to 600 m.

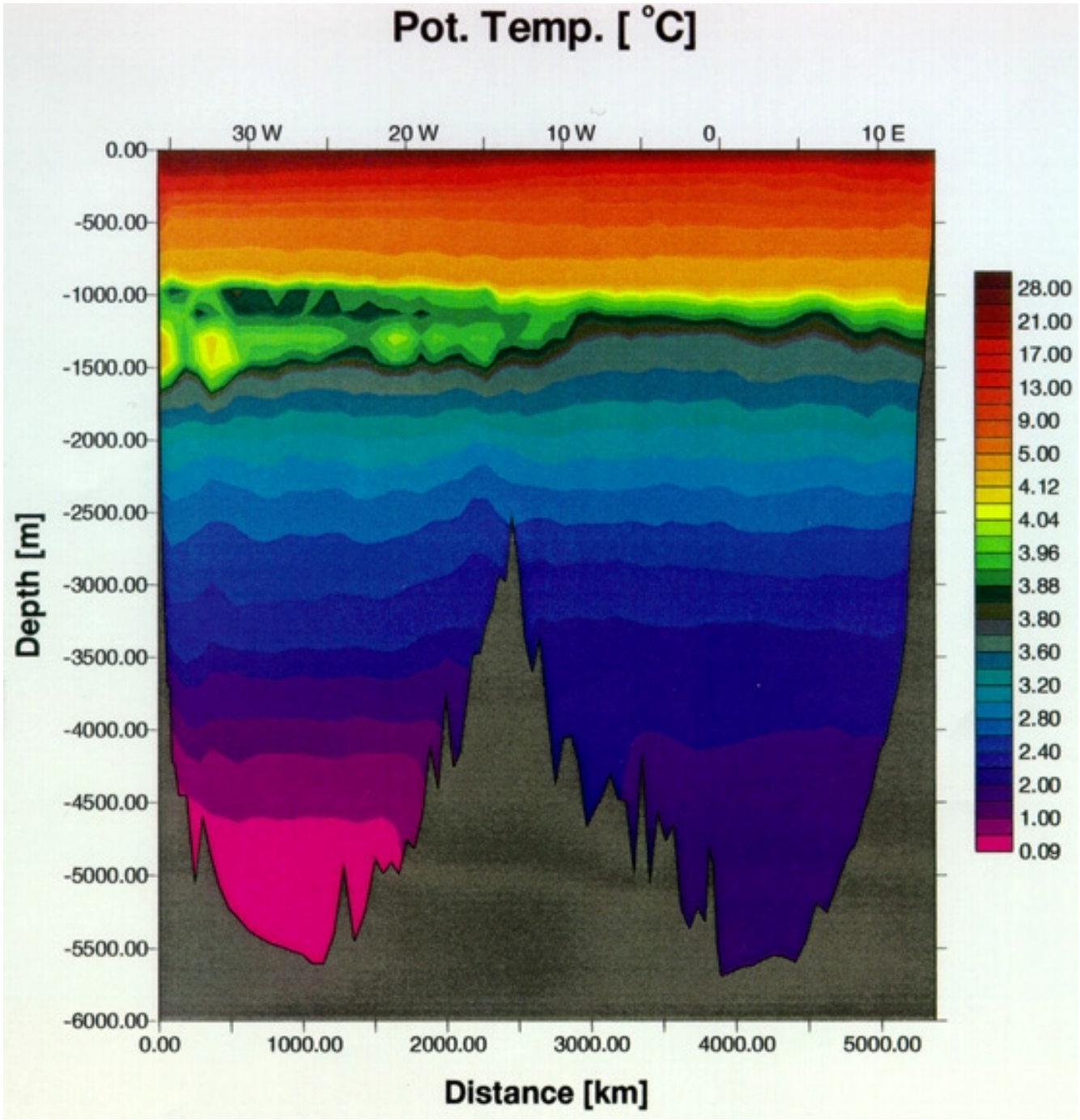

Fig. 7: WOCE Hydrographic Programme Section A8 along 11°20'S, occupied with METEOR during cruise M 28/1 from April 01 to May 07, 1994. Distribution of potential temperature.

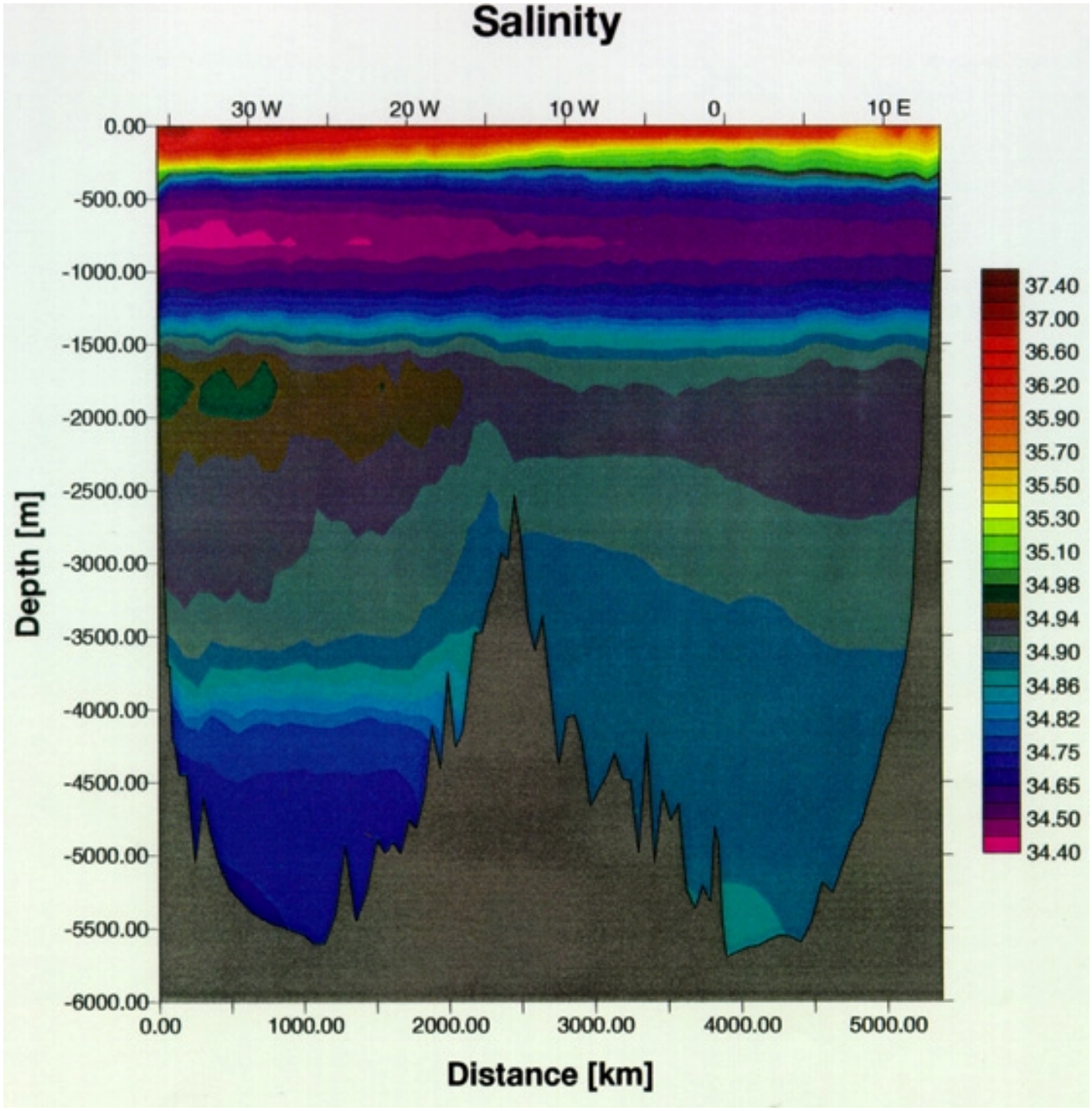

Fig. 8: As fig. 7, salinity (uncalibrated)

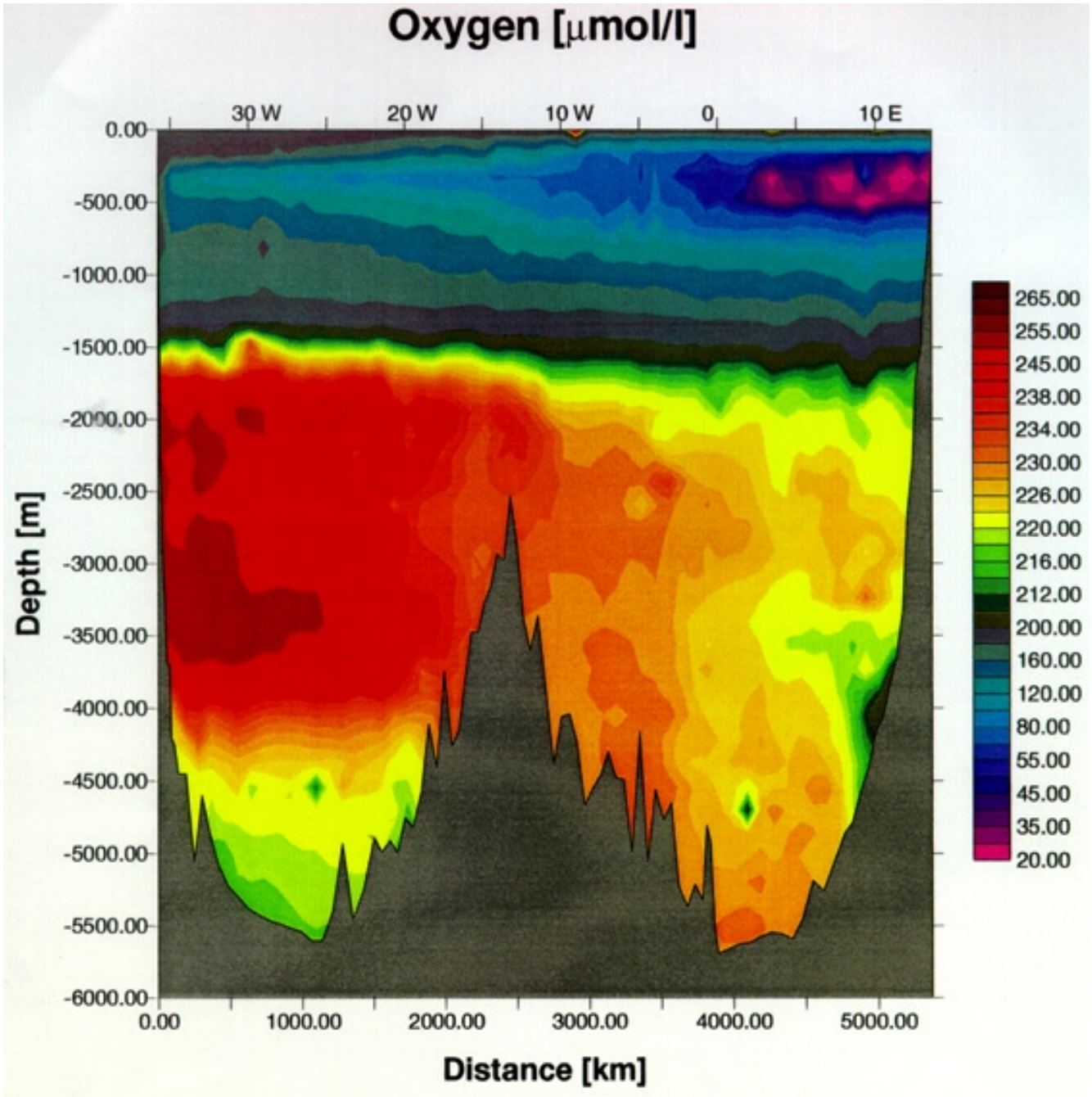

Fig. 9: As fig. 7, dissolved oxygen

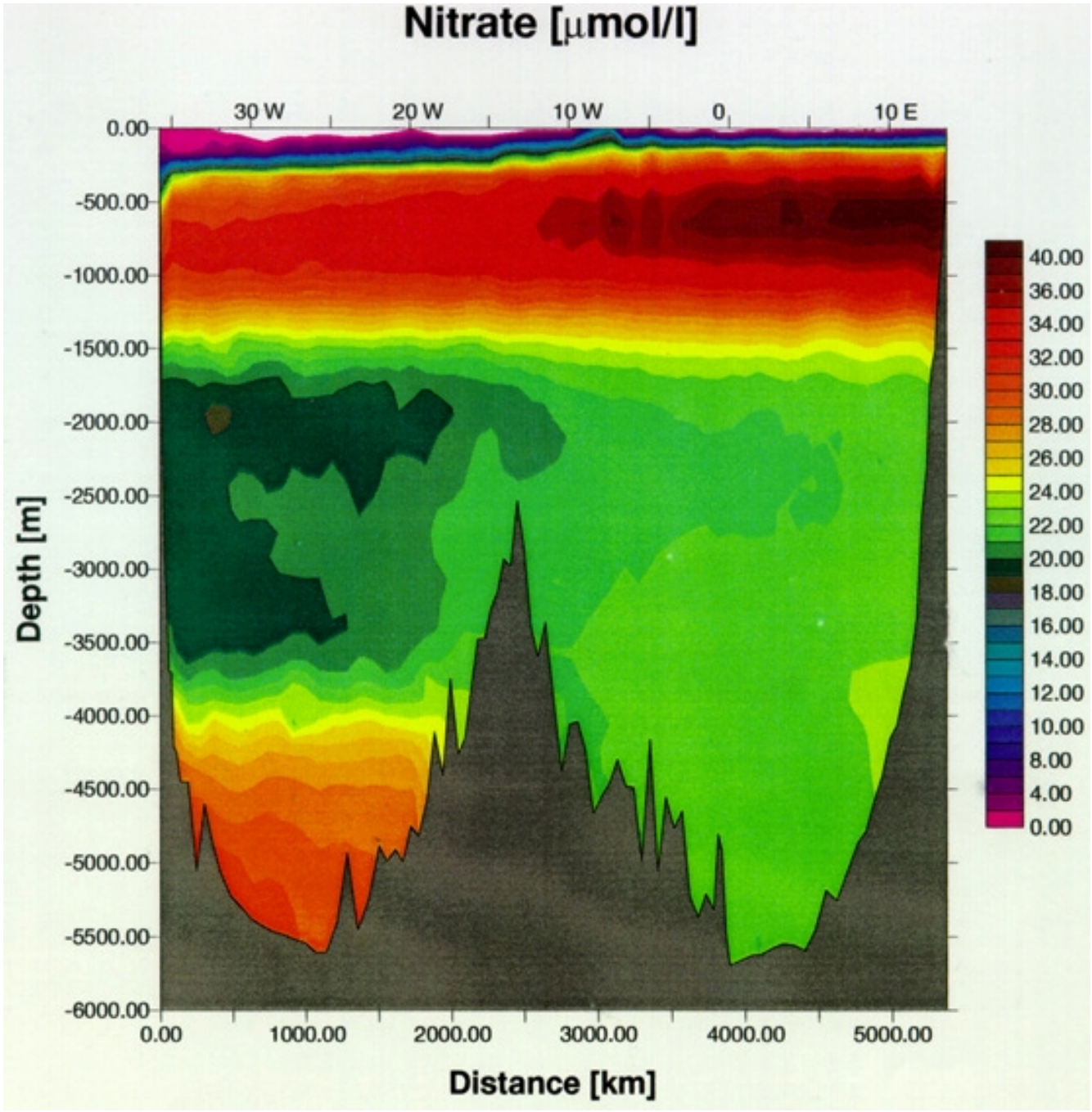

Fig. 10: As fig. 7, nitrate

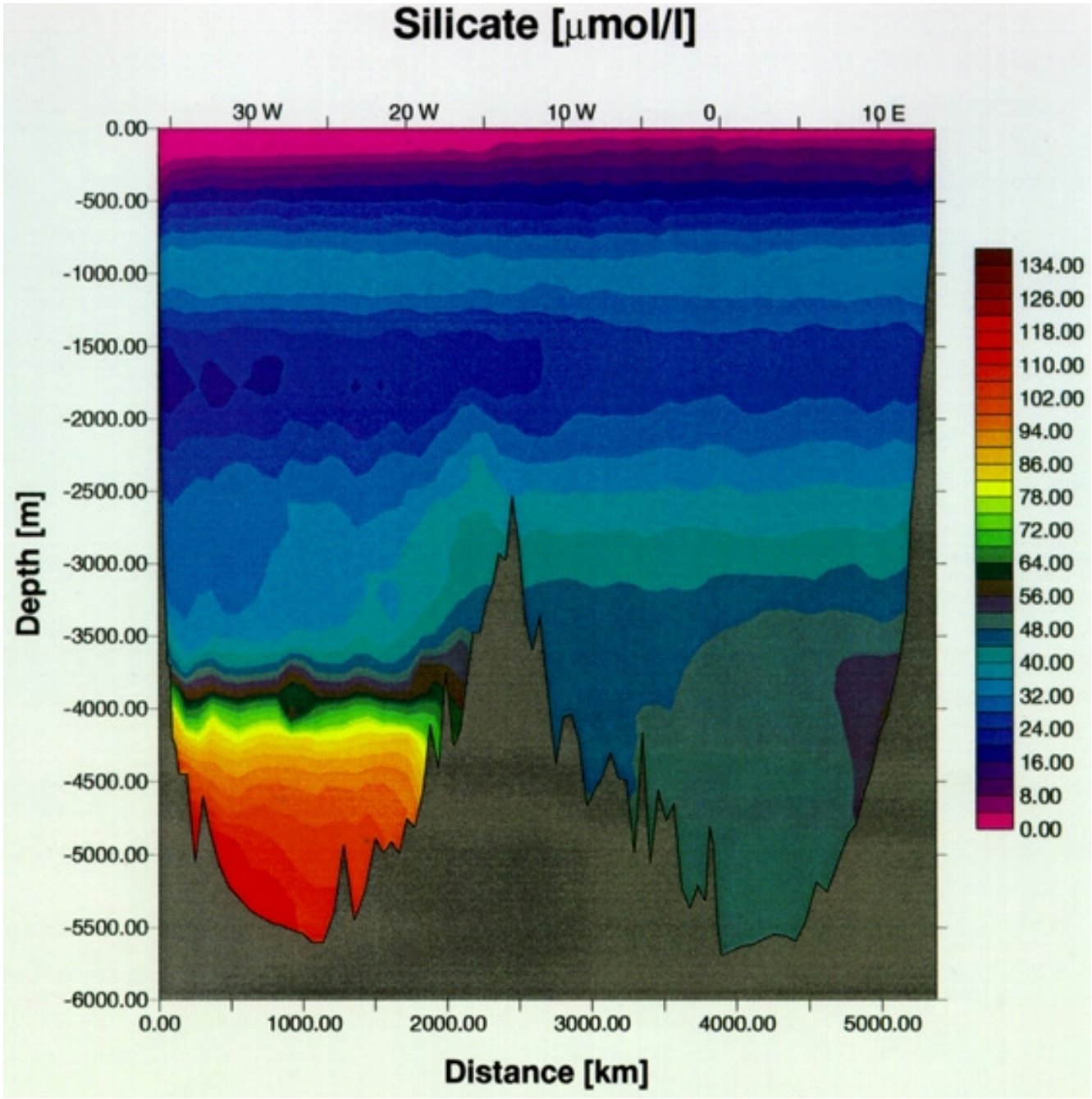

Fig. 11: As fig. 7, silicate

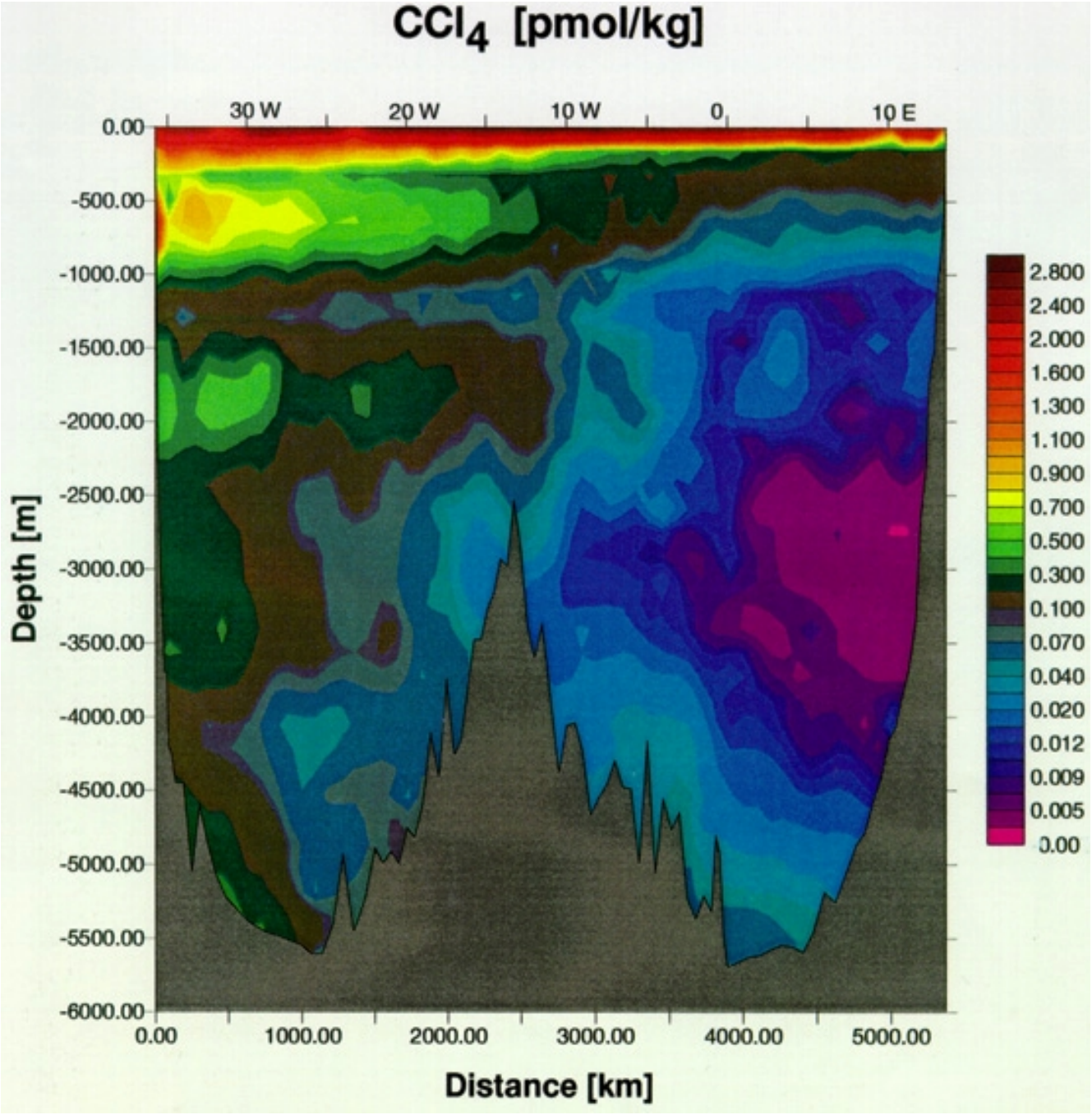

Fig. 12: As fig. 7, CCl_4

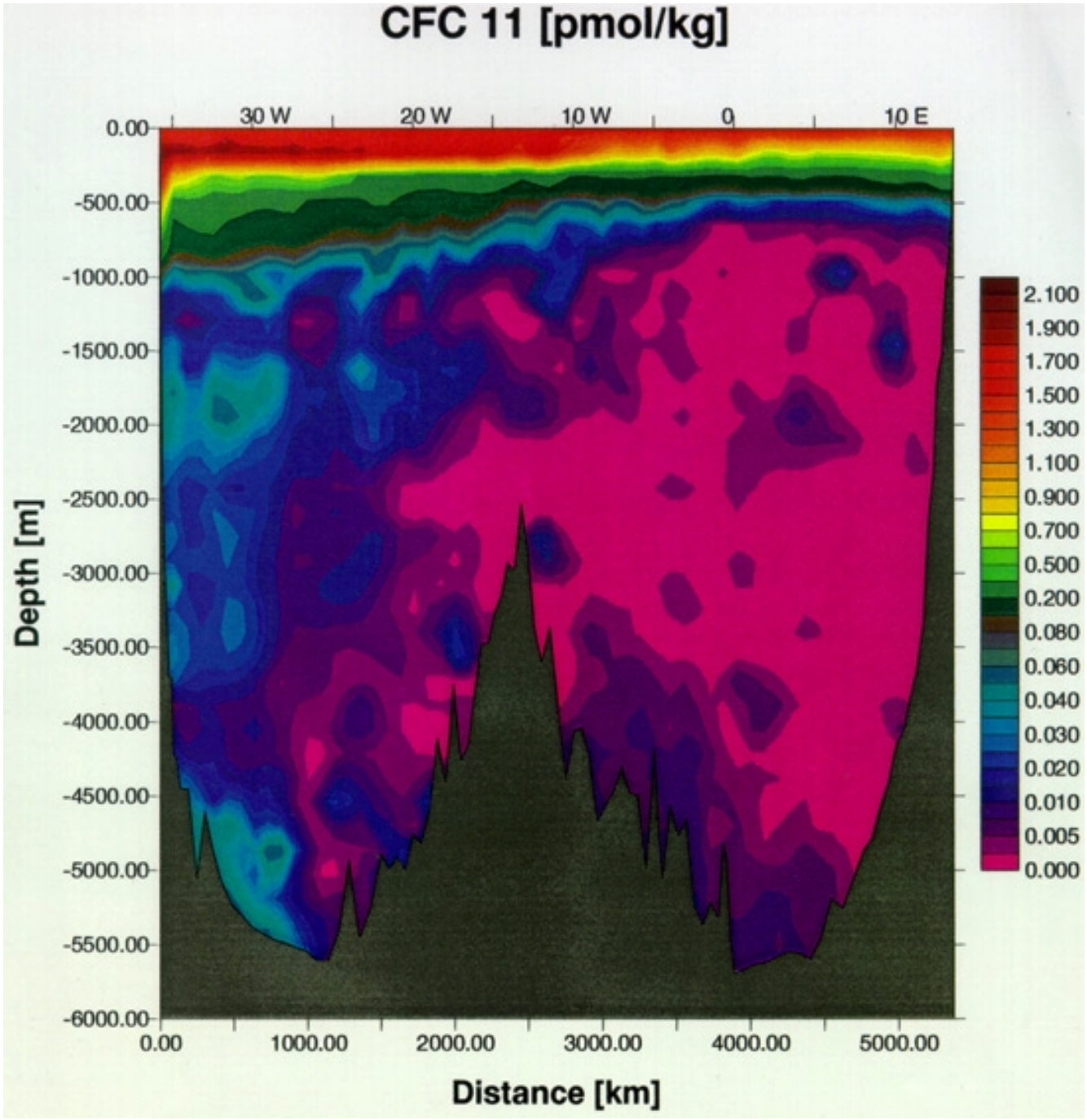

Fig. 13: As fig. 7, F-11

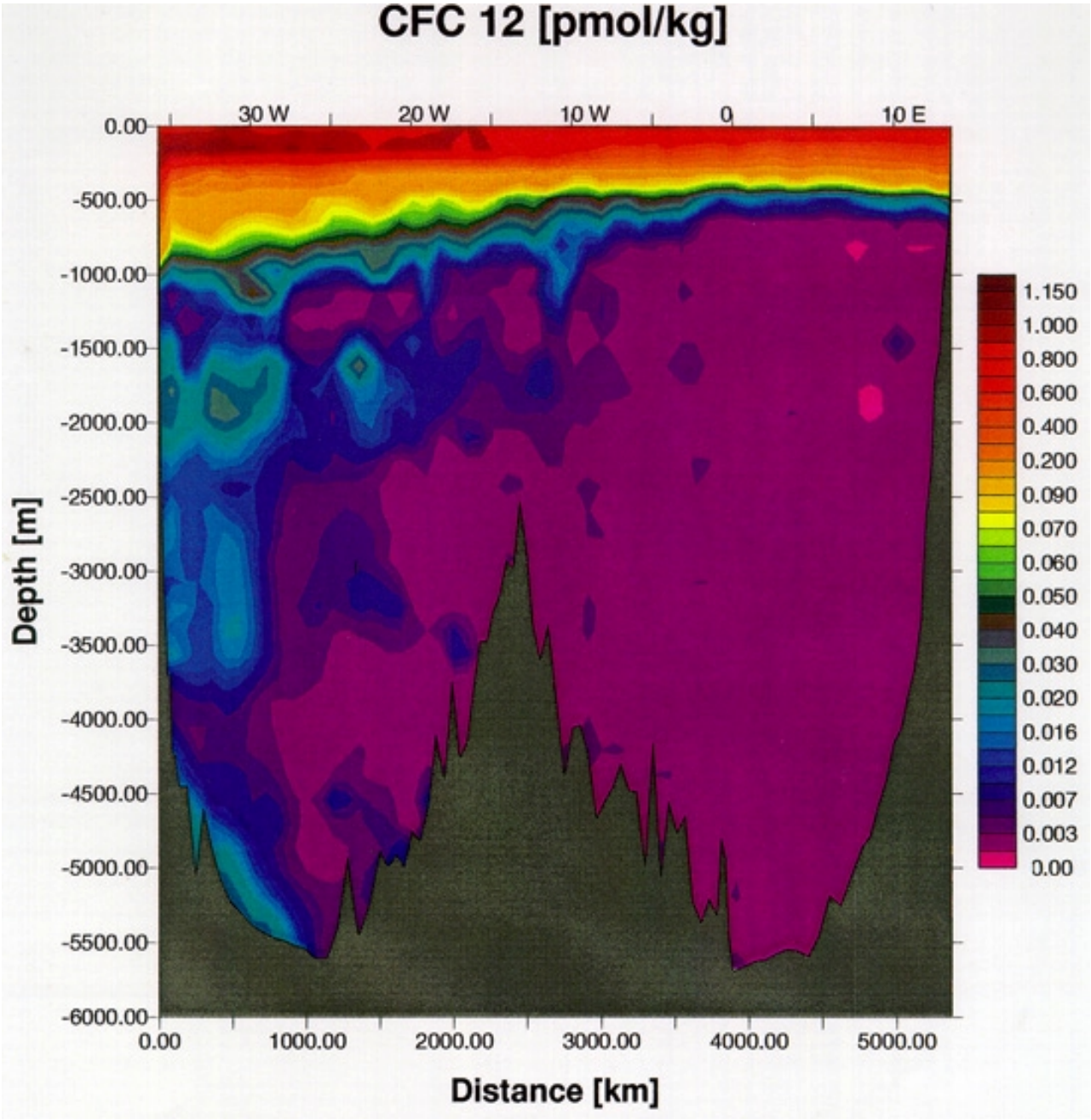

Fig. 14: As fig. 7, F-12

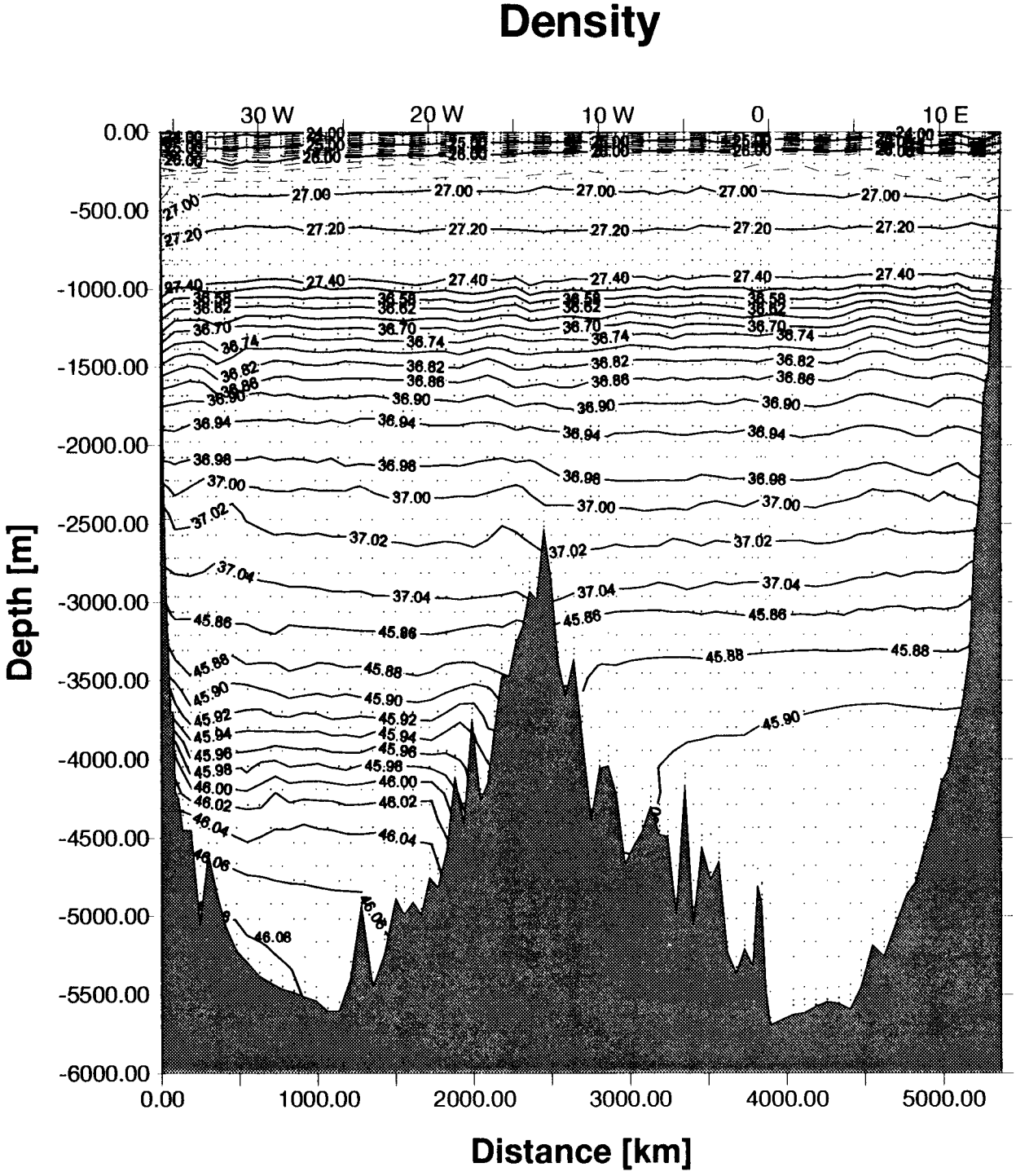

Fig. 15: As fig. 7, potential density referred to the surface until 1000 m depth, to 2000 dbar between 1000 and 3000 m depth, and to 4000 dbar for depths greater 3000 m. Dots indicate the more than 3700 spots where bottles were closed.

Below the SACW, two cores of waters of antarctic origin are identified: At 800 m depth the Antarctic Intermediate Water (AAIW) with its salinity minimum, and at 1000 m depth the Upper Circumpolar Deep Water (UCPDW) with its temperature minimum and silicate maximum. They can be traced throughout the section until the African shelf break. While these water masses origin from the south, note that, both, the tongues of the AAIW and of the UCPDW are cut by the above mentioned fronts in anthropogenic tracers F-11 and CCl_4 at about 5˚W which indicates their relatively weak renewal rates in the eastern basin as compared to that in the western basin.

Next, all three components of North Atlantic Deep Water (NADW) are identified: At 1300 m depth the core of the Upper North Atlantic Deep Water (UNADW) with its temperature maximum, at 1900 m the Mid North Atlantic Deep Water (MNADW) with its salinity maximum and silicate minimum, and at 3200 m the oxygen rich Lower North Atlantic Deep Water (LNADW). Note some lenses of NADW just east of the western boundary; they may indicate re-circulation cells discussed recently (De MADRON and WHEATHERLY, 1994). In the west, the CFC values are relatively low within the UNADW because of its 'old' components of Mediterranean origin. A maximum in CFCs is found in the MNADW, and they still have high values in the LNADW. Again, a front in CFC values separates the NADWs in the western from those of the eastern basin.

Lower Circumpolar Deep Water (LCPDW) is formed when Weddell Sea Deep Water mixes with Circumpolar Deep Water on its way north. Formerly denoted as Antarctic Bottom Water (AABW) (PETERSON and WHITWORTH, 1989), it carries low temperature and salinity bottom water along the western boundary northward. Because of its Weddell Sea compound, it is also marked by relatively high CFC values. A slight increase of the F-11 concentration at the western slope of the Mid-Atlantic Ridge seems to indicate a re-circulation cell of bottom water. LCPDW also was clearly distinguishable in the CO_2 parameters (not shown here).

Two further interesting result are found in the deep Angola Basin. First, we observe an increase of, both, CCl_4 and F-11 values at the bottom which is intensified at the western side of the basin. Thus there is evidence that the bottom water of the Angola Basin is ventilated by a western boundary current (WARREN and SPEER, 1991) which carries compounds of bottom waters that have been at the surface within the last 30 years. While other hydrographic and chemical parameters indicate a fairly homogenous water mass below 4000 m, F-11 and CCl_4 outline a structure that indicates a circulation and slow upwelling of bottom waters within the basin. Only very few samples measured at about 3000 m depth in the eastern part of the Angola Basin show CCl_4 concentrations below their detection limit.

The second interesting feature in the Angola Basin is observed at 4000 m depth on the continental break: A low oxygen and high silicate water mass with a small increase of CCl_4 and extremely slight increase only of F-11. Whereas in the CFCs the signal is confined to only very few samples just above the bottom, it is broader and therefore significant in oxygen and silicate. Maybe the idea of a Congo River turbidity plume is evident here (BENNEKOM and BERGER, 1984).

5.2 Deep Basin Experiment

5.2.1 Water Mass Distribution in the Subtropical South Atlantic
(O. Boebel, C. Schmid, W. Zenk)

The data base for this paragraph consists of two quasi-meridional hydrographic sections (Fig. 16) occupied between 21˚ and 39˚S during M 28/2. The longer section (Fig. 17) contains 21 CTD stations covering the east side of the Brazil Basin, crossing Hunter Channel, running right into the central Argentine Basin. The supplementing shorter section (Fig. 18), featuring 7 CTD stations, connects the southern end of the long section between the Subtropical Convergence at roughly 40˚S with the southern extend of Vema Channel. Thermosalinograph records also shown in Fig. 17 and 18, are reproduced without further corrections. Comparisons with near-surface CTD data revealed no systematic differences for temperature data. However, a significant shift of 0.038 ± 0.050 PSU between 35 salinity samples (taken during CTD stations) and the displayed continuous salinity record was determined. The shown surface salinity needs to be reduced by the calculated offset for future analyses.

CTD stations were taken (a) for a detailed investigation of the vertical structure and zonal flow of the Antarctic Intermediate Water (AAIW) at approximately 900 m depth and (b) for the determination of in situ density at float launch sites (see chapter 7.2.5). Due to ship time limitations both sections had to be compiled from CTD profiles not exceeding 1500 dbar. Only selected stations cover tile whole water column. Their complete data are processed in our θ/S-diagram (Fig. 19). Nominally all deep stations were taken with a sediment sampler as described in chapter 5.8.

Both CTD-sections are shown jointly with continuous thermosalinograph data and their belonging bottom profiles. Gaps in these data (DVS) were linearly interpolated, or in case of bathymetry eliminated by soundings from CTD stations (Profile 36-33, 32-16). Fig. 16 shows the track lines of the long (Profile 37-2) and the short section (Profile 37-43) embedded in the local bathymetry. Please note, station notation is given by CTD profile numbers. An equivalence Stat. No. vs Profile contains chapter 7.2.1. The central box in Fig. 46 contains CTD stations at Hunter Channel as displayed in Fig. 20 and described further down.

The most pronounced structure of both sections shown in Figs. 17 and 18, is given by the Subtropical Convergence at their common southern end (<-38˚ = > 38˚S). North of 38˚S thermosalinograph records with their strong fluctuations (horizontal interleaving) confirm the abrupt transition between the southern rim of the subtropical gyre of the South Atlantic at 38˚S and the northern extend of the Southern Ocean (see Fig. 18e). The deep reaching front at the convergence is most developed in the upper 500 dbar. Nevertheless, it can be traced down to the bottom of our sections (1500 dbar), though with reduced horizontal gradients. Sloping isopygnals associated with the frontal region, represent the dynamical signature of the eastward flowing South Atlantic Current (STRAMMA and PETERSON, 1990).

Farther north we identify the well-known variety of water masses in the subtropical South Atlantic: In the centre of the subtropical gyre, i.e., north of 28˚S, we find the characteristic shallow salinity maximum at approximately 60 dbar. The next deeper extremum on the θ/S-diagram (Fig. 19) occurs below the main thermocline. It is marked by the salinity minimum of the Antarctic Intermediate Water (AAIW). The Smin core at approximately $\sigma\theta$ = 27.18 or $\sigma 1$ = 31.75 kg m3 drops from < 600 dbar at the Subtropical Convergence to almost 1000 dbar between 36' and 37˚S, from where on we observe a slow decrease of the pressure level to 700 dbar at the northern end of the long section. The core salinity is lowest in the frontal region (< 34.2 PSU). It increases up to 34.4 PSU towards the north. Temperatures range from 3-4˚C in the south , where 3.5-4˚C are more characteristic for the northern end. In terms of potential density Intermediate Water ranges from 27.00 < $\sigma\theta$ < 7.35 kg m3 or 31.50 < $\sigma 1$ < 31.90 kg m3.

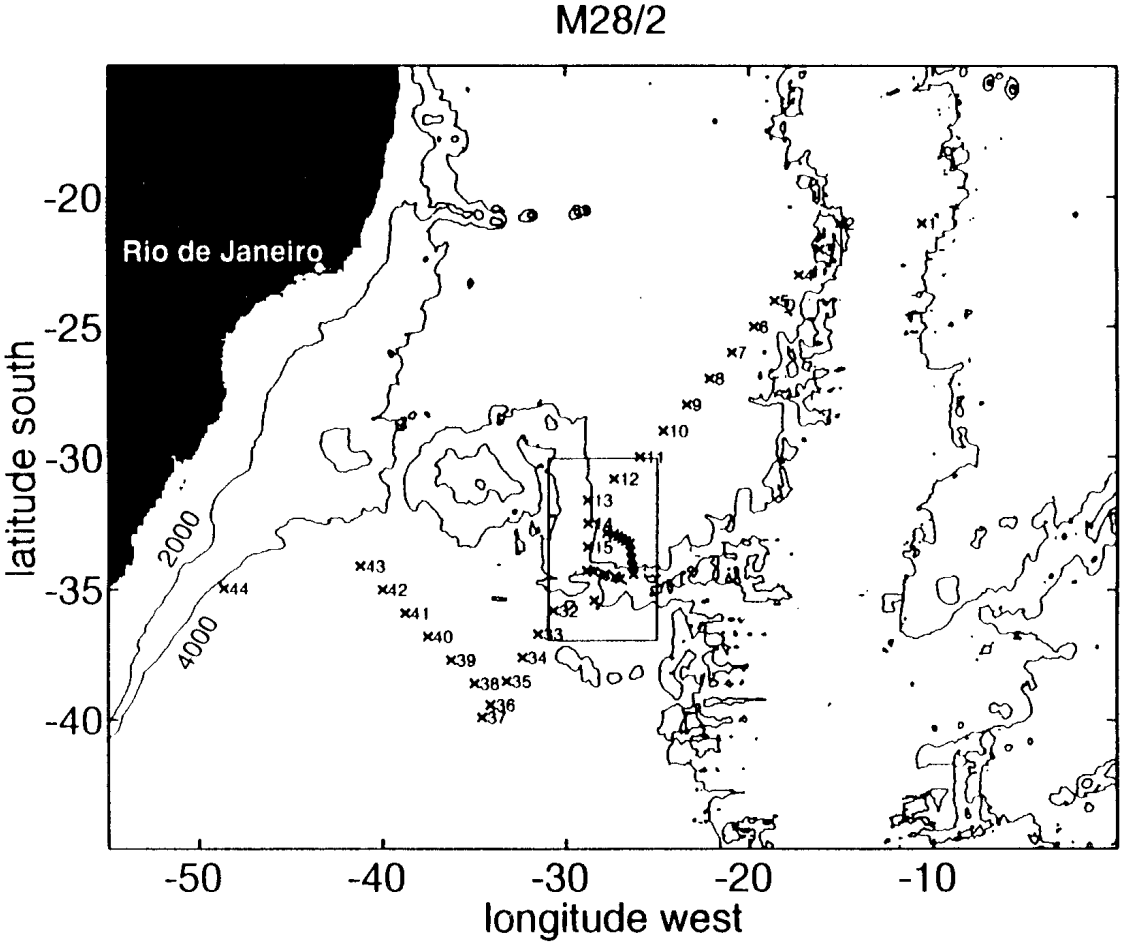

Fig. 16: During M 28/2 METEOR occupied two quasi-meridional hydrographic sections in the Brazil Basin and in the Argentine Basin. Numbers indicate CTD profiles, corresponding station numbers are listed in chapter 7.2.1. Most of the CTD stations cover only the upper 1500 dbar, sufficiently deep enough for the investigation of the Antarctic Intermediate Water. Stations in the box were taken in the Hunter Channel region as described in chapter 5.2.2.

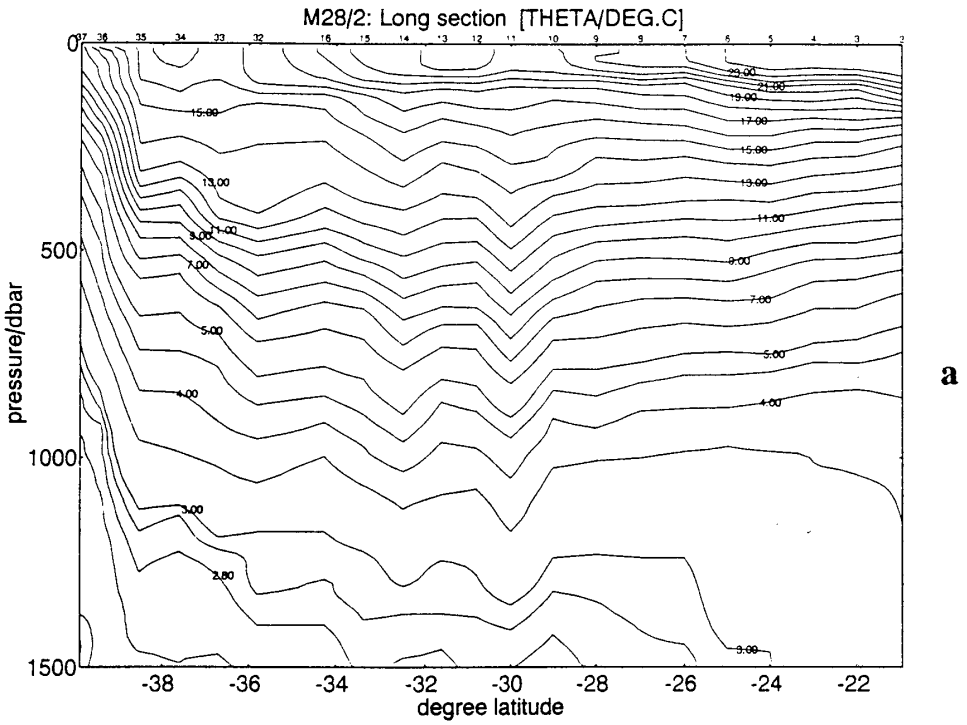

a

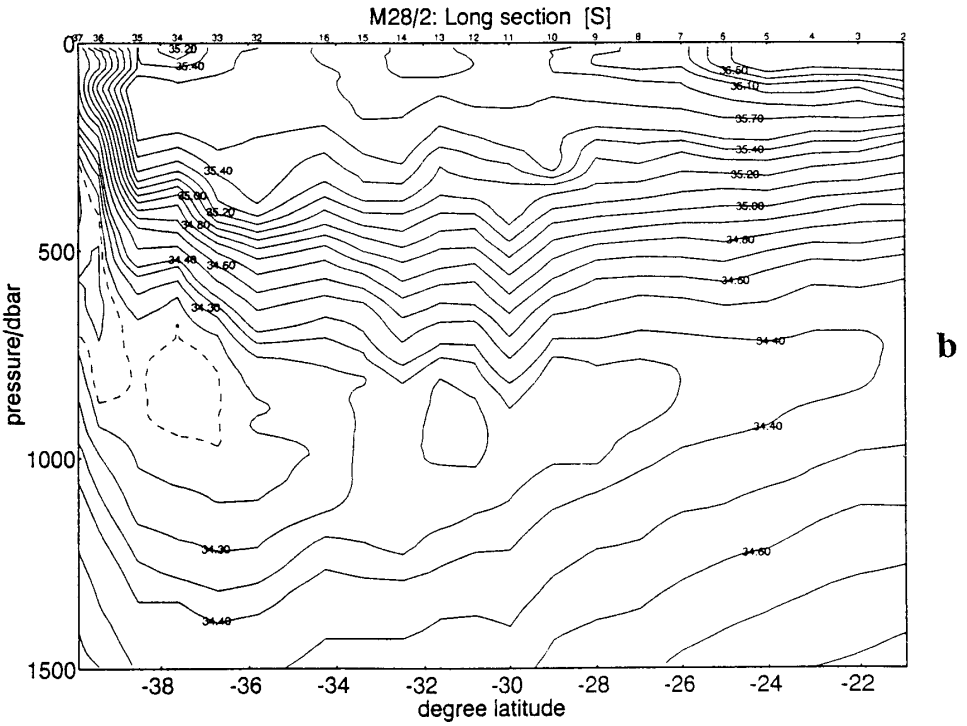

b

Fig. 17a-b: CTD-sections ($p \leq 1500$ dbar) through the southern subtropical gyre of the western South Atlantic. The long section (A2) was taken en route to Hunter Channel and farther to the Subtropical Convergence.

a) Potential temperature (ºC),
b) Salinity (PSU),

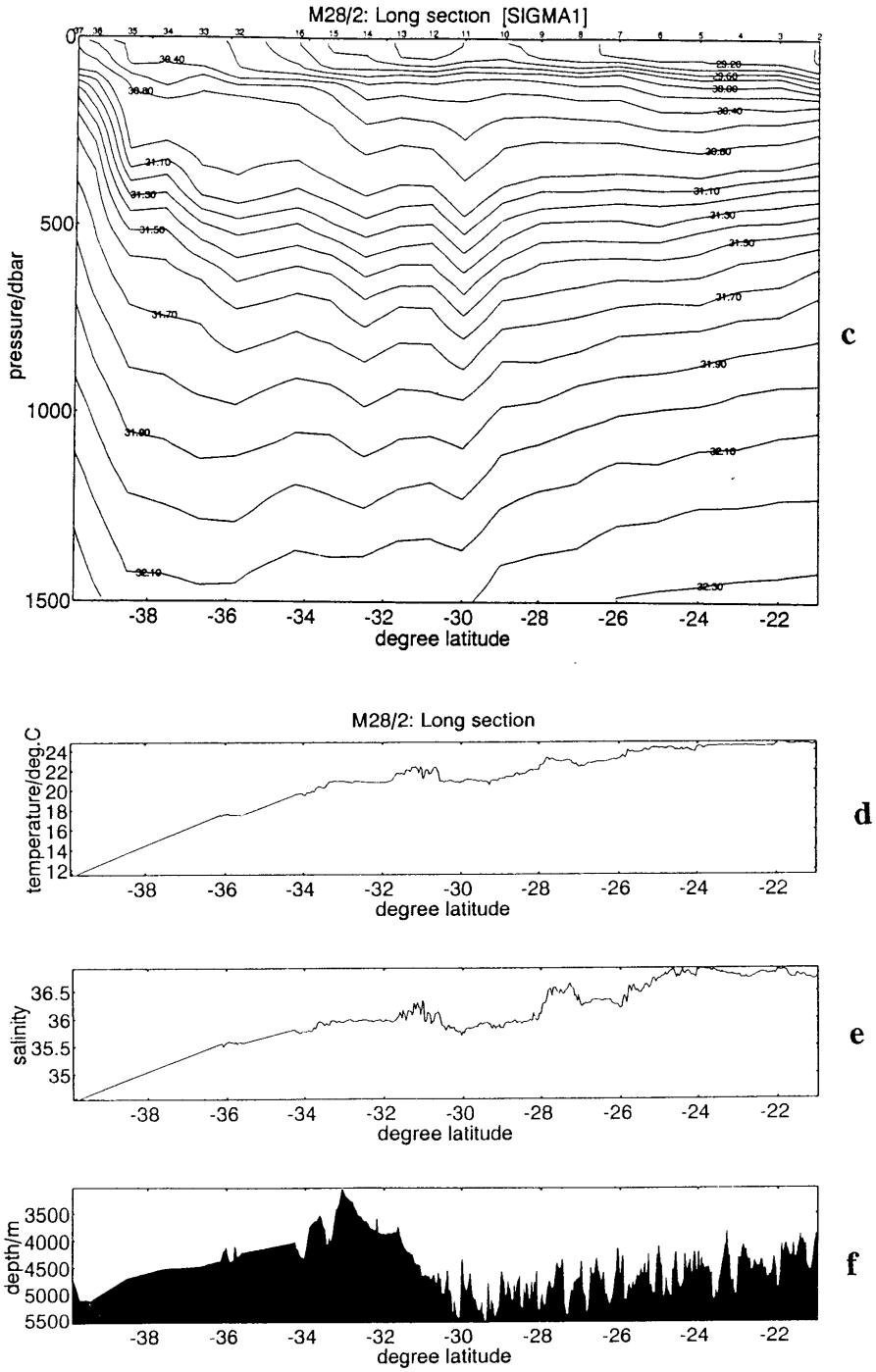

Fig. 17c-f: CTD-sections ($p \leq 1500$ dbar) through the southern subtropical gyre of the western South Atlantic. The long section (A2) was taken en route to Hunter Channel and farther to the Subtropical Convergence.

c) Density σ_1 (kg m^{-3}),
d) thermosalinograph records of temperature,
e) uncorrected salinity,
f) bathymetry recorded simultaneously by METEOR.

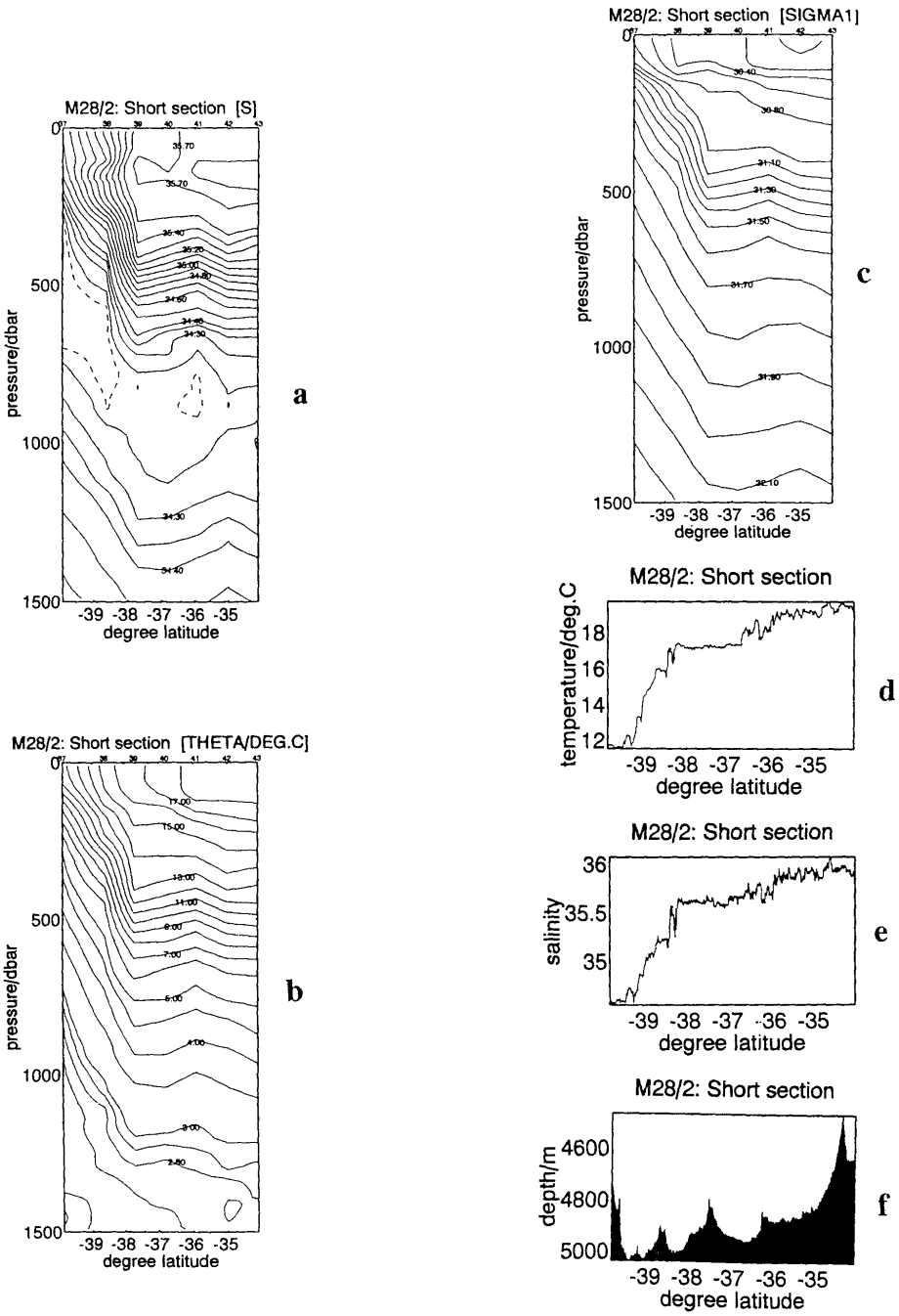

Fig. 18a-f: CTD-sections ($p \leq 1500$ dbar) through the southern subtropical gyre of the western South Atlantic. The short section (A3) was taken on the north-westbound track towards the Vema Channel extention.

a) Potential temperature (°C),
b) Salinity (PSU),
c) Density σ_1 (kg m^{-3}),
d) thermosalinograph records of temperature,
e) uncorrected salinity,
f) bathymetry recorded simultaneously by METEOR.

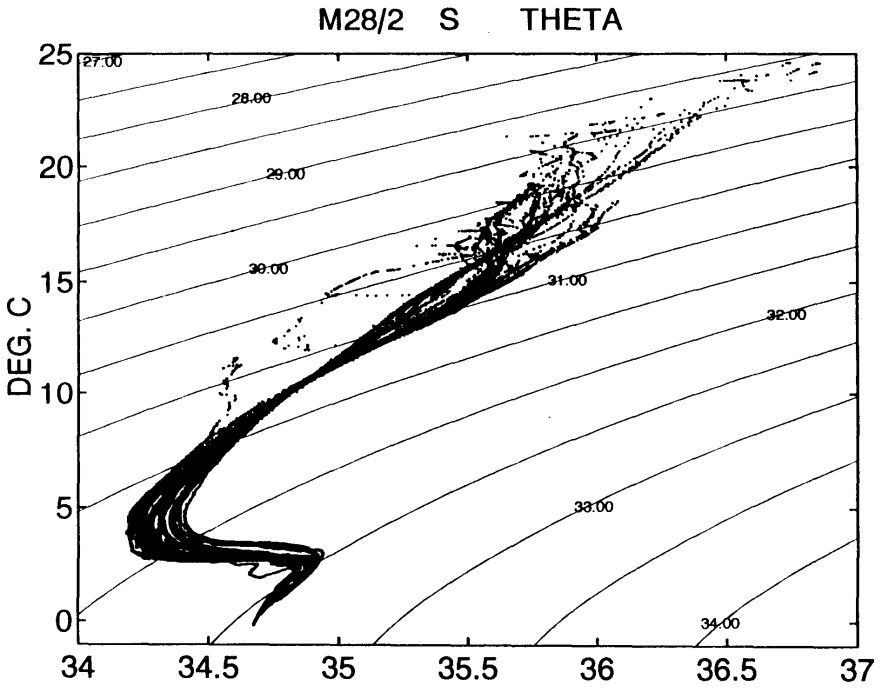

Fig. 19: Potential temperature (ºC) vs salinity (PSU) from all deep stations of M 28/2 (chapter 7.2.1). Lines of equal densities (kg m^{-3}) are referred to 1000 dbar (σ_1).

Three different low temperature gradient regions were observed. The first at 36˚S reaches down to 400 dbar at 14˚C. It resembles Maderia Mode Water (SIEDLER et al., 1987) found in the eastern North Atlantic. This thermocline mode water is formed at the northern boundary of the subtropical gyre by deep wintertime convection and is degenerated during the course of the year. Deeper down at ~38˚S (Fig. 17 and 18) we identify remainders of the upper Circumpolar Water (2.7˚C, 34.4 PSU) beneath the deep core of Antarctic Intermediate Water. Unfortunately no oxygen data for further identification of this water mass are available from M 28/2. The third and most extended thermostat (~3.4˚C) layer is found between 21˚ and 26˚S (Fig. 17a) at pressures >1000 dbar. The concurrent increase of salinity from 34.40 to > 34.80 PSU indicates a mixture of upper Circumpolar Water with North Atlantic Deep Water (NADW). While vertical mixing in this water mass cannot have much effect on the temperature since the vertical temperature gradient is small, strong fluxes of salinity presumably exist between layers (K. SPEER in SIEDLER and ZENK, 1992). Finally we point out two submesoscale pygnocline depressions (Profiles 11, 14) and/or three domes (Profiles 12, 13, 16, 34) which cannot be interpreted by the available CTD data (Fig. 17c) alone. Perhaps RAFOS floats launched every degree of latitude concurrently with CTD stations along both sections, will allow a conclusive analysis of these dynamical signals. Float deployment locations are summarized in chapter 7.2.5.

5.2.2 Water Exchange through Hunter Channel

(T.J. Müller, J. Pätzold, G. Siedler, C. Schmid, W. Zenk)

Under the auspices of the Deep Basin Experiment of WOCE a large fraction of observations has been focused on the bottom water exchange across the Rio Grande Ridge. During two METEOR cruises (M 15 and M 22) we concentrated our efforts in close cooperation with the Woods Hole Oceanographic Institution primarily on the inflow of Weddell Sea Deep Water and of Antarctic Bottom Water (AABW) through Vema Channel (ZENK et al., 1993). Cruise M 28/2 put special emphasis on the recovery of a moored current meter at the Hunter Channel, deployed in December 1992. Logistical constrains (see chapter 4.2) allowed a modest extent of bathymetric work started jointly with the University of Bremen and the Alfred-Wegener-Institut, Bremerhaven, during M 15 in 1991 (K. HEIDLAND in SIEDLER and ZENK, 1992). Fig. 20 shows the course of the 4000 m isobath according to a digitized chart of the South Atlantic (NGCD, 1993) together with CTD stations and mooring locations (H1-H6, R). Fig. 21 depicts a partial view of the sill region in the central Hunter Channel prepared from all available METEOR Hydrosweep data (M 15, M 22, M 28).

Hydrography

As in Fig. 16 CTD stations in Fig. 20 are labeled by their profile numbers (see chapter 7.2.1). Fig. 22 and 23 display two hydrographic sections of deep and bottom water ($p > 3000$ dbar) distribution at Hunter Channel. The quasi-zonal section (Fig. 22) was obtained as a byproduct of the work on the moored current meter array. Unfortunately ship time did not allow for a higher spatial resolution of this section. Nevertheless, previous results such as a significant through flow of Antarctic Bottom Water (SPEER et al., 1992) are impressively confirmed. As in the survey in February 1991 (M 15) we recognize a queezing of property lines in the east near the bottom of Fig. 22. Geostrophic speeds of 0 (+1 cm s^{-1}) relative to the depth of the 2°C (potential) temperature isoline were calculated. Furthermore it is worth mentioning that in 1991 the lowest temperature above the sill at the same location was approximately 0.2°C higher. A similar trend towards higher bottom temperature at the entrance of the Brazil Basin was observed already between Lower Santos Plateau and Vema Channel farther to the west of Hunter Channel two years earlier (ZENK and HOGG, subm.).

The second deep hydrographic section (Fig. 23) consists of a nearly meridional (Profile 31-26) and a zonal part (Profile 26-22) north, respectively, east of the inner Hunter Channel. It was planned according to the known bottom hydrography (Fig. 20), focussing on the region where the through flow of the bottom water still appears to be topographically constrained, but where station spacing (nominally 25 km) allows for sufficient resolution of transport calculations.

Fig. 23 contains the actual bottom contours measured during M 28/2. Unfortunately major deficits in station coverage occurred afterwards such as the deep channels (or blind troughs ?) between Profile 31-30 and 25-26. Unfavourable weather conditions did not allow us to fill these gaps during the remaining ship time. Apparently the majority of

bottom water leaves the Hunter region towards the east between Profile 25-24. Only minor contributions at more intermediate depths (< 4000 m) are advected northward through Profile 27-26, which at least partially seems to recirculate between Profile 28-27. During M 28/2 we have observed no significant deep northward flow west of Profile 29. Such a flow has previously been suggested as part of an anticyclonic circulation around Rio Grande Rise (see Fig. 9 in SPEER and ZENK, 1993). Actually mooring R (Fig. 20) at Profile 13 (Stat. 306) had been launched in December 1993 with the intention to monitor this interior western boundary current. Results from moored current meters are shown in the following paragraph.

Moored Current Meter Array

Between 1991 and 1992 (M 15, M 22) an array of current meters had monitored deep advection along the western segment of the southern boundary of the Brazil Basin. A joint data report by the Woods Hole Oceanographic Institution and the Institut für Meereskunde Kiel summarizes the obtained results (TARBELL et al., 1994). After the recovery of this large array parts of it were re-moored farther to the east in the Hunter Channel and on the Rio Grande Ridge (Fig 24). Data presented here are complimentary to the former data set from the Vema Channel and the other more westerly regions. A total of 25 Aanderaa Current Meters, two 200 m long thermistor chains and an Acoustic Doppler Current Meter operated in seven moorings (Code H1-6 for Hunter Channel, R for Rio Grande Rise).

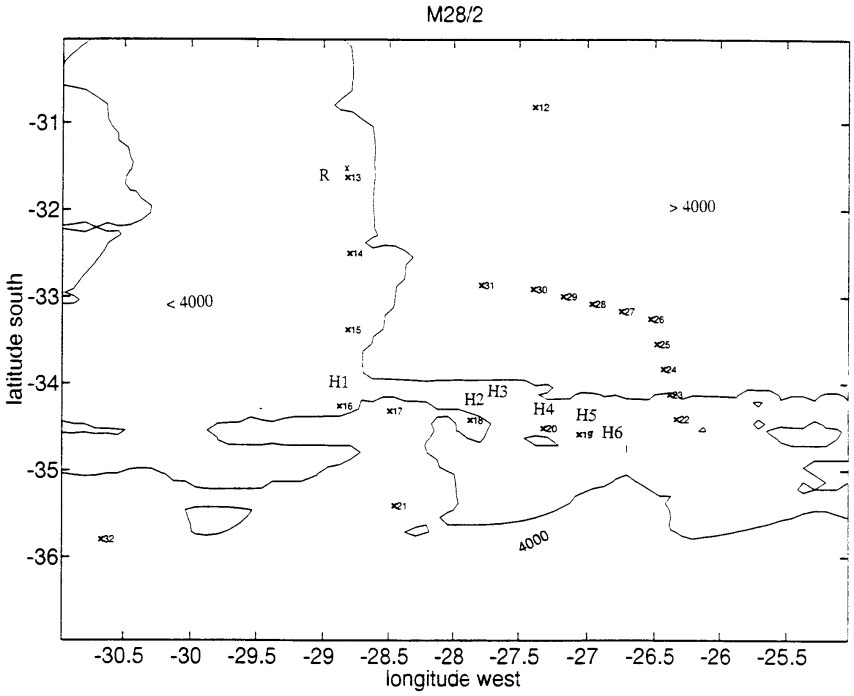

Fig. 20: Zoomed distributions of stations from the Hunter Channel region in the center box of Fig. 16. Isolines represent the 4000 m line as available in digital form (NGDC, 1993). Crosses denote deep CTD stations labeled by their profile numbers. Station numbers are listed in chapter 7.2.1. H1-6 stands for a moored current meter array across Hunter Channel. Mooring R was situated in the eastern flank of the Rio Grande Ridge.

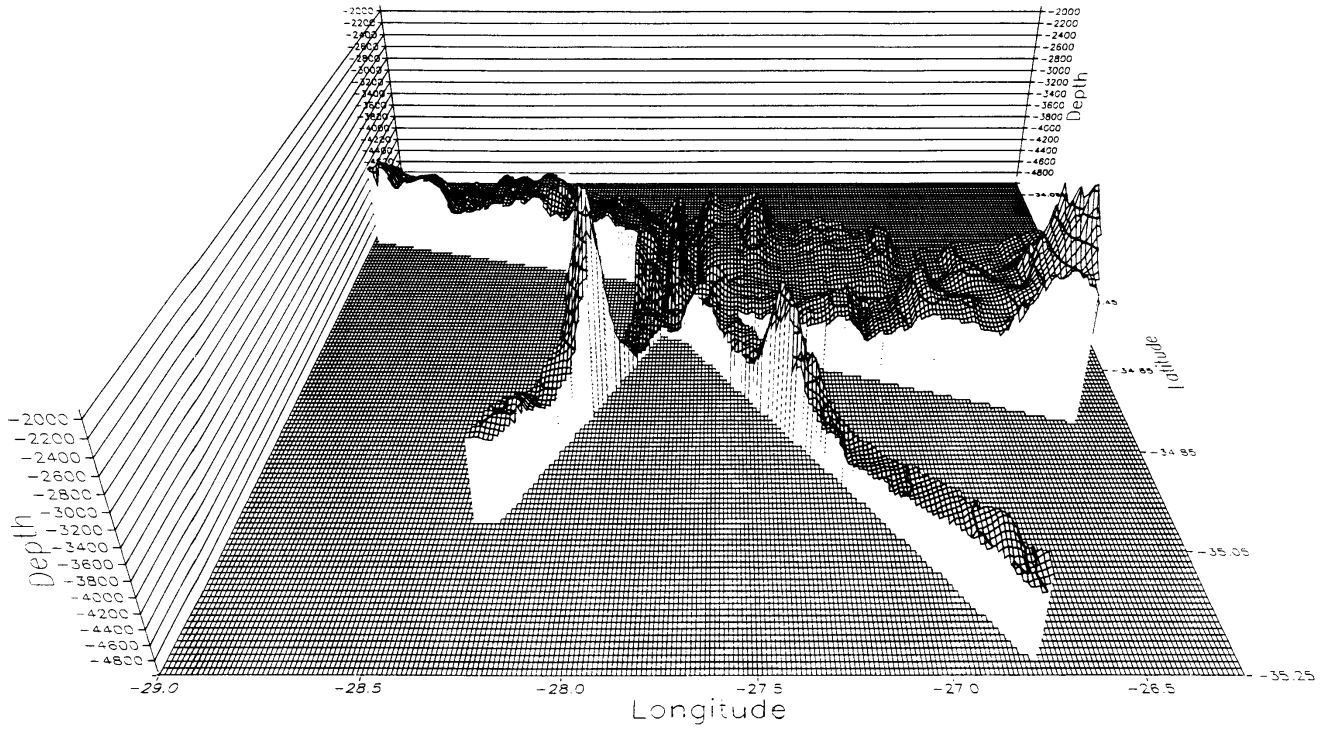

Fig. 21: 3-dimensional representation of the Hunter Channel. The synthesis of the bathymetry was compiled according to three METEOR surveys (M 15, M 22, M 28) by Hydrosweep in cooperation with the University of Bremen and the Alfred-Wegener-Institut, Bremerhaven (SIEDLER and ZENK, 1992).

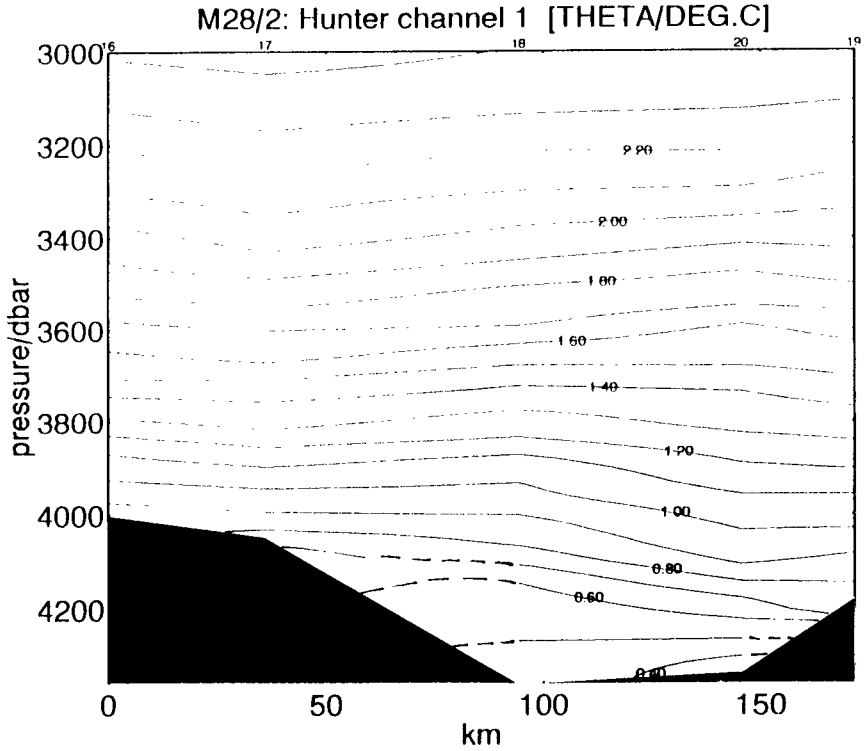

Fig. 22: a) Potential temperature (ºC)

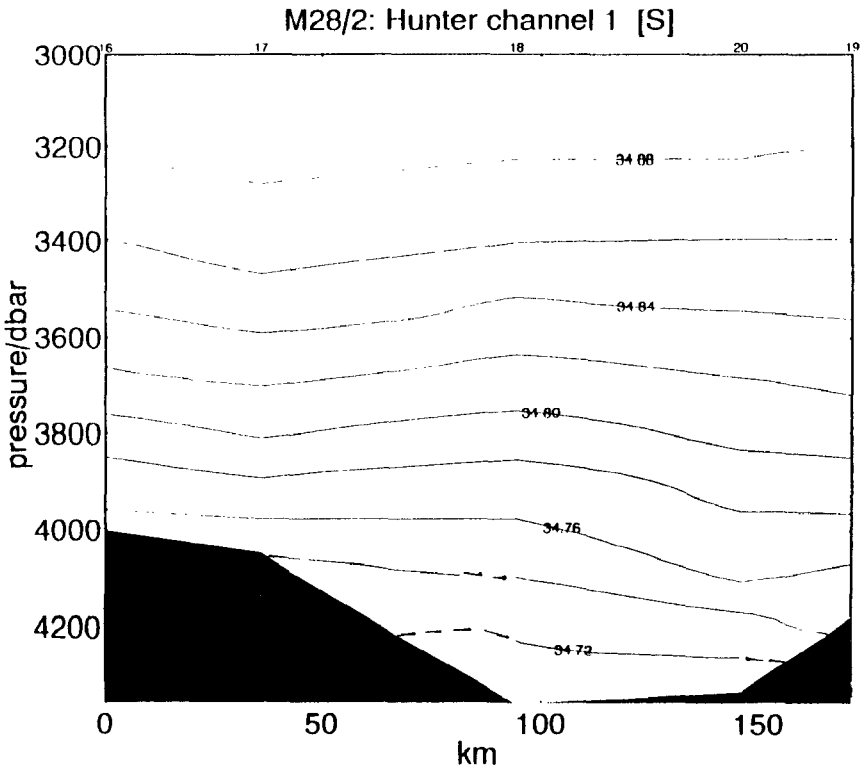

Fig. 22: b) Salinity (PSU)

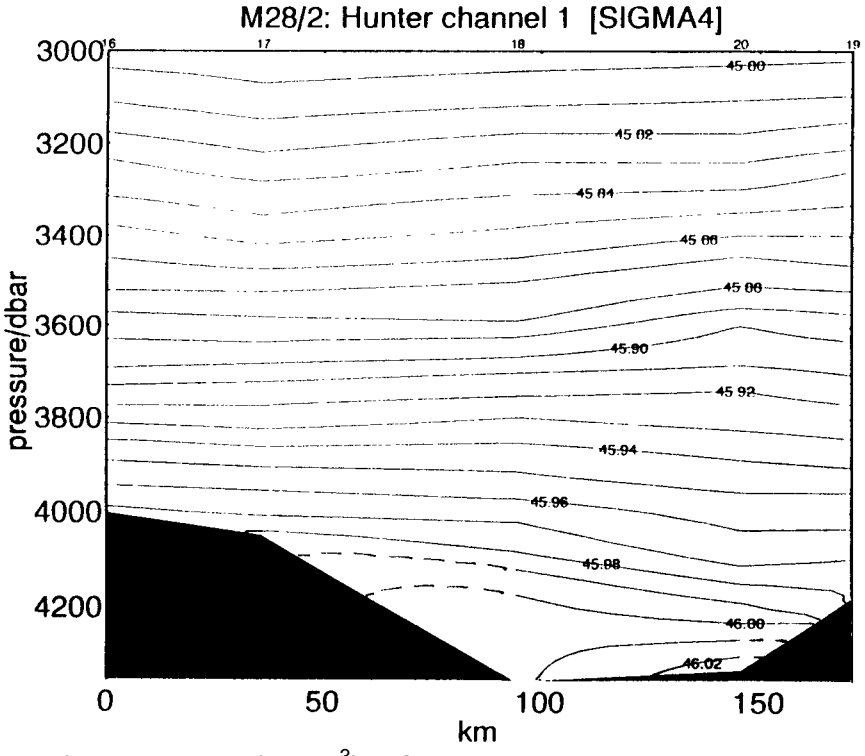

Fig. 22: c) Density σ_4 (kg m^{-3}) referred to 4000 dbar

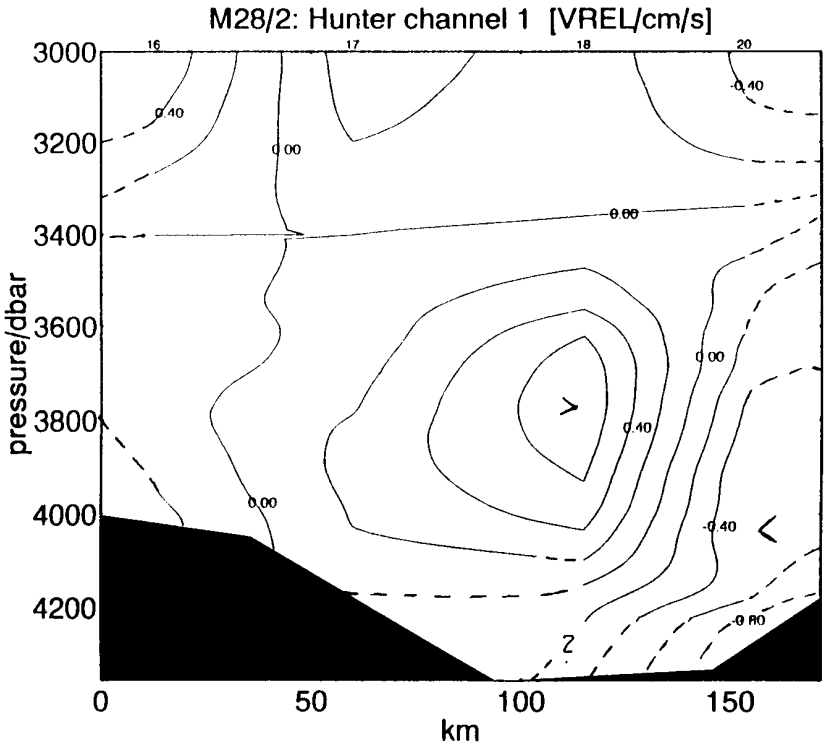

Fig. 22a-d: Deep CTD-section (p ≥ 3000 dbar) of the outflow of Antarctic Bottom Water through the Hunter Channel. This section 1 was obtained during the recovery work on mooring sites H1-6. Due to DVS failure no detailed bathmetry between stations is available. Note the pintching of property lines on the lower right side. These compressions represent the dynamics of the bottom water flow entering the Brazil Basin.

d) Geostrophic current speed (cm/s) relative to the depth of the 2ºC potential temperature isoline. Negative speeds (of Antarctic Bottom Water) are directed towards the North.

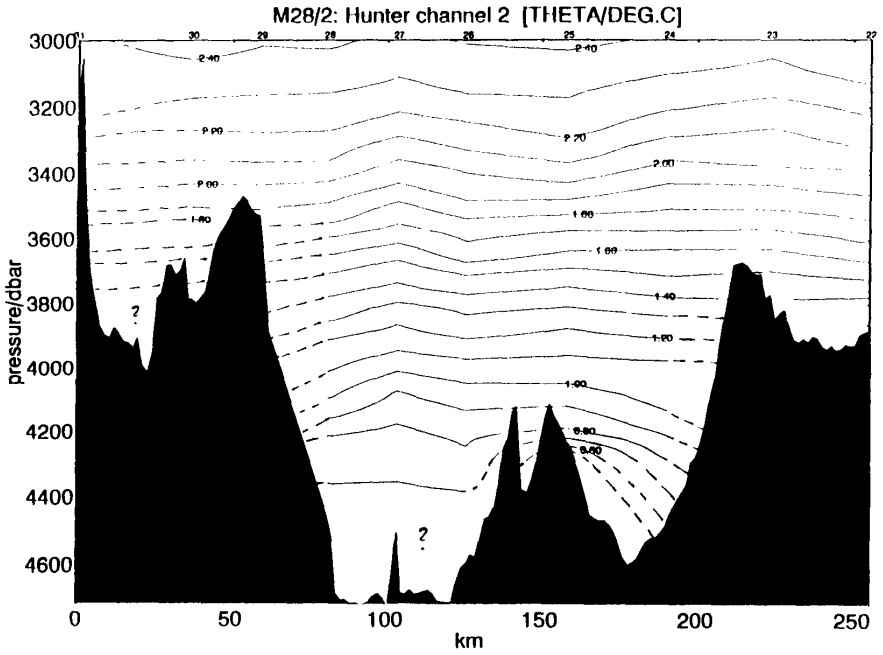

Fig. 23: a) Potential temperature (°C)

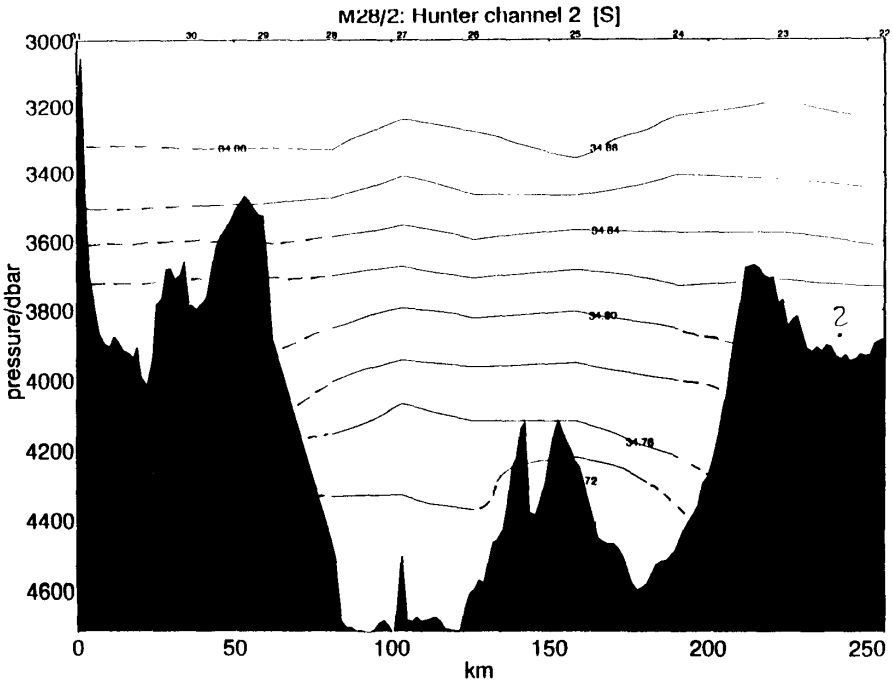

Fig. 23: b) Salinity (PSU)

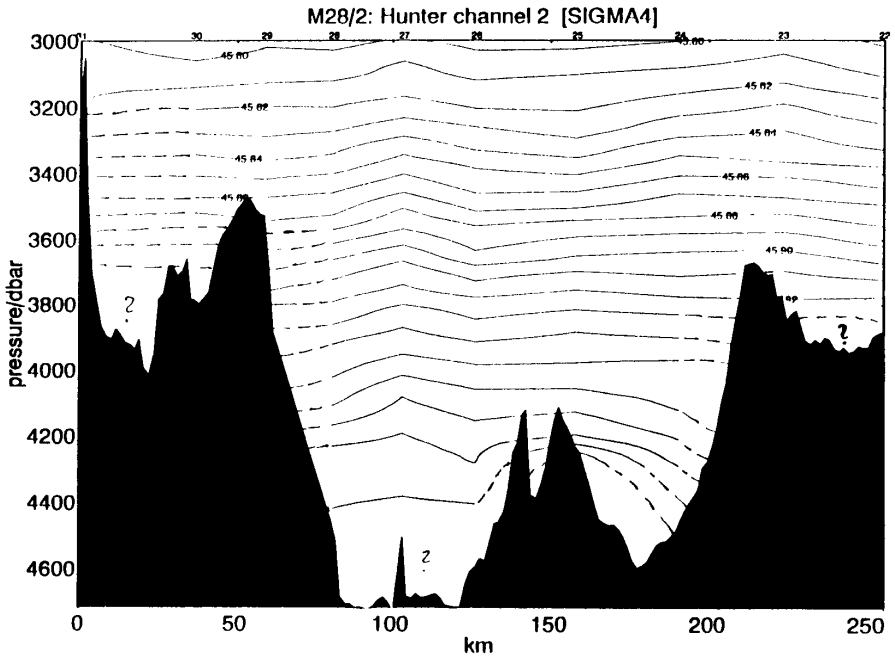

Fig. 23: c) Density σ_4 (kg m^{-3}) referred to 4000 dbar

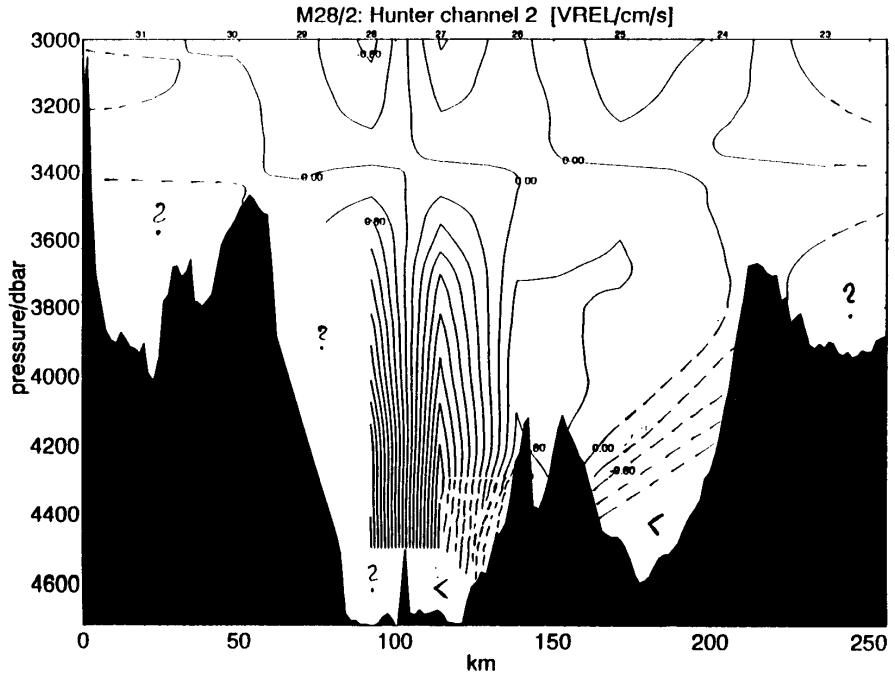

Fig. 23a-d: Deep CTD-section (p ≥ 3000 dbar) of the outflow of Antarctic Bottom Water just north of the Hunter Channel. This section 2 was plotted from profiles 31-22. Bathmetry between stations was measured by METEOR. The main outflow across the Hunter Sill into the Brazil Basin was obtained between profiles 27, 26 and 25, 24.

d) Geostrophic current speed (cm/s) relative to the depth of the 2ºC potential temperature isoline. Negative speeds (of Antarctic Bottom Water) are directed towards the North (Profiles 31-26) or towards the East (Profiles 26-22).

Chapter 7.2.4 contains all mooring durations and locations. The latter are also displayed in Figs. 20 and 21. Locations of related CTD stations from the deployment (M 22) and the recovery cruises (M 28) are summarized in Table 6. The table contains three different estimated depths which must be explained by the rough bottom topography, characteristic for the Hunter Channel (see Fig. 22). In selected cases we therefore give two numbers for the vertical position of our instruments: Clearance from bottom and instrument depth. The more reliable vertical distance relative to the surface or to the bottom is labeled by bold numbers.

Data from moored instruments were processed in the usual fashion (MOLLER, 1981). Problems occurred with larger numbers of Aanderaa Current Meters (RCM8): Both vector averaged components in slow current regimes appeared to have a stronger uncorrelated tendency towards zero. In order to conserve a rough estimate of the recorded direction, zeros in calculated speed series were artificially set to 1 cm s^{-1}, the threshold speed of the instruments. Besides other operational details, Table 7 displays the percentage of changed threshold values of the Aanderaa Current Meters. Since we were forced to shift identical instruments from the Vema to the Hunter regime during METEOR cruise M 22/4, time did not allow for a detailed ship borne analysis of the obtained data sets. Unfortunately this did not prevent us from running into problems we had encountered before with vector averaging Aanderaa Current Meters. (TARBELL et al., 1994).

The data from the moored Acoustic Doppler Current Meter (ADCP) in H6 were downloaded from the instrument to a personal computer aboard METEOR. These binary data later were transferred to the VAX of the Institut für Meereskunde computer centre in Kiel, where they were converted into time series of MK4 and ASCII coded vertical current profiles. The processing of auxiliary parameters like pitch, roll, heading and instrument depth followed. The latter quantity is displayed in Figs. 25-54. It represents a pseudo-pressure time series inferred from the strongest bin echo of the ADCP. A detail comparison of the upper real pressure record with the calculated depths reveals an excellent agreement between both methods (VIESBEK and FISCHER, 1995).

All thermistor chain data from H4 and H5 in Fig. 37 and 39 were adjusted to the available CTD profiles. Since these moored instruments stopped due to a lack of data storage capabilities earlier then the adjacent Aanderaa Current Meters, their temperature time series were used as transfer standards for the recovery calibration checks of the thermistor chains. The biggest problem with this calibration fine tuning appeared to be the determination of equal observation levels of the thermistor chains and the CTD profiles. As is shown in Table 6 and Fig. 21 the Hunter Channel is full of strong gradients in the bottom topography. A pre-cruise laboratory calibration of both thermistor chains did not deliver accuracies desirable and necessary for abyssal applications.

The complete set of time series of all available Aanderaa Current Meters together with selected ADCP data (see overview in Fig. 55) are displayed in Figs. 24-54. With expectation of the displayed pressure and pseudo-pressure filtered, daily averaged means are shown. All progressive vector diagrams from the H-mooring are shown in not more then two different scales. Thermistor chain data were shifted by -0.2˚C, referenced to the upper sensor.

Tab. 6: Moorings with corresponding CTD stations during launch (M 22) and recovery cruises (M 28).

Mooring		**M22**					**M28**			
		December 1992					**May 1994**			
		Nearest CTD			**Launch**	**Estim.**	**Recovery**	**Nearest CTD**		
ID		**Station #**	**Profile #**	**Depth (m)**	**Station #**	**Depth (m)**	**Station #**	**Station #**	**Profile #**	**Depth (m)**
Hunter Channel										
353	H1	603	46	4031	602	4112	309	309	16	4115
354	H2	-	-	-	604	4292	313	313	18	4390
355	H3	-	-	-	605	(4436)	312	-	-	-
356	H4	608	48	4319	606	4336	318	318	20	4370
357	H5	607	47	4301	607	(4836)[2)]	316	316	19	4235
358	H6	609	49	4326	609	4303	315	(325	24	4530)[3)]
Rio Grande Rise										
363	R	612	50	3806	612	3719	306	306	13	3780

Remarks:
( ) Questionable data
1) Rough estimate. For details see cruise report M 22 by SIEDLER et al. (1993)
2) According to bridge log, log sheet of mooring group shows 4485 m.
- no CTD data available
3) Station downstream of Hunter array in core of bottom water

Tab. 7: Performance of moorings in Hunter Channel (H1-6) and on Rio Grande Rise (R). RCM_ = Aanderaa Current Meter, V = current vector, T = thermistor, MAFOS = sound recorder, ADCP = Acoustic Doppler Current Profiler.

Mooring #	ID	Instrument Typ	Serial #	Instr. Depth (m)	Clearence from Bottom (m)	Max. Cycles	k %	Notes
353101	H1	RCM8/VTP	8412	175		6380	0	
353102	H1	MAFOS	10	875		-	-	no data
353103	H1	RCM8/VT	8295	925		-	-	no data
353104	H1	RCM8/VT	9730	2025		6380	38.9	
353105	H1	RCM8/VT	10077	3125		6380	36.8	
353106	H1	RCM8/VT	6159	3830		6380	49.5	
353107	H1	RCM8/VT	6160	4105		6380	47.1	
354101	H2	RCM5/VTC	8365	4000		6382	32.4	
354102	H2	RCM5/VT	7624	4335		6382	16.1	
355101	H3	RCM8/VTP	9323	905		6376	20.4	Pres = no data
355102	H3	RCM8/VT	10502	2005		6376	20.3	
355103	H3	RCM8/VT	10504	3155		6376	23.7	
355104	H3	RCM5/VT	8575	4310		6304	-	Dir = no data
355105	H3	RCM5/VT	4562	4530		-	-	no data
356101	H4	RCM5/VT	4354	4100		6380	13.8	
356102	H4	Aa Recorder	1293	4102-		5180	-	
		Th Chain	1259	4302				
356103	H4	RCM5/VT	8411	4315		-	-	no data
357101	H5	RCM8/VT	9832		252	6367	13.1	
357102	H5	Aa Recorder	1294		250-50	5216	-	
		Th Chain	1960					
357103	H5	RCM8/VT	9728		15	6367	8.9	
358101	H6	ADCP	389	(4-147)		5818	-	
358102	H6	RCM8/VTC	9732	900		6357	38.5	
358103	H6	RCM8/VTC	10663	2000		6357	75.6	
358104	H6	RCM8/VTC	9313	3100		6357	53.6	
358105	H6	RCM5/VT	4563	3980		6357	-	Temp only
358106	H6	RCM5/VT	7927	4310		6357	55.0	
363101	R	RCM8/VTP	10501	3485		6308	8.2	
363102	R	RCM8/VTC	10664	3705		6308	14.2	

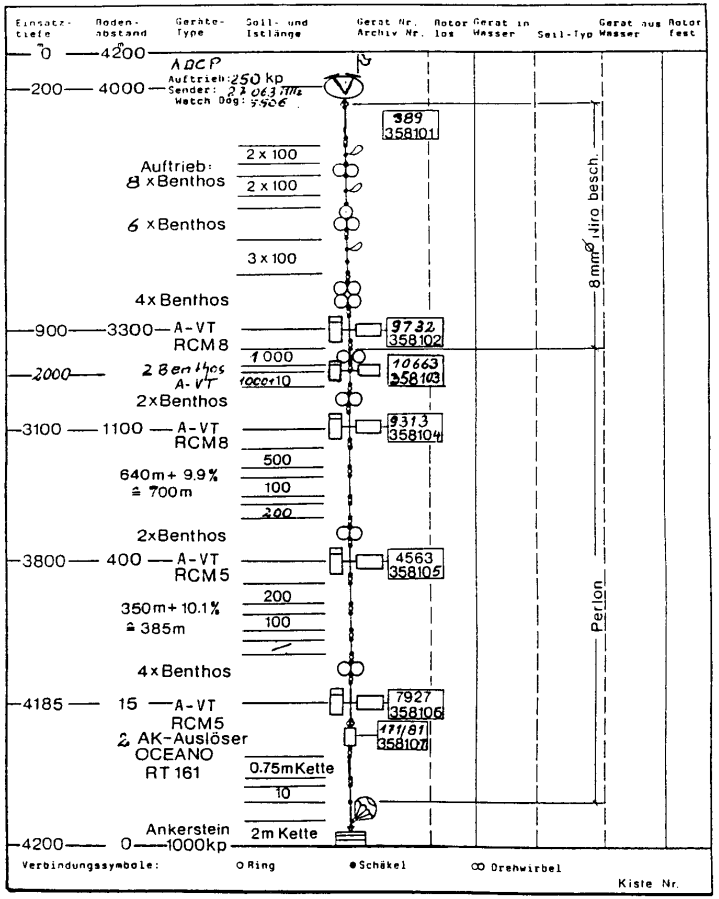

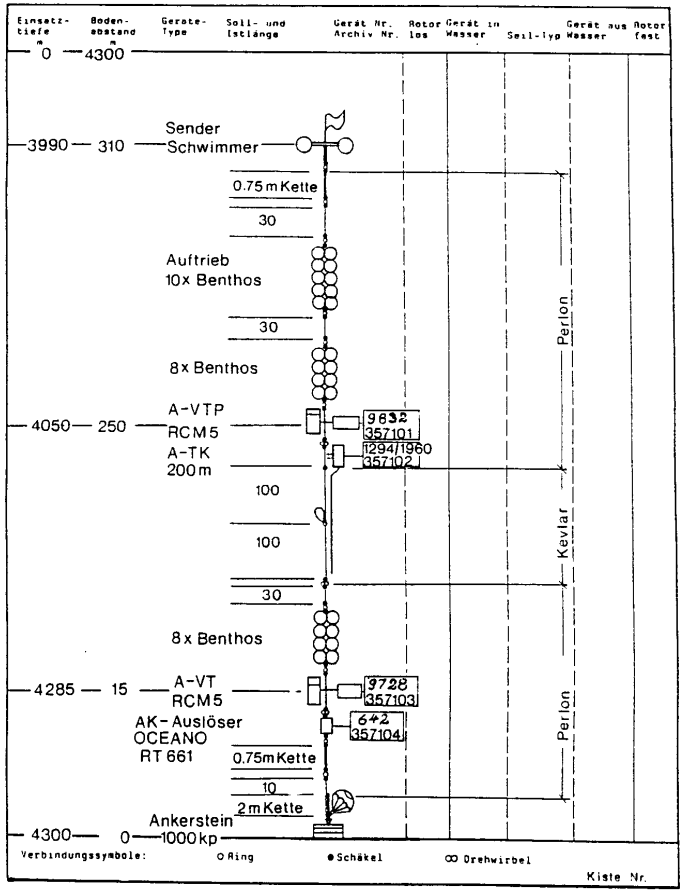

Fig. 24: Typical mooring configurations of the Institut für Meereskunde Kiel. Mooring H6 is on the left side. On the right side the thermistor chain mooring H5 is displayed.

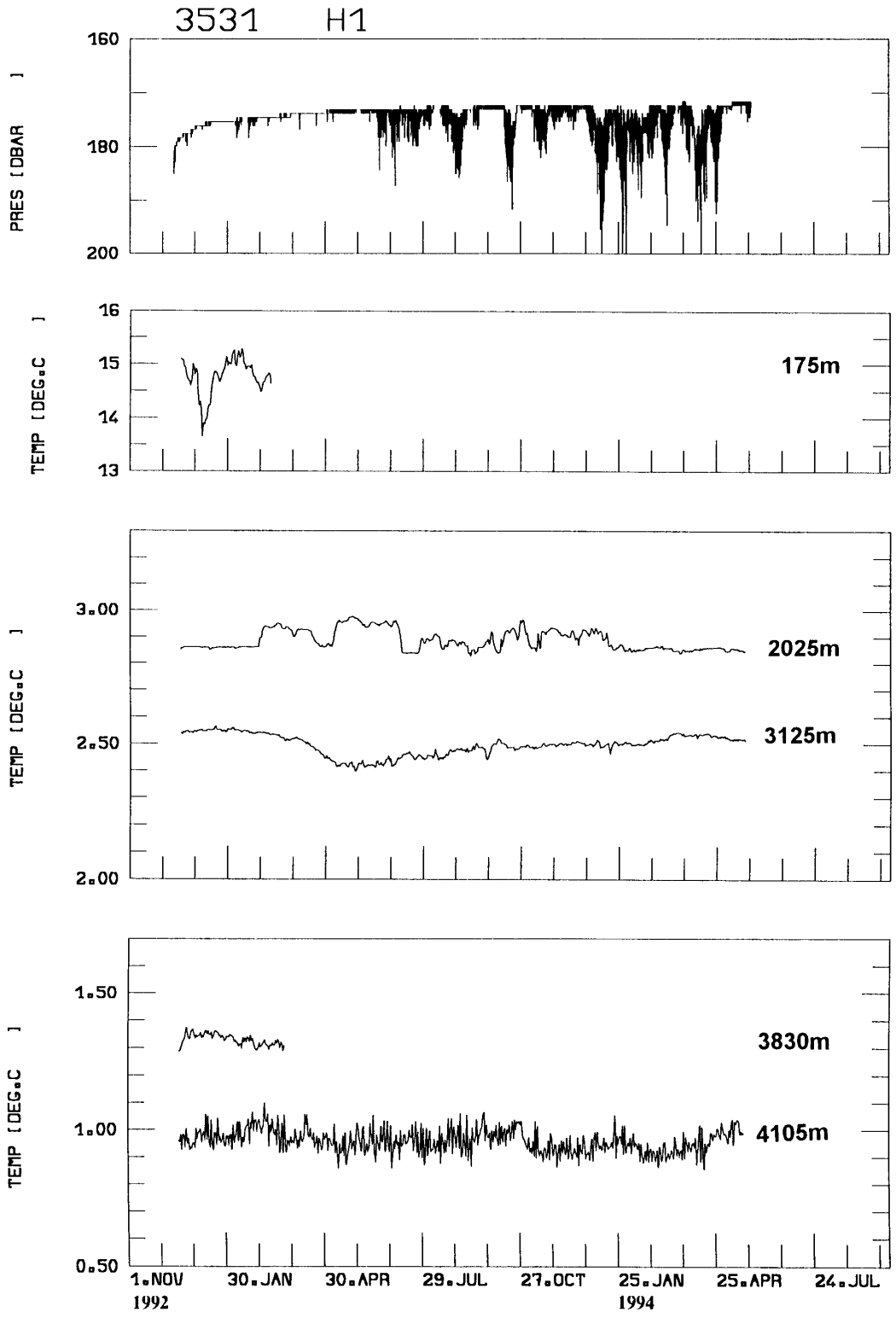

Fig. 25: Pressure (top) and temperature times series from mooring H1 on the west side of the Hunter Channel. Only pressure data were not low-pass filtered.

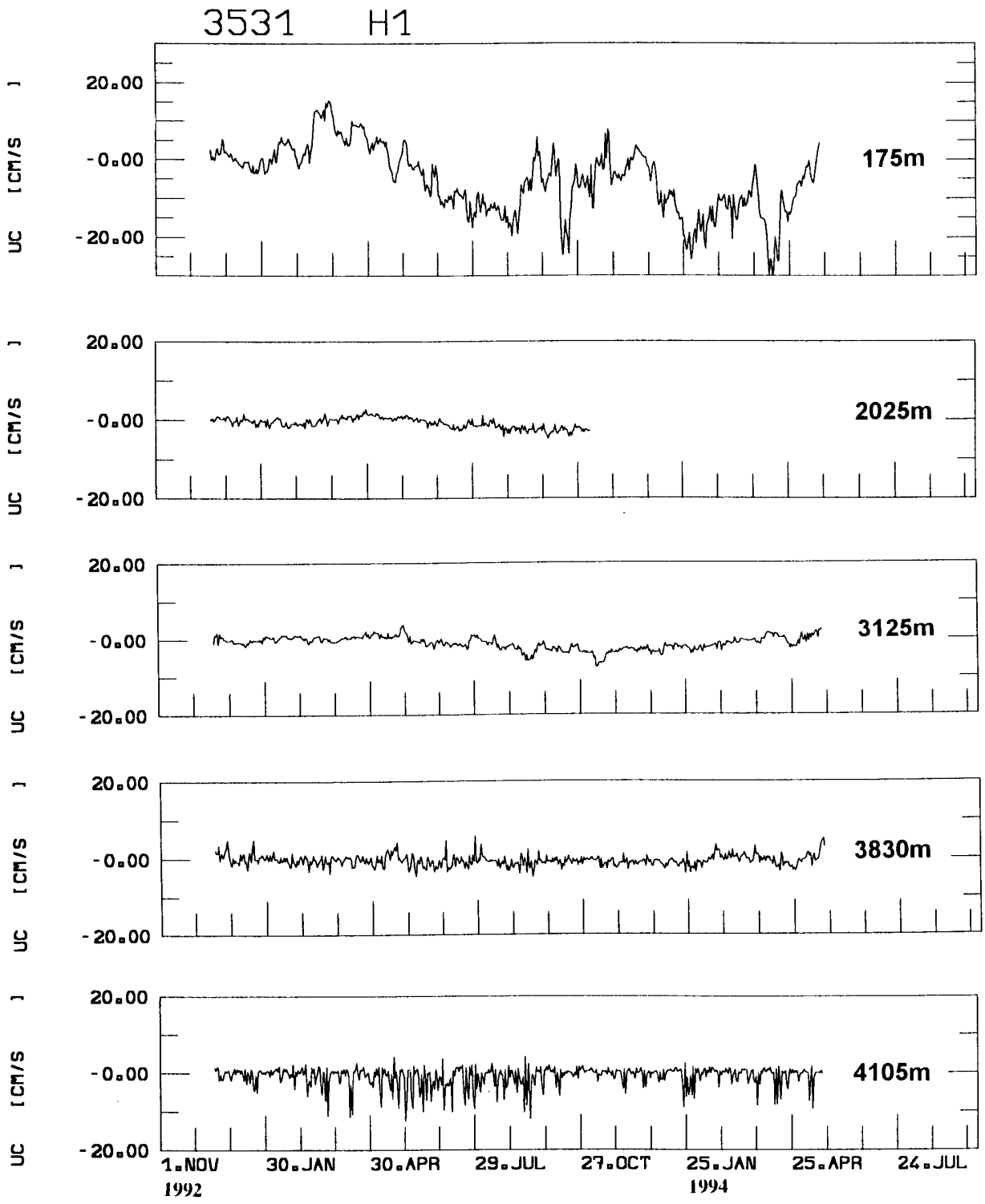

Fig. 26: Time series of zonal current components (UC) from mooring H1.

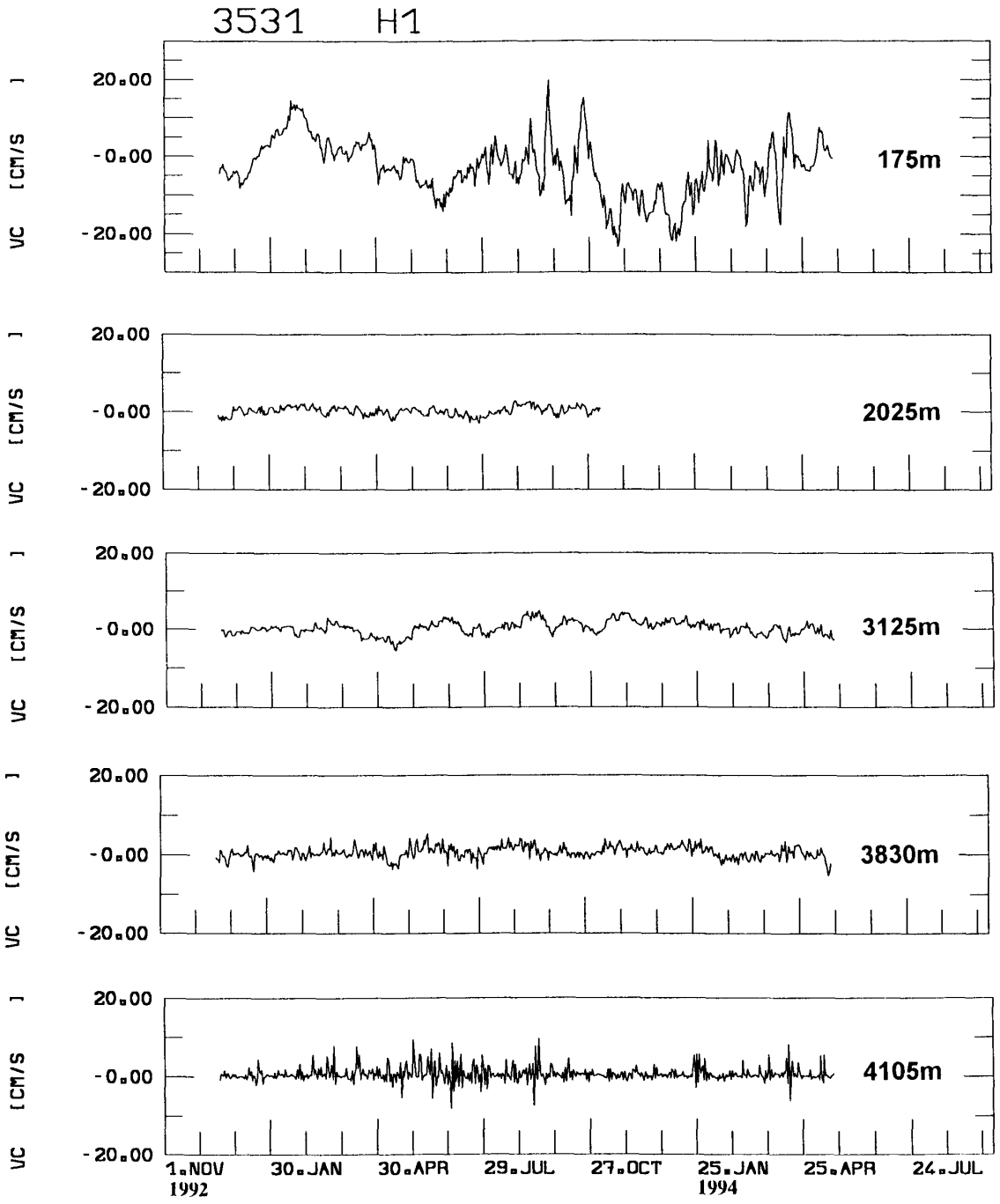

Fig. 27: Time series of meridional current components (VC) from mooring H1.

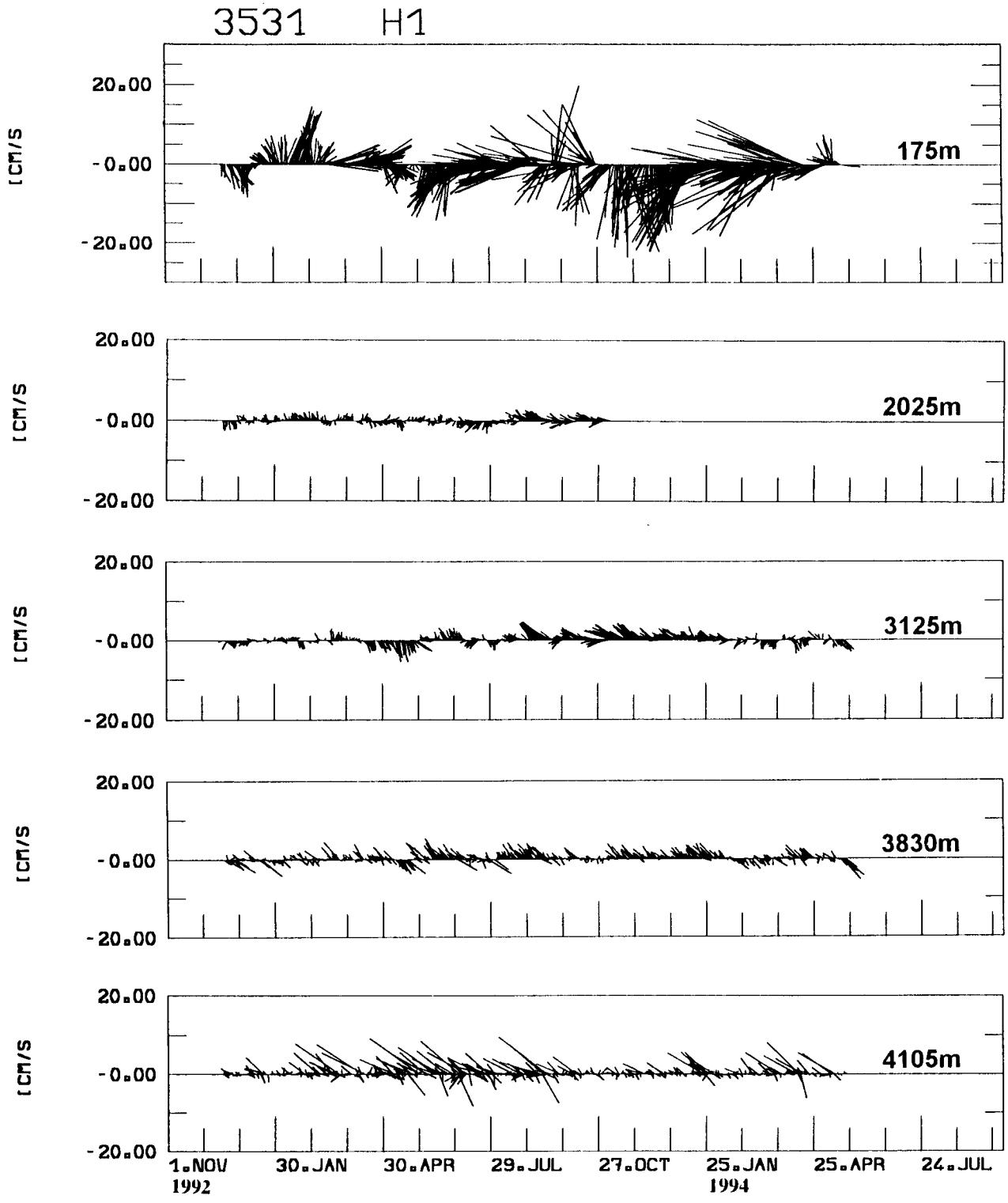

Fig. 28: Stick plot diagrams of current vectors from mooring H1. North is upward.

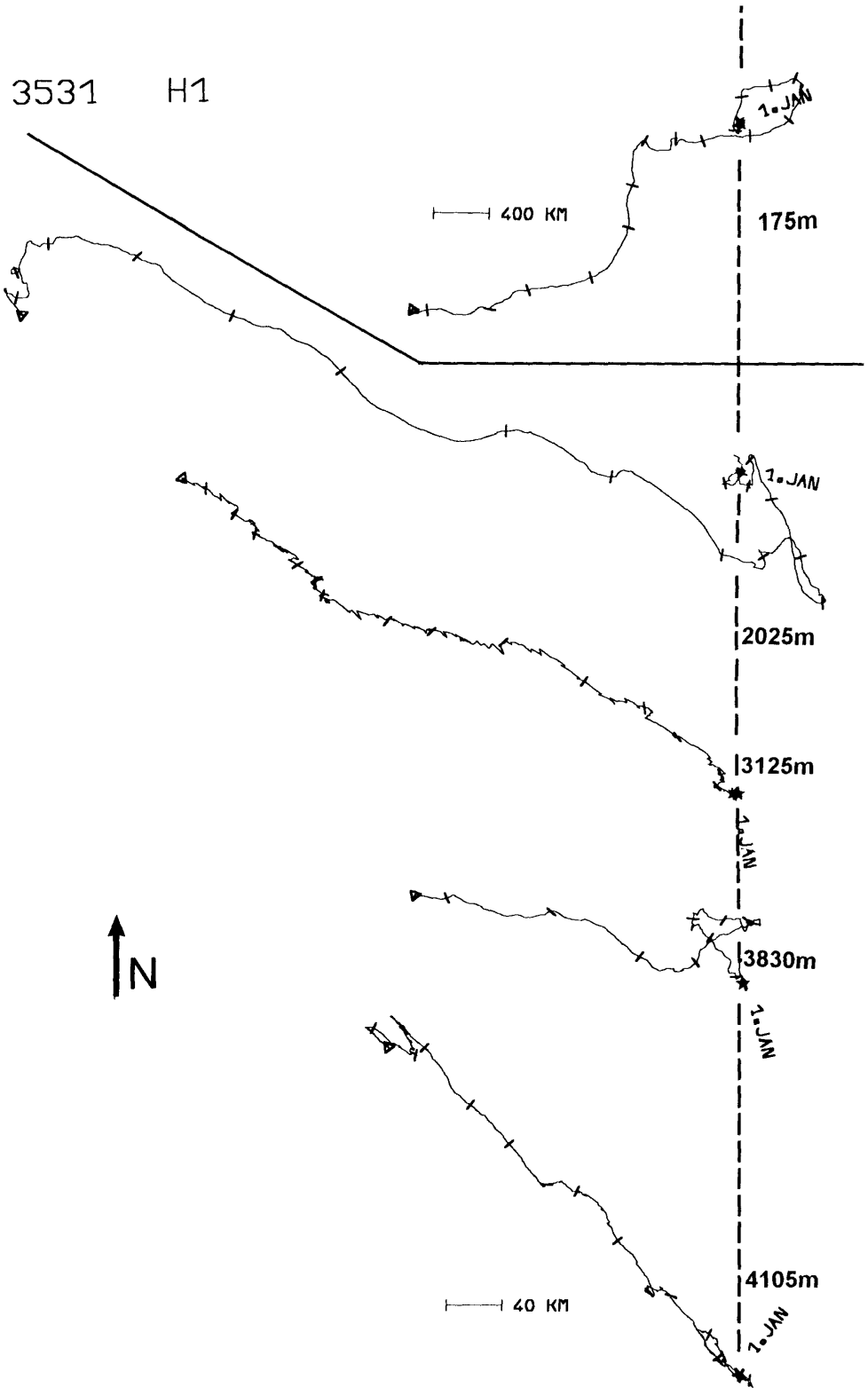

Fig. 29: Progressive vector diagrams of currents from mooring H1. Starting points are given by asterisks. Tics separate 30 days intervals.

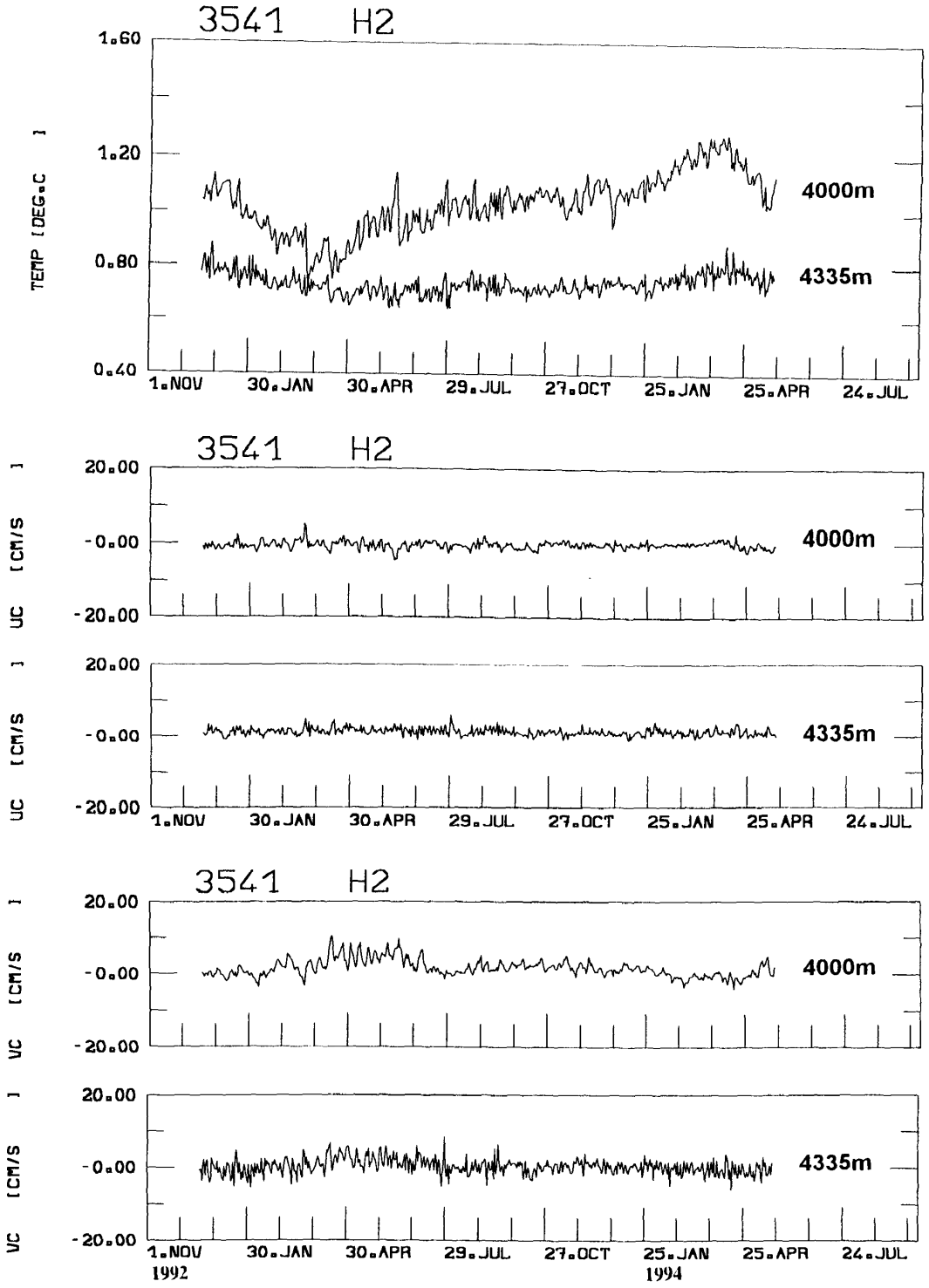

Fig. 30: Times series of temperature (top), zonal current components (UC), and meridional current components (VC) from mooring H2.

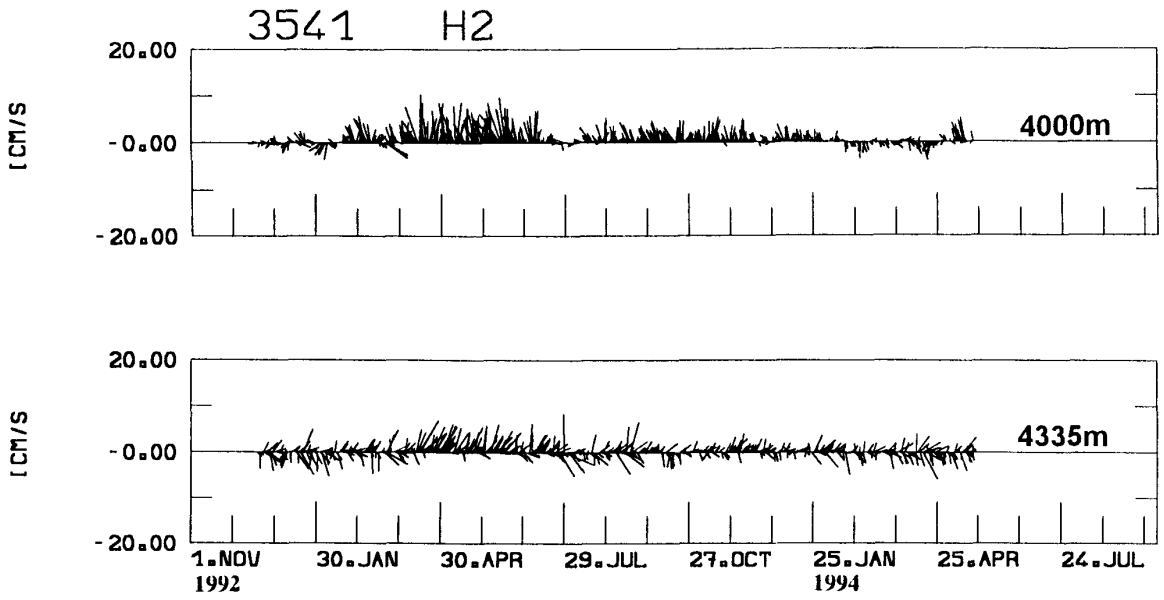

Fig. 31: Stick plot diagrams of current vectors from mooring H2 (top). North is upward. Progressive vector diagrams of currents from mooring H2 (bottom). Tics are separated by 30 days.

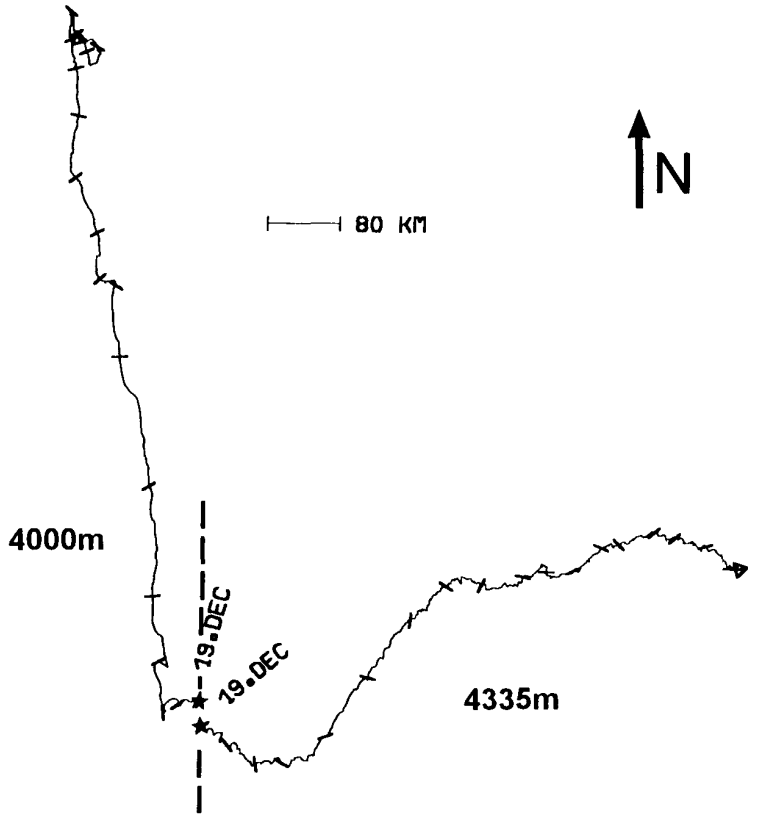

Fig. 32: Salinity (S) and temperature time series from mooring H3.

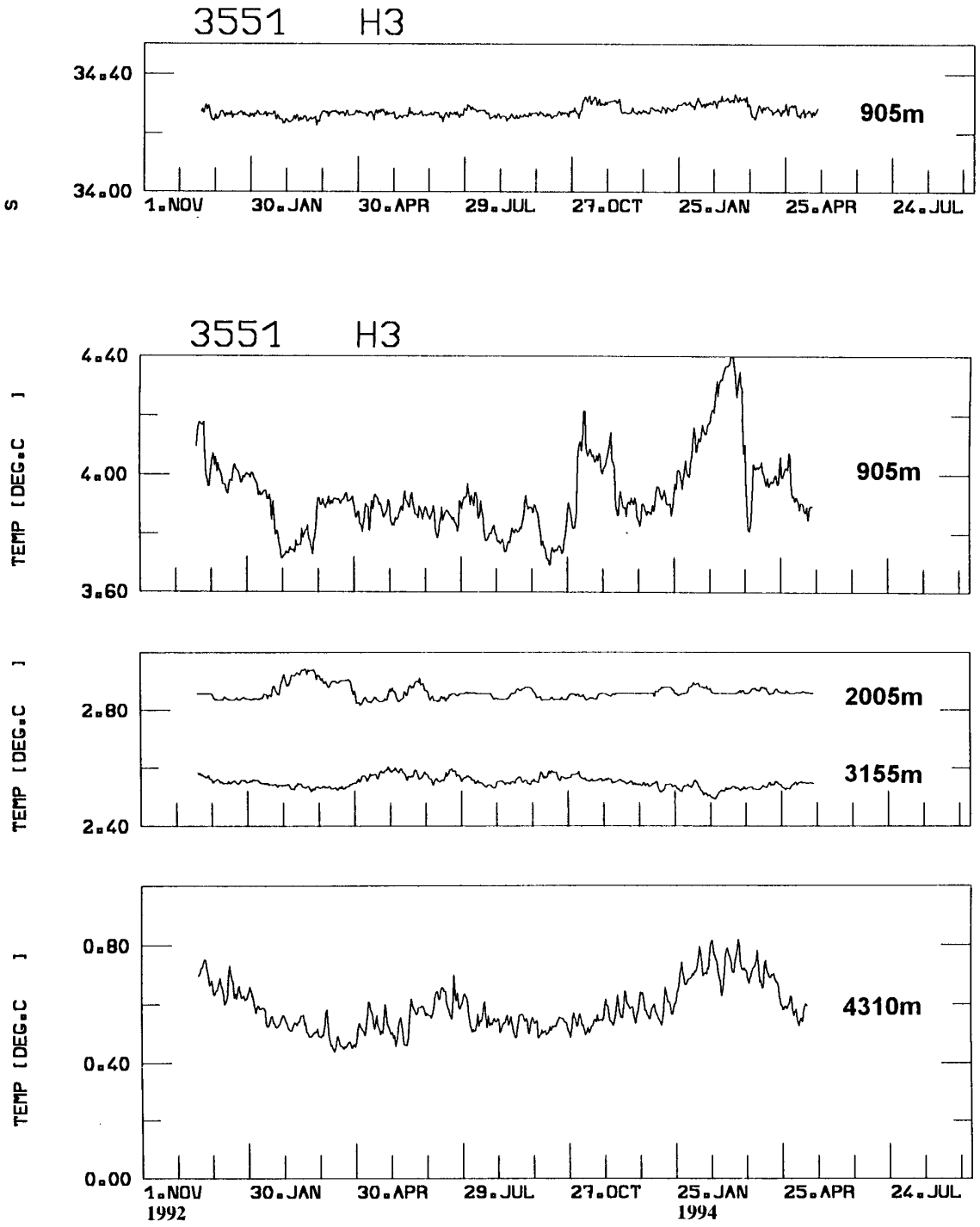

Fig. 33: Times series of zonal current components (UC) from mooring H3.

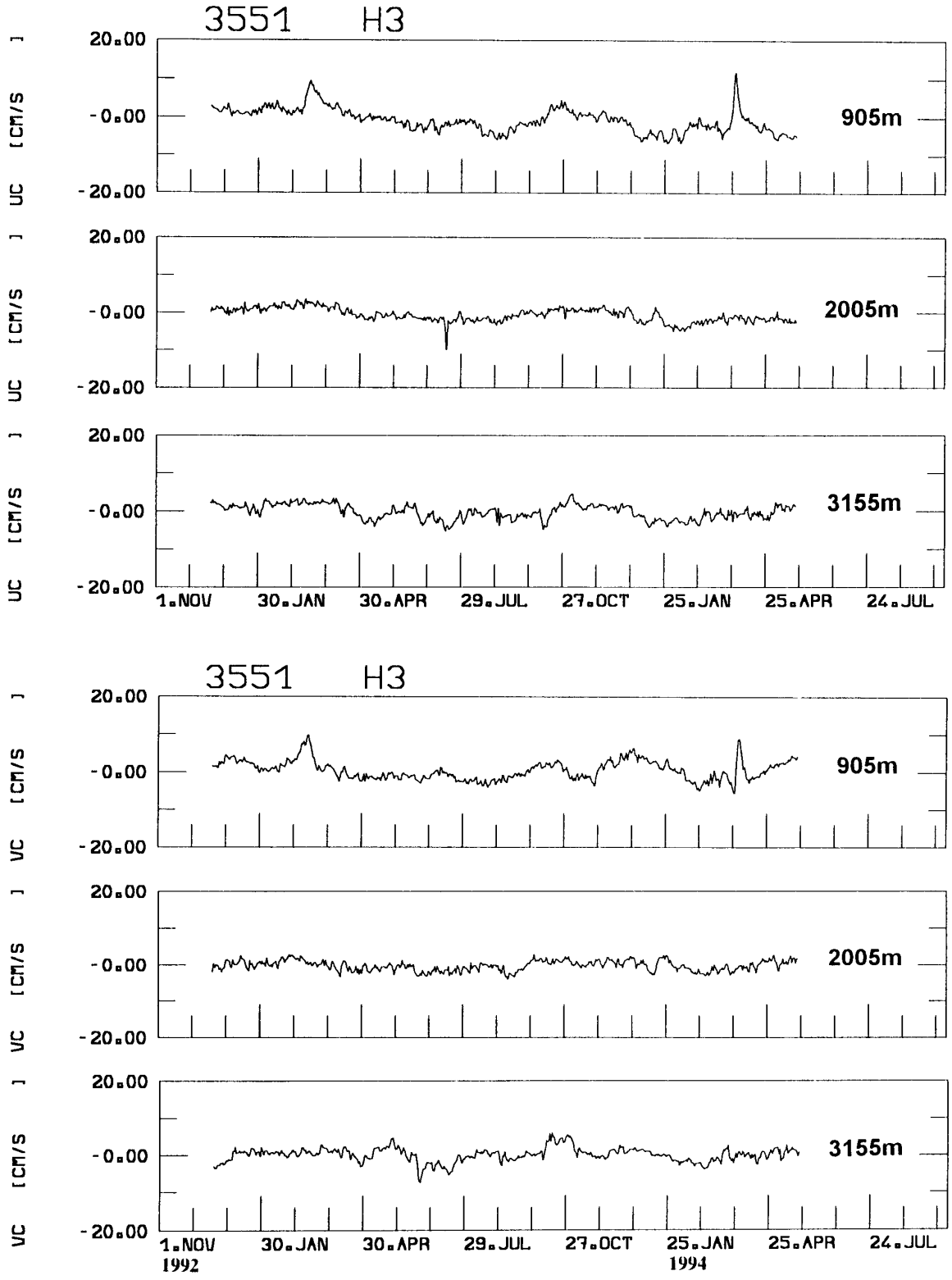

Fig. 34: Time series of meridional current components (VC) from mooring H3.

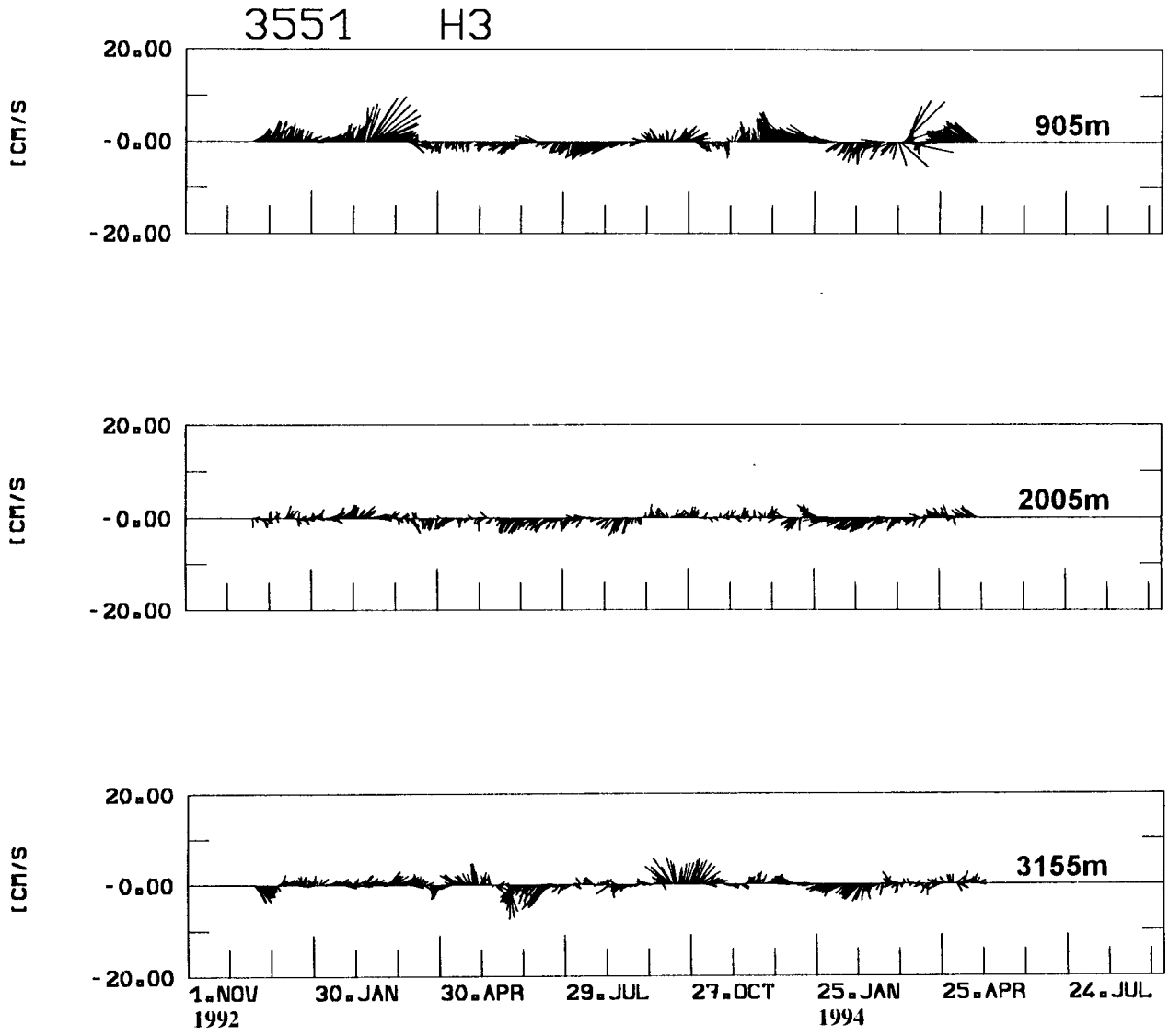

Fig. 35: Stick plot diagrams of current vectors from mooring H3. North is upward.

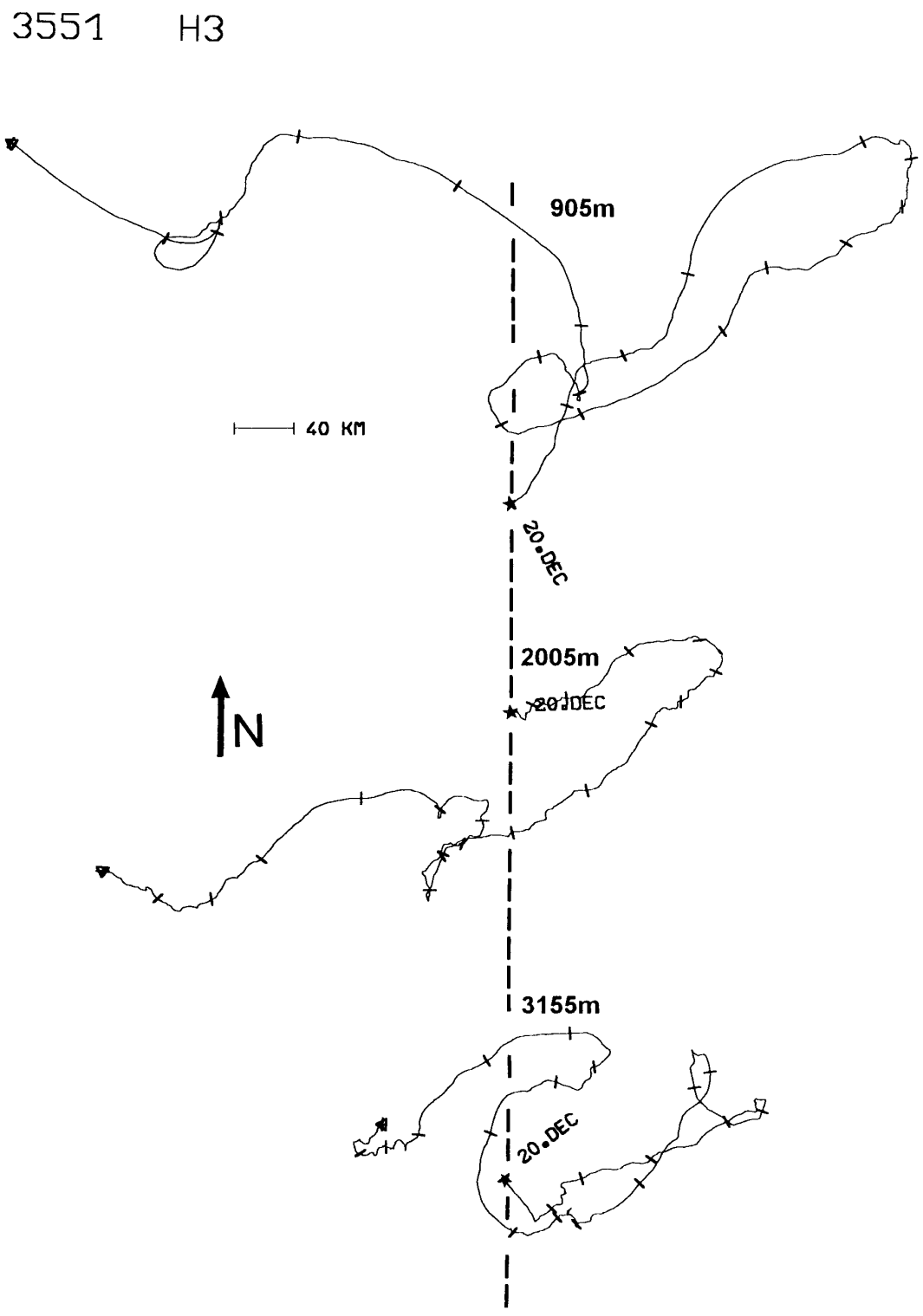

Fig. 36: Progressive vector diagrams of currents from mooring H3. Tics separate 30 days intervals.

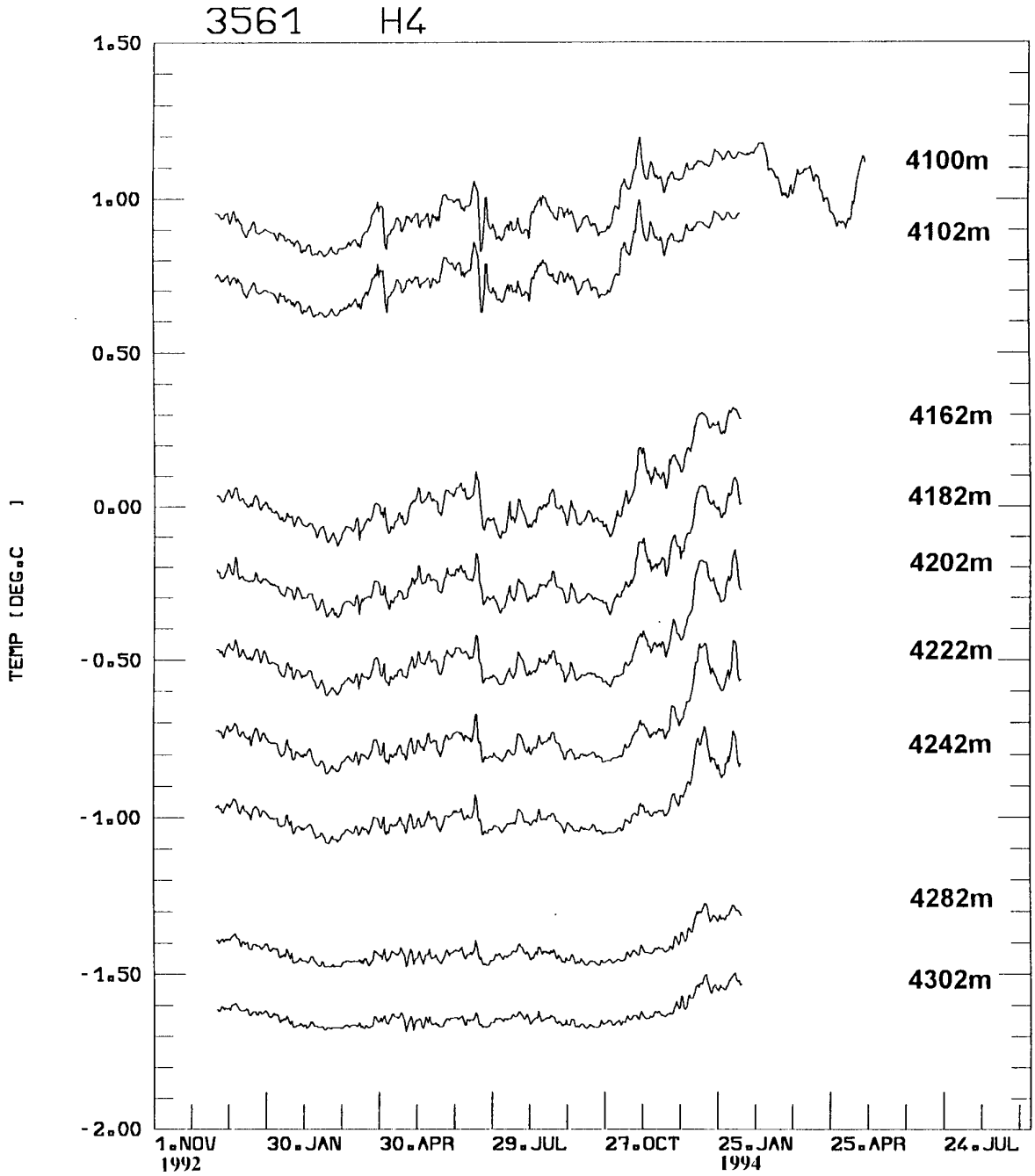

Fig. 37: In situ temperature times series from thermistor chain mooring H4. For better readability individual temperature curves are shifted by -0.5ºC, the uppermost curve serves as reference. Only the current meter on the top of the 200 m long thermistor chain recorded for the total mooring deployment (top). The data storage capacity of the thermistor chain below expired earlier. Gaps under the second curve stand for two sensors without records. The lower gap represents an additional sensor that failed. Temperature were adjusted to the nearest CTD station (see Table 6). Numbers on the right side indicate sensor depths.

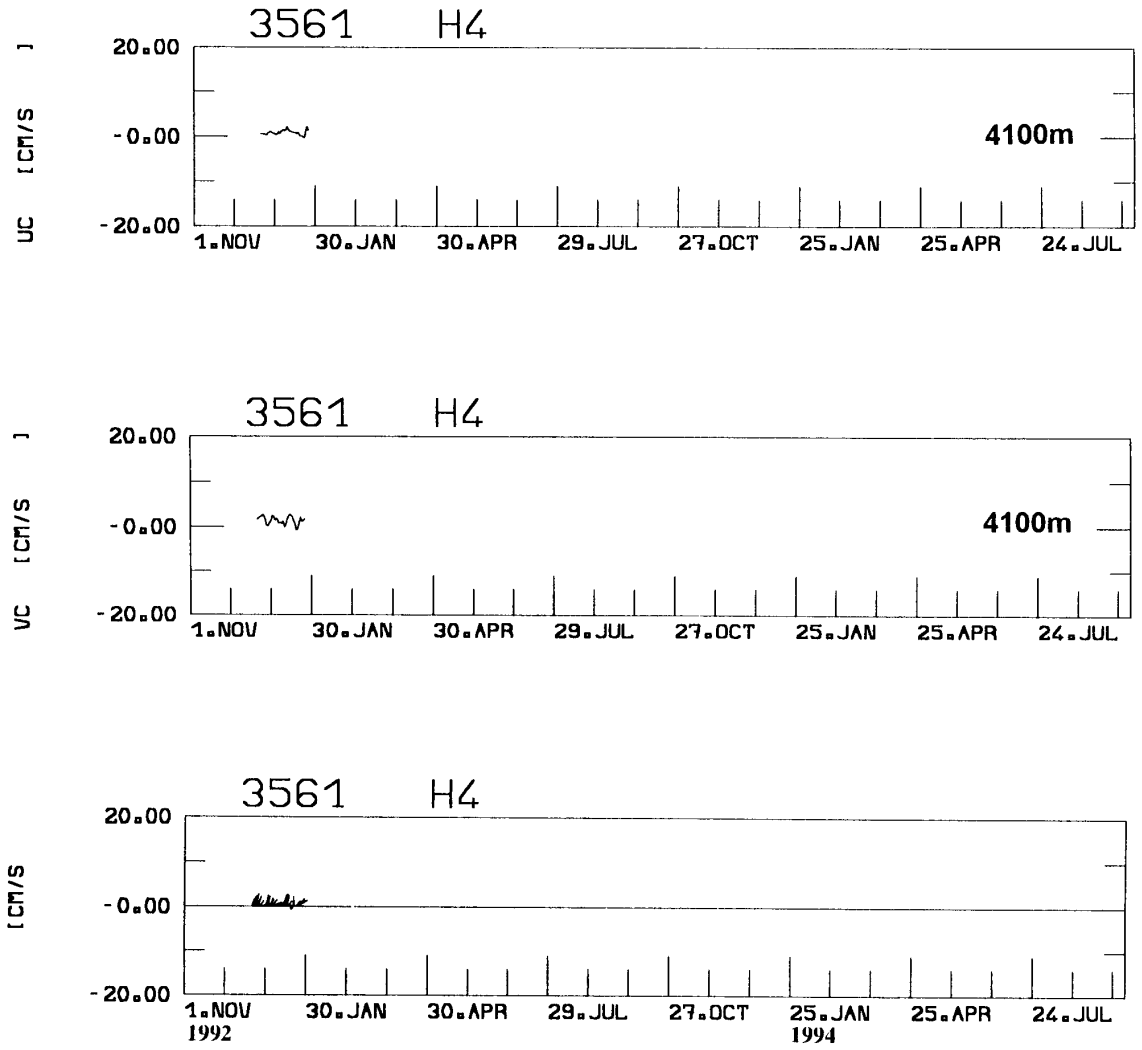

Fig. 38: Times series of the zonal (UC) and the meridional (VC) current components together with the stick plot diagram (North is upward) from mooring H4.

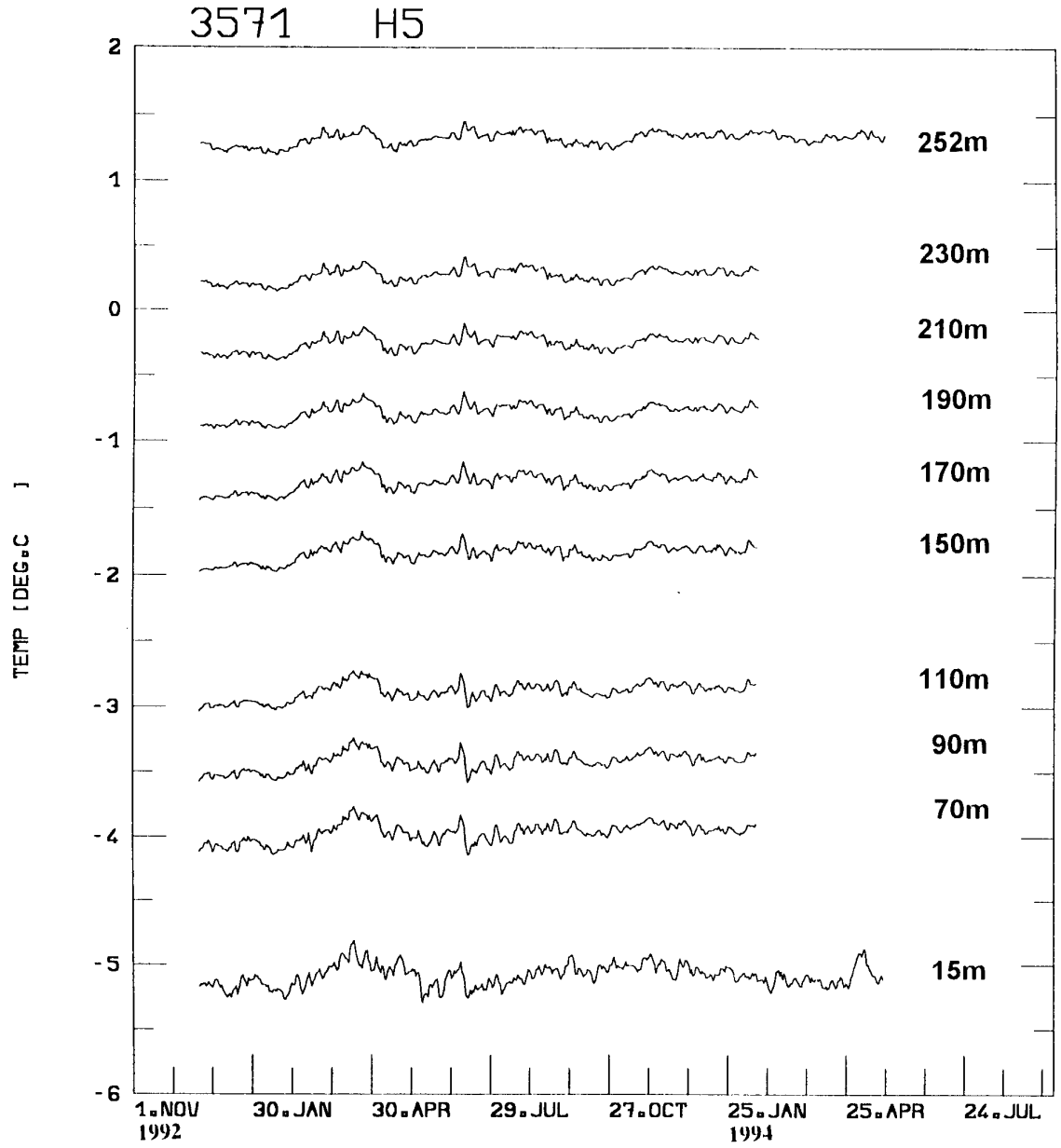

Fig. 39: Preliminary temperature time series from thermistor chain mooring H5. Due to extreme bottom roughness at the sill of Hunter Channel depth determinations of sensors are difficult. On the right side distances from the bottom for individual sensors are displayed, which were 20 m apart except for the top curve. This contains the temperature record of the upper current meter. The data storage capacity of the thermistor chain expired early. For better readability individual temperature curves are shifted by –0.5ºC, the uppermost curve serves as graphical reference. Gaps in the vertical stand for missing records of defect sensors.

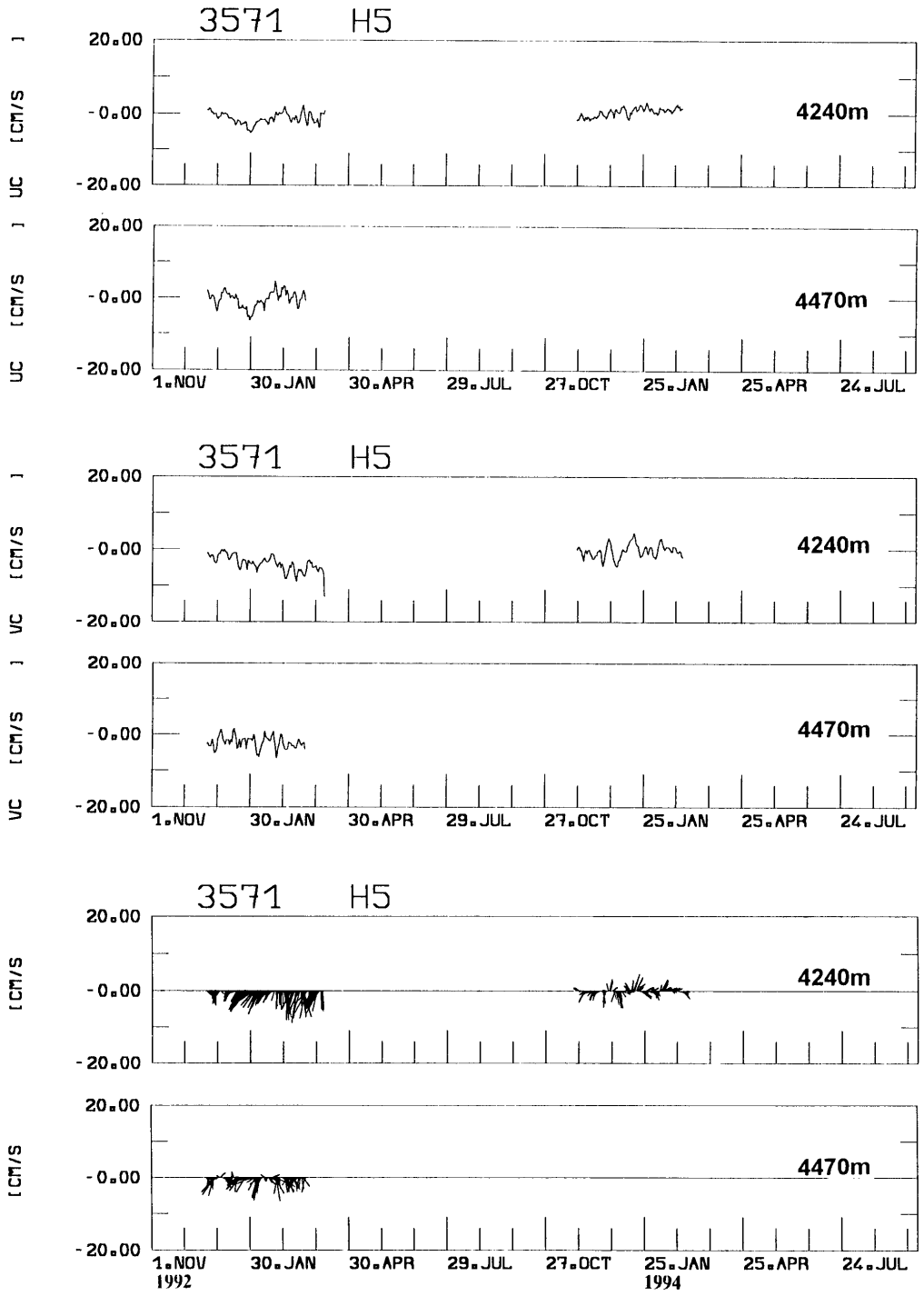

Fig. 40: Time series of zonal (UC) and meridional (VC) current components together with stick plot diagrams (North is upward) from mooring H5. The interrupt in the time series of the 4240 m level is caused by technical problems of the used Aanderaa Current Meter.

3571 H5

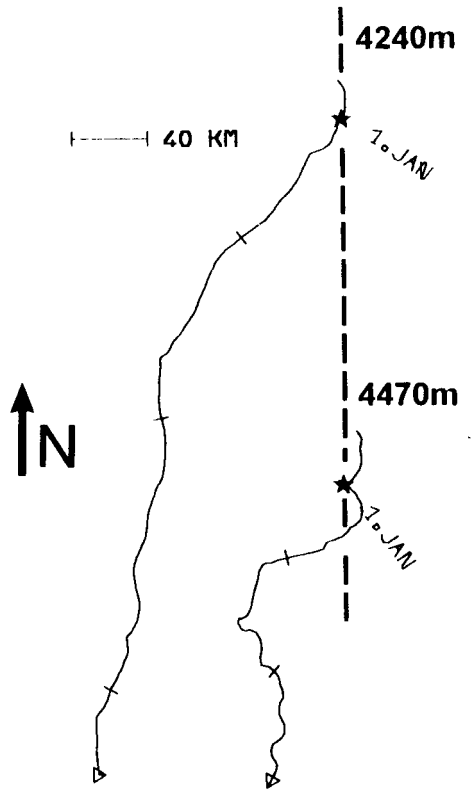

Fig. 41: Progressive vector diagrams of currents from mooring H5. From the upper level only the first sub-series (see Fig. 40) is shown. This indicates 30 days intervals.

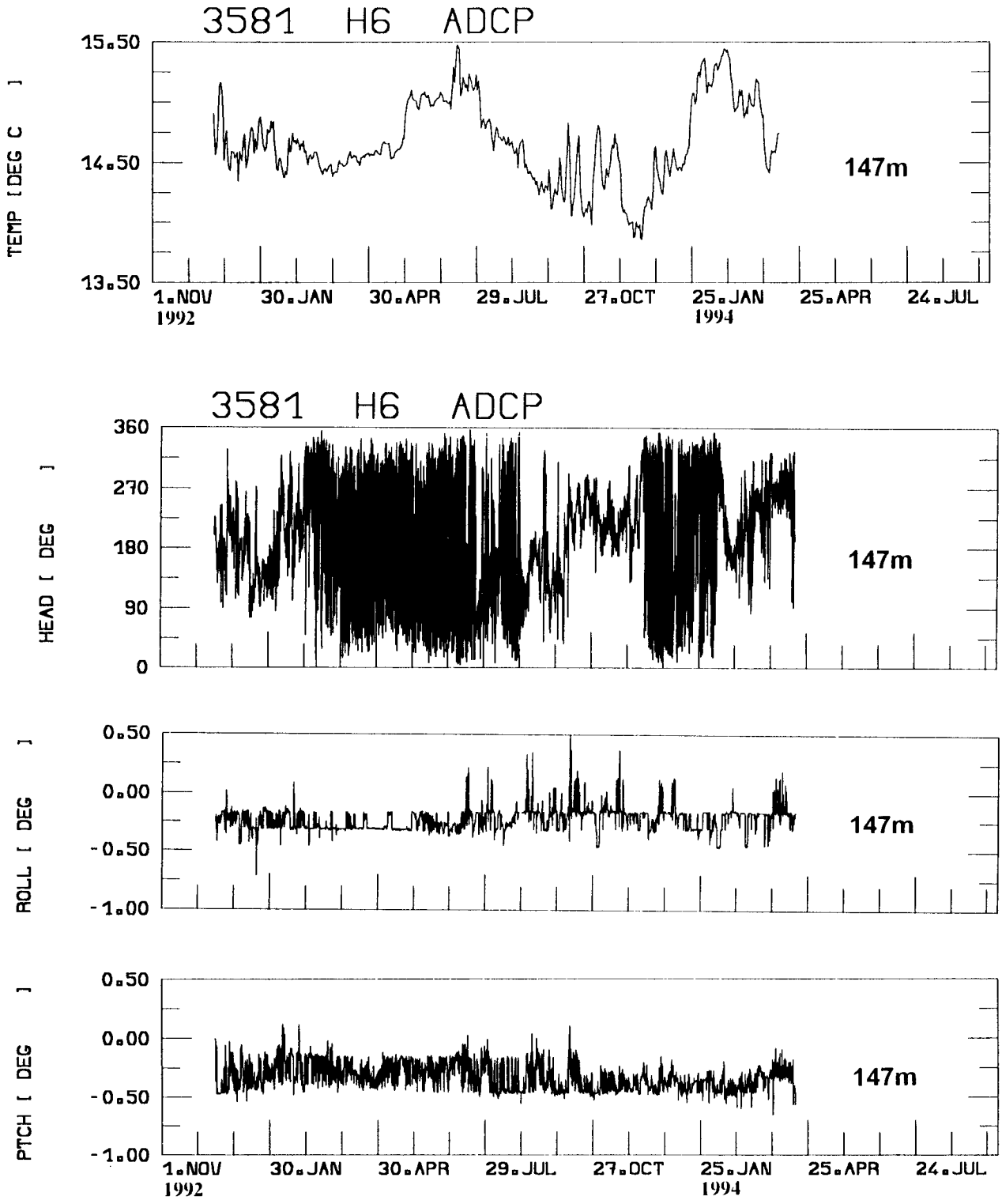

Fig. 42: Temperature (top) and auxiliary parameters of the Acoustic Doppler Current Profiler on the top of mooring H6. Only the temperature time series has been low-passed filtered.

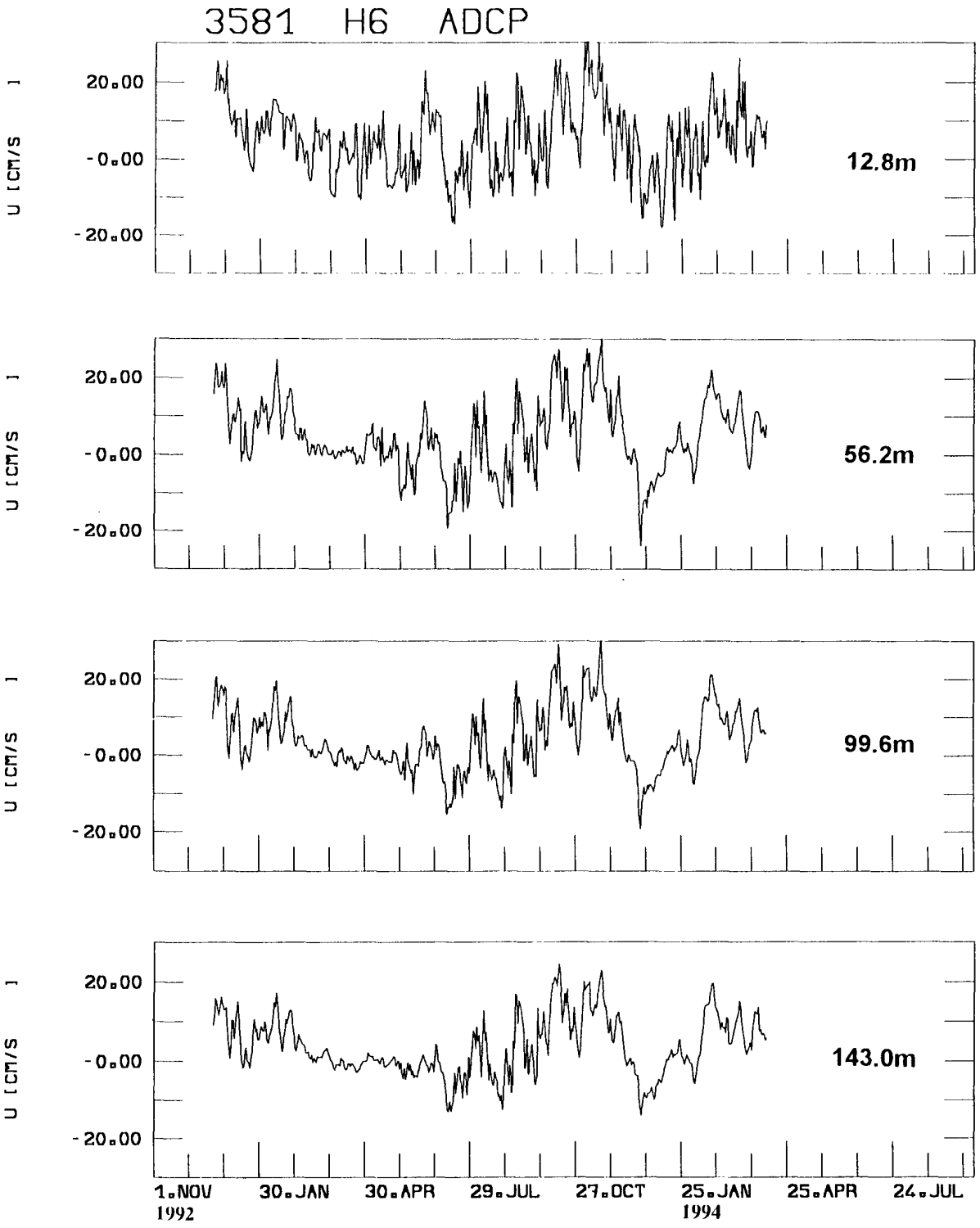

Fig. 43: Time series of zonal current components (UC) at selected depths from the Acoustic Doppler Current Profiler on top of the mooring H6. Bin size was 8.7 m.

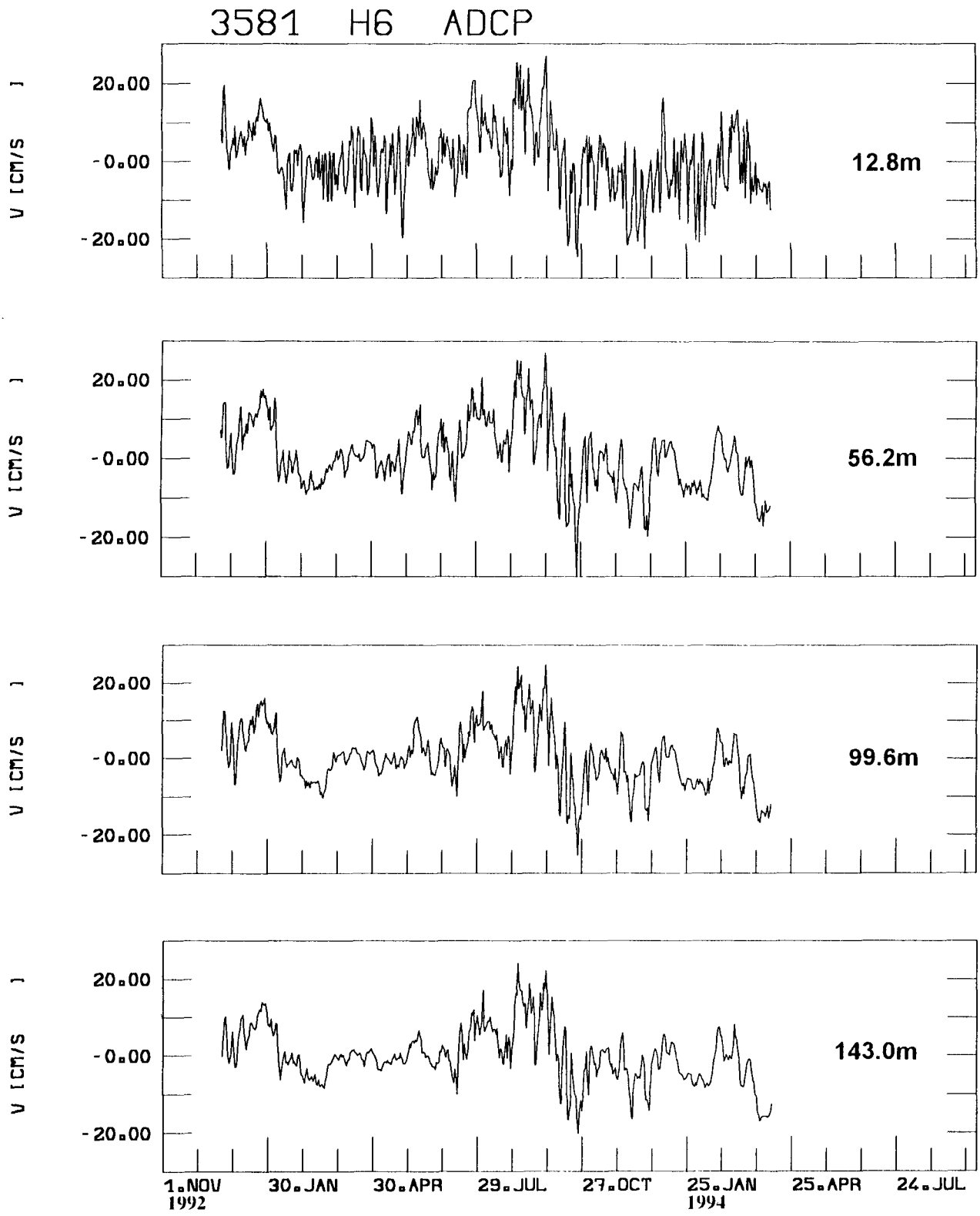

Fig. 44: Time series of meridional current components (VC) at selected depths from the Acoustic Doppler Current Profiler on top of mooring H6. Bin size was 8.7 m.

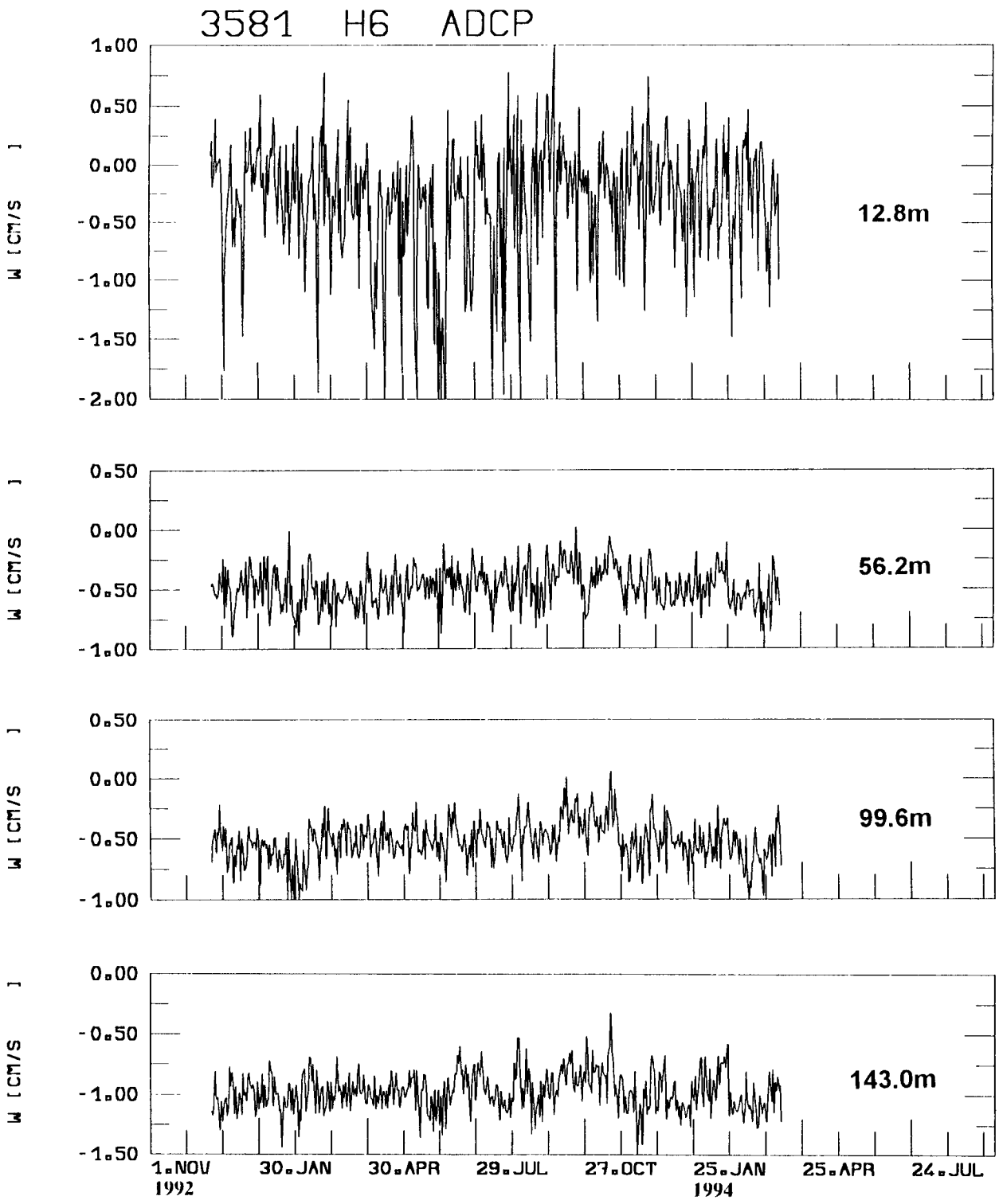

Fig. 45: Uncorrected time series of vertical current components (W) at selected depths as recorded by Acoustic Doppler Current Profiler on top of mooring H6. Bin size was 8.7 m.

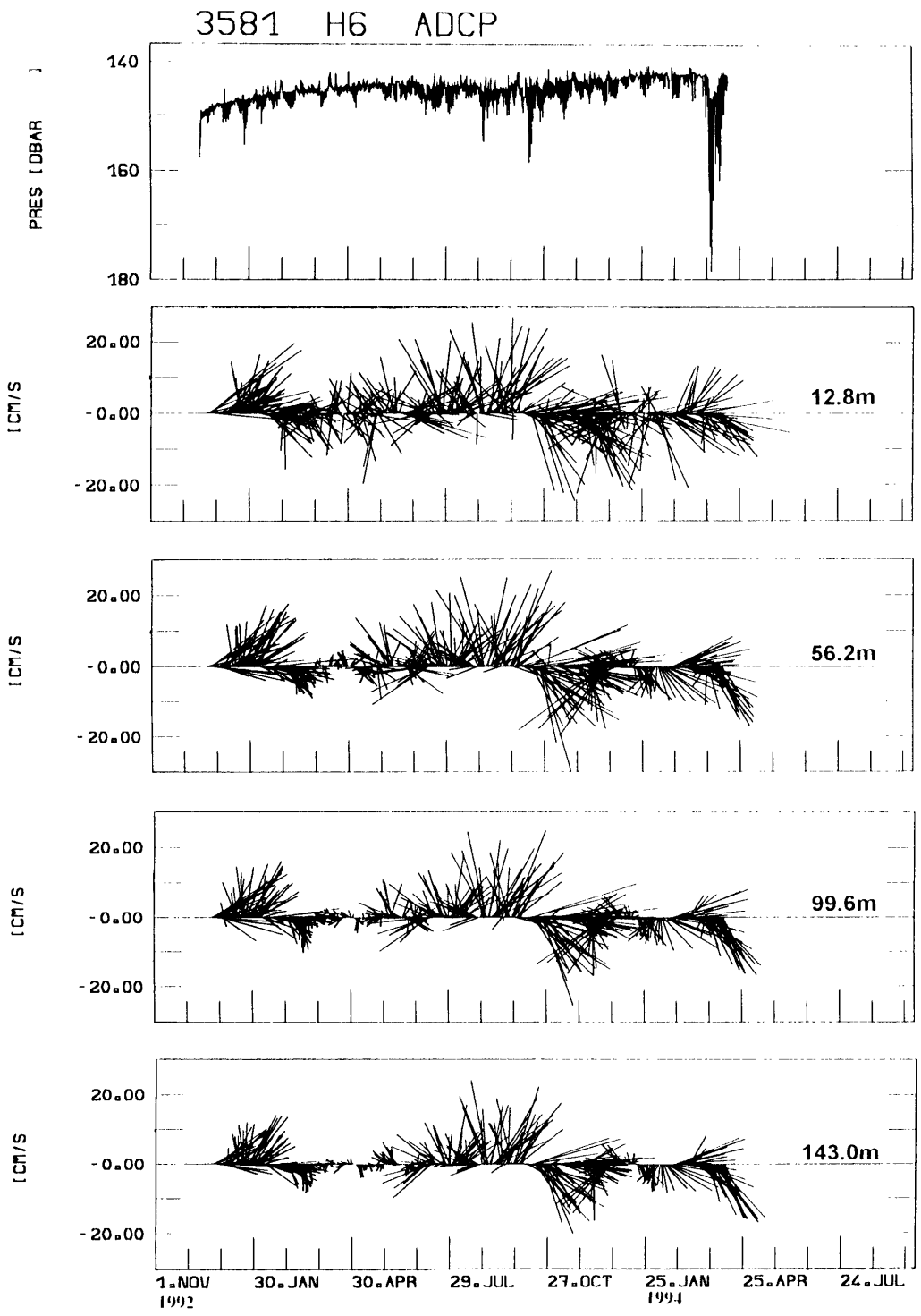

Fig. 46: Pseudo-pressure (PRESS) time series for the ADCP in mooring H6 as inferred from the backscatter record (according to VIESBEK and FISCHER, 1995). Below PRESS stick plot diagrams of ADCP current vectors at selected depth above the top instrument (ADCP) of mooring H6 is displayed. North is upward.

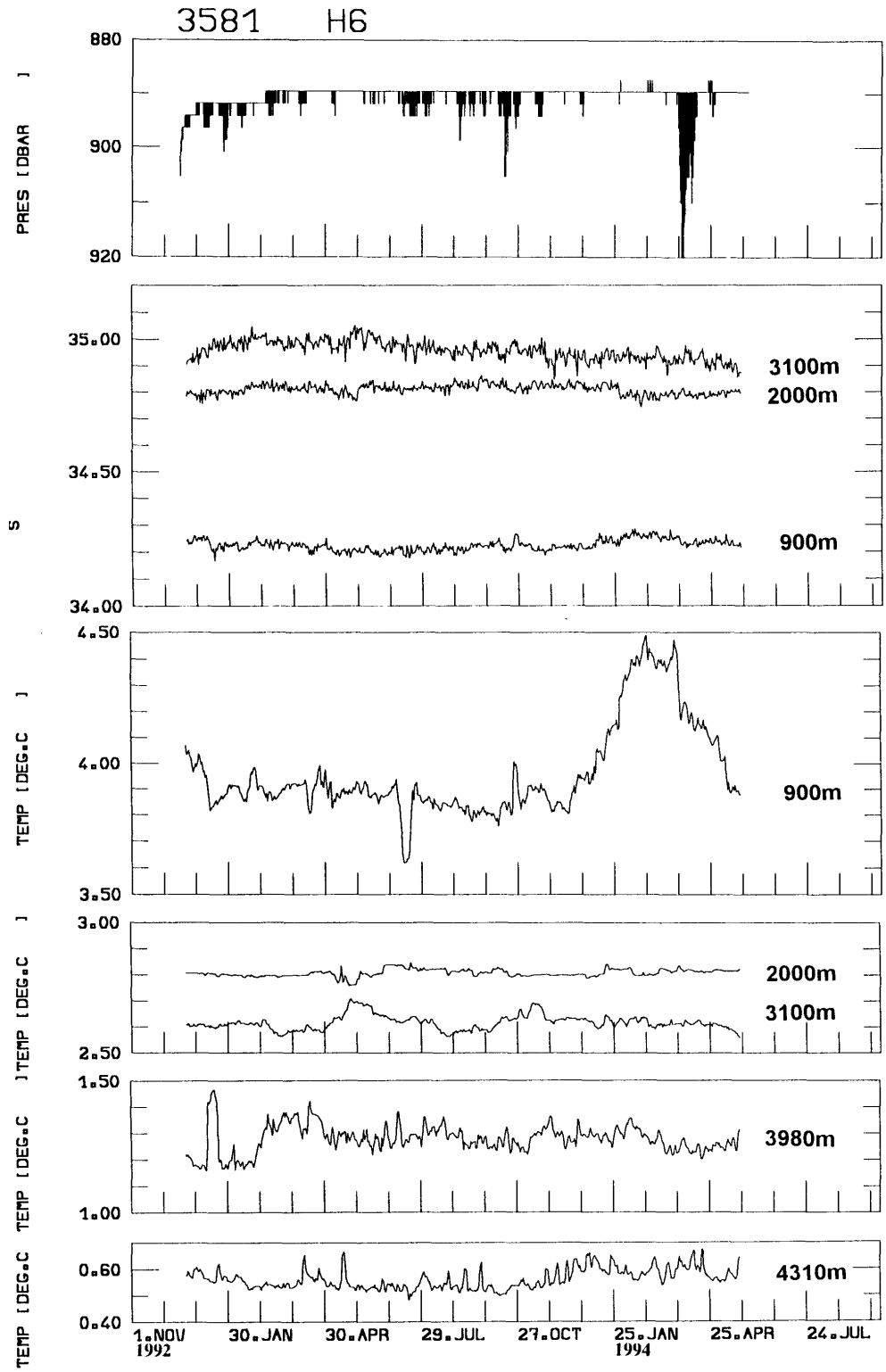

Fig. 47: Time series of pressure (top), salinity (S), and temperatures from mooring H6. As before all time series were low-press filtered, except for pressure.

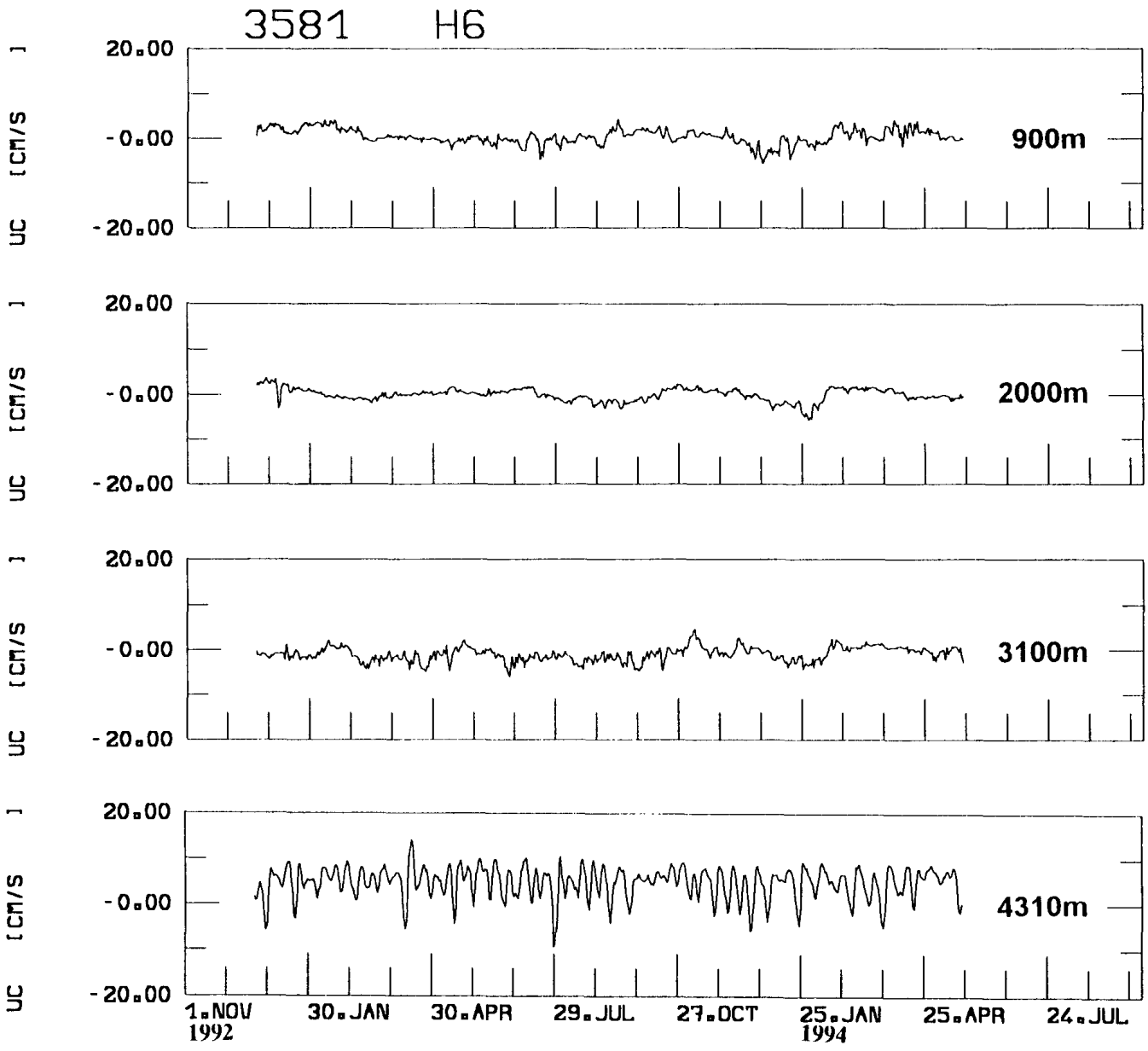

Fig. 48: Time series of zonal current components (UC) from mooring H6.

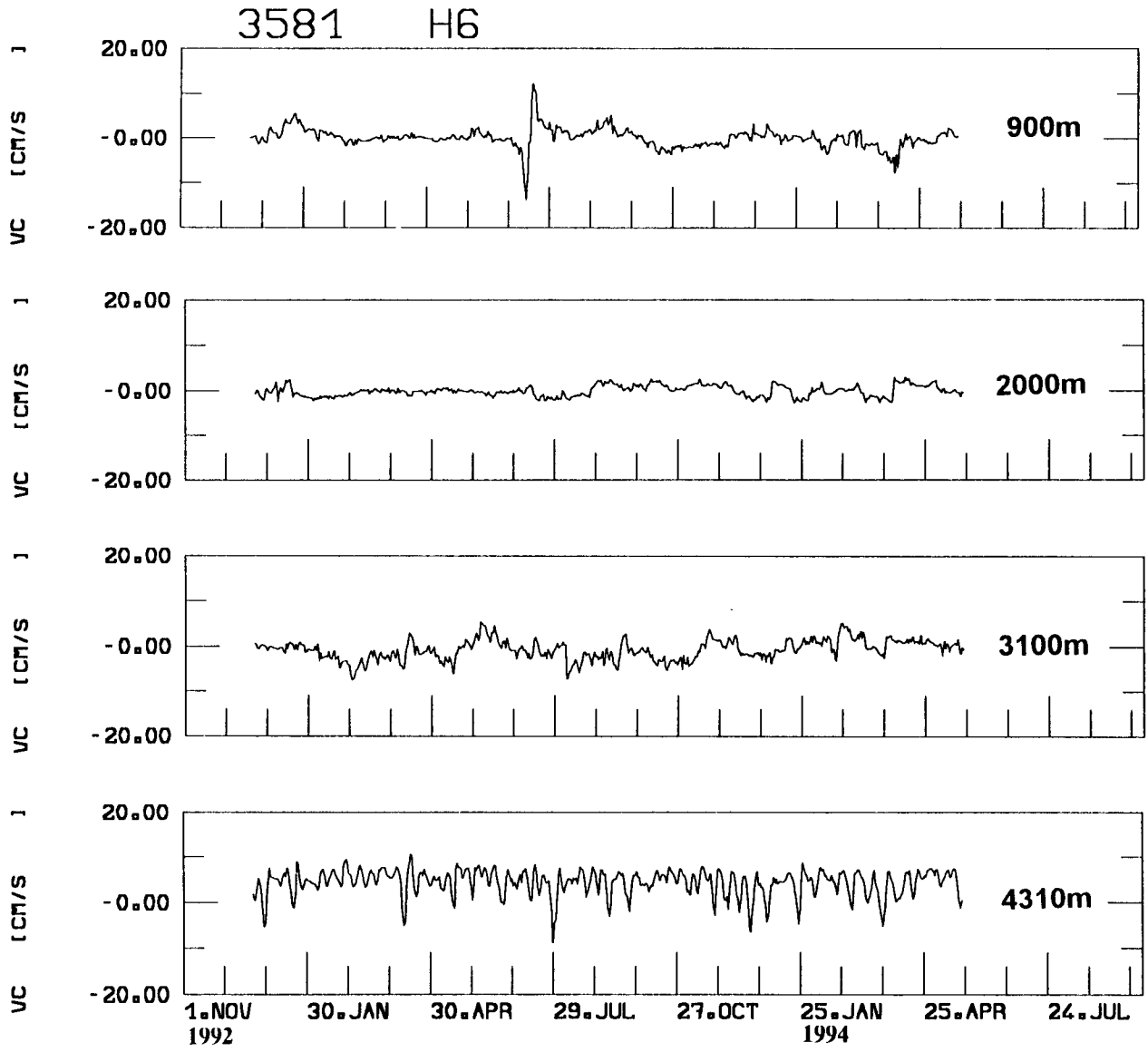

Fig. 49: Time series of meridional current components (VC) from mooring H6.

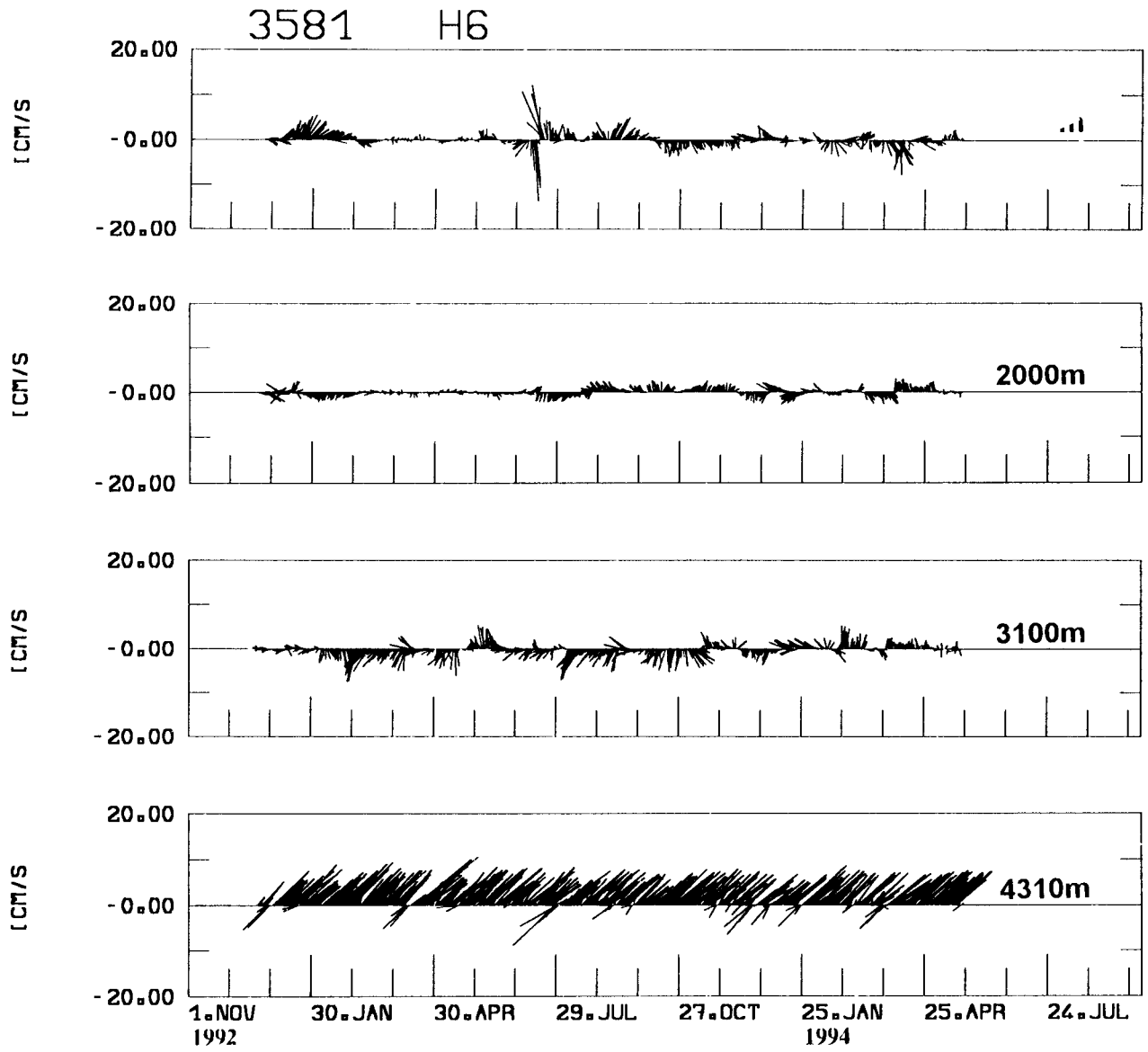

Fig. 50: Stick plot diagrams of current vectors from mooring H6. North is upward.

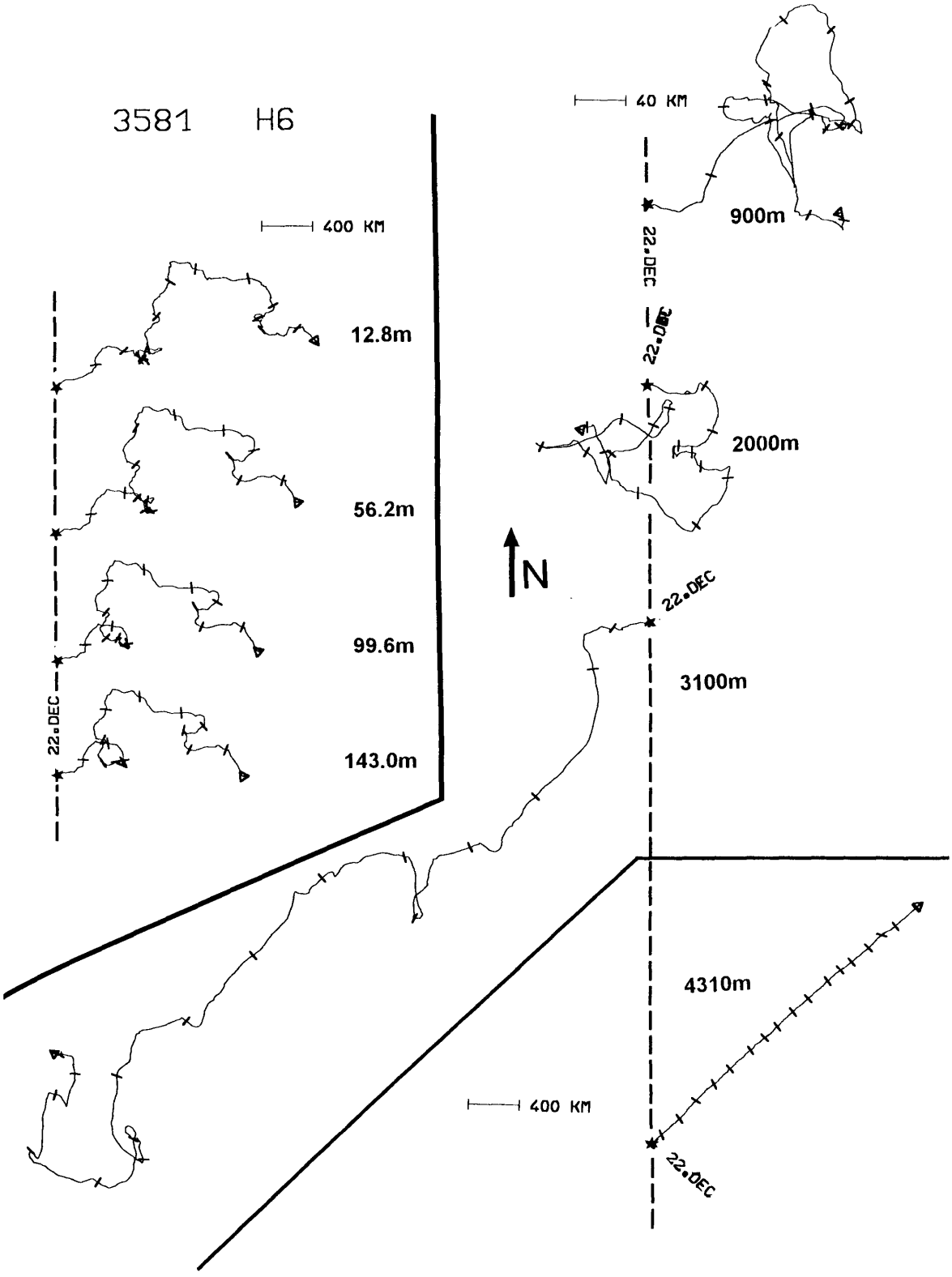

Fig. 51: Progressive vector diagrams of currents from mooring H6. Tics indicate 30 days intervals.

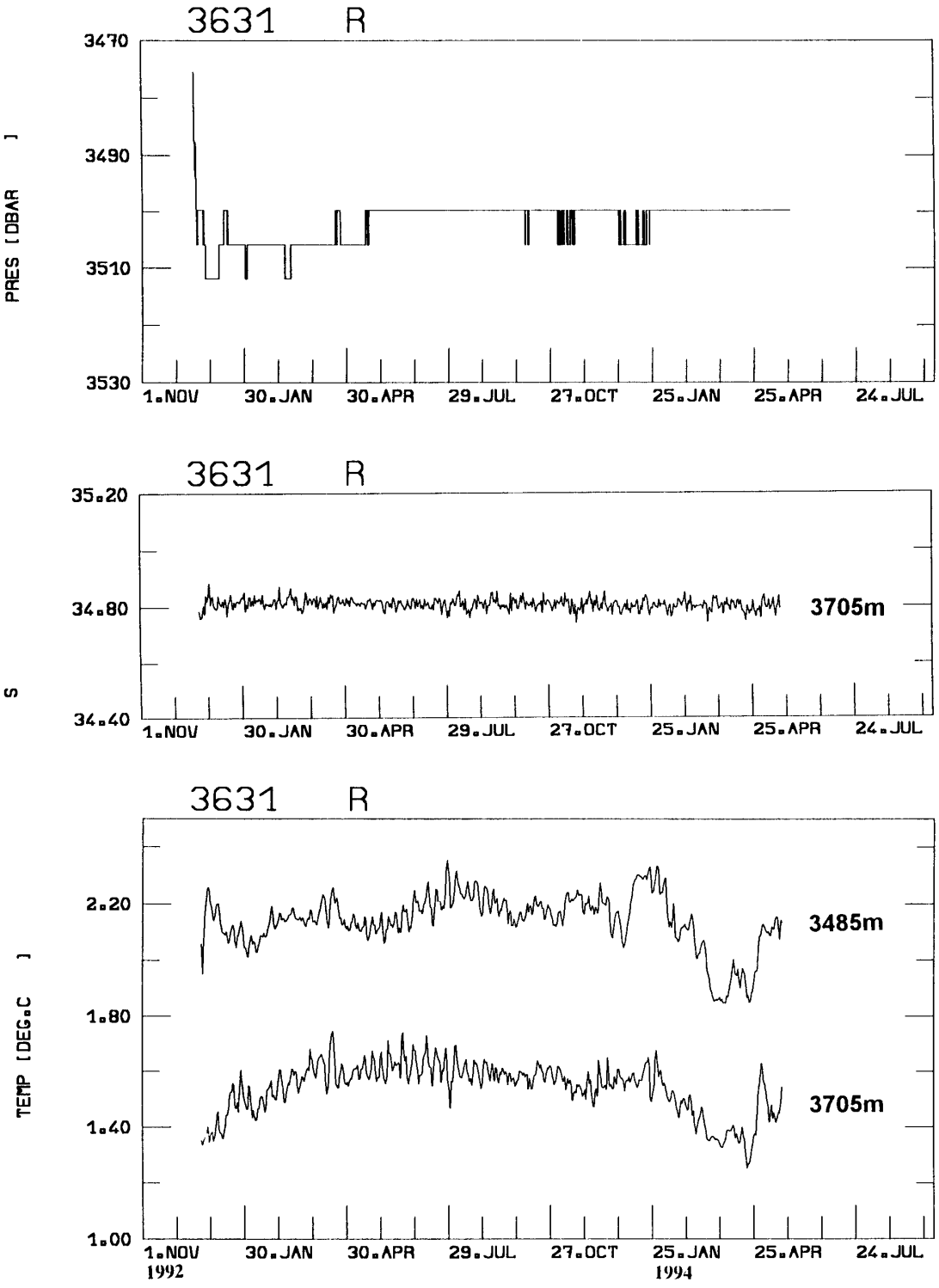

Fig. 52: Time series of pressure (top), salinity (S), and temperatures from mooring R at the eastern flank of the Rio Grande Rise. As before all time series were low-pass filtered, except for pressure.

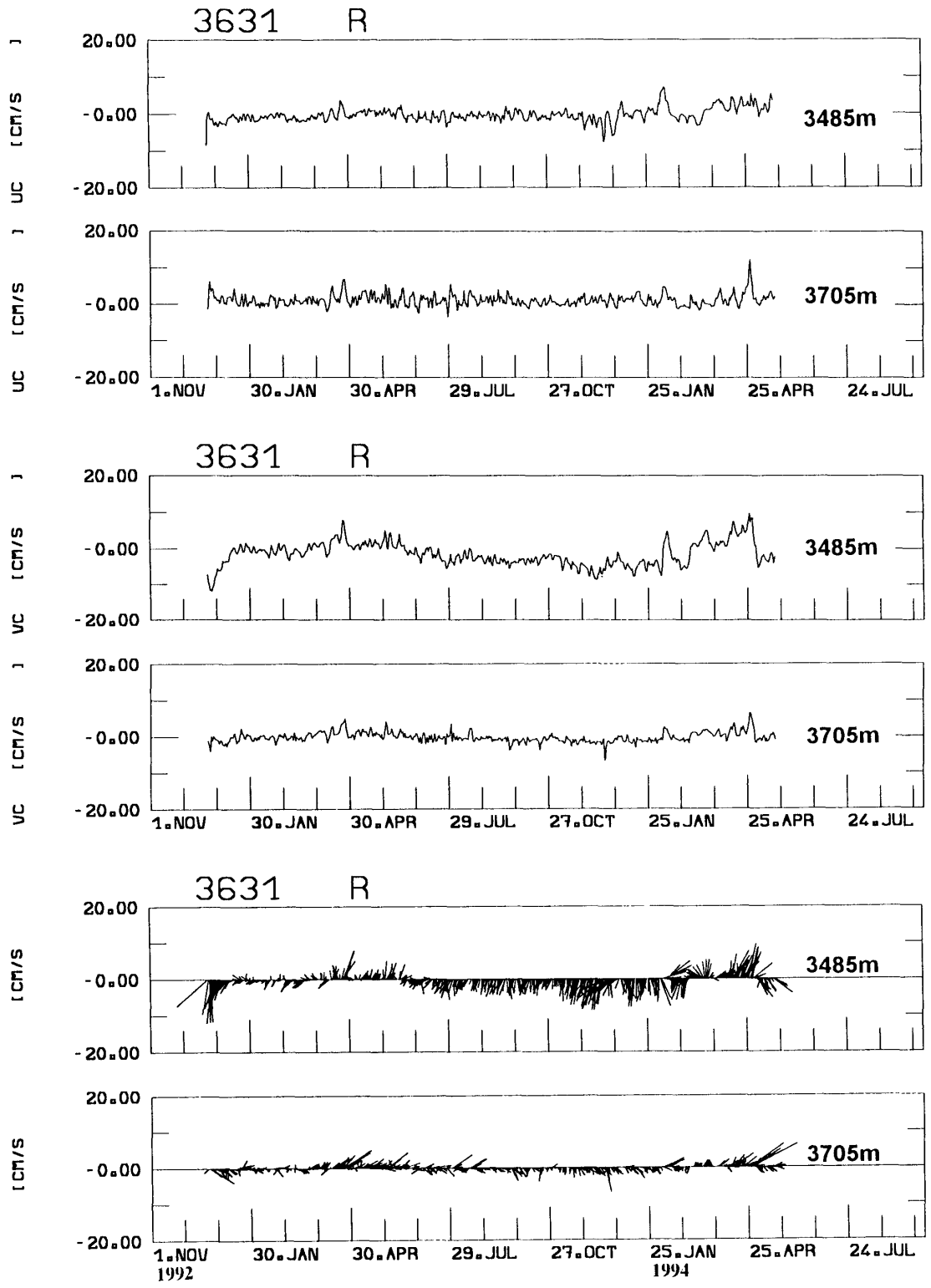

Fig. 53: Time series of zonal (UC) and meridional (VC) current components together with stick plot diagrams (North is upward) from mooring R.

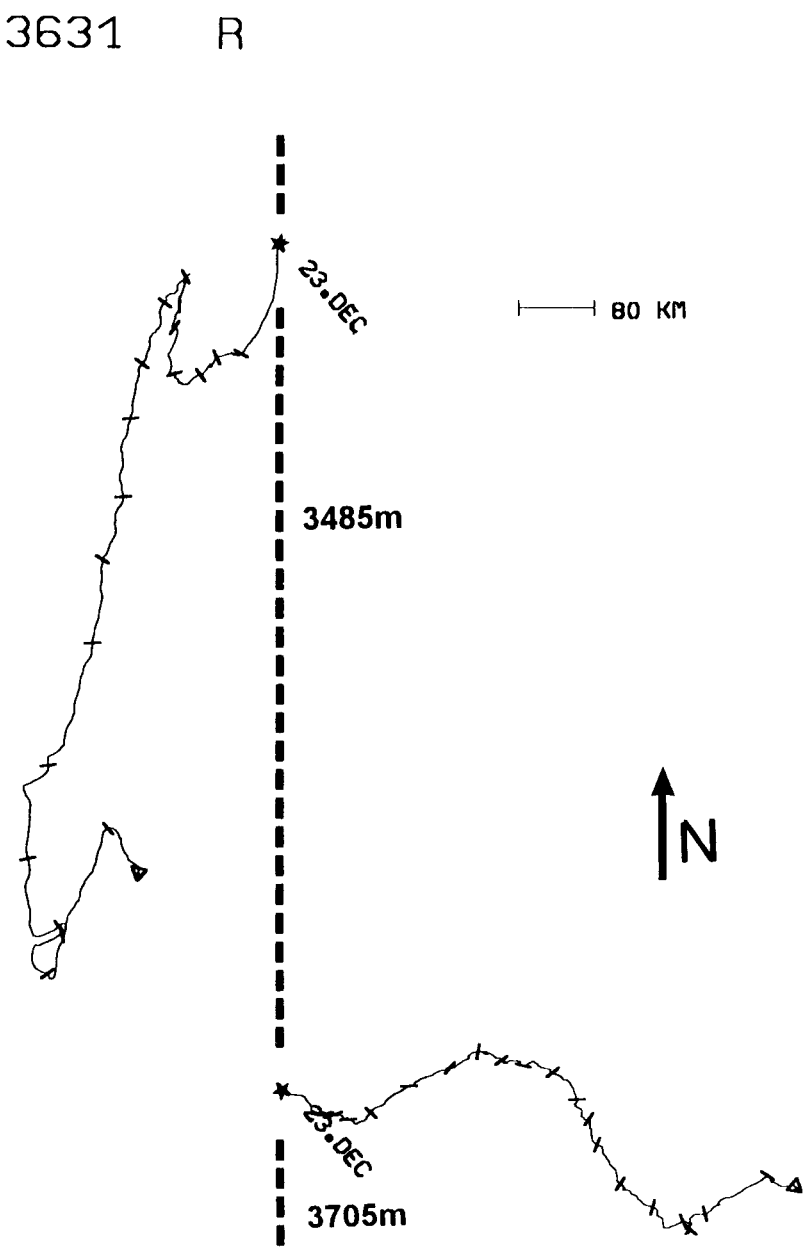

Fig. 54: Progressive vector diagrams of currents from mooring R. Tics were separated by 30 days.

5.3 Near Surface Circulation from Satellite Tracked Drifters (W. Krauß)

During M 28/1 and M 29/2 a total of 30 satellite tracked buoys has been deployed in the central part of the South Atlantic in order to fill the gaps in the present pattern. Fig. 56 depicts the trajectories obtained until April 30, 1994. All deployments have been made from RV METEOR and RV POLARSTERN. After completion of the programme in 1995, mean values of the velocity field will be assimilated into a numerical model in order to simulate the 3-dimensional mean circulation of the South Atlantic.

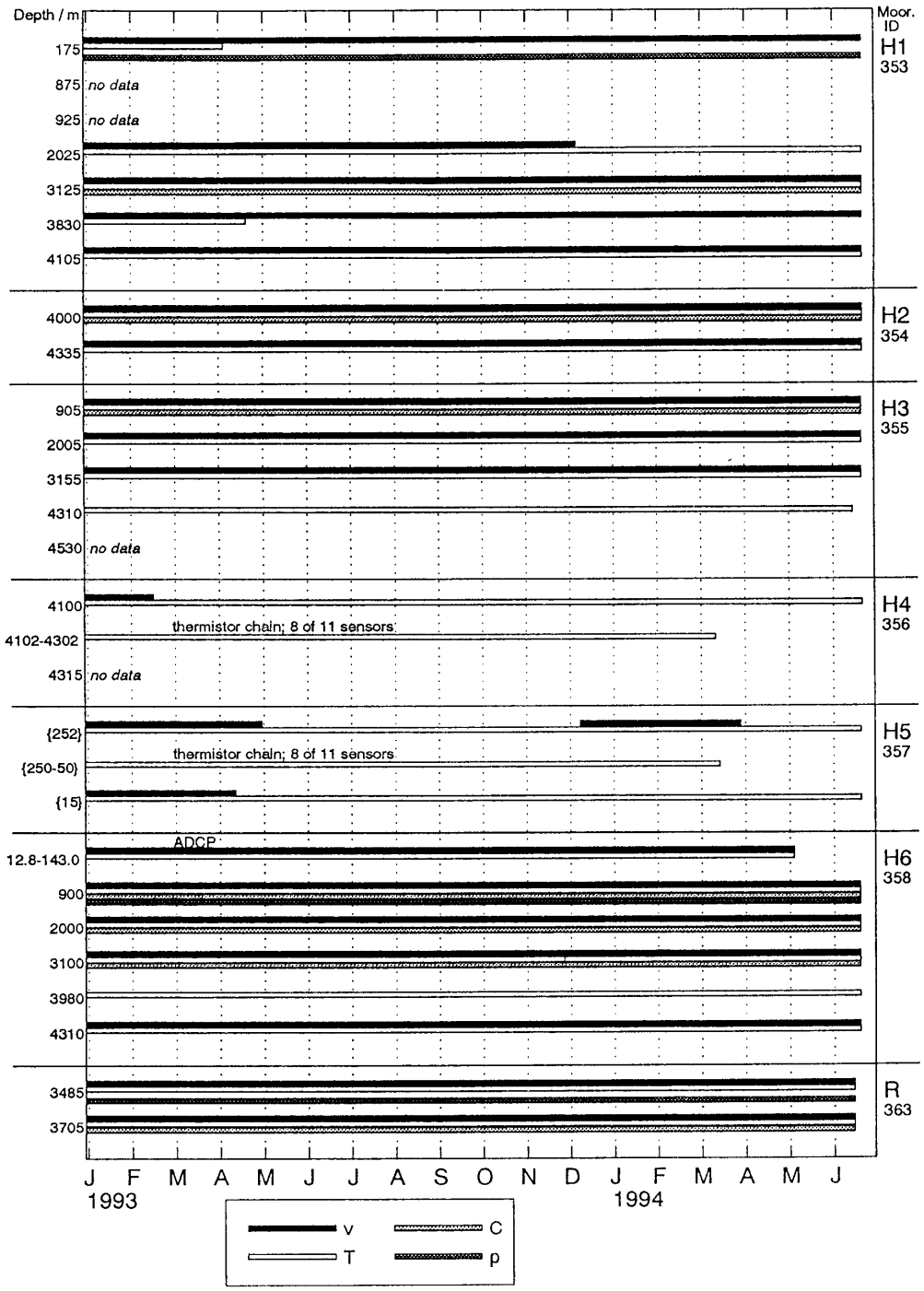

Fig. 55: Performance of moored instruments in the Hunter Channel (H1-6) and on the Rio Grande Rise (R). Temperatures are represented by light beams, current vectors by black beams. Other parameters are displayed by dark beams. More information on the individual records contains Table 7. Depths in {} indicate clearance from bottom. V=vector, C=electrical conductivity, T=temperature, p=pressure, ADCP=Acoustic Doppler Current Profiler.

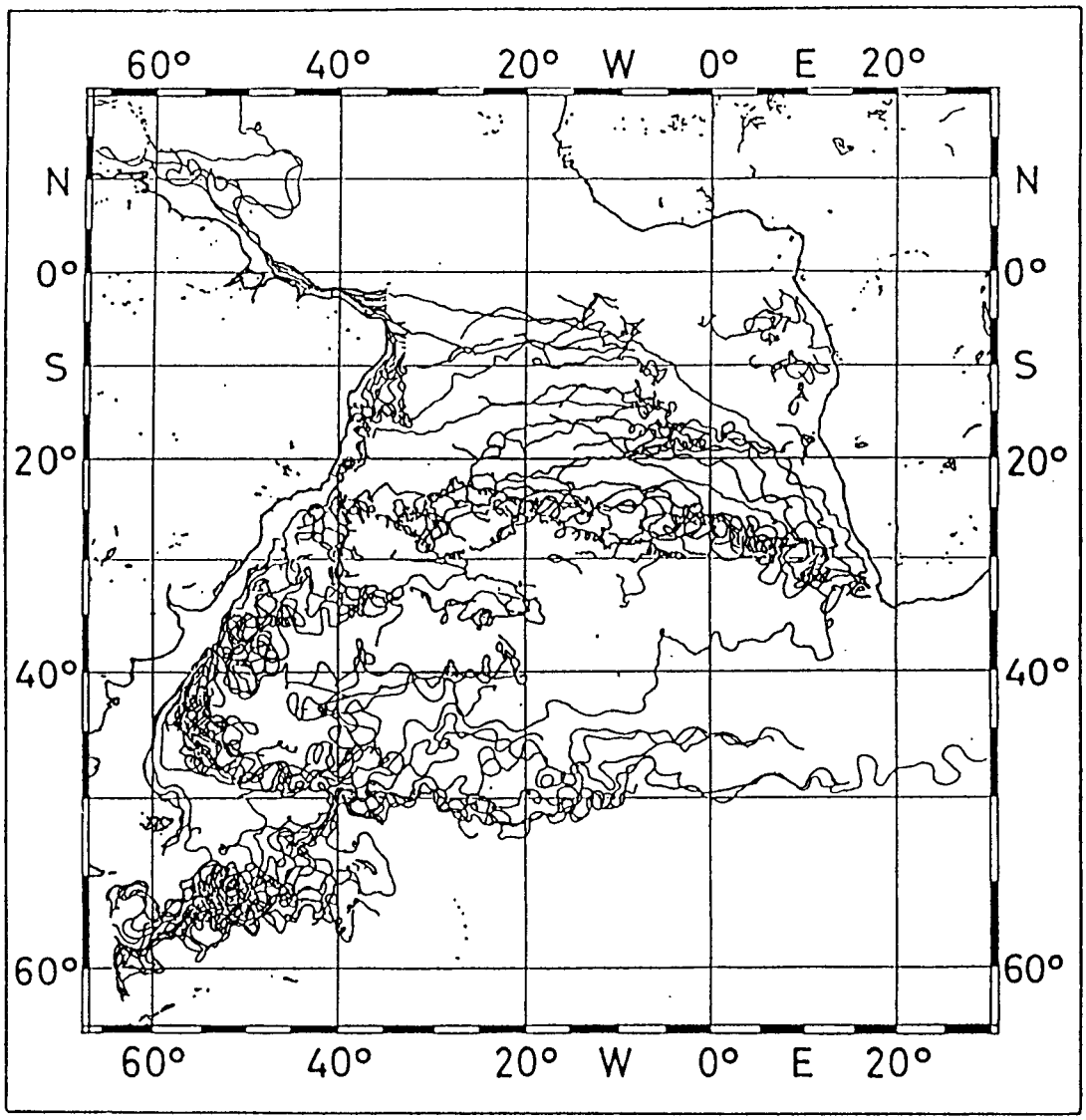

Fig. 56: Trajectories of the WOCE drifting buoy data set (status: April 30, 1994)

5.4 **GEK Observations** (T. Knutz)

On both legs of M 28 the GEK system operated without any failure. The only area the GEK could not be used was the eastern shelf area of Africa because of missing clearance. The GEK data were sampled with 50 kHz. Averaged data were recorded every minute. Environmental data from the ship's data acquisition system DVS were available in two minute intervals.

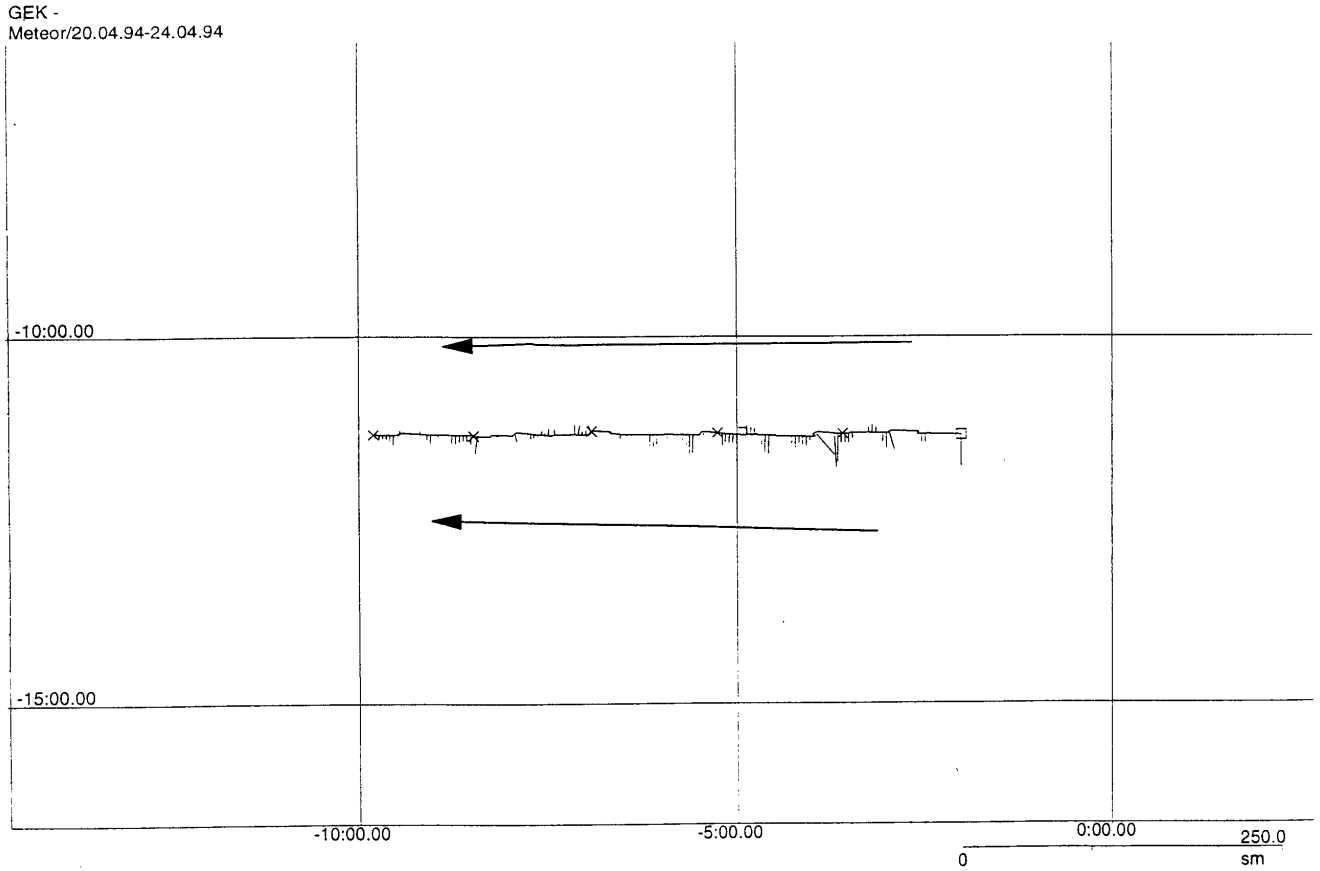

Fig. 57: GEK, 20 April –24 April 1994

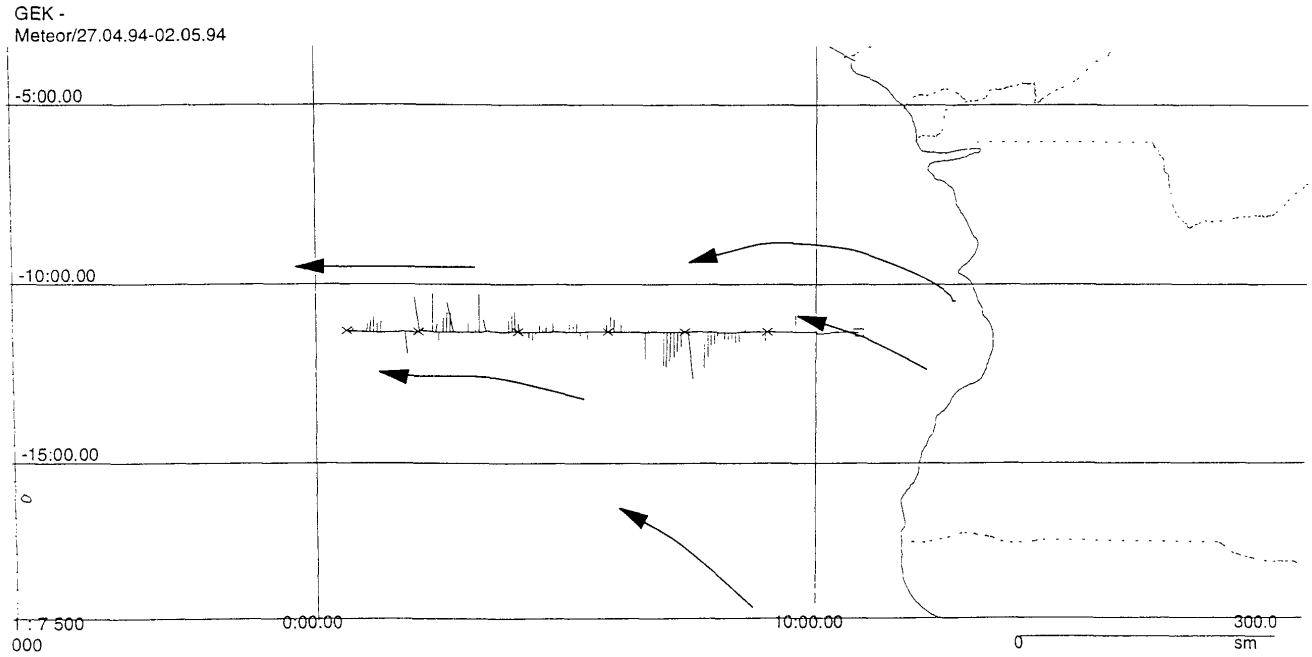

Fig. 58: GEK, 27 April – 02 May 1994

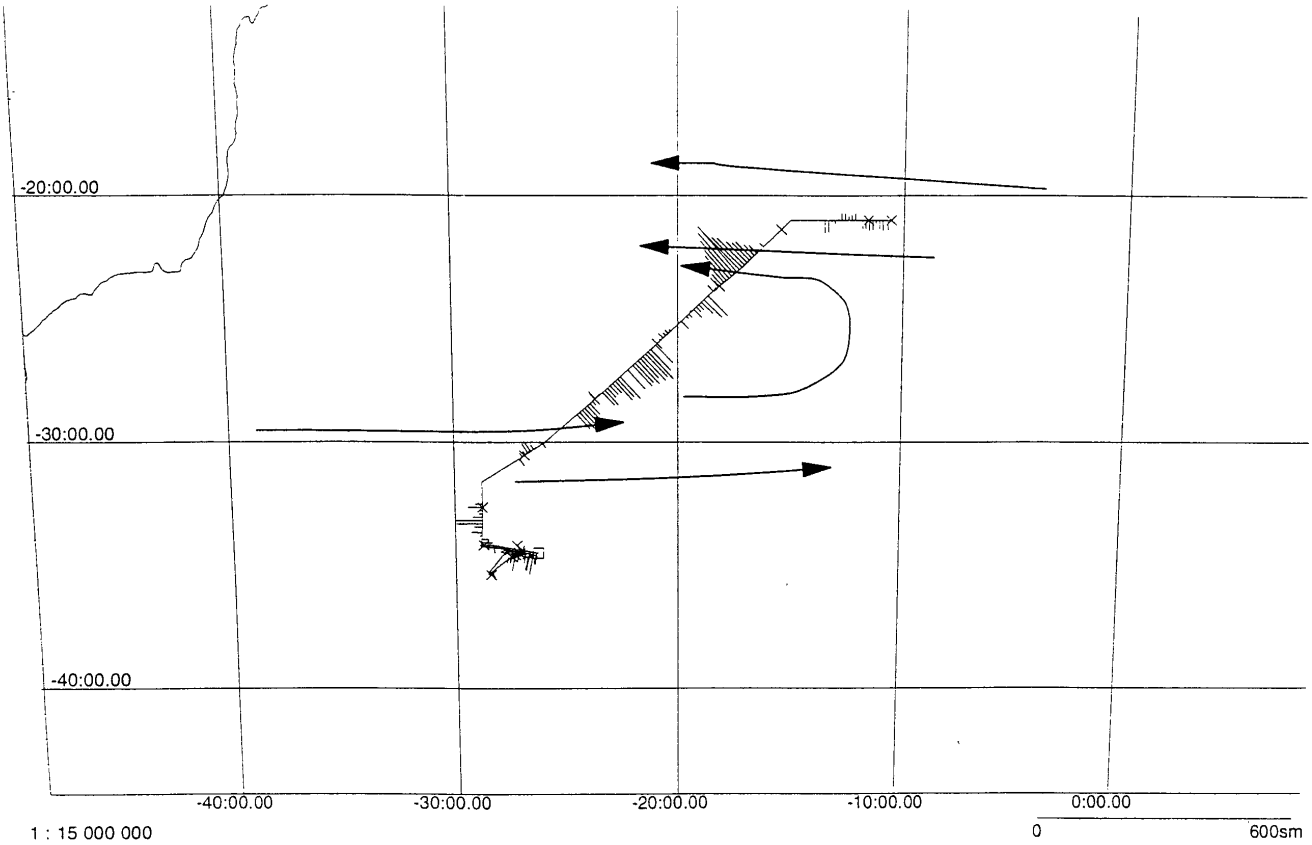

Fig. 59: GEK, 20 May – 02 June 1994

There was a principal difference between both legs. On M 28/1 the time between two CTD stations was in the range of 1 to 3 hours. In contrast during M 28/2 long distances without interruptions could be used for continuous GEK operation. Before and after each station a GEK zero control had to be done. During this time no data for current interpretation could be recorded.

In a previous data interpretation the GEK data had been linked together with position and meteorological data from the ship's DVS system. A course plot including GEK signals proportional to ocean currents has been constructed for both legs (Figs. 57-59). The vectors plotted rectangular to the ship's heading are GEK signals in mV. The numbers at the vectors are mean values. The registered signals in the range from 0.15 to 0.8 mV represent ocean currents in the range from 0.2 to 0.7 m/s. An exact calculation of ocean currents from the GEK signal will be realized in a second step of interpretation.

The GEK signals shown in the plots are time averaged in dependence of the geographical scale of the plots. In addition to the GEK signals current arrows are plotted within Figs. 57-59. These current arrows were taken from the atlas, "Quarterly Surface Current Charts of the Atlantic Ocean" published by the Hydrographic Department of the Admirality (1945). The numbers at the butts of the arrows give the rate in miles per day representative for three month (February, March, April or May, June, July). 10 miles per day represents an averaged velocity of 0.2 m/s. The

averaged currents described by the arrows are in the same scale as the GEK signals. In all plots a good correlation between the GEK signals and global current field is given. Differences can be caused by local effects as sudden wind changes or superimposed eddy motion. In Fig. 57 no significant current rectangular to the ship's heading could be recorded. The shown GEK signals represent currents in the range of 0.1 m/s. This is in good agreement with the global current in direction of the ship's course. In Fig. 58 is given a southern component by the 0.8 mV signal in the eastern area and a northern current (0.5 mV) component in the western part of the course plot. The signals plotted in Fig. 59 give a good example for GEK measurements as frontal zone detection system. The measurements have been taken in the area of subtropical convergence (United States Naval Oceanographic Office (1955)) with high seasonal variability. The reversing current as described by the arrows could be registrated with high geographical resolution by the GEK system.

In the future data processing the GEK signals will be calculated with the earth magnetic field and compared with meteorological observations, ship drift, ADCP data and CTD measurements.

5.5 Biological Oceanography and Taxonomy along 11˚30'S

(C. Zelck, H.-Ch. John)

5.5.1 Quantitative Data

5.5.1.1. General

Microscopic analysis was possible on board for 25 NEU upper net samples and 10 complete MCN stations from the Brazilian slope and adjacent oceanic area (see chapter 7.2.6). Analysis includes quantitative extraction of taxa Gammaridea and Hyperiidae, Hexapoda and fish, plus a qualitative record on the coarse taxonomic composition of the remaining plankton. The following chapters will exclusively focus on fish from the station sequence 169 - 189 (see Fig. 60). From these samples, the total catch of fish amounts to 3843 specimens, and a still insufficient identification of 79 taxa.

5.5.1.2 Taxonomy

From this station sequence alone, larval forms of 4 taxa appear to be undescribed, further 10 taxa are known to science, but are new for the team and the larval collection of the Zoologisches Museum Hamburg. These species belong to the complex of coastal (neritic) species, which are extremely difficult to identify. It is anticipated that further analysis might yield additional taxonomic findings.

5.5.1.3 Cross-slope Ecological Patterns

5.5.1.3.1 Abundance Patterns

NEU and MCN samples provide conforming results, though there is very little overlap in the species composition obtained by each sampler (Scaridae type 1, parrot fish, making the only

notable exception), and NEU samples are notorious for their diurnal changes in species composition (HEMPEL and WEIKERT, 1972), and catch per unit of effort (cpue).

Oceanic NEU samples yielded the typical pattern of higher daytime cpue (Fig. 61a; compare LOPES and JOHN, 1986, and literature therein), with prevailing beloniform taxa (flying fishes *Oxyporhamphus micropterus* and several species of Exocoetidae). Upper slope and shelf stations off northeast Brazil might prove to differ in diurnal periodicity and lacked the typical oceanic nighttime species of family Myctophidae (*Myctophum nitidulum, M. affine, Centrobranchus nigroocellatus*). However, the latter micronektonic groups showed low abundances in off-shore waters, too. From NEU samples as well as MCN (Fig. 61b, columns divided into cpue per stratum) it becomes apparent that upper slope waters (Sta. 169 - 174) yielded much higher cpue than open ocean waters.

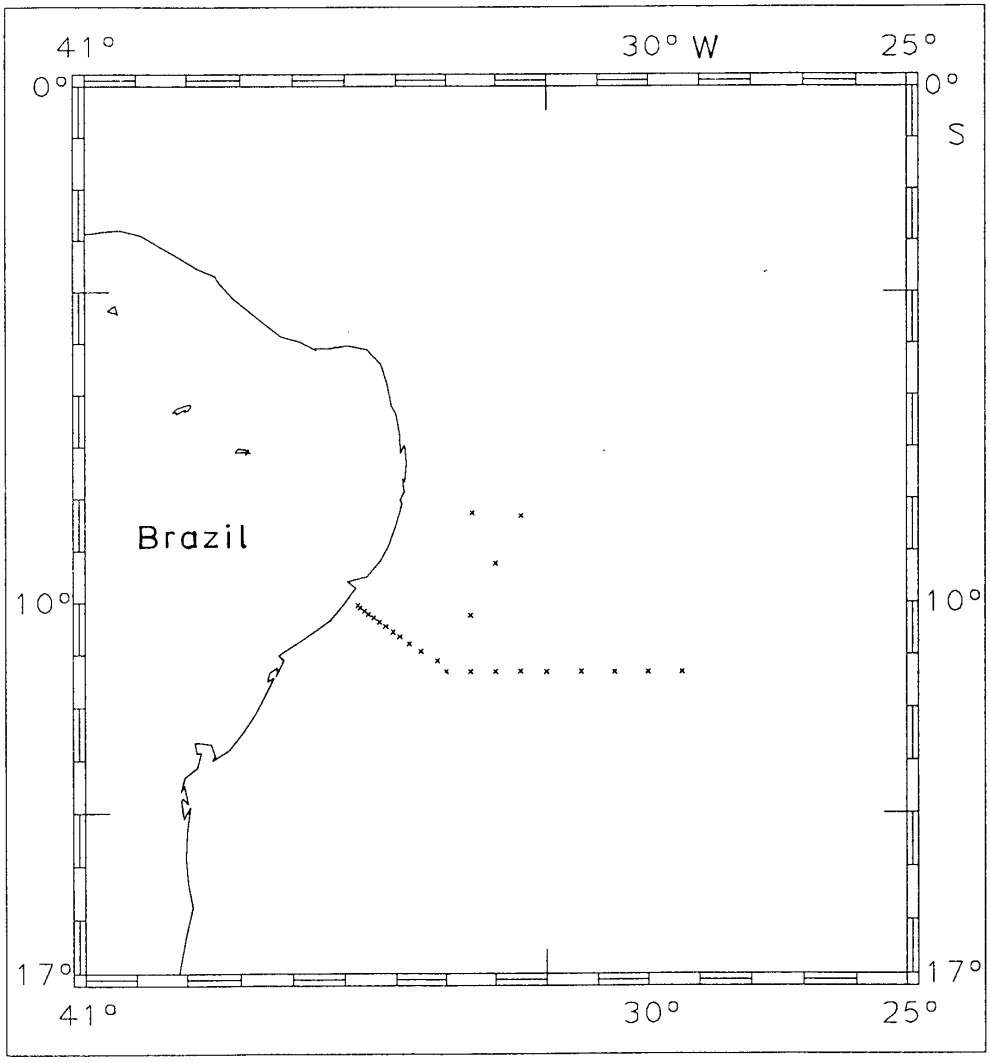

Fig. 60: The location of ship station nos. 165 – 189. The consecutive series are Sta. 169 (coastal) to 189 (off-shore) discussed in text.

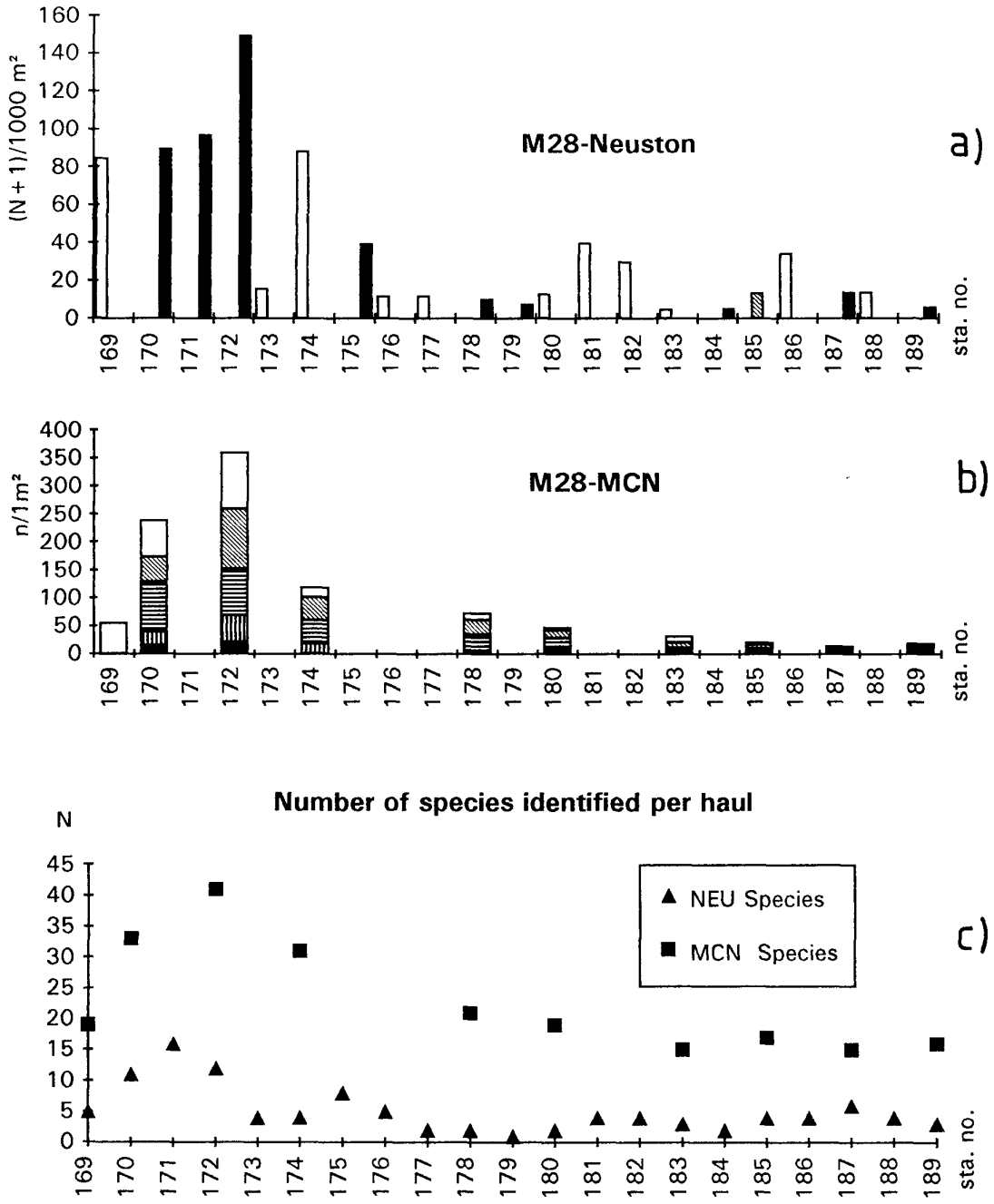

Fig. 61: Abundance values of fish larvae and numbers of species identified.
Top (61a): Neustonic fish. The shading of columns represents light conditions during catch.
Middle (61b): MCN fish larvae per step, upper part of column (light) indicating upper 25 m, and lowest part (dark) 150 – 200 m. Sta. 169 is biased to low values
Bottom (61c): Number of species per station in MCN (squares) and NEU (triangles). MCN Sta. 169 may be an underestimate.

5.5.1.3.2 Diversity and Species Composition

A similar relation is revealed by the number of species identified (the MCN-values are likely to be underestimates due to identification problems) shown in Fig. 61c, neritic ecosystems being more diverse than oceanic ones. The neustonic realm is, due to its environmental stress, a habitat suited only for especially adapted organisms (HEMPEL and WEIKERT, 1972), and has thus a lower diversity than the epipelagic and mesopelagic layer sampled by the MCN. It seems to be an advection-related ecological signal, that diversity in the MCN decreases further off-shore than in the NEU (see below).

A preliminary calculation of the percentages of neritic and oceanic species among total catch (Fig. 62) yields some differences between NEU and MCN. For NEU there is a sharp decline of oceanic species from Sta. 178 - 176, while such a decline in MCN only amounts to some 20 % (there are less identification problems and consequently more precise values for oceanic elements). On the contrary, neritic species reach further off-shore in MCN samples than NEU samples (the entire neritic curve in Fig. 62b is likely to increase by some 20 % after better taxonomic analysis and inclusion of less conspicuous elements into the group).

The boundary between the neritic and oceanic regime was much sharper and closer to the shore than found for the South Brazil Current, but there too oceanic elements are found in shelf waters (compare ANDRES et al., 1992; ZELCK, 1993).

It is furthermore noteworthy, that species like tropical oceanic-ubiquitous *Diogenichthys atlanticus* or *Vinciguerria nimbaria* were expected, but in fact proved absent or rare off Brazil (and somewhat deeper than in the NE Atlantic). On the other hand, catches of *Sudis atrox, Evermanella* or tuna exceeded by far previous catches.

5.5.1.3.3 Vertical Distribution and Implication for Cross-slope Zonations

An overall relative vertical distribution of fish larvae is given in Fig. 63. Generally some 50 % of all larvae were caught in the upper 50 m, and almost consistently some 80 % were contributed in the upper 100 m (Sta. 169 is an exception and biased as only half the bottom depth was sampled due to opening-closing problems).

As for the defined station sequence so far only about half of the samples with vertical resolution could be sorted, a detailed analysis on species level and differing individual depth preferences was hardly feasible. Differing vertical patterns are exemplified by species Scaridae type I, having an extended-shallow pattern (Fig. 64), and an oceanic deep group. Scaridae I occurred also in NEU samples seawards up to Sta. 175. However, in the MCN this species was encountered regularly up to and including Sta. 180, and with a shift towards deeper occurrences there. As we have a general pattern of a more restricted coastal regime in the NEU than in the MCN, we presume that off-shore displacement of surface plankton is restricted by the westward flowing South Equatorial Current, while at mid-depths an eastward transport (by a South Equatorial Undercurrent?) apparently takes place to some 120 n.m. from the shelf edge. Nevertheless, considerable advection of oceanic species also occurred up to the shelf edge (Fig. 62), and perhaps at depths of between 50 and 200 m (Fig. 64) by along-slope currents.

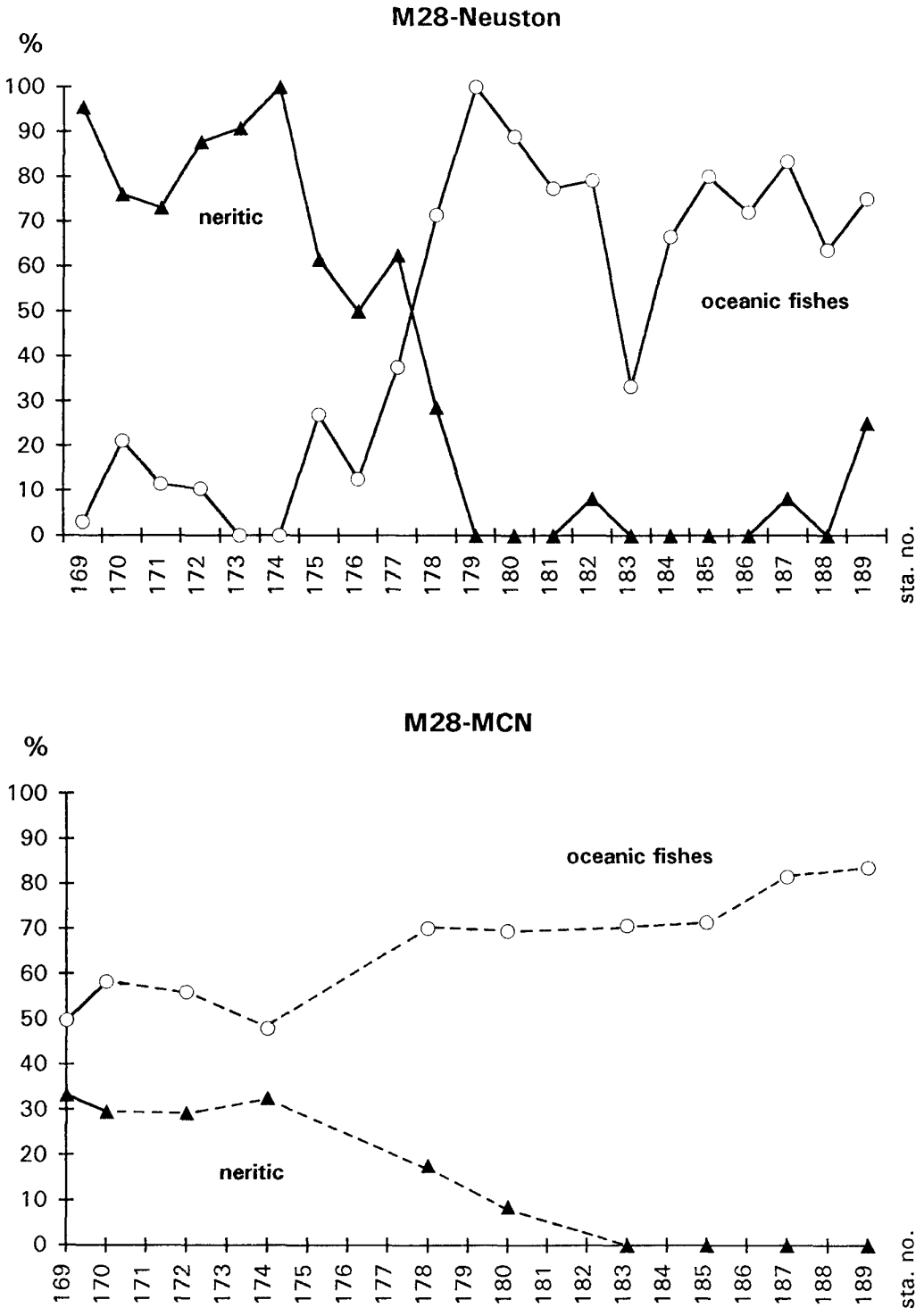

Fig. 62: The relative percentages of neritic (triangles) respectively oceanic species (circles) among total catch of NEU (top) and MCN (bottom). MCN-neritic values may be underestimate.

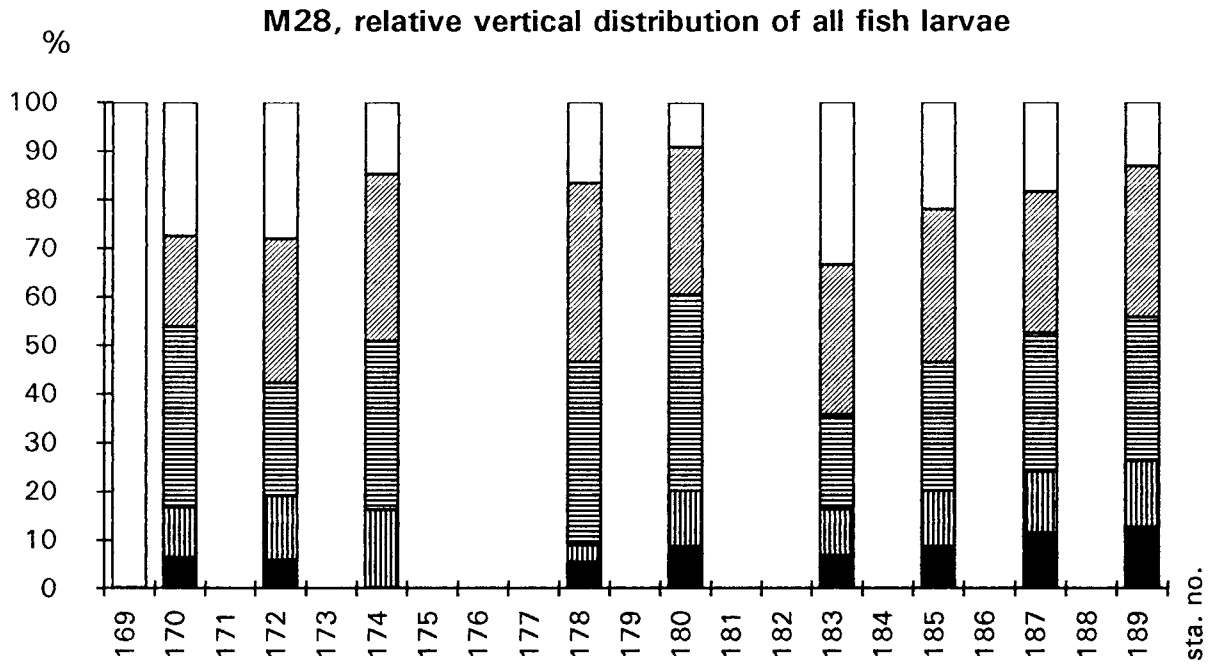

Fig. 63: The relative vertical distribution of total fish larvae in MCN-catches (shadings as for Fig. 61b).

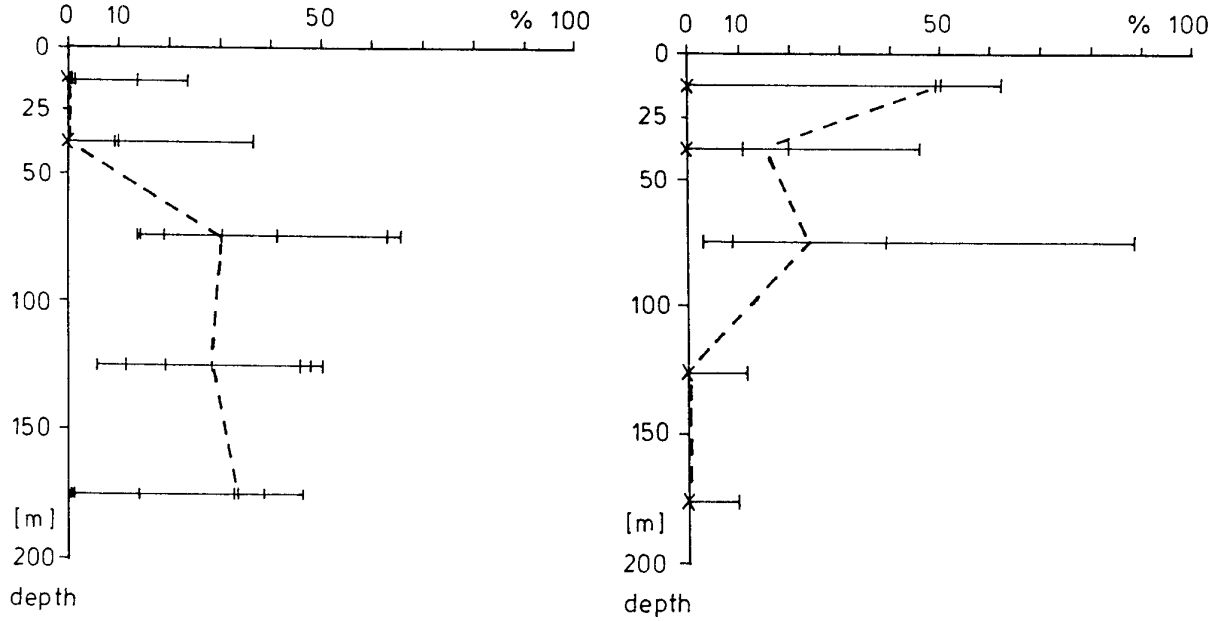

Fig. 64: The relative vertical distributions of oceanic-deep species group Alepisauroidei (left-hand, 7 hauls and 145 specimens) and coastal, extended-shallow species Scaridae I (right-hand, 4 hauls and 300 specimens). The interrupted lines connect median values.

5.5.2 The Plankton Material from the Central Atlantic to Angola: Findings, Hints and Expectations

5.5.2.1 General

It was impossible to microscopically analyze any further plankton sample. All following statements are based on macroscopical investigation during preservation of the sample, though some individual species or specimens in question had been picked out for closer identification under the microscope. Any numerical estimates may become void after microscopical analysis of larval numbers. Hoping that the team can be maintained as it is, a thorough analysis of the entire, huge load of material will take about four years. The priority to work from the Brazilian coast eastwards was set a long time ago.

5.5.2.2 Plankton Biomass Volumes and Micronekton Numbers

As already stated for Brazil, from Sta. 189 onwards and until having crossed the Mid-Atlantic Ridge, plankton biomass and numbers of adult Myctophidae remained at a comparatively low level. Myctophids were mainly "slendertails" and *Myctophum affine*, considered by us as typical for the low productive central gyre zones.

Immediately after crossing the Mid-Atlantic Ridge, both values increased distinctly. Checking regularly adult Myctophidae (following a request of myctophid taxonomists demanding *Lepidophanes* specimens), we were able to identify and deep freeze 4 *L. guentheri* immediately after catch for genetical analysis (Sta. 242 and 247). These specimens were transferred from board directly to P.A. Hulley in Cape Town. Other Myctophidae (e.g. *Diaphus sp.*) were often identified to generic level only, as there was not enough time (and literature) for thorough identification.

Somewhat down current of the Dampier/Cardno Seamount group we caught a tiny but adult dragonet (Callionymidae, Sta. 218, 200 - 150 m). Though not acquainted with this complex and difficult family, it might prove to become a new species. At Sta. 257 a beautiful larva of *Loweina rara* made a nice addition to our existing series of smaller larvae of this species, an amended description is in progress.

In the samples adjacent to the mentioned seamounts, plankton biomass and numbers of micronekton increased furthermore. Apparently this was less a seamount effect than a general East Atlantic feature, as both values remained high towards the slope of Angola. We estimated both figures to be two orders of magnitude higher than in the Brazilian off-shore area, sometimes we had problems to hose down the plankton in the nets. Sta. 264 yielded high numbers of transforming *V. nimbaria* and will perhaps reveal even higher larval numbers. While high numbers of myctophids occurred until the very last and shallow station (Sta. 290) above the Angola shelf edge, plankton volumes decreased distinctly at stations 289 and 290. Angolan ichthyoplankton obtained a neritic characteristic (larvae of Serranidae, Scorpaenidae and Carangidae becoming abundant) from Sta. 285 onwards. These stations seemed to differ also in vertical distribution, as plankton biomasses decreased sharply below 50 in depth, conforming with sharp density gradients below 30 m.

5.5.2.3 The Juvenile Life Stage of *Bathylagus argyrogaster*

Exciting results yielded Sta. 283. The MCN caught 3 juvenile specimens of *Bathylagus argyrogaster* (deep-sea smelt) at depths 150 - 100 m, 50 - 25 m, and 25 - 0 m. They were coloured unlike larvae or adults, but like typical epipelagic species, with blue dorsum and silver ventral side. According to literature the dorsal colour of adults is black or brown (BLACHE, 1964; NORMAN, 1930). The species is generally considered to be endemic of the Gulf of Guinea and bathypelagic (BLACHE, 1964), but KOBYLYANSKIY (1985) stated a mesopelagic range. BLACHE (1964) provided evidence that juveniles might have a shallower distribution than adults. Larvae have been described on the basis of METEOR material (HERMES and OLIVAR, 1987), and are known to be swept with the NE Atlantic Upwelling Undercurrent up to Cape Blanc. Three larvae have been reported from off Namibia (HERMES and OLIVAR, 1987), and at least one additional larger South Atlantic larva was caught now at M 28, Sta. 283. In the mean time we learned, that larvae are stenobathic 60 - 90 in, and follow deflections of the undercurrent caused by gyres like the Guinea Dome or the Mauritanian Central Gyre (own, unpublished data). We think this new finding might be connected with the Angola Dome plus the southward undercurrent, and it will shed new light upon a previously unknown epipelagic life stage of this otherwise deep-sea species.

5.6 Atmospheric Physics and Chemistry along 11˚30S

(J. Brinkmann, G. Schebeske)

Although needed for a better understanding of the atmosphere as well as input information for different theoretical models (for example on cloud formation and radiation balance) the amount of data on marine aerosol is very crude.

During M 28/1 measurements of different physical and chemical properties of the marine atmosphere have been carried out. Furthermore investigations of the oceanic surface layer had been made. These measurements have to be seen in comparison to previous measurements made during the last few years in other areas of the Atlantic Ocean.

As we did not have any permission to work within the 200 sm-zone off-shore from the Brazilian coast our measurements began on April 6, after having left that zone and were finished on May 6, near the Angolan coast.

The preliminary conclusions are described below:

1 Two optical particle counters in combination with a diffusion box and two impactors were used to measure the number size distribution of the marine aerosol particles in the size range of 0.002 micrometer to about 50 micrometer radius. Initial results show relatively homogeneous concentrations during most of the time of the cruise. First investigations of our data in the lower particle size range are shown in Fig. 65. The spectrum is an average of all the measurements done during the cruise in that particular range of particle size. In correspondence with the model distribution of marine aerosole (JAENICKE, 1987) the spectrum is of bimodal nature. The absolute values of our mean size distribution have to be validated in further tests. However, the shift of both of the models seems to be of special interest. This phenomenon will be investigated in detail in future examination of our data.

The particles in the super micrometer range show a clear diel behaviour with higher concentrations during the night.

A noticeable increase in the concentrations measured next to the coast took place very late, i.e. about 500 km off-shore, which is probably due to the southerly winds next to the African coast. We also observed a slight rise in the aerosol particle concentration while crossing the shipping route South Africa - Europe.

Besides these effects we also found an increase in the concentration in the upper size range of the particles from April 27 to April 28. Comparing Fig. 66a and 66b it can be seen that there had been a doubling of particle concentration in both of the two channels measuring the bigger particles while the channel counting the small ones remained indicating a relatively constant number concentration. This effect took place when we had a slight change in the weather conditions: The sky became more cloudy, the wind strengthened. So reasons might be the minor convection and an enhanced production of big particles due to the wind. Examinations of the filter samples will give more information of the nature of these additional particles.

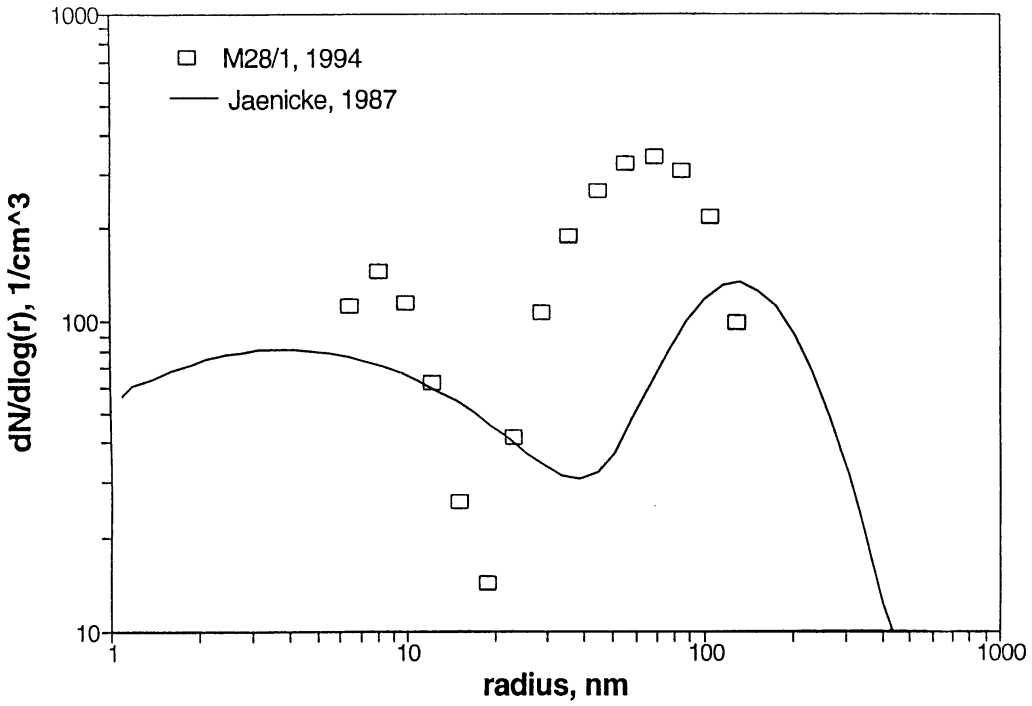

Fig. 65: Marine aerosole; number size distribution of aerosol particles; symboles: Mean distribution, measured during M 28/1, South Atlantic; solid line: Model distribution, calculated by means of the parameters and equations given in JAENICKE, 1987.

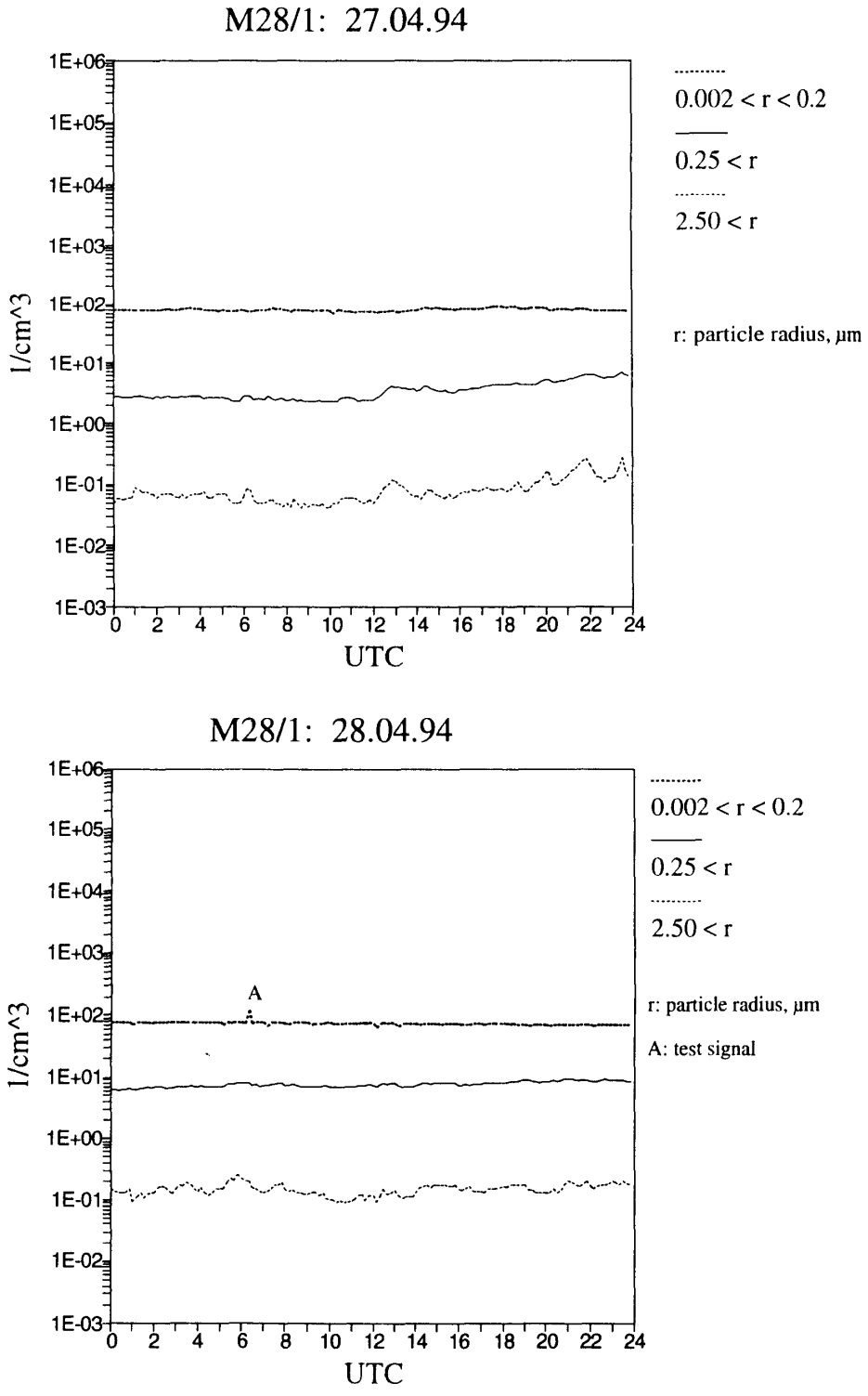

Fig. 66: Number concentration of aerosol particles in different size ranges, 10 min. means, measured during M 28/1;
a) April 27, 1994;
b) April 28, 1994.

2 Soot is a very effective absorber and thus of great importance for the radiation balance of the atmosphere. Nevertheless the amount of particulate carbon in an unpolluted area is poorly known, although recently some measurements have been made. We measured articulate carbon measured in various ways. Different sets of filters will be analyzed with optical and pyrolytic methods in order to get some information on the total and the black carbon. First investigations of the deposits on the filters, i.e. the degree of greyish-ness, showed an obvious dependence from the distance to the coast. The filters will also be used to compare the different analytical methods because up to now there is no standardized procedure for determining particulate carbon in the atmosphere.

3 During the period given above we sampled aerosol particles daily in three size classes by means of two different impactors. These specimens will be analyzed by energy dispersive

X-ray analysis and a protein dye technique in order to determine the amount of biological or biologically contaminated particles. The analysis can not be done on board in detail but, as expected, the relative amount of soil derived particles seems to be distinctly higher in front of the Angolan coast than in the middle of the South Atlantic.

Analogous investigations had been made with samples got on two previous cruises showing differing results. At the moment we cannot explain this behaviour but hopefully these new measurements give some further information. The differences might be due to dimethylsulfide.

4 Dimethylsulfide (DMS) is unstable in air and oxidizes to sulfate to form particles. So it is of some interest to correlate DMS with the total particle concentration as well as with the particles of biological origin. DMS in air has been sampled and analyzed automatically. During the cruise 1400 samples have been analyzed. The concentration was between 150 ng and 400 ng per cubic meter air. It was found a slight increase in the concentration while approaching the African coast. The diurnal course of DMS with an afternoon minimum could be confirmed.

5 DMS in ocean water was sampled by means of a membrane pump four times a day at 00, 06, 12, and 18 local time. All together 120 samples were analyzed. The water contained between 120 ng and 480 ng DMS per liter. We also found a slight increase while getting closer to the Angolan coast.

6 The above mentioned samples had been analyzed for chlorophyll and phaeophytin, too. Because there had been no way to calibrate the measurements on board the absolute amounts can not given here but will follow. An increase of the measured signal of chlorophyll concentration in oceanic water increased parallel with the atmospheric DMS.

5.7 **Radiative Physics** (W. Emery, M. Suarez)

The world's ocean serve as an vast reservoir of heat in the ocean/atmosphere engine. For this reason, it is impossible to accurately model global climate without first understanding the heat exchanges between the ocean and atmosphere. Since the advent of weather satellites, scientists have been allowed to gather data from around the world in a matter of hours or days. One of the key quantities measured in this fashion is global sea surface temperature (SST).

In the past, satellite radiometric measurements have been calibrated using SST measurements taken from drifting buoys or ships which is not physically correct. These methods measure the temperature of the seawater at a depth of a meter or more, that is, bulk temperature. Satellites, however, only measure the radiation emitted from the upper few microns, or skin temperature. Due to the latent heat released by evaporation, sensible heat and the net long wave radiative emission, the skin temperature is generally cooler than the bulk temperature. It is possible though, during periods of high wind or strong solar insulation, that the skin may be of the same or higher temperature than the water below. The difference between the bulk and skin temperatures can occasionally be as large as 1˚C or more (SCHLUESSEL et al., 1990; WICK et al., 1992). While this difference may seem negligible, ROBINSON et al. (1984) suggests that an accuracy of 0.2˚C is necessary for satellite measurements to be useful in global climate prediction. For this reason a more accurate, radiometric method of sea surface temperature calibration has been developed.

As part of M 28/2 we employed a prototype multi-channel infrared sea-truth calibration radiometer (MISTRC) designed and built by OPHIR Corp., Littleton, Colorado. The experimental set up was patterned after a system developed by scientists in Hamburg and Kiel, Germany. Key aspects of the system include a bucket of continuously circulating ocean water which serves as a continuous calibration reference, and that the radiometer views the ocean at approximately the Brewster angle in order to minimize reflected radiation.

The radiometer has two independent optical trains, one operating in the short wave infrared (IR) and one operating in the thermal IR. The short wave head has filters at 3.7 and 4.0 μm and additional vertically polarized filters to further suppress the effects of reflected radiation. In the long wave region, the MISTRC has filters at 10.8 and 11.8 μm which are closer to the standard Barnes PRT-5 and Heimann KT-19 radiometers. These wave lengths are also similar to those on the advanced very high resolution radiometer (AVHRR) flying on the NOAA satellites and the along track scanning radiometer (ATSR) flying aboard ERS-1.

In addition to using the radiometric SST measurements to calibrate space borne radiometers, these measurements also give the opportunity to study the bulk-skin temperature difference. By understanding this difference, it may be possible to determine the bulk temperature from satellite measured skin temperature, or alternately to predict the temperatures calculated from satellites based on bulk measurements.

In order to help better our understanding of the temperature difference and the heat fluxes involved, an entire suite of atmospheric, oceanographic and radiometric measurements are taken. Atmospheric variables include dry and wet bulb temperature, pressure and surface wind as well as the profiles taken by radiosonde balloons. The primary oceanographic variable used is the bulk temperature from the hull mounted sensors and the thermosalinograph, however salinity and temperature profiles are also taken for their importance in upper ocean stability. Upward looking pyranometers and pyrgeometers are used to measure the down-welling solar and terrestrial irradiance.

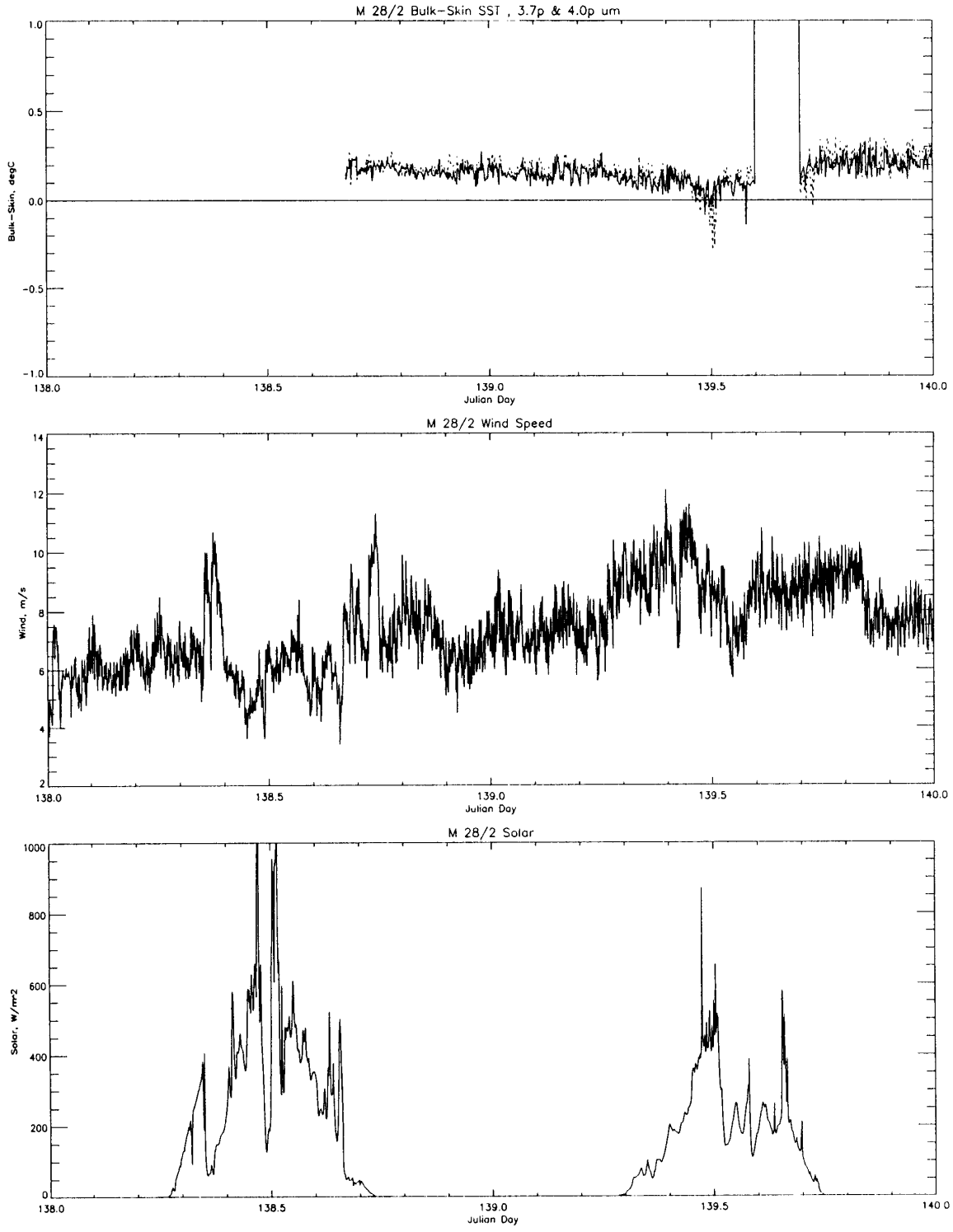

Fig. 67: Plots of bi-daily time series of radiative parameters. On top bulk-skin temperature deviations using the short wave polarized radiometer channels (3,7 and 4,0 μm) are displayed. The middle part contains wind speed. The lower plot shows down-welling solar irradiance.

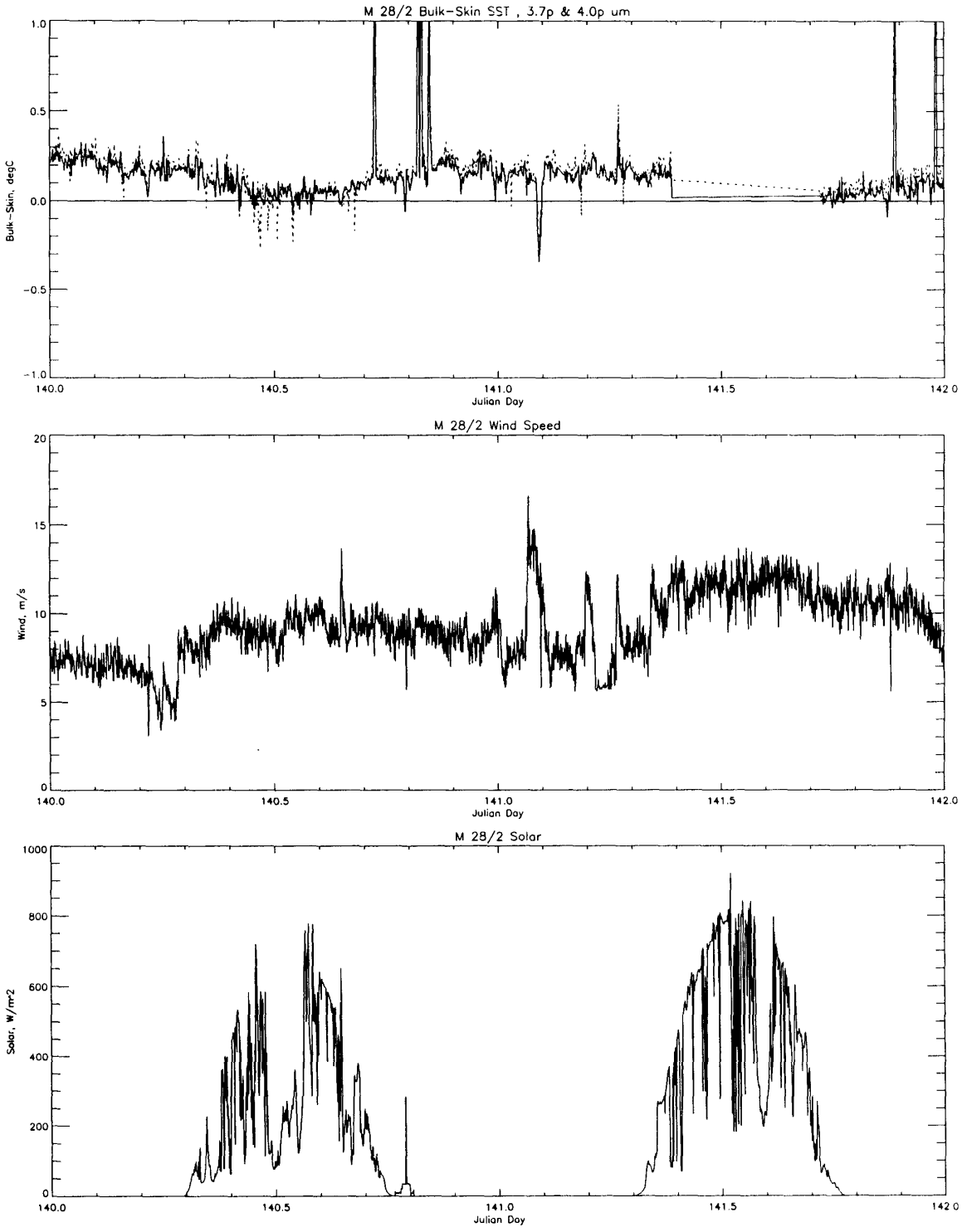

Fig. 68: Plots of bi-daily time series of radiative parameters. On top bulk-skin temperature deviations using the short wave polarized radiometer channels (3,7 and 4,0 μm) are displayed. The middle part contains wind speed. The lower plot shows down-welling solar irradiance.

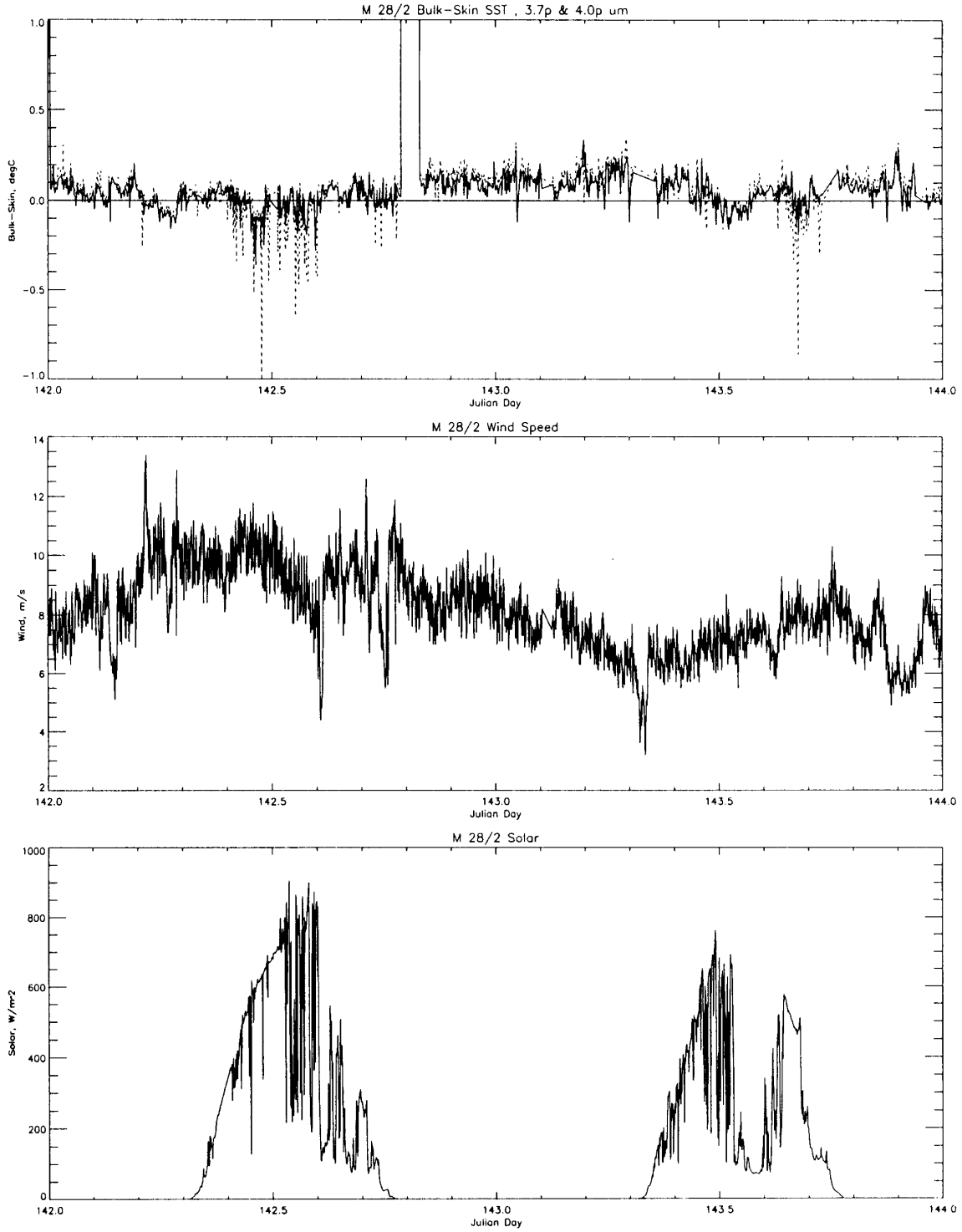

Fig. 69: Plots of bi-daily time series of radiative parameters. On top bulk-skin temperature deviations using the short wave polarized radiometer channels (3,7 and 4,0 μm) are displayed. The middle part contains wind speed. The lower plot shows down-welling solar irradiance.

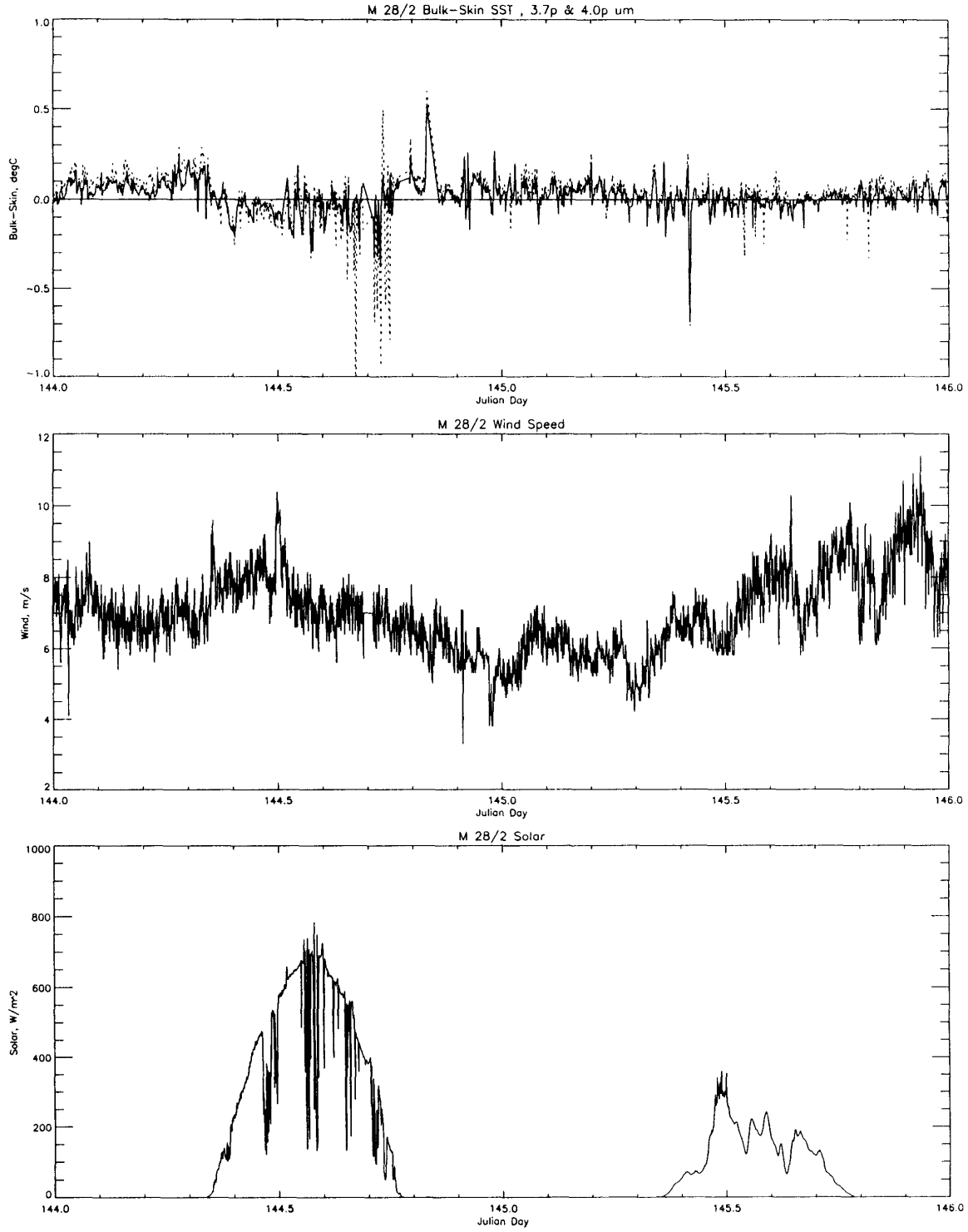

Fig. 70: Plots of bi-daily time series of radiative parameters. On top bulk-skin temperature deviations using the short wave polarized radiometer channels (3,7 and 4,0 μm) are displayed. The middle part contains wind speed. The lower plot shows down-welling solar irradiance.

Preliminary results from the first eight days of system operation are shown in Figs. 67-70 in the form of four bi-daily time series plots. The Julian day, 138 corresponds to May 18, 1994 and so forth. On each page, the top plot is of the bulk-skin temperature deviation using the short wave polarized radiometer channels, the middle plot is of surface wind speed and the bottom plot is of down-welling solar irradiance.

Important things to note are that the surface temperature deviation is generally positive, that is, the skin temperature is cooler than the bulk temperature. Also note that this difference changes sign (i.e., a warm skin) during periods of intense insulation. A notable exception to the latter is at the beginning of Julian day 141, May 21, when the temperature deviation dips below zero shortly after midnight. This dip corresponds with a large wind event which may have disturbed the skin layer. Whether this was, in fact, the case or whether the wind simply caused an inaccuracy in the calibration is difficult to say, but this behavior is not typical. Towards the end of day 144, May 24, the data begins to behave poorly. This was approximately the time we began having mechanical and electrical problems with our data.

For the last two weeks of M 28/2, the preliminary results of our data do not look good. Unfortunately, this is often the case with prototypical instruments. Our radiometer is currently back home at OPHIR for post-cruise inspection and recalibration. It is hoped that with the help of the scientists and technicians at OPHIR we may be able to salvage data from the final two weeks. It should be duly noted that this was the second experiment using the MISTRC radiometer and on its first voyage it performed flawlessly. Every time radiometric SST measurements are made, it adds to the wealth of knowledge about bulk-skin temperature deviation and improves the foundation for further research.

5.8 **Marine Geology** (R. Cordes, J. Funk)

Sediment and water samples have been taken during the M28/2 (see chapter 7.2.7) on a section across the subtropical South Atlantic (Angola Basin, Brazil Basin, Hunter Channel and Argentine Basin).

On 22 stations a minicorer was used to sample the sediment surface. The corer (Fig. 71) works similar to the multicorer which was successfully used on a number of cruises before. The minicorer, however, only has four tubes and is of low weight so that it is possible to use it below a CTD probe. The big advantage is only to need a few minutes extra time per station to get a deep water profile in combination with sediment samples from the uppermost 10 - 30 cm of the underlying sediments at the same time.

The aim of the geological sampling during leg 2 was to obtain core material and water samples for paleo-oceanographic studies from the last glacial to recent times. The studies are carried out within the framework of the "Sonderforschungsbereich 261" at the Department of Geosciences of the University of Bremen.

On the water samples, stable oxygen isotopes, isotope composition of $\sum CO_2$ and nutrients will be measured to improve the GEOSECS-data set (Geochemical Ocean Section Study) of the Atlantic and to investigate the relationship between nutrients and the $^{12}C/^{13}C$-ratio.

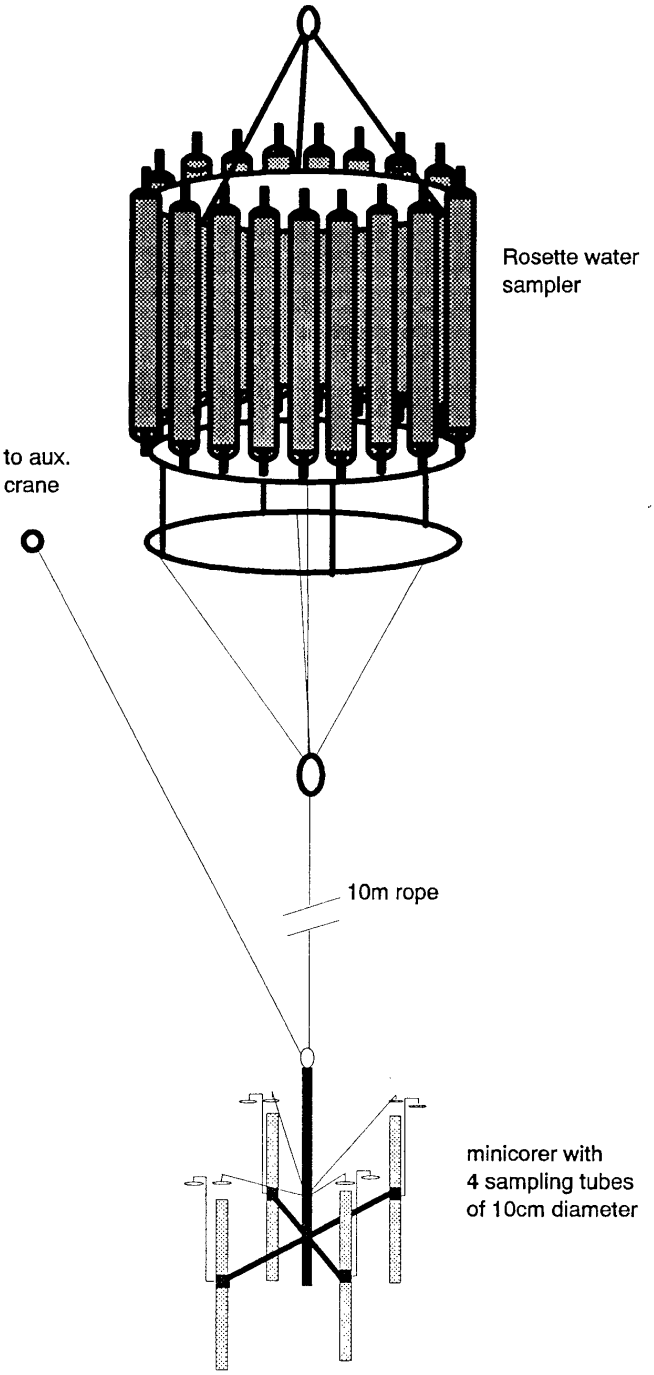

Fig. 71: Scheme of the minicorer. It is fixed by a 10 in rope below the rosette. As the outrigger of the main crane is not high enough, it has to be fixed to an auxiliary crane by an additional rope. It is brought out before the rosette, the auxiliary rope is unhooked and fixed to the rosette as soon as the 10 m main rope comes tight. It is recovered the reversed way. Bringing out and recovering the rosette with the minicorer using the auxiliary crane takes about 10 minutes additional time per sampling station compared to the rosette without minicorer.

5.8.1 Sediment Sampling

The four tubes of the minicorer were sampled as follows:
First tube: The uppermost 5 cm were cut in 1 cm thick slices, which were filled in Kautex-bottles and than preserved with Rose Bengal. Below that depth each 5 cm a one 1 cm thick slice was taken and filled up unpreserved. These samples will be used to determine the foraminiferal assemblage and the stable oxygen and carbon isotope-composition of the foraminifera.

Second tube: These samples were completely frozen up. Diatom and radiolaria assembleges will be studied on the sediment.

Third tube: Here also the uppermost 5 cm were cut in 1 cm slices. Each was filled into a petridish and then frozen to -20˚C. The C/N-ratio of the organic material will be measured on these samples.

Fourth tube: This tube was completely frozen for the archives.

5.8.2 Water Sampling

The water samples were taken with a CTD-rosette including 24 Niskin bottles (10 l) which were closed at different water depths.

All water samples will be analyzed for the stable oxygen isotopes composition of the water and $^{13}C/^{12}C$ -ratio of the $\sum CO_2$. Besides measurements of nutrients are planned, to study the coupling between the $^{13}C/^{12}C$-ratio of the $\sum CO_2$ and the nutrients.

For the measurement of $^{13}C/^{12}C$-ratio the water was carefully filled into 250 ml glass bottles to avoid contamination with air, and immediately poisoned with 1 ml of a saturated $HgCl_2$ solution. Later the bottle was sealed air tight with wax and stored in the cooling storage at 4˚C. The samples for the measurement $^{18}O/^{16}O$-ratio were prepared in the same way but were not poisoned. Both samples were returned to the laboratory at the Department of Geosciences at Bremen for further preparation.

Samples for nutrient measurements were taken twice from each depth to test different preservation methods. The water was filled into 10 ml scintillation bowls. One series was frozen to -20˚C the other one was poisoned with $HgCl_2$ and stored at 4˚C. Both series were returned to the Department of Geosciences at Bremen and will be analyzed there.

5.9 Environmental Chemistry (R. Rieger, M. Schneider, K. Ballschmiter)

5.9.1 Compounds of Interest

Chlorinated paraffins (CP) are known as complex mixtures of polychlorinated n-alkanes, which are characterized by the chain length of the food stocks and the grade of chlorination. These compounds are synthesized in industrial scale (100000 t/year Europe) for various products, i.e. lubricants, plasticizers and fire retardants. Thus a significant input into the environment occurs.

Due to the high stability of CP under environmental conditions they are not biodegradable but persistent. Only less data is available about the global occurrence and distribution of CP. In sewage sludge of different European cities CP levels are known in the μg/kg range and in the ng/l range in the South Atlantic. This project aimed at the confirmation of the occurrence of CP in the marine environment of the South Atlantic. Furthermore a temporary change in the level and/or pattern of CP might be determined.

Alkyl nitrates are, besides the more investigated molecules ozone and peroxyacetyl nitrate, components of the photochemical smog. Their atmospheric occurrence is related to the photo oxidation of anthropogenic and biogenic hydrocarbons and the steady increase in NO_X emission. The atmospheric life times are in the range of some weeks and allow therefore a long range transport to the unpolluted marine troposphere. Only little information is available about levels and pattern of alkyl nitrates in the South Atlantic region in relation of anthropogenic and biogenic hydrocarbon sources. Due to the relative high hydrolytic resistance of alkyl nitrates samples of surface water and water from the micro layer have been taken to investigate the distribution to these compartments. The micro layer possesses in order to higher temperatures increased activity of marine micro organisms. Biotic transformation of alkyl nitrates could be possibly seen by determining the enantiomeric ratios of chiral alkyl nitrates.

Furthermore the polychlorinated biphenyls (PCBs) have been analyzed as well as which serve as trace components.

5.9.2 Sampling Methods

5.9.2.1 Sampling of Surface Seawater

For sampling of surface seawater a solid phase extraction technique was employed which enables sampling of volumes up to 1000 liters. Surface seawater was provided by a bulk water inlet at the bow of the ship, two meters below the sea surface, and was served directly by a water tap in the laboratory. The seawater sampling apparatus consisted of two glass cartridges with a volume of 200 ml which were connected to the seawater tap. For solid phase extraction various polymeric materials are available which are appropriate to the sampling of the different molecules. Chlorinated paraffins were extracted on "Amberlite XAD-2", a cross-linked styrene-divinylbenzene copolymer with slight polar properties suitable for sampling chlorinated paraffins showing the same attributes. Alkyl nitrates contain more polarity and therefore "Amberlite XAD-7", an acryl ester polymer with medium polarity, has to be used.

The cartridges were packed with 90 g of XAD-2 or XAD-7 respectively, conditioned with 4 liters of seawater and spiked for quantification with internal standards (1,1,1,2,2,3,3-heptachloro propane, ε-hexachloro cyclo-hexane and tetrachloro naphthalene). A flow rate of approximately 400 ml per minute lead to sampling volumes of 300 to 550 liters which were determined by a water gauge. The first cartridge performs the sampling part, while the second should indicate the break through of the compounds. To exclude any contamination of the ship, no water samples were taken during stops. The essential blank tests were also carried out by performing the same procedures with an XAD cartridge (filling, conditioning, spiking with internal standard) except sampling,

Chapter 7.2.8 and 7.2.9 schedules the sampling positions, dates and volumes for precise sample characterization.

5.9.2.2 Sampling of Surface Micro Layer

The surface micro layer is known for its ability to concentrate natural and man-made compounds, like hydrocarbons or pesticides, compared to the bulk water below the surface. The thickness of the sampled micro layer is about 30 μm. Several methods of sampling this particular layer were developed. In this study a simple screen technique (GARRET, 1965) was used. A rectangular steel framed screen (16-mesh) is lowered vertically into the water, oriented horizontally and raised through the micro layer yielding app. 50 ml of film water which is drained through an outlet tubing. Sampling was carried out on weather side of a rubber raft which cruised at least 100 m away from the vessel to minimize any contamination. A four liter sample was taken at every site which was extracted twice by a liquid phase extraction with 50 ml hexane (nanograde) using a high speed stirring device. In total 12 samples of micro layer were taken at 11 sampling sites (chapter 7.2.10).

5.9.2.3 High Volume Air Sampling

High volume air sampling was performed using two High Volume Samplers (Ströhlein), which were placed on the upper deck of the ship.

Air is sucked through an adsorbent bed where the components of interest are trapped. Activated silica gel or a mixture of charcoal and silica gel were used for the sampling of CP. In case of alkyl nitrate sampling silica gel covered with 10% ethylene glycol is known to be effective. The volume of a single air sample ranged from 300 -1200 m^3. After sampling the material was sealed in glass flasks to avoid any contamination. Sampling efficiency is controlled by internal standard compounds, which are spiked in a well known amount. In total 44 air samples has been taken. Chapter 7.2.11 outlines the specific sampling data of the individual air samples.

5.9.2.4 Low Volume Sampling

The above described high volume sampling technique is only useful in the investigation of low volatile compounds such as chlorinated paraffins and alkyl nitrates with at least eight carbon atoms. Alkyl nitrates smaller than octyl nitrates cannot be retained quantitatively on the silica gel bed if amounts of approximately 300,000 liters of air are sampled. This is due to a general decrease in the break through volume with increasing volatility of the different compounds. The volatilities of methyl nitrate (C-1) up to heptyl nitrates (C-7) are in the range of dichloro methane and tetrachloro ethanes respectively. Low volume sampling technique of these compounds on a Tenax adsorption phase (phenylether polymer) is useful. The Tenax adsorption bed is packed in glass tubes (length 15 cm, inner diameter 0.4 mm). To avoid contamination during the transport and storage before sampling, the tubes were sealed by melting them in a second glass tube. On sampling date the outer tube is cracked with a glass cutter and the sampling tube is connected to a small air sampling pump. Diurnal volumes of 30 - 70 liters of air have been taken (see chapter 7.2.12). Air volumes were directly measured by connecting the outlet of the sampling pump with a gas counter. After sampling the tubes have been immediately resealed. The sampling efficiency

can be proved, because most samples are taken using two Tenax glass tubes in a row. The first tube represents the sample while the second will show a possible break through. Moreover blanks of this sampling technique will be checked. Therefore two Tenax tubes were opened on the ship and sealed afterwards without sampling. On M 28/2 twenty one low volume air samples have been taken. Explicit sample characterization (position, date, volumes) is depicted in chapter 7.2.12. Sampling locations are displayed in Fig. 72.

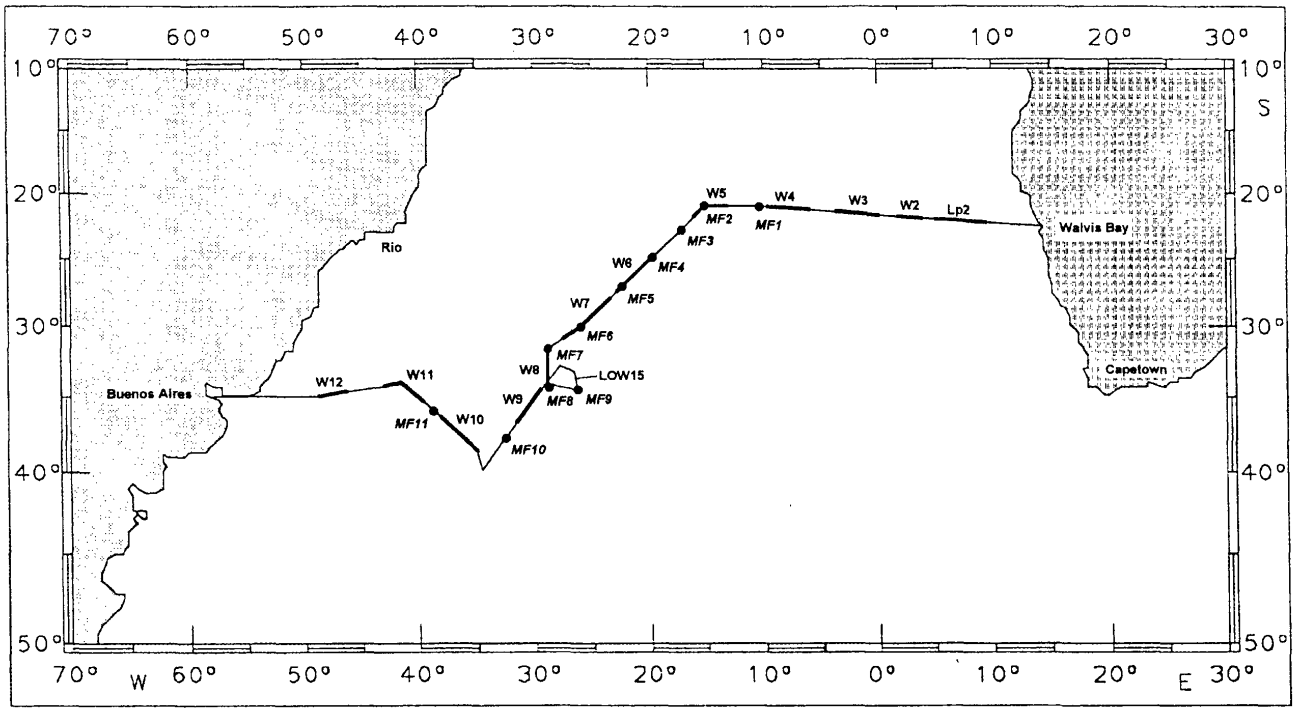

Fig. 72: Locations of environmental chemistry samples

5.9.3 Analytical Methods

All samples were spiked with internal standards, sealed and carried to Germany. Organic trace analysis requires high sensitive instrumentation (e.g. mass spectrometer) and the exclusion of any sample contamination. Several control samples (blanks) document the background level. Thus sample preparation and analysis were not carried out on METEOR but at the University of Ulm under controlled background conditions (clean benches).

In cases of High Volume Air Sampling and Surface Seawater Sampling the adsorbents are eluted by organic solvents, cleaned-up and concentrated to a volume of 100 - 500 µl prior to analytical measurement. For analysis high resolution gas chromatography with electron capture detection (HRGC-ECD) and mass selective detection (HRGC-MSD) were applied. The sensitive detection of CP in negative chemical ionization mass spectrometry (NCI-MS) opens a classification into short-chain, intermediate and long-chain CP which gives more detailed information about the composition of a particular CP mixture.

Analysis of alkyl nitrates in high volume air samples required high pre-concentration of the eluted samples. A new liquid chromatographic separation procedure has been developed using silica gel with defined activity and chromatographic solvent fractions of different polarity. This improved the detection limit by the separation of disturbing components before gas chromatographic analysis.

The low volume air samples are analyzed using gas chromatographic separation with electron capture detection (ECD). The adsorbed molecules are not eluted from the Tenax material with a solvent. Due to their high volatility the glass tube is directly fitted into a special injector port of the gas chromatograph. Thermal desorption is carried out by heating the glass tube quickly up to 250˚C. At the entrance of the chromatographic column the desorbed molecules are cold trapped with liquid nitrogen to enable a synchron starting of the separation. After separation, compound identification and quantification is carried out by comparison with reference compounds and internal calibration.

5.9.4 Preliminary Results

5.9.4.1 Chlorinated Paraffins

Chlorinated paraffins were detected in all seawater samples and surface micro layer samples in ng/l concentrations, whereas in air samples CP were not detectable.

In seawater the total CP concentration varied between 0.5 ng/l and 10 ng/l. Short-chain CP ranged from 0.1 ng/l to 4.8 ng/l at a limit of quantification (LOQ) of 0.1 ng/l. Levels of intermediate CP were between 0.5 ng/l and 5.0 ng/l at a LOQ of 0.5 ng/l whereas long-chain CP were not detected at a limit of detection (LOD) of 0.5 ng/l (Fig. 73).

Acceptable recoveries of the internal standards and traces of short-chain and intermediate CP in the break through samples document good sampling efficiencies.

The course of short-chain and intermediate CP levels displays a ground level in the low ng/l range. The increased levels of sample W3 (21˚S/0˚E) and sample W11 (35˚S/40˚W) are effected by the South Equatorial Current and the Brazil Current gyre respectively. Sample W11 is influenced by effluents from the Rio de La Plata which are transported north-easterly by the Brazil Current gyre.

The surface micro layer indicated total CP concentrations between 100 and 650 ng/l. Levels of short-chain CP ranged from 50 ng/l to 200 ng/l and intermediate CP from 75 to 500 ng/l at LOQ of 20 ng/l and 50 ng/l respectively (Fig. 74). Furthermore traces of long-chain CP were detected due to the effective accumulation of hydrophobic compounds by the micro layer which is in this case equivalent to a concentration factor of 100 compared with seawater. The course of CP levels in the micro layer is consistent to seawater and emphasizes the slightly increased levels at 15˚W and 27˚W. The ratio short-/intermediate CP however is different due to increased enrichment of more lipophilic intermediate and long-chain CP by the micro layer. Air samples of the lower troposphere were also investigated for chlorinated paraffins using the same analytical methods.

At a limit of detection of 0.1 ng/m^3 CP were not detected in any air sample. This fact is emphasized by calculating an expected concentration in air using the known seawater concentrations and the gas -water-distribution-coefficient (K_{gw}) derived from water solubility and vapor pressure. The expected concentrations in air are significantly below the limit of detection.

These data confirm the occurrence of short-chain, intermediate and long-chain chlorinated paraffins in the hydrosphere of the South Atlantic ocean, which had been reported by KRAMER and BALLSCHMITER (1987), and document the global distribution of these anthropogenic compounds. These results also support the theory that chlorinated paraffins are mainly transported via hydrosphere primarily adsorbed on organic particulate matter rather than via atmosphere.

5.9.4.2 Alkyl Nitrates in Air Samples

Alkyl nitrates could be analyzed on Tenax as well as in high volume samples. In case of the low volume samples we detected the spectrum of methyl nitrate (C1) up to C6-nitrates (2M3C5, 2M4C5, 3C6, 2C6). In IUPAC nomenclature the nitrate group is called "nitroxy" group. For peak labeling we used here a much more simpler and in case of mono-functional nitrates already conventional nomenclature. The longest alkyl chain is taken for the skeleton of the molecule (e.g. C7 means longest chain has seven C-atoms). In case of branched alkyl nitrates the alkyl side chains possess higher priorities than the nitroxy group, what implies that the alkyl side chains receive the smaller numbers. This is important because alkyl nitrates are formed via photo-oxidation from hydrocarbons and so the hydrocarbon skeletons can be compared. If the nitroxy group would have the higher priority same alkyl skeletons would be named different. A general example is 2,4M5C7 what indicates a heptyl chain with to methyl groups at the 2 and 4 position and the nitroxy group at the 5 position.

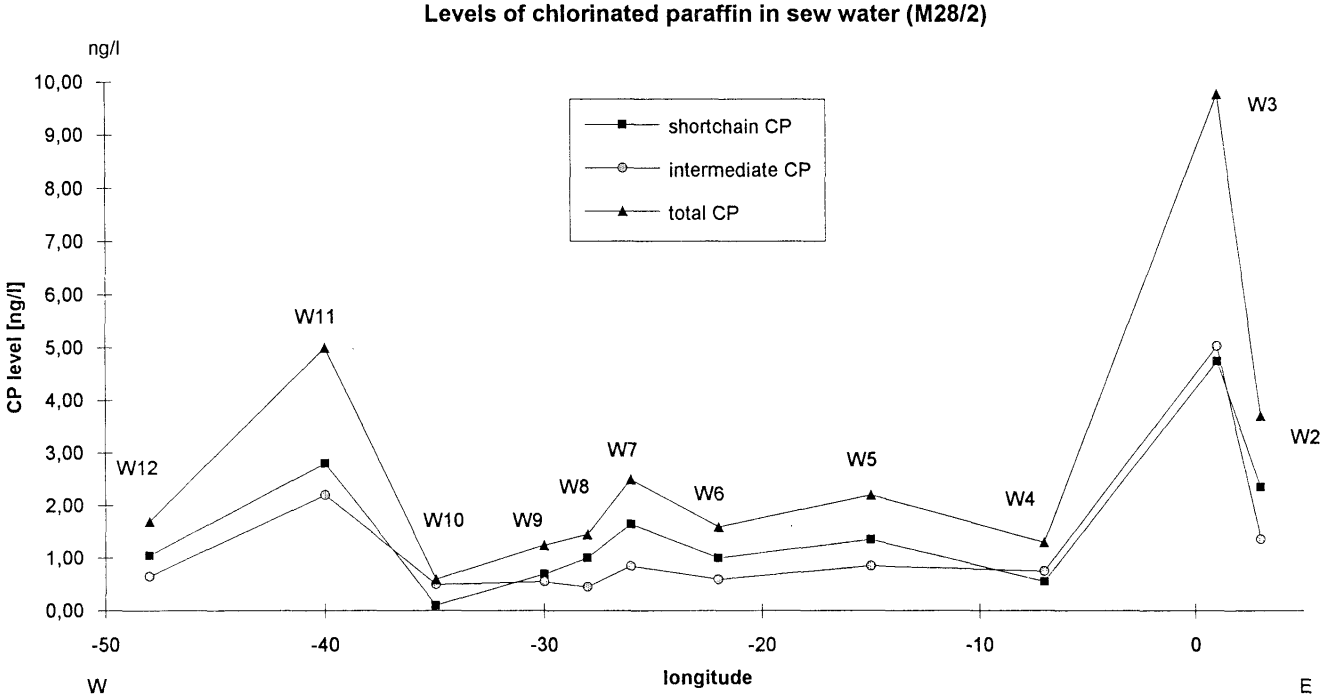

Fig. 73: Levels of chlorinated paraffin in surface seawater

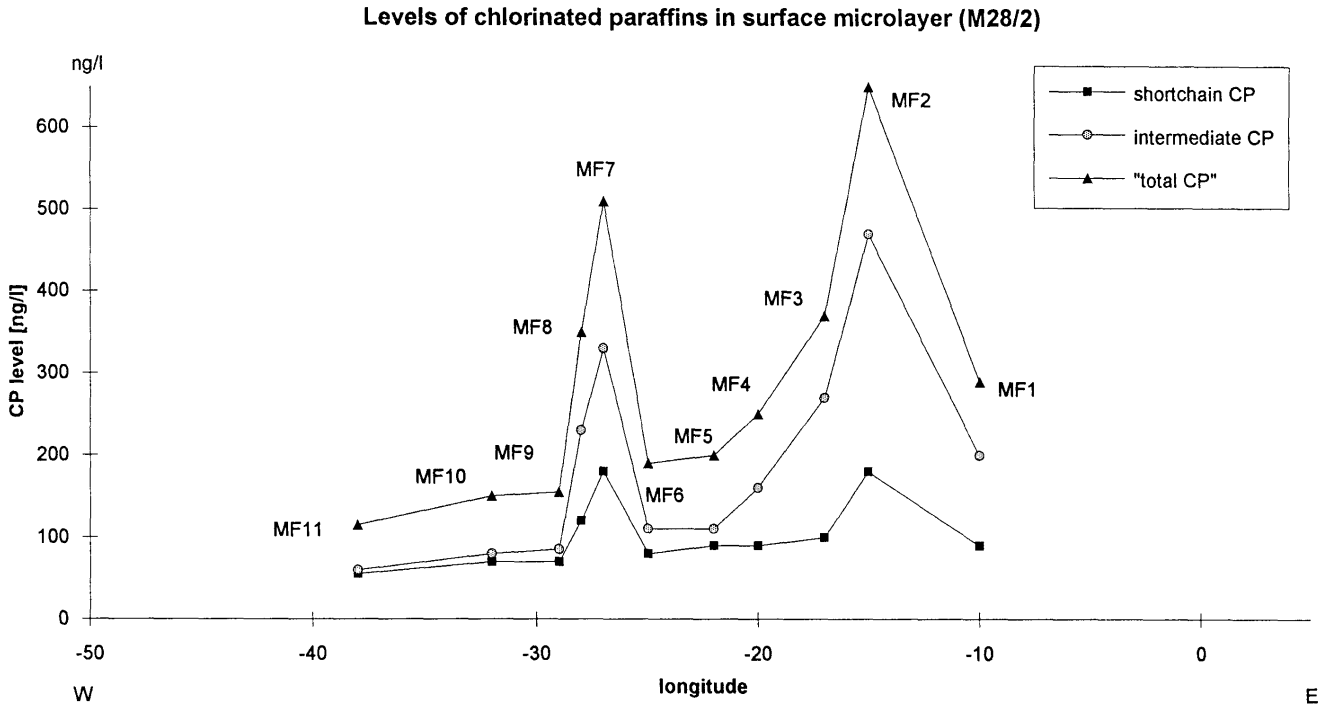

Fig. 74: Levels of chlorinated paraffin in the micro layer

Figure 75 depicts the separation of a 52.2 liter low volume air sample (LOW15) with high resolution gas chromatography and electron capture detection (HRGC-ECD) after thermal desorption from the Tenax material. The detected alkyl nitrate peaks are marked by asterisks and painted black. Beside the alkyl nitrates we determined high volatile halogenated hydrocarbons especially tetrachloro methane, tetrachloro ethylene and bromoform. Following table explains the abbreviations used in Figure 75 for halogenated hydrocarbons.

CH2BrCl	Bromo-chloro methane
CHCl3	Chloroform
111TCE	111-Trichloro ethane
CC14	carbon tetrachloride
Tri	Trichloro ethylene
CHBrCl2	Bromo-dichloro methane
Per	Tetrachloro ethylene
CHBr2Cl	Dibromo-chloro methane
CHBr3	Bromoform
TCP (Int.St.)	123Trichloro propane (internal standard)
PCE	Pentachloro ethane
HCE	Hexachloro ethane

Nevertheless the sample includes several unknown components predominantly in the medium volatile region (C6 - C8 nitrates). In case of an immense increase in the complexity of possible branched alkyl nitrates, reference compounds have to be synthesized for further identification.

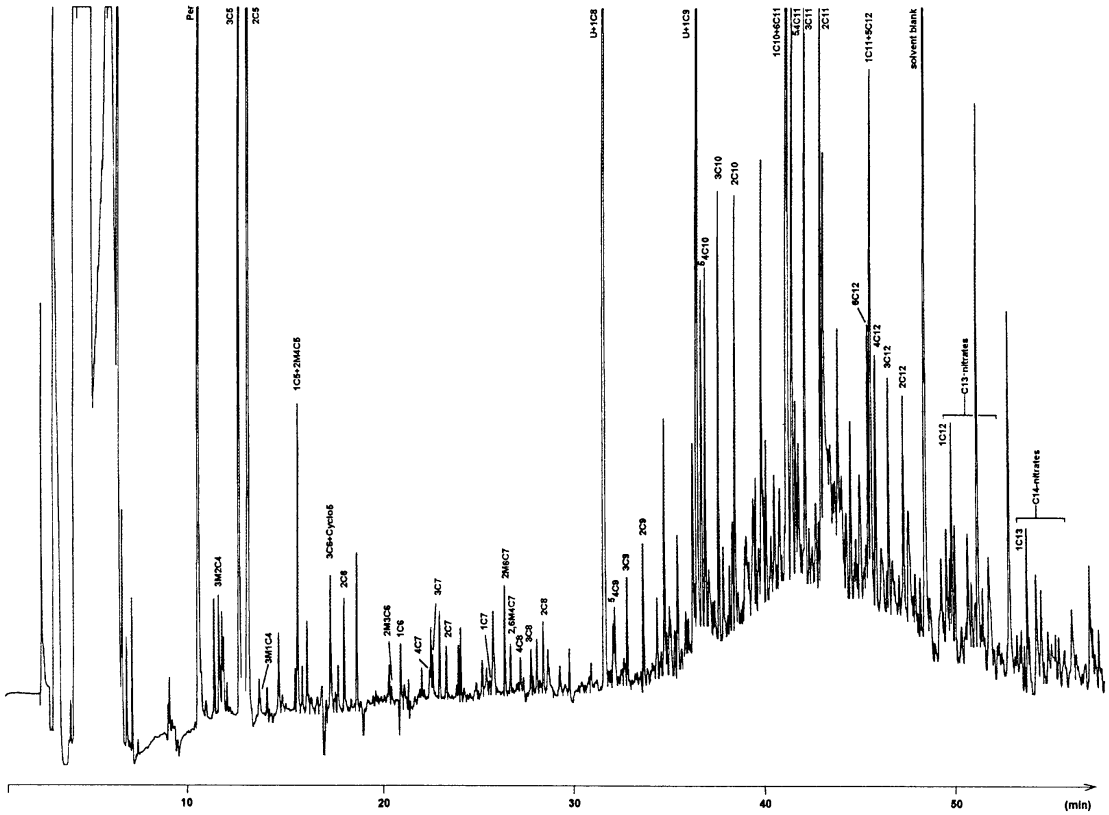

Fig. 75: HRGC/ECD: Alkyl nitrates in a low volume air sample (LOW 15; aliquot 52.2 1)

The analysis of the high volume samples required intense effort in pre-separation before a possible gas chromatographic analysis of alkyl nitrates. Figure 76 exhibits an excellent high resolution gas chromatogram with mostly alkyl nitrates. We detected alkyl nitrates from C-6 up to C-14 with the typical separation pattern deriving from the n-alkanes, e.g. all n-nonyl nitrates are present in their correct relative concentrations. We obtained a maximum at C-11 nitrates. Interpretation of this result is yet very difficult. Detailed results are potential if the separation technique of C-15 - C-25 alkyl nitrates can be improved.

It must be noted that Figure 76 only depicts a fraction of the high volume air sample. The whole air sample consists of a very complex composition. Gas chromatographic analysis without pre-separation would lead to no quantitative determination of alkyl nitrates. Furthermore we could prove that also the branched alkyl nitrates are present in this fraction. Hence, several of the unlabeled peaks should represent branched alkyl nitrates.

Alkyl nitrates are not commercially available, therefore nearly all compounds have to be synthesized and reference standards have to be prepared for quantitative analysis. First quantitative estimations can be made. The concentrations of high volatile alkyl nitrates (low volume sampling) range in the medium to upper pg/m^3, while the long-chain alkyl nitrates are present in the lower pg/m^3 region. The much higher concentrations of short-chain alkyl nitrates are conform with present results. Only high volume sampling makes the detection of long-chain alkyl nitrates possible, because it involves an enrichment factor of approximately 100 relative to

the low volume sampling technique. Figure 75 shows the whole low volume air sample (52.21), while Figure 76 represents an aliquot of 5,800 l of the sampled 975,000 l air. These first results hint to further conclusions of global distribution or formation of alkyl nitrates in "unpolluted" air masses of the southern hemisphere.

5.9.4.3 Polychlorinated Biphenyls (PCB)

All seawater and micro layer samples were investigated for a set of 12 PCB; congeners (PCB 28, PCB 49, PCB 52, PCB; 87, PCB; 101, PCB 110, PCB, 118, PCB 138, PCB 149, PCB 151, PCB 153, PCB 180) which serve as trace components for environmental distribution effects.

The total PCB level as the sum of 12 congeners in the seawater ranged between 60 pg/l and 140 g/l which documents a very low background level in the South Atlantic. However a significant elevated PCB burden was observed in sample W11 (35˚S/40˚W) due to the input from Rio de la Plata by the Brazil Current gyre. The micro layer again performs a concentration effect resulting in PCB; levels between 2,800 pg/l and 5,000 pg/l. Slightly increased levels at 15˚W and 27˚W are consistent to CP levels at these positions (Figs. 77-78).

The composition of the PCB patterns in seawater and micro layer are very similar and correspond to a mixture of low chlorinated and high chlorinated technical PCB. The increase of highly chlorinated PCB congeners in sample W11 hints to an input from the hydrosphere (Rio de La Plata, Brazil Current gyre).

Furthermore other organohalogen compounds of anthropogenic and biogenic origin were also detected and are under further investigation.

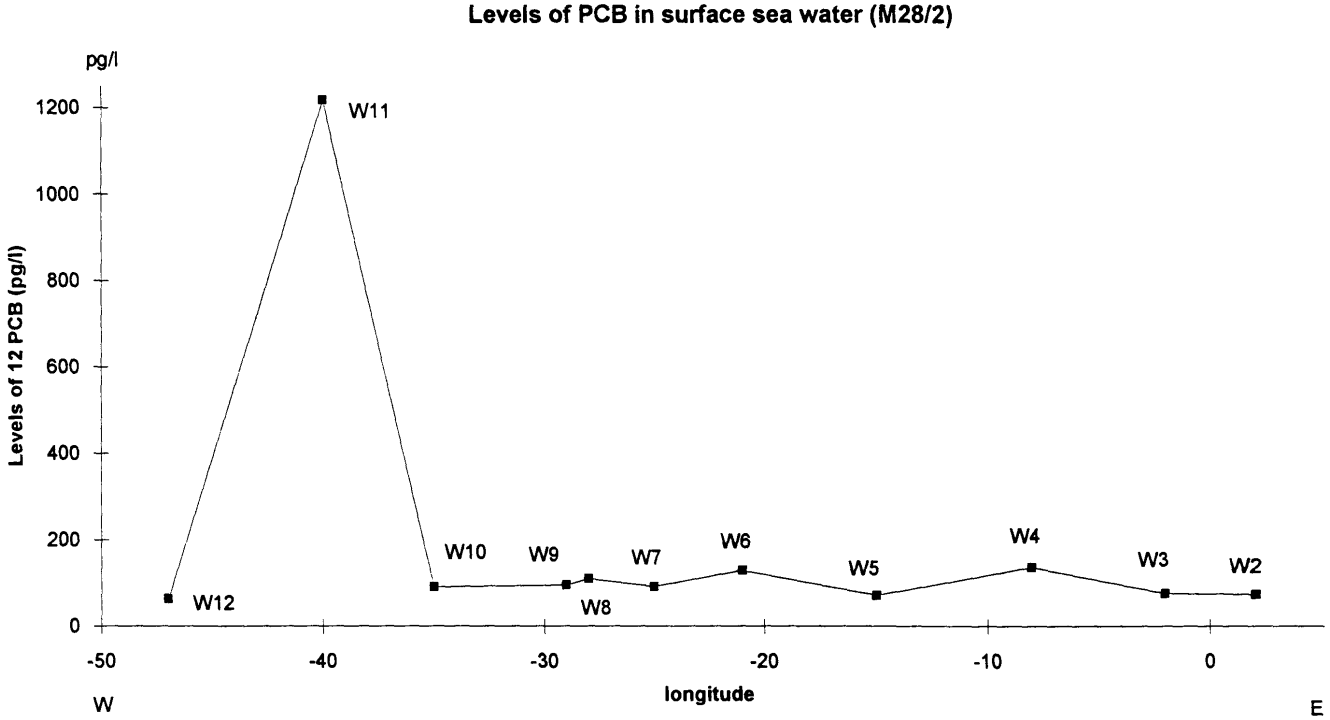

Fig. 76: HRGC/ECD: Alkyl nitrates in a high volume air sample (Lp2; aliquot 5,800 1)

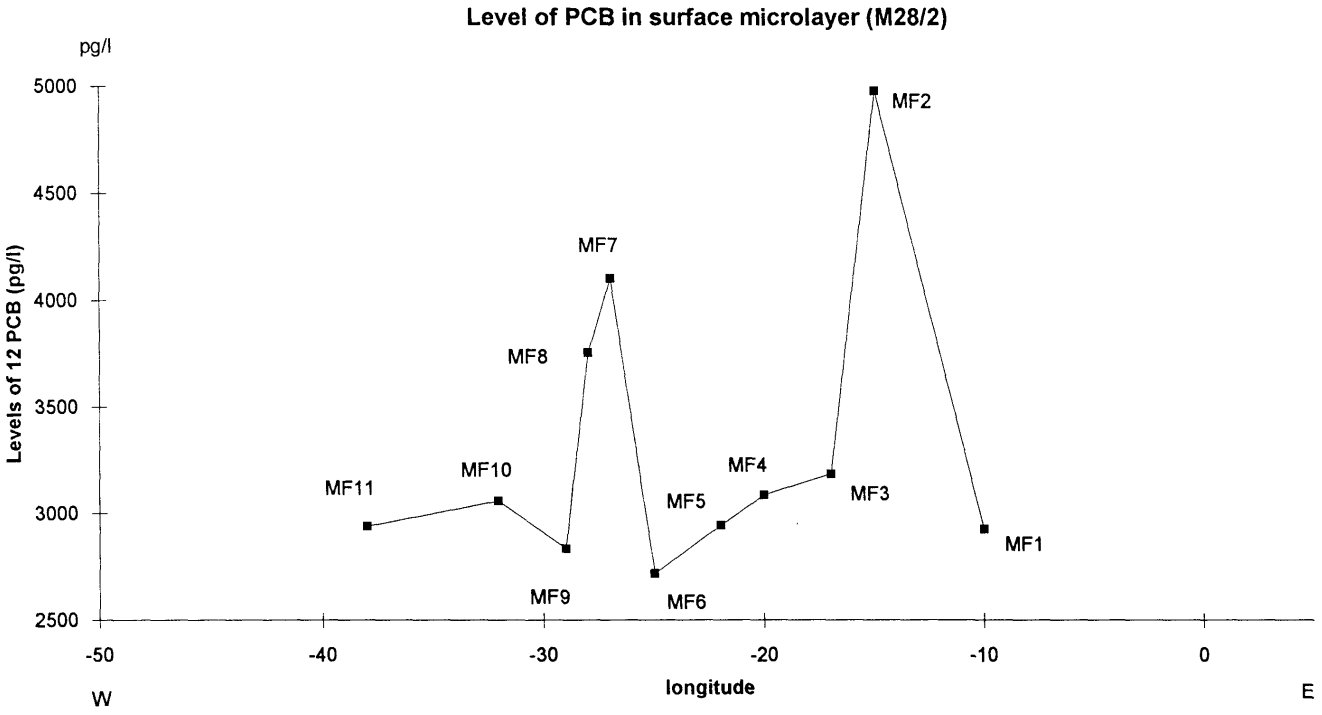

Fig. 77: Level of ∑12 PCB in surface seawater

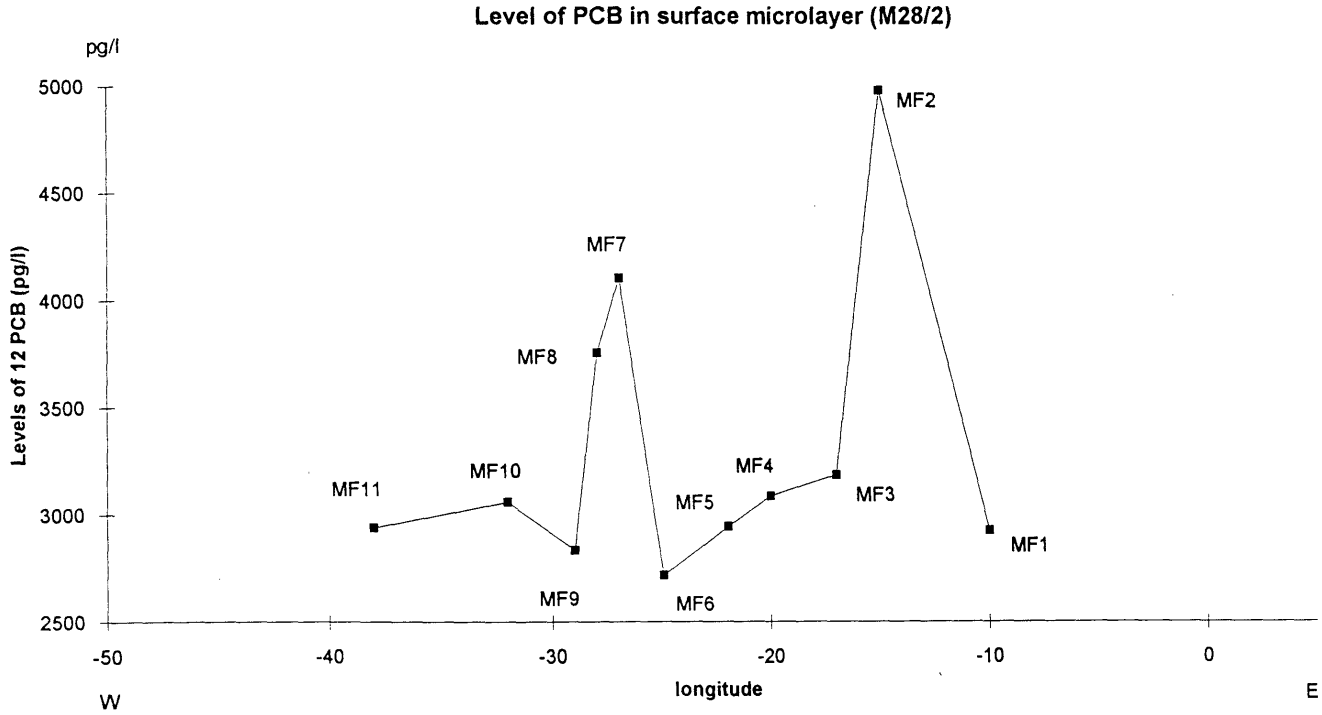

Fig. 78: Level of ∑12 PCB in surface micro layer

6 Ship's Meteorological Station (K. Flechsenhar)

6.1 Weather and Meteorological Conditions during Leg M 28/1

METEOR left the northeast Brazilian harbor Recife on March 29, 1994, steered south to southeastward doing station operations in coastal waters and reached the position 11˚20S/34˚W, which is the starting point of the projected WOCE section, on April 4. From this position on it was to steer exactly east, doing all projected station operations on the same latitude. On April 4, the longitude 30˚W was crossed.

Until April 9, METEOR sailed through the region of weak pressure gradients, which lies between the subtropical South Atlantic high centered at 28˚S/5˚W and the equatorial low pressure zone. The Intertropical Convergence Zone (ITC) was placed in the western Atlantic just north of the equator and curved eastward up to 15˚N over Central Africa. Just south of the equator weak tropical disturbances moved westward, which could be noticed by some short showers near METEOR. Here weak easterly winds were dominating, height of swell 1.5 to 2 m.

From April 10 on, the eastsoutheasterly winds increased up to Bft 5, temporarily 6 at the northern parts of the above mentioned high, swell 2 to -3 in. On April 13, 20˚W and on April 19, 10˚W was passed with east to southeast winds of 4 to 5 Bft and 2.5 m swell. On April 26, the Meridian 0 was crossed with southeast winds of 3 to 4 Bft and a long swell of about 3 in from the southeast. On May 2, METEOR passed the Meridian 10˚E. Here the wind veered south to southwest and decreased, caused by a stationary low over the Congo Basin. The swell decreased to 1 m. On May 4, 11˚20 S was left at 13˚E in the coastal waters of Angola for the first time. Until May 7, METEOR cruised near the coast of Angola doing station operations and then started her voyage down to Walvis Bay, Namibia. In the last part of the voyage the dominating cold up-welling waters caused fog and low clouds. The wind increased too. On May 11, METEOR moored in Walvis Bay.

6.2 Weather and Meteorological Conditions during Leg M 28/2

METEOR left the harbor of Walvis Bay, Namibia, on May 15, 1994, and sailed first to the position 21˚S/10˚W, where the station operations started. From this position on they steered west to southwest, doing all the projected station operations, and reached the Hunter Channel area (34˚S/28˚W) on May 27, where further station and mooring operations were done. Until May 25, the weather was fair, influenced by the stable subtropical South Atlantic high. But a steady 2 to 3 m high swell made the ship roll, specially at the stations, disturbing the participants and causing some lack of sleep. On May 25, a cyclogenetic process occurred near South Brazil, creating a storm centre, which moved eastsoutheast and caused winds Bft 6 to 7. After a rather calm period on May 28/29, another storm cyclone created in the same area, bringing gale Bft 9 with gusts of 11 to the heaving ship on May 30. From May 31 to the 3rd of June, a high was dominating, so the search operations for a trifting sound-producer on May 31/June I could be done under good weather conditions, good sight and clear sky, but with a swell of 2 to 3 m. On June 4, another storm cyclone approached from the Northwest, meeting METEOR at the position 33˚S/27˚W. After a while of high pressure influence with fair weather, METEOR reached the position 40˚S/35˚W on June 7. There the ship found itself at the edge of a large storm cyclone with centre

between the Falkland Islands/Malvinas and the South Sandwich Islands. Here the wind increased to Bft 7 to 8, becoming 4 to 6 later, and the swell increased up to 4 m, causing heavy pitching and rolling. From June 6 on, the influence of a large high over Argentina was to be noticed by stable weather and a rather cool and steady southwest to west wind. This high moved gradually eastward. So from June 10 on, METEOR met winds (Bft 6 to 7) from ahead. On June 12, the wind became weak, on June 13, they arrived at the Rio de la Plata with moderate winds from southeast to east and a rainy weather. On June 14, METEOR moored in Buenos Aires, Argentina.

7 Lists

7.1 Leg M 28/1

7.1.1 List of Stations

Station No.	Date	Time	Device	Activity	Length of wire	Speed	Winch	Latitude	Longitude
Station # 164									
	29.03.94	UTC-3	GEK	z/W, Schiff ADCP				08º07.5S	34º16.6W
		17.30	(Kontinuierliches Messen mit ADCP; GEK - Messungen zwischen den einzelnen Stationen)						
Station # 165									
		23.12	CTD/Ro/WS	z/W	SL 4648 m		W 03	08º16.9S	33º28.0W
	30.03.94	01.52	CTD/Ro/WS	a/D				08º16.5S	33º27.4W
		02.05	CTD/Ro/WS/ADCP	z/W	SL 991 m		W 02	08º16.5S	33º27.4W
		02.49	CTD/Ro/WS/ADCP	a/D				08º16.5S	33º27.4W
		02.55	NEUSS	z/W		V =2.3 Kn		08º16.3S	33º27.3W
		03.30	NEUSS	a/D				08º14.7S	33º26.2W
Station # 166									
		10.01	CTD/Ro/WS/ADCP	z/W	SL 999 m		W 02	08º19.9S	32º29.9W
		10.55	CTD/Ro/WS/ADCP	a/D				08º20.0S	32º29.7W
		11.10	CTD/Ro/WS	z/W	SL 4800 m		W 03	08º19.8S	32º29.9W
		12.23	CTD/Ro/WS	a/D				08º19.4S	32º29.8W
		13.59	NEUSS	z/W		V = 2.3 Kn		08º19.1S	32º29.7W
		14.32	NEUSS	a/D				08º17.5S	32º29.4W
Station # 167									
		21.06	CTD/Ro/WS	z/W	SL 4079 m		W 03	09º15.1S	33º00.0W
		23.37	CTD/Ro/WS	a/D				09º14.8S	32º59.9W
		23.58	CTD/Ro/WS/ADCP	z/W	SL 995 m		W 02	09º14.9S	33º00.0W
	31.03.94	00.28	CTD/Ro/WS/ADCP	a/D				09º14.9S	33º00.0W
		00.58	MSN	z/W	SL 400 m	V = 2.3 Kn	W 09	09º14.7S	32º59.9W
		02.00	MSN	a/D				09º11.2S	32º59.6W
		01.18	NEUSS	z/W		V = 2.3 Kn		09º13.4S	32º59.8W
		01.44	NEUSS	a/D				09º11.9S	32º59.7W
Station # 168									
		08.52	CTD/Ro/WS/ADCP	z/W	SL 994 m		W 02	10º15.1S	33º30.1W
		09.43	CTD/Ro/WS/ADCP	a/D				10º15.1S	33º29.9W

Station No.	Date	Time	Device	Activity	Length of wire	Speed	Winch	Latitude	Longitude
		10.00	CTD/Ro/WS	z/W	SL 4801 m		W 03	10º15.0S	33º30.0W
		12.46	CTD/Ro/WS	a/D				10º15.3S	33º29.3W
		13.01	MSN	z/W	SL 70 m	V = 2.3 Kn	W 09	10º14.9S	33º29.3W
		13.22	MSN	a/D				10º14.1S	33º29.3W
		13.04	NEUSS	z/W		V = 2.3 Kn		10º14.8S	33º29.3W
		13.36	NEUSS	a/d				10º13.6S	33º29.2W
		14.07	MSN	z/W	SL 375 m	V = 2.3 Kn	W 09	10º13.2S	33º28.8W
		14.53	MSN	a7D				10º11.6S	33º28.3W
Wetter: SE 4 See 2 1012.7hPa c L 27.7ºW 28.9									
Station # 169									
	01.04.94	14.22	CTD/R o/WS/ADCP	z/W	SL 80 m		W 02	10º03.6S	35º45.1W
		14.29	CTD/R o/WS/ADCP	a/D				10º03.6S	35º45.0W
		14.37	CTD/R o/WS	z/W	SL 187 m		W 03	10º03.6S	35º44.9W
		15.05	CTD/R o/WS	a/D				10º03.6S	35º44.9W
		15.09	MSN	z/W	SL 127 m	V = 2.3 Kn	W 09	10º03.5S	35º44.9W
		15.30	MSN	a/D				10º02.8S	35º44.7W
		15.12	NEUSS	z/W		V = 2.3 Kn		10º03.3S	35º44.8W
		15.42	NEUSS	a/D				10º02.2S	35º44.4W
Station # 170									
		16.35	CTD/Ro/WS/ADCP	z/W	SL 499 m		W 02	10º06.2S	35º42.5W
		17.06	CTD/Ro/WS/ADCP	a/D				10º05.9S	35º42.4W
		17.28	CTD/Ro/WS	z/W	SL 763 m		W 03	10º06.2S	35º42.5W
		18.51	CTD/Ro/WS	a/D				10º05.1S	35º41.9W
		18.58	MSN	z/W	SL 342 m	V = 2.3 Kn	W 09	10º05.0S	35º41.8W
		19.45	MSN	a/D				10º02.9S	35º41.2W
		19.03	NEUSS	z/W		V = 2.3 Kn		10º04.8S	35º41.8W
		19.33	NEUSS	a/D				10º03.3S	35º41.4W
Station # 171									
		21.00	MSN	z/W	SL 280 m	V = 2.3 Kn	W 09	10º12.7S	35º38.3W
		21.42	MSN	a/D				10º11.0S	35º37.7W
		21.04	NEUSS	z/W		V = 2.3 Kn		10º12.8S	35º38.1W
		21.33	NEUSS	a/D				10º11.4S	35º37.8W
		22.03	CTD/Ro/WS/ADCP	z/W	SL 999 m		W 02	10º10.2S	35º36.9W
		22.45	CTD/Ro/WS	a/D				10º09.7S	35º36.5W
		23.09	CTD/Ro/WS	z/W	SL 2196 m		W 03	10º10.2S	35º37.0W
	02.04.94	01.07	CTD/Ro/WS	a/D				10º09.2S	35º36.0W

Station No.	Date	Time	Device	Activity	Length of wire	Speed	Winch	Latitude	Longitude
Station # 172									
		02.03	MSN	z/W	SL 331 m	V = 2.3 Kn	W 09	10º15.8S	35º33.6W
		02.50	MSN	a/D				10º14.0S	35º32.6W
		02.10	NEUSS	z/W		V = 2.3 Kn		10º15.4S	35º33.4W
		02.50	NEUSS	a/D				10º14.0S	35º32.6W
		03.04	CTD/Ro/WS/ADCP	z/W	SL 1001 m		W 02	10º14.2S	35º32.5W
		03.52	CTD/Ro/WS/ADCP	a/D				10º13.7S	35º32.0W
		04.20	CTD/Ro/WS	z/W	SL 2635 m		W 03	10º14.2S	35º32.5W
		07.06	CTD/Ro/WS	a/D				10º12.5S	35º31.4W
Station # 173									
		08.08	MSN	z/W	SL 391 m	V = 2.3 Kn	W 09	10º19.8S	35º27.0W
		08.54	MSN	a/D				10º17.5S	35º26.6W
		08.13	NEUSS	z/W		V = 2.3 Kn		10º19.6S	35º27.0W
		08.43	NEUSS	a/D				10º18.0S	35º26.8W
		09.14	CTD/Ro/WS/ADCP	z/W	SL 1002 m		W 02	10º18.0S	35º26.4W
		10.15	CTD/Ro/WS/ADCP	a/D				10º17.1S	35º28.8W
		10.44	CTD/Ro/WS	z/W	SL 3036 m		W 03	10º17.9S	35º26.5W
		13.00	CTD/Ro/WS	a/D				10º16.4S	35º26.0W
Station # 174									
		14.10	MSN	z/W	SL 358 m	V = 2.3 Kn	W 09	10º24.7S	35º21.6W
		14.58	MSN	a/D				10º22.8S	35º21.3W
		14.17	NEUSS	z/W		V = 2.3 Kn		10º24.3S	35º21.5W
		14.49	NEUSS	a/D				10º22.8S	35º21.3W
		15.16	CTD/Ro/WS/ADCP	z/W	SL 1008 m		W 02	10º23.0S	35º20.0W
		16.11	CTD/Ro/WS/ADCP	a/D				10º22.4S	35º19.8W
		16.36	CTD/Ro/WS	z/W	SL 3294 m		W 03	10º23.0S	35º20.0W
		19.15	CTD/Ro/WS	a/D				10º21.9S	35º19.7W
Station # 175									
		20.32	CTD/Ro/WS/ADCP	z/W	SL 1002 m		W 02	10º28.2S	35º12.5W
		21.35	CTD/Ro/WS/ADCP	a/D				10º27.6S	35º11.9W
		22.12	CTD/Ro/WS	z/W	SL 3713 m		W 03	10º28.0S	35º12.6W
	03.04.94	00.47	CTD/Ro/WS	a/D				10º26.7S	35º11.8W
		00.51	NEUSS	z/W		V = 2.3 Kn		10º26.5S	35º11.7W
		01.24	NEUSS	a/D				10º25.0S	35º11.5W
Station # 176									
		02.48	CTD/Ro/WS/ADCP	z/W	SL 1004 m		W 02	10º34.5S	35º04.0W

Station No.	Date	Time	Device	Activity	Length of wire	Speed	Winch	Latitude	Longitude
		03.44	CTD/Ro/WS/ADCP	a/D				10º34.4S	35º03.6W
		04.07	CTD/Ro/WS	z/W	SL 3975 m		W 02	10º34.5S	35º04.1W
		06.56	CTD/Ro/WS	a/D				10º33.4S	35º03.7W
		07.00	NEUSS	z/W		V = 2.3 Kn		10º33.1S	35º03.5W
		07.33	NEUSS	a/D				10º31.8S	35º02.9W
Wetter: El 4 See 2 c 1013.OhPa L 27.6ø W 28.8ø									
Station # 177									
		08.54	CTD/Ro/WS/ADCP	z/W	SL 1011 m		W 02	10º39.9S	34º56.0W
		09.49	CTD/Ro/WS/ADCP	a/D				10º39-6S	34º56.0W
		10.11	CTD/Ro/WS	z/W	SL 4051 m		W 03	10º39.9S	34º56.0W
		12.47	CTD/Ro/WS	a/D				10º38.8S	34º55.8W
		12.54	MSN	z/W	SL 446 m	V = 2.3 Kn	W 09	10º38.5S	34º55.9W
		13.46	MSN	a/D				10º36.6S	34º56.9W
		12.57	NEUSS	z/W		V = 2.3 Kn		10º38.4S	34º55.9W
		13.27	NEUSS	a/D				10º37.1S	34º56.7W
Station # 178									
		15.34	CTD/Ro/WS/ADCP	z/W	SL 1004 m		W 02	10º48.0S	34º44.5W
		16.32	CTD/Ro/WS/ADCP	a/D				10º47.5S	34º44.5W
		16.55	CTD/Ro/WS	z/W	SL 4312 m		W 03	10º47.2S	34º44.8W
		19.38	CTD/Ro/WS					10º46.5S	34º45.0W
		19.48	MSN	z/W	SL 420 m	V = 2.3 Kn	W 09	10º46.1S	34º44.9W
		20.35	MSN	a/D				10º43.9S	34º44.4W
		19.51	NEUSS	z/W		V = 2.3 Kn		10º46.0S	34º44.9W
		20.23	NEUSS	a/D				10º44.5S	34º44.6W
Station # 179									
		22.43	CTD/Ro/WS/ADCP	z/W	SL 1005 m		W 02	10º57.0S	34º30.9W
		23.55	CTD/Ro/WS/ADCP	a/D				10º56.9S	34º30.9W
	04.04.94	00.02	CTD/Ro/WS	z/W	SL 4468 m		W 03	10º57.0S	34º30.9W
		02.53	CTD/Ro/WS	a/D				10º55.7S	34º30.6W
		02.57	MSN	z/W	SL 522 m	V = 2.3 Kn	w 09	10º55.5S	34º30.5W
		03.51	MSN	a/D				10º53.1S	34º29.9W
		02.59	NEUSS	z/W		V = 2.3 Kn		10º55.4S	34º30.4W
		03.32	NEUSS	a/D				10º53.8S	34º30.4W
Station # 180									
		06.28	CTD/Ro/WS/ADCP	z/W	SL 644 m		W 02	11º08.0S	34º11.0W
		07.23	CTD/Ro/WS/ADCP	a/D				11º07.7S	34º10.9W
		07.30	CTD/Ro/WS	z/W	SL 4571 m		W 03	11º07.6S	34º10.9W

Station No.	Date	Time	Device	Activity	Length of wire	Speed	Winch	Latitude	Longitude
		10.15	CTD/Ro/WS	a/D				11º06.3S	34º10.9W
		10.22	MSN	z/W	SL 445 m	V = 2.3 Kn	W 09	11º06.2S	34º10.8W
		11.08	MSN	a/D				11º04.2S	34º09.7W
		10.24	NEUSS	z/W		V = 2.3 Kn		11º06.1S	34º10.7W
		10.55	NEUSS	a/D				11º04.8S	34º10.0W
Wetter: El 1/2 See 0 b/c 1011.1hPa L 27.4ø W 28.9ø									
Station # 181									
		13.10	CTD/Ro/WS	z/W	SL 4618 m		W 03	11º20.0S	34º00.0W
		16.09	CTD/Ro/WS	a/D				11º19.2S	34º00.5W
		16.15	MSN	z/W	SL 466 m	V = 2.3 Kn	W 09	11º19.0S	34º00.4W
		17.14	MSN	a/D				11º16.7S	33º59.3W
		16.18	NEUSS	z/W		V = 2.3 Kn		11º18.9S	34º00.4W
		16.51	NEUSS	a/D				11º17.6S	33º59.8W
		21.01	CTD/Ro/WS	z/W	SL 1511 m			11º19.9S	34º00.0W
		22.22	CTD/Ro/WS	a/D				11º19.8S	34º00.0W
Station # 182									
	05.04.94	01.20	CTD/Ro/WS/ADCP	z/W	SL 994 m		W 02	11º20.0S	33º30.0W
		02.12	CTD/Ro/WS/ADCP	a/D				11º19.9S	33º30.0W
		02.16	CTD/Ro/WS	z/W	SL 4980 m		W 03	11º19.9S	33º30.0W
		05.34	CTD/Ro/WS	a/D				11º19.8S	33º29.9W
		05.40	MSN	z/W	SL 453 m	V = 2.3 Kn	W 09	11º19.6S	33º29.7W
		06.35	MSN	a/D				11º17.1S	33º28.8W
		05.42	NEUSS	z/W		V = 2.3 Kn		11º19.5S	33º29.7W
		06.15	NEUSS	a/D				11º18.0S	33º29.2W
Station # 183									
		09.28	CTD/Ro/WS/ADCP	z/W	SL 992 m		W 02	11º20.0S	32º59.9W
		10.23	CTD/Ro/WS/ADCP	a/D				11º20.0S	32º59.8W
		10.27	CTD/Ro/WS	z/W	SL 4766 m		W 03	11º20.0S	32º59.8W
		13.18	CTD/Ro/WS	a/D				11º19.9S	32º59.9W
		13.22	MSN	z/W	SL 413 m	V = 2.3 Kn	W 09	11º19.7S	32º59.8W
		14.05	MSN	a/D				11º18.1S	32º58.8W
		13.24	NEUSS	z/W		V = 2.3 Kn		11º19.6S	32º59.8W
		13.55	NEUSS	a/D				11º18.4S	32º59.1W
Station # 184									
		16.52	CTD/Ro/WS/ADCP	z/W	SL 995m	WT 4850 m	W 02	11º20.0S	32º30.0W
		18.00	CTD/Ro/WS/ADCP	a/D				11º19.7S	32º30.2W
		18.05	CTD/Ro/WS	z/W	SL 4889 m	WT 4884 m	W 03	11º19.3S	32º30.3W

Station No.	Date	Time	Device	Activity	Length of wire	Speed	Winch	Latitude	Longitude
		20.58	CTD/Ro/WS	a/D				11º18.9S	32º30.3W
		21.05	MSN	z/W	SL 458 m	V = 2.3 Kn	W 09	11º18.6S	32º30.2W
		21.57	MSN	a/D		V = 2.3 Kn		11º18.6S	32º30.1W
		21.40	NEUSS	a/D				11º17.3S	32º29.4W
Station # 185									
	06.04.94	00.44	CTD/Ro/WS/ADCP	z/W	SL 993 m	WT 5060 m	W 02	11º20.0S	32º00.0W
		01.43	CTD/Ro/Ws/ADCP	a/D				11º20.0S	32º00.0W
		01.47	CTD/Ro/WS	z/W	SL 5067 m	WT 5060 m	W 03	11º20.0S	32º00.0W
		04.58	CTD/Ro/WS	a/D				11º19.9S	31º59.6W
		05.05	MSN	z/W	SL 466 m	V = 2.3 Kn	W 09	11º19.8S	31º59.5W
		06.05	MSN	a/D				11º17.3S	31º58.3W
		05.07	NEUSS	z/W		V = 2.3 Kn		11º19.7S	31º59.4W
		05.40	NEUSS	a/D				11º18.3S	31º58.8W
Station # 186									
		09.49	CTD/Ro/WS/ADCP	z/W	SL 994 m	WT 5220 m	W 02	11º20.0S	31º19.9W
		10.44	CTD/Ro/WS/ADCP	a/D				11º19.7S	31º20.0W
		10.49	CTD/Ro/WS	z/W	SL 5256 m	WT 5220 m	W 03	11º19.6S	31º20.0W
		13.57	CTD/Ro/WS	a/D				11º19.3S	31º20.0W
		14.02	MSN	z/W	SL 459 m	V = 2.3 Kn	W 09	11º19.1S	31º19.9W
		14.54	MSN	a/D				11º17.2S	31º18.7W
		14.02	NEUSS	z/W		V = 2.3 Kn		11º19.1S	31º19.9W
		14.36	NEUSS	a/D				11º17.9S	31º19.1W
Wetter: E'l 1/2 S 0 b/C 1010.6hPa L 27.1ø W 28.7ø									
Station # 187									
		18.55	CTD/Ro/WS/ADCP	z/W	SL 997 m	WT 5296 m	W 02	11º20.0S	30º40.0W
		20.02	CTD/Ro/WS/ADCP	a/D				11º20.0S	30º40.0W
		20.09	CTD/Ro/WS	z/W	SL 5327 m	WT 5296 m	W 03	11º20.0S	30º40.0W
		23.05	CTD/Ro/WS	a/D				11º20.1S	30º40.0W
		23.12	MSN	z/W	SL 474 m	V = 2.3 Kn	W 09	11º19.9S	30º39.8W
		00.04	MSN	a/D				11º17.2S	30º39.5W
		23.16	NEUSS	z/W		V = 2.3 Kn		11º19.7S	30º39.9W
		23.46	NEUSS	a/D				11º18.1S	30º39.6W
Station # 188									
	02.05.94	04.10	CTD/Ro/WS/ADCP	z/W	SL 993 m	WT 5382 m	W 02	11º20.0S	30º00.0W
		05.22	CTD/Ro/WS/ADCP	a/D				11º20.1S	30º00.0W
		05.32	CTD/Ro/WS	z/W	SL 5412 m	WT 5382 m	W 03	11º20.1S	29º59.9W
		08.33	CTD/RO/WS	a/D				11º19.9S	29º59.9W

Station No.	Date	Time	Device	Activity	Length of wire	Speed	Winch	Latitude	Longitude
		08.40	MSN	z/W	SL 491 m	V = 2.3 Kn	W 09	11º19.8S	29º59.9W
		09.30	MSN	a/D				11º17.4S	30º00.0W
		08.42	NEUSS	z/W		V = 2.3 Kn		11º19.7S	29º59.9W
		09.14	NEUSS	a/D				11º18.1S	29º59.9W
Station # 189									
		13.43	CTD/Ro/WS/ADCP	z/W	SL 996 m	WT 5480 m	W 02	11º20.0S	29º20.0W
		14.39	CTD/Ro/WS/ADCP	a/D				11º19.9S	29º20.0W
		14.44	CTD/Ro/WS	z/W	SL 5460 m	WT 5429 m	W 03	11º20.0S	29º20.0W
		18.00	CTD/Ro/WS	a/D				11º19.8S	29º19.8W
		18.15	MSN	z/W	SL 532 m	V = 2.3 Kn	W 09	11º19.3S	29º19.7W
		19.17	MSN	a/D				11º16.2S	29º18.9W
		18.17	NEUSS	z/W		V = 2.3 Kn		11º19.2S	29º19.6W
		18.48	NEUSS	a/D				11º17.6S	29º19.3W
Station # 190		UTC-2							
	08.04.94	02.15	CTD/Ro/WS/ADCP	z/W	SL 999 m	WT 5467 m	W 02	11º19.9S	28º40.0W
		01.15	CTD/Ro/WS/ADCP	a/D				11º19.9S	28º39.9W
		03.10	CTD/Ro/WS	z/W	SL 5503 m	WT 5520 m	W 03	11º19.9S	28º39.9W
		04.00	CTD/Ro/WS	a/D				11º19.9S	28º39.8W
		04.07	MSN	z/W	SL 534 m	V = 2.3 Kn	W 09	11º19.7S	28º39.7W
		05.25	MSN	a/D				11º16.6S	28º39.0W
		04.09	NEUSS	z/W		V = 2.3 Kn		11º19.6S	28º39.7W
		05.01	NEUSS	a/D				11º17.8S	28º39.4W
Station # 191									
		09.23	CTD/Ro/WS/ADCP	z/W	SL 995 m	WT 5488 m	W 02	11º20.0S	28º00.0W
		10.14	CTD/Ro/WS/ADCP	a/D				11º20.0S	28º00.0W
		10.19	CTD/Ro/WS	z/W	SL 5526 m	WT 5489 m	W 03	11º20.0S	28º00.0W
		13.23	CTD/Ro/WS	a/D				11º20.1S	28º00.0W
Station # 192									
		17.40	CTD/Ro/WS/ADCP	z/W	SL 993 m	WT 5509 m	W 02	11º20.0S	27º20.0W
		19.00	CTD/Ro/WS/ADCP	a/D				11º20.0S	27º20.0W
		19.04	CTD/Ro/WS	z/W	SL 650 m	WT 5510 m	W 03	11º20.0S	27º20.0W
		19.50	CTD/Ro/WS	a/D	Messung abgebrochen, Winde defekt)				
		20.10	CTD/Ro/WS	z/W	SL 5549 m	WT 5566 m	W 02	11º20.0S	27º20.0W
	09.04.94	00.44	CTD/Ro/WS	a/D				11º20.0S	27º20.0W
		00.48	MSN	z/W	SL 468 m	V = 2.3 Kn	W 09	11º19.9S	27º20.1W
		01.42	MSN	a/D				11º17.7S	27º19.2W
		00.51	NEUSS	z/W		V = 2.3 Kn		11º19.7S	27º20.0W

Station No.	Date	Time	Device	Activity	Length of wire	Speed	Winch	Latitude	Longitude
		01.23	NEUSS	a/D				11º18.4S	27º19.5W
Station # 193									
		05.50	CTD/Ro/WS	z/W	SL 5581 m	WT 5537 m	W 02	11º20.0S	26º40.0W
		09.12	CTD/Ro/WS	a/D				11º20.0S	26º40.0W
		09.30	CTD/Ro/WS/ADCP	z/W	SL 995 m	WT 5537 m	W 02	11º20.0S	26º40.0W
		10.29	CTD/Ro/WS/ADCP	a/D				11º20.0S	26º40.0W
Wetter: SE'l 5 See 2 c 1013.0hPa L 27.0ø W 27.8ø									
Station # 194									
		15.16	CTD/Ro/WS/ADCP	z/W	SL 993 m	WT 5678 m	W 02	11º20.0S	26º00.0W
		16.16	CTD/Ro/WS/ADCP	a/D				11º20.0S	26º00.0W
		16.22	CTD/Ro/WS	z/W	SL 5607 m	WT 5601 m	W 10/12	11º20.0S	26º00.0W
		20.10	CTD/Ro/WS	a/D				11º20.0S	26º00.0W
		20.23	MSN	z/W	SL 622 m	V = 2.3 Kn	W 09	11º19.9S	25º59.8W
		21.26	MSN	a/D				11º17.2S	25º57.1W
		20.23	NEUSS	z/W		V = 2.3 Kn		11º19.8S	25º59.7W
		20.55	NEUSS	a/D				11º18.6S	250583W
Station # 195									
	10.04.94	01.32	CTD/Ro/WS/ADCP	z/W	SL 998 m	WT 5702 m	W 02	11º20.0S	25º20.0W
		02.25	CTD/Ro/WS/ADCP	a/D				11º19.9S	25º20.0W
		02.34	CTD/Ro/WS	z/W	SL 5625 m	WT 5680 m	W 10/12	11º19.9S	25º20.0W
		06.30	CTD/Ro/WS	a/D				11º20.0S	25º20.0W
Station # 196									
		10.49	CTD/Ro/WS/ADCP	z/W	SL 994 m	WT 5399 m	W 02	11º10.0S	24º40.0W
		11.44	CTD/Ro/WS/ADCP	a/D				11º20.0S	24º40.0W
		11.52	CTD/Ro/WS	z/W	SL 5403 m	WT 5399 m	W 10/12	11º20.0S	24º40.0W
		15.02	CTD/Ro/WS	a/D				11º19.9S	24º40.0W
Station # 197									
		19.35	CTD/Ro/WS/ADCP	z/W	SL 999 m	WT 4954 m	W 02	11º20.0S	24º00.0W
		20.37	CTD/Ro/WS/ADCP	a/D				11º19.9S	24º00.0W
		20.56	CTD/Ro/WS	z/W	SL 4931 m	WT 4928 m	W 10/12	11º10.0S	23º59.9W
	11.04.94	00.12	CTD/Ro/WS	a/D				11º20.0S	24º00.0W
		00.19	MSN	z/W	SL 410 m	V = 2.3 Kn	W 09	11º19.8S	24º00.0W
		01.10	MSN	a/D				11º17.8S	23º58.8W
		00.22	NEUSS	z/W		V = 2.3 Kn		11º19.7S	23º59.9W
		00.54	NEUSS	a/D				11º18.5S	23º59.2W
Station # 198									
		05.22	CTD/Ro/WS/ADCP	z/W	SL 999 m	WT 5448 m	W 02	11º20.0S	23º20.0W

Station No.	Date	Time	Device	Activity	Length of wire	Speed	Winch	Latitude	Longitude
		06.26	CTD/Ro/WS/ADCP	a/D				11º20.0S	23º20.0W
		06.34	CTD/Ro/WS	z/W	SL 5453 m	WT 5459 m	W 10/12	11º20.0S	23º20.0W
		10.07	CTD/Ro/WS	a/D				11º20.0S	23º20.0W
		10.14	MSN	z/W	SL 569 m	V = 2.3 Kn	W 09	11º19.8S	23º19.9W
		11.13	MSN	a/D				11º17.5S	23º17.7W
		10.46	NEUSS	z/W		V = 2.3 Kn		11º19.7S	23º19.8W
		10.48	NEUSS	a/D				11º18.5S	23º18.7W
Station # 199									
		15.36	CTD/Ro/WS/ADCP	z/W	SL 1001 m	WT 5228 m	W 02	11º10.0S	22º40.0W
		16.40	CTD/Ro/WS/ADCP	a/D				11º20.0S	22º40.0W
		16.48	CTD/Ro/WS	z/W	SL 5140 m	WT 5240 m	W 10/12	11º20.0S	22º40.0W
		20.19	CTD/Ro/WS	a/D				11º20.0S	22º40.0W
Station # 200									
	12.04.94	00.49	CTD/Ro/WS/ADCP	z/W	SL 993 m	WT 4888 m	W 02	11º20.0S	22º00.0W
		01.48	CTD/Ro/WS/ADCP	a/D				11º20.1S	22º00.0W
		01.52	CTD/Ro/WS	z/W	SL 4841 m	WT 4883 m	W 10/12	11º20.1S	22º00.0W
		05.35	CTD/Ro/WS	a/D				11º20.2S	21º59.7W
Station # 201									
		08.51	CTD/Ro/WS/ADCP	z/W	SL 999 m	WT 4979 m	W 02	11º20.0S	21º30.0W
		09.47	CTD/Ro/WS/ADCP	a/D				11º20.0S	21º30.0W
		09.55	CTD/Ro/WS	z/W	SL 4905 m	WT 4989 m	W 10/12	11º20.2S	21º30.0W
		13.31	CTD/Ro/WS	a/D				11º20.0S	21º30.0W
		13.37	MSN	z/W	SL 418 m	V = 2.3 Kn	W 09	11º19.9S	21º29.9W
		14.28	MSN	a/D				11º17.8S	21º29.6W
		13.40	NEUSS	z/W		V = 2.3 Kn		11º19.8S	21º29.9W
		14.11	NEUSS	a/D				11º18.5S	21º29.7W
Station # 202									
		17.29	CTD/Ro/WS/ADCP	z/W	SL 992 m	WT 4916 m	W 02	11º20.0S	20º59.9W
		18.42	CTD/Ro/WS/ADCP	a/D				11º20.0S	21º00.0W
		18.50	CTD/Ro/WS	z/W	SL 4851 m	WT 4869 m	W 10/12	11º20.0S	21 º00.0W
		22.23	CTD/Ro/WS	a/D				11º19.9S	21 º00.0W
Station # 203									
	13.04.94	01.42	CTD/Ro/WS/ADCP	z/W	SL 996 m	WT 5039 m	W 02	11º20.0S	20º30.0W
		02.42	CTD/Ro/WS/ADCP	a/D				11º19.9S	20º29.9W
		02.46	CTD/Ro/WS	z/W	SL 4977 m	WT 5023 m	W 10/12	11º20.0S	20º29.9W
		07.03	CTD/Ro/WS	a/D				11º20.0S	20º30.0W
		07.12	MSN	z/W	SL 487 m	V = 2.3 Kn	W 09	11º19.9S	20º29.9W

Station No.	Date	Time	Device	Activity	Length of wire	Speed	Winch	Latitude	Longitude
		08.05	MSN	a/D				11º18.1S	20º28.3W
		07.15	NEUSS	z/W		V = 2.3 Kn		11º19.9S	20º29.9W
		07.45	NEUSS	a/D				11º18.8S	20º29.0W
Station # 204									
		11.15	CTD/Ro/WS/ADCP	z/W	SL 997 m	WT 4753 m	W 02	11º20.0S	20º00.0W
		12.07	CTD/Ro/WS/ADCP	a/D				11º20.0S	20º00.0W
		Wetter E 4/5 See 2 c 1012.9hPa L 26.4ø W 27.5ø							
		12.18	Test mit Dummy		SL 4415 m	WT 4710 m	W 03	11º20.0S	20º00.0W
		14.48	Dummy	a/D				11º19.9S	20º00.0W
		14.54	CTD/Ro/WS	z/W	SL 4713 m	WT 4751 m	W 03	11º19.9S	20º00.0W
		18.15	CTD/Ro/WS	a/D				11º20.0S	19º59.9W
		18.25	Drifter m. Segel	z/W				11º19.8S	19º59.7W
Station # 205									
		21.32	CTD/Ro/WS/ADCP	z/W	SL 993 m	WT 4837 m	W 02	11º20.0S	19º30.0W
		22.00	CTD/Ro/WS/ADCP	a/D				11º20.0S	19º30.0W
		22.39	CTD/Ro/WS	z/W	SL 4743 m	WT 4796 m	W 03	11º20.0S	19º30.0W
	14.04.94	01.39	CTD/Ro/WS	a/D				11º20.0S	19º29.9W
		01.46	MSN	z/W	SL 485 m	V = 2.3 Kn	W 09	11º19.8S	19º29.9W
		02.43	MSN	a/D				11º17.2S	19º29.3W
		01.49	NEUSS	z/W		V = 2.3 Kn		11º19.7S	19º29.8W
		02.20	NEUSS	a/D				11º18.1S	19º29.5W
Station # 206									
		05.40	CTD/Ro/WS/ADCP	z/W	SL 1001 m	WT 4573 m	W 02	11º10.0S	19º00.0W
		06.43	CTD/Ro/WS/ADCP	a/D				11º20.0S	19º00.0W
		06.50	CTD/Ro/WS	z/W	SL 4542 m	WT 4565 m	W 03	11º20.0S	19º00.0W
		09.47	CTD/Ro/WS	a/D				11º20.1S	18º59.9W
		09.54	Drifter m. Segel	z/W				11º20.1S	18º59.8W
Station # 207									
		12.48	CTD/Ro/WS/ADCP	z/W	SL 995 m	WT 4115 m	W 02	11º20.0S	18º30.0W
		13.45	CTD/Ro/WS/ADCP	a/D				11º20.1S	18º29.9W
		13.54	CTD/Ro/WS	z/W	SL 4083 m	WT 4114 m	W 03	11º20.0S	18º30.0W
		16.40	CTD/Ro/WS	a/D				11º20.1S	18º29.8W
Station # 208									
		19.30	CTD/Ro/WS/ADCP	z/W	SL 994 m	WT 4411 m	W 02	11º20.0S	18º00.0W
		20.28	CTD/Ro/WS/ADCP	a/D				11º20.0S	18º00.0W
		20.34	CTD/Ro/WS	z/W	SL 4326 m	WT 4417 m	W 03	11º20.0S	18º00.0W
		23.55	CTD/Ro/WS	a/D				11º19.9S	17º59.8W

Station No.	Date	Time	Device	Activity	Length of wire	Speed	Winch	Latitude	Longitude
		UTC-1							
	15.04.94	00.00	MSN	z/W		V = 2.3 Kn	W 09	11º19.9S	17º59.6W
		00.45	MSN	a/D				11º18.6S	17º57.6W
		00.05	NEUSS	z/W		V = 2.3 Kn		11º19.9S	17º59.5W
		00.35	NEUSS	a/D				11º18.9S	17º58.0W
Station # 209									
		04.00	CTD/Ro/WS/ADCP	z/W	SL 193 m	WT 3733 m	W 02	11º20.0S	17º30.0W
		04.20	CTD/Ro/WS/ADCP	a/D				11º20.0S	17º30.0W
		04.25	CTD/Ro/WS	z/W	SL 3724 m	WT 3743 m	W 03	11º20.0S	17º30.0W
		07.00	CTD/Ro/WS	a/D				11º20.0S	17º29.9W
		07.08	Drifter m. Segel	z/W				11º20.0S	17º29.8W
Station # 210									
		10.05	CTD/Ro/WS/ADCP	z/W	SL 1018 m	WT 4265 m	W 02	11º20.0S	17º00.0W
		10.53	CTD/Ro/WS/ADCP	a/D				11º20.0S	17º00.0W
		10.58	CTD/Ro/WS	z/W	SL 3236 m	WT 4259 m	W 03	11º19.9S	17º00.0W
		13.32	CTD/Ro/WS	a/D				11º19.9S	16º59.9W
		13.38	MSN	z/W	SL 62 m	V = 2.3 Kn	W 09	11º19.8S	16º59.8W
		13.42	MSN	a/D	(Kabelbruch im Gerdt)			11º19.7S	16º59.6W
		13.41	NEUSS	z/W		V = 2.3 Kn		11º19.7S	16º59.7W
		14.15	NEUSS	a/D				11º18.4S	16º59.1W
Station # 211									
		16.40	CTD/Ro/WS/ADCP	z/W	SL 995 m	WT 4164 m	W 02	11º20.0S	16º35.0W
		17.36	CTD/Ro/WS/ADCP	a/D				11º20.0S	16º35.0W
		17.43	CTD/Ro/WS	z/W	SL 4120 m	WT 4148 m	W 03	11º20.0S	16º35.0W
		20.25	CTD/Ro/WS	a/D				11º20.0S	16º35.0W
		20.32	MSN	z/W	SL 581 m	V = 2.3 Kn	W 09	11º19.8S	16º34.9W
		21.35	MSN	a/D				11º16.5S	16º34.4W
Station # 212									
	16.04.94	00.08	CTD/Ro/WS/ADCP	z/W	SL 115 m	WT 3843 m	W 02	11º20.0S	16º10.0W
		00.17	CTD/Ro/WS/ADCP	a/D				11º20.0S	16º10.0W
		00.19	CTD/Ro/WS/ADCP	z/W	SL 995 m	WT 3843 m	W 02	11º20.0S	16º10.0W
		01.13	CTD/Ro/WS/ADCP	a/D				11º20.0S	16º10.0W
		01.17	CTD/Ro/WS	z/W	SL 3743 m	WT 3819 m	W 03	11º20.0S	16º09.9W
		04.00	CTD/Ro/WS	a/D				11º20.0S	16º10.0W
Station # 213									
		06.35	CTD/Ro/WS/ADCP	z/W	SL 995 m	WT 3470 m	W 02	11º20.0S	15º45.0W

Station No.	Date	Time	Device	Activity	Length of wire	Speed	Winch	Latitude	Longitude
		07.29	CTD/Ro/WS/ADCP	a/D				11º20.0S	15º45.0W
		07.34	CTD/Ro/WS	z/W	SL 3434 m	WT 3472 m	W 03	11º20.0S	15º45.0W
		09.45	CTD/Ro/WS	a/D				11º20.0S	15º45.0W
		09.51	MSN	z/W	SL 486 m	V = 2.3 Kn	W 09	11º19.8S	15º44.9W
		10.47	MSN	a/D				11º17.4S	15º43.3W
		09.54	NEUSS	z/W		V = 2.3 Kn		11º19.7S	15º44.8W
		10.26	NEUSS	a/D				11º18.3S	15º43.9W
		10.54	Drifter m. Segel	z/W				11º17.2S	15º43.1W
Wetter: E'l 5 See 2 c 1014.7hPa L 26.7ø W 26.3ø									
Station # 214									
		13.21	CTD/Ro/WS/ADCP	z/W	SL 995 m	WT 3476 m	W 02	11º20.0S	15º20.0W
		14.18	CTD/Ro/WS/ADCP	a/D				11º20.0S	15º20.0W
		14.22	CTD/Ro/WS	z/W	SL 3488 m	WT 3476 m	W 03	11º20.0S	15º20.0W
		16.50	CTD/Ro/WS	a/D				11º19.9S	15º19.9W
Station # 215									
		19.25	CTD/Ro/WS/ADCP	z/W	SL 993 m	WT 3269 m	W 02	11º20.0S	14º55.0W
		20.19	CTD/Ro/WS/ADCP	a/D				11º20.0S	14º55.0W
		20.24	CTD/Ro/WS	z/W	SL 3252 m	WT 3270 m	W 03	11º20.0S	14º55.0W
		22.28	CTD/Ro/WS	a/D				11º20.0S	14º55.0W
		22.35	MSN	z/W	SL 478 m	V = 2.3 Kn	W 09	11º19.8S	14º54.9W
		23.40	MSN	a/D				11º17.1S	14º53.4W
		22.38	NEUSS	z/W		V = 2.3 Kn		11º19.7S	14º54.8W
		23.09	NEUSS	a/D				11º18.4S	14º54.1W
Station # 216									
	17.04.94	02.02	CTD/Ro/WS/ADCP	z/W	SL 995 m	WT 3075 m	W 02	11º20.0S	14º30.0W
		02.58	CTD/Ro/WS/ADCP	a/D				11º20.0S	14º30.0W
		03.02	CTD/Ro/WS	z/W	SL 3014 m	WT 3047 m	W 03	11º20.0S	14º30.0W
		05.20	CTD/Ro/WS	a/D				11º19.9S	14º29.9W
Station # 217									
		07.45	CTD/Ro/WS/ADCP	z/W	SL 1061 m	WT 2935 m	W 02	11º20.0S	14º05.0W
		08.40	CTD/Ro/WS/ADCP	a/D				11º20.0S	14º05.0W
		08.44	CTD/Ro/WS	z/W	SL 2926 m	WT 2947 m	W 03	11º20.0S	14º05.0W
		10.44	CTD/Ro/WS	a/D				11º20.0S	14º05.0W
Station # 218									
		13.27	CTD/Ro/WS/ADCP	z/W	SL 995 m	WT 2937 m	W 02	11º20.0S	13º40.0W
		14.21	CTD/Ro/WS/ADCP	a/D				11º20.0S	13º40.0W
		14.24	CTD/Ro/WS	z/W	SL 2950 m	WT 2976 m	W 03	11º20.0S	13º40.0W

Station No.	Date	Time	Device	Activity	Length of wire	Speed	Winch	Latitude	Longitude
		16.34	CTD/Ro/WS	a/D				11º20.0S	13º39.8W
		16.40	MSN	z/W	SL 582 m	V = 2.3 Kn	W 09	11º19.9S	13º39.7W
		17.40	MSN	a/D				11º17.7S	13º37.6W
		16.45	NEUSS	z/W		V = 2.3 Kn		11º19.7S	13º39.5W
		17.19	NEUSS	a/D				11º18.4S	13º38.2W
Station # 219									
		20.05	CTD/Ro/WS/ADCP	z/W	SL 1001 m	WT 2535 m	W 02	11º20.0S	13º15.0W
		20.49	CTD/Ro/WS/ADCP	a/D				11º20.0S	13º15.0W
		20.52	CTD/Ro/WS	z/W	SL 2524 m	WT 2534 m	W 03	11º20.0S	13º15.0W
		22.44	CTD/Ro/WS	a/D				11º20.0S	13º15.0W
Station # 220									
	18.04.94	01.25	CTD/Ro/WS/ADCP	z/W	SL 994 m	WT 2863 m	W 02	11º20.0S	12º50.0W
		02.16	CTD/Ro/WS/ADCP	a/D				11º20.0S	12º50.1W
		02.20	CTD/Ro/WS	z/W	SL 2865 m	WT 2863 m	W 03	11º20.0S	12º50.0W
		04.34	CTD/Ro/WS	a/D				11º20.0S	12º50.0W
Station # 221									
		07.12	CTD/Ro/WS/ADCP	z/W	SL 995 m	WT 3398 m	W 02	11º20.0S	12º25.0W
		08.06	CTD/Ro/WS/ADCP	a/D				11º19.9S	12º25.0W
		08.10	CTD/Ro/WS	z/W	SL 3363 m	WT 3436 m	W 02	11º20.0S	12º25.0W
		10.22	CTD/Ro/WS	a/D				11º20.0S	12º25.0W
		10.29	MSN	z/W	SL 672 m	V = 2.3 Kn	W 09	11º19.9S	12º24.9W
		11.31	MSN	a/D				11º17.5S	12º22.5W
		10.31	NEUSS	z/W		V = 2.3 Kn		11º19.8S	12º24.8W
		11.03	NEUSS	a/D				11º18.5S	12º23.5W
Station # 222									
		13.53	CTD/Ro/WS/ADCP	z/W	SL 1004 m	WT 3604 m	W 02	11º20.0S	12º00.0W
		14.46	CTD/Ro/WS/ADCP	a/D				11º20.1S	12º00.0W
		14.49	CTD/Ro/WS	z/W	SL 3579 m	WT 3602 m	W 03	11º20.1S	12º00.0W
		17.41	CTD/Ro/WS	a/D				11º20.0S	12º00.0W
Station # 223									
		20.50	CTD/Ro/WS/ADCP	z/W	SL 993 m	WT 3363 m	W 02	11º20.0S	11º30.0W
		21.37	CTD/Ro/WS/ADCP	a/D				11º20.0S	11º30.0W
		21.41	CTD/Ro/WS	z/W	SL 3347 m	WT 3357 m	W 03	11º20.0S	11º30.0W
		23.53	CTD/Ro/WS	a/D				11º19.9S	11º30.0W
Station # 224									
	19.04.94	03.06	CTD/Ro/WS/ADCP	z/W	SL 1003 m	WT 3826 m	W 02	11º20.0S	11º00.0W
		04.04	CTD/Ro/WS/ADCP	a/D				11º20.0S	11º00.0W

Station No.	Date	Time	Device	Activity	Length of wire	Speed	Winch	Latitude	Longitude
		04.10	CTD/Ro/WS	z/W	SL 3771 m	WT 3848 m	W 03	11º20.0S	11º00.0W
		06.56	CTD/Ro/WS	a/D				11º20.0S	11º00.0W
		07.03	MSN	z/W	SL 502 m	V = 2.3 Kn	W 09	11º19.9S	10º59.9W
		08.00	MSN	a/D				11º18.0S	10º58.2W
		07.06	NEUSS	z/W		V = 2.3 Kn		11º19.8S	10º59.8W
		07.36	NEUSS	a/D				11º18.6S	10º58.8W
Station # 225									
		11.08	CTD/Ro/WS/ADCP	z/W	SL 997 m	WT 4373 m	W 02	11º20.0S	10º30.0W
		12.00	CTD/Ro/WS/ADCP	a/D				11º20.0S	10º30.0W
		12.02	CTD/Ro/WS	z/W	SL 4364 m	WT 4373 m	W 03	11º20.0S	10º30.0W
		14.49	CTD/Ro/WS	a/D				11º20.0S	10º30.0W
Station # 226									
		18.05	CTD/Ro/WS/ADCP	z/W	SL 995 m	WT 4065 m	W 02	11º20.0S	10º00.0W
		19.15	CTD/Ro/WS/ADCP	a/D				11º20.0S	10º00.0W
		19.20	CTD/Ro/WS	z/W	SL 4054 m	WT 4070 m	W 03	11º20.0S	10º00.0W
		21.50	CTD/Ro/WS	a/D				11º20.0S	10º00.0W
Station # 227									
	20.04.94	00.47	CTD/Ro/WS/ADCP	z/W	SL 995 m	WT 4040 m	W 02	11º20.0S	09º30.0W
		01.57	CTD/Ro/WS/ADCP	a/D				11º20.0S	09º30.0W
		02.00	CTD/Ro/WS	z/W	SL 4026 m	WT 4054 m	W 03	11º20.0S	09º30.0W
		04.49	CTD/Ro/WS	a/D				11º20.0S	09º30.0W
		04.56	MSN	z/W	SL 499 m	V = 2.3 Kn	W 09	11º19.9S	09º29.9W
		05.50	MSN	a/D				11º18.2S	09º27.9W
		04.58	NEUSS	z/W		V = 2.3 Kn		11º19.8S	09º29.8W
		05.32	NEUSS	a/D				11º18.7S	09º28.6W
Station # 228									
		08.28	CTD/Ro/WS/ADCP	z/W	SL 1002 m	WT 4211 m	W 02	11º20.0S	09º00.0W
		09.43	CTD/Ro/WS/ADCP	a/D				11º20.0S	09º00.0W
		09.47	CTD/RO/WS	z/W	SL 4227 m	WT 4221 m	W 03	11º20.0S	09º00.0W
		12.28	CTD/Ro/WS	a/D				11º20.0S	09º00.0W
Wetter: SE 5 See 2 c 101 1.3hPa L 25.4ø W 26.5ø									
		15.42	CTD/Ro/WS/ADCP	z/W	SL 996 m	WT 4635 m	W 02	11º20.0S	08º30.0W
		16.46	CTD/Ro/WS/ADCP	a/D				11º20.0S	08º29.9W
		21.01	CTD/Ro/WS	z/W	SL 4535 m	WT 4647 m	W 03	11º20.0S	08º30.0W
		24.00	CTD/Ro/WS	a/D				11º20.0S	08º30.0W
Station # 230									
	21.04.94	03.06	CTD/Ro/WS/ADCP	z/W	SL 995 m	WT 4553 m	W02	11º20.0S	08º00.0W

Station No.	Date	Time	Device	Activity	Length of wire	Speed	Winch	Latitude	Longitude
		04.18	CTD/Ro/WS/ADCP	a/D				11º20.0S	08º00.0W
		04.22	CTD/Ro/WS	z/W	SL 4514 m	WT 4553 m	W 03	11º20.0S	08º00.0W
		07.21	CTD/Ro/WS	a/D				11º20.0S	08º00.0W
		07.27	MSN	z/W	SL 510 m	V = 2.3 Kn	W 09	11º19.8S	07º59.8W
		08.20	MSN	a/D				11º17.8S	07º58.0W
		07.30	NEUSS	z/W		V = 2.3 Kn		11º19.7S	07º59.7W
		08.00	NEUSS	a/D				11º18.5S	07º58.8W
Station # 231									
		11.24	CTD/Ro/WS/ADCP	z/W	SL 995 m	WT 4464 m	W 02	11º20.0S	07º30.0W
		12.22	CTD/Ro/WS/ADCP	a/D				11º20.0S	07º30.0W
		12.25	CTD/Ro/WS	z/W	SL 4439 m	WT 4452 m	W03	11º20.0S	07º30.0W
		15.07	CTD/Ro/WS	a/D				11º20.0S	07º30.0W
Station # 232									
		18.28	CTD/Ro/WS/ADCP	z/W	SL 997 m	WT 4999 m	W 02	11º20.0S	07º00.0W
		19.26	CTD/Ro/WS/ADCP	a/D				11º20.0S	07º00.0W
		19.32	CTD/Ro/WS	z/W	SL 4283 m	WT 4304 m	W03	11º20.0S	07º00.0W
		22.53	CTD/Ro/WS	a/D				11º20.0S	07º00.0W
		22.59	MSN	z/W	SL 497 m	V = 2.3 Kn	W 09	11º19.8S	06º59.9W
		23.54	MSN	a/D				11º17.6S	06º58.7W
		23.12	NEUSS	z/W		V = 2.3 Kn		11º19.7S	06º59.9W
		23.34	NEUSS	a/D				11º18.3S	06º59.1W
Station # 233		UTC 0							
	22.04.94	03.24	CTD/Ro/WS/ADCP	z/W	SL 998 m	WT 4479 m	W 02	11º20.0S	06º30.0W
		04.28	CTD/Ro/WS/ADCP	a/D				11º20.0S	06º30.0W
		04.35	CTD/Ro/WS	z/W	SL 4469 m	WT 4477 m	W 03	11º20.0S	06º30.0W
		07.31	CTD/Ro/WS	a/D				11º20.0S	06º30.0W
Station # 234									
		10.38	CTD/Ro/WS/ADCP	z/W	SL 998 m	WT 4514 m	W 02	11º20.0S	06º00.0W
		11.26	CTD/Ro/WS/ADCP	a/D				11º20.0S	06º00.0W
		11.33	CTD/Ro/WS	z/W	SL 4505 m	WT 4504 m	W 03	11º20.0S	06º00.0W
		14.25	CTD/Ro/WS	a/D				11º20.0S	06º00.0W
Station # 235									
		17.35	CTD/Ro/WS/ADCP	z/W	SL 994 m	WT 5002 m	W 02	11º20.0S	05º30.0W
		18.37	CTD/Ro/WS/ADCP	a/D				11º20.0S	05º30.0W
		18.44	CTD/Ro/WS	z/W	SL 5009 m	WT 5001 m	W 03	11º20.0S	05º30.0W
		21.37	CTD/Ro/WS	a/D				11º20.0S	05º30.0W
		21.45	MSN	z/W	SL 613 m	V = 2.3 Kn	W 09	11º19.8S	05º29.8W

Station No.	Date	Time	Device	Activity	Length of wire	Speed	Winch	Latitude	Longitude
		22.47	MSN	a/D				11º17.7S	05º27.0W
		21.48	NEUSS	z/W		V = 2.3 Kn		11º19.8S	05º29.7W
		22.18	NEUSS	a/D				11º18.7S	05º28.2W
Station # 236									
	23.04.94	01.38	CTD/Ro/WS/ADCP	z/W	SL 1007 m	WT 4145 m	W 02	11º20.0S	05º00.0W
		02.35	CTD/Ro/WS/ADCP	a/D				11º20.0S	05º00.0W
		02.41	CTD/Ro/WS	z/W	SL 4131 m	WT 4166 m	W 03	11º20.0S	05º00.0W
		05.32	CTD/Ro/WS	a/D				11º20.0S	05º00.0W
Station # 237									
		08.37	CTD/Ro/WS/ADCP	z/W	SL 997 m	WT 5057 m	W 02	11º20.0S	04º30.0W
		09.32	CTD/Ro/WS/ADCP	a/D				11º19.9S	04º30.0W
		09.37	CTD/Ro/WS	z/W	SL 5061 m	WT 5062 m	W 03	11º19.9S	04º30.0W
		12.46	CTD/Ro/WS	a/D				11º20.0S	04º30.0W
Wetter: SSE 5 See 2 c 1015.51lPa L 24.7ø W 25.9ø									
Station # 238									
		16.48	CTD/Ro/WS/ADCP	z/W	SL 994 m	WT 4552 m	W 02	11º20.0S	04º00.0W
		17.53	CTD/Ro/WS/ADCP	a/D				11º20.0S	04º00.0W
		17.58	CTD/Ro/WS	z/W	SL 4528 m	WT 4554 m	W 03	11º20.0S	04º00.0W
		20.49	CTD/Ro/WS	a/D				11º20.0S	03º59.9W
		20.58	MSN	z/W	SL 585 m	V = 2.3 Kn	W 09	11º19.9S	03º59.5W
		21.31	MSN	a/D				11º18.8S	03º56.1W
		21.00	NEUSS	z/W		V = 2.3 Kn		11º19.8S	03º59.4W
		21.31	NEUSS	a/D				11º19.3S	03º57.7W
Station # 239									
	24.04.94	00.42	CTD/Ro/WS/ADCP	z/W	SL 996 m	WT 4762 m	W 02	11º20.0S	03º30.0W
		01.38	CTD/ro/WS/ADCP	a/D				11º20.0S	03º30.0W
		01.41	CTD/Ro/WS	z/W	SL 4770 m	WT 4762 m	W 03	11º20.0S	03º30.0W
		04.49	CTD/Ro/WS	a/D				11º20.0S	03º30.0W
Station # 240									
		07.50	CTD/Ro/WS/ADCP	z/W	SL 1002 m	WT 4650 m	W 02	11º20.0S	03º00.0W
		08.47	CTD/Ro/WS/ADCP	a/D				11º20.0S	03º00.0W
		08.52	CTD/Ro/WS	z/W	SL 4645 m	WT 4652 m	W 03	11º20.0S	03º00.0W
		11.40	CTD/Ro/WS	a/D				11º20.0S	02º59.9W
		11.46	MSN	z/W	SL 447 m	V = 2.3 Kn	W 09	11º19.9S	02º59.8W
		12.37	MSN	a/D				11º19.3S	02º57.6W
		11.48	NEUSS	z/W		V = 2.3 Kn		11º19.9S	02º59.6W
		12.20	NEUSS	a/D				11º19.5S	02º58.2W

Station No.	Date	Time	Device	Activity	Length of wire	Speed	Winch	Latitude	Longitude
Station # 241									
		15.18	CTD/ro/WS/ADCP	z/W	SL 996 m	WT 5210 m	W 02	11º20.0S	02º30.0W
		16.24	CTD/ro/WS/ADCP	a/D				11º20.0S	02º29.7W
		16.45	CTD/Ro/WS	z/W	SL 5220 m	WT 5225 m	W 03	11º20.0S	02º30.0W
		20.03	CTD/Ro/WS	a/D				11º20.0S	02º30.0W
Station # 242									
		22.52	CTD/Ro/WS/ADCP	z/W	SL 999 m	WT 5383 m	W 02	11º20.0S	02º00.0W
		23.50	CTD/Ro/WS/ADCP	a/D				11º19.9S	01º59.7W
	25.04.94	00.15	CTD/Ro/WS	z/W	SL 5381 m	WT 5382 m	W 03	11º20.0S	01º59.9W
		03.41	CTD/Ro/WS	a/D				11º20.0S	02º00.0W
		03.46	MSN	z/W	SL 560 m	V = 2.3 Kn	W 09	11º19.9S	01º59.8W
		04.40	MSN	a/D				11º19.3S	01º56.9W
		03.49	NEUSS	z/W		V = 2.3 Kn		11º19.9S	01º59.6W
		04.20	NEUSS	a/D				11º19.5S	01º58.0W
Station # 243									
		07.11	CTD/Ro/WS/ADCP	z/W	SL 996 m	WT 5211 m	W 02	11º20.0S	01º30.0W
		08.12	CTD/Ro/WS/ADCP	a/D				11º20.0S	01º30.0W
		08.17	CTD/Ro/WS	z/W	SL 5216 m	WT 5219 m	W 03	11º20.0S	01º29.8W
		11.19	CTD/Ro/WS	a/D				11º20.0S	01º29.9W
Station # 244									
		14.12	CTD/Ro/WS/ADCP	z/W	SL 1014 m	WT 5326 m	W 02	11º20.0S	01º00.0W
		15.12	CTD/Ro/WS/ADCP	a/D				11º20.0S	01º00.0W
		15.15	CTD/Ro/WS	z/W	SL 5327 m	WT 5322 m	W 03	11º20.0S	01º00.0W
		18.37	CTD/Ro/WS	a/D				11º20.0S	01º00.0W
Station # 245									
		20.18	CTD/Ro/WS/ADCP	z/W	SL 997 m	WT 4798 m	W 02	11º20.0S	00º45.0W
		21.04	CTD/Ro/WS/ADCP	a/D				11º20.0S	00º45.0W
		21.09	CTD/Ro/WS	z/W	SL 4720 m	WT 4780 m	W 03	11º20.0S	00º45.0W
		23.53	CTD/Ro/WS	a/D				11º20.0S	00º45.0W
	26.04.94	00.00	MSN	z/W	SL 455 m	V = 2.3 Kn	W 09	11º20.0S	00º44.8W
		00.53	MSN	a/D				11º20.0S	00º42.3W
		00.05	NEUSS	z/W		V = 2.3 Kn		11º20.1S	00º44.5W
		00.36	NEUSS	a/D				11º20.1S	00º43.1W
Station # 246									
		02.15	CTD/Ro/WS/ADCP	z/W	SL 995 m	WT 4930 m	W 02	11º20.0S	00º30.0W
		03.12	CTD/Ro/WS/ADCP	a/D				11º20.0S	00º30.0W
		03.16	CTD/Ro/WS	z/W	SL 4916 m	WT 4930 m	W 03	11º20.0S	00º30.0W

Station No.	Date	Time	Device	Activity	Length of wire	Speed	Winch	Latitude	Longitude
		06.30	CTD/Ro/WS	a/D				11º20.0S	00º30.0W
		06.35	MSN	z/W	SL 572 m	V = 2.3 Kn	W 09	11º19.9S	00º29.8W
		07.37	MSN	a/D				11º18.0S	00º27.6W
		06.38	NEUSS	z/W		V = 2.3 Kn		11º19.8S	00º29.7W
		07.10	NEUSS	a/D				11º18.7S	00º28.5W
Station # 247									
		08.59	CTD/Ro/WS/ADCP	z/W	SL 996 m	WT 5462 m	W 02	11º20.0S	00º15.0W
		09.47	CTD/Ro/WS/ADCP	a/D				11º20.1S	00º15.0W
		09.51	CTD/Ro/WS	z/W	SL 5469 m	WT 5473 m	W 03	11º20.1S	00º15.0W
		13.06	CTD/Ro/WS	a/D				11º20.2S	00º14.9W
		13.13	MSN	ZIW	SL 471 m	V = 2.3 Kn	W 09	11º20.2S	00º14.7W
		14.00	MSN	a/D				11º19.9S	00º12.4W
		13.16	NEUSS	ZIW		V = 2.3 Kn		11º20.1S	00º14.5W
		13.48	NEUSS	a/D				11º20.0S	00º13.1W
Station # 248									
		15.35	CTD/Ro/WS/ADCP	z/W	SL 994 m	WT 5701 m	W 02	11º20.0S	00º00.1W
		16.40	CTD/Ro/WS/ADCP	a/D				11º20.0S	00º00.0
		16.44	CTD/Ro/WS	z/W	SL 5697 m	WT 5694 m	W 03	11º20.0S	00º00.0
		20.41	CTD/Ro/WS	a/D				11º20.1S	00º00.0
Station # 249									
	27.04.94	00.40	CTD/Ro/WS/ADCP	z/W	SL 5605 m	WT 5608 m	W 02	11º20.0S	00º40.0E
		04.25	CTD/Ro/WS/ADCP	a/D				11º20.0S	00º40.0E
		0433	MSN	z/W	SL 480 m	V = 2.3 Kn	W 09	11º19.9S	00º40.3E
		05.22	MSN	a/D				11º18.9S	00º42.6E
		04.36	NEUSS	z/W		V = 2.3 Kn		11º19.9S	00º40.4E
		05.07	NEUSS	a/D				11º19.2S	00º42.0E
Station # 250									
		09.03	CTD/Ro/WS/ADCP	z/W	SL 1094 m	WT 5590 m	W 02	11º20.0S	01º20.0E
		10.02	CTD/Ro/WS/ADCP	a/D				11º20.0S	01º20.0E
		10.06	CTD/Ro/WS	z/W	SL 5590 m	WT 5627 m	W 03	11º20.0S	01º19.9E
		13.23	CTD/Ro/WS	a/D				11º20.0S	01º20.0E
		13.31	Drifter m. Segel	z/W				11º19.9S	01º20.0E
Station # 251									
		19.20	CTD/Ro/WS/ADCP	z/W	SL 993 m	WT 5621 m	W 02	11º20.0S	02º00.0E
		20.21	CTD/Ro/WS/ADCP	a/D				11º20.0S	02º00.0E
		20.25	CTD/Ro/WS	z/W	SL 5589 m	WT 5574 m	W 03	11º20.0S	02º00.0E
		23.48	CTD/Ro/WS	a/D				11º20.0S	02º00.0W

Station No.	Date	Time	Device	Activity	Length of wire	Speed	Winch	Latitude	Longitude
		23.57	MSN	z/W	SL 525 m	V = 2.3 Kn	W 09	11º19.9S	02º00.0E
	28.04.94	00.51	MSN	a/D				11º18.2S	02º02.0E
		00.01	NEUSS	z/W		V = 2.3 Kn		11º19.8S	02º00.0E
		00.31	NEUSS	a/D				11º18.8S	02º01.4E
Station # 252									
		04.50	CTD/Ro/WS/ADCP	z/W	SL 994 m	WT 5570 m	W 02	11º20.0S	02º40.0E
		05.55	CTD/Ro/WS/ADCP	a/D				11º20.0S	02º40.0E
		06.01	CTD/Ro/WS	z/W	SL 5585 m	WT 5572 m	W 03	11º20.0S	02º40.0E
		09.17	CTD/Ro/WS	a/D				11º20.0S	02º40.0E
		09.24	Drifter m. Segel	z/W				11º20.0S	02º40.0E
Station # 253									
		13.25	CTD/Ro/WS/ADCP	z/W	SL 995 m	WT 5558 m	W 02	11º20.0S	03º20.0E
		14.28	CTD/Ro/WS/ADCP	a/D				11º20.0S	03º20.0E
		14.32	CTD/Ro/WS	z/W	SL 5588 m	WT 5566 m	W 03	11º20.0S	03º20.0E
		18.08	CTD/Ro/WS	a/D				11º20.0S	03º20.0E
		18.13	MSN	z/W	SL 512 m	V = 2.3 Kn	W 09	11º19.9S	03º20.2E
		19.08	MSN	a/D				11º18.6S	03º22.5E
		18.16	NEUSS	z/W		V = 2.3 Kn		11º19.8S	03º20.3E
		18.46	NEUSS	a/D				11º19.0S	03º21.5E
Station # 254									
		23.03 UTC+1	CTD/Ro/WS/ADCP	z/W	SL 1094 m	WT 5554 m	W 02	11º20.0S	04º00.0E
	29.04.94	01.00	CTD/Ro/WS/ADCP	a/D				11º20.0S	04º00.0E
		01.05	CTD/Ro/WS	z/W	SL 5573 m	WT 5556 m	W 03	11º20.0S	04º00.0E
		04.52	CTD/Ro/WS	a/D				11º20.1S	04º00.0E
		05.00	Drifter m. Segel	z/W				11º20.2S	04º00.1E
Station # 255									
		09.01	CTD/Ro/WS/ADCP	z/W	SL 995 m	WT 5596 m	W 02	11º20.0S	04º40.0E
		09.56	CTD/Ro/WS/ADCP	a/D				11º20.0S	04º40.0E
		10.00	CTD/Ro/WS	z/W	SL 5560 m	WT 5590 m	W03	11º20.0S	04º40.0E
		13.17	CTD/Ro/WS	a/D				11º20.1S	04º39.9E
		13.22	MSN	z/W	SL 470 m	V = 2.3 Kn	W 09	11º20.1S	04º40.1E
		14.13	MSN	a/D				11º19.4S	04º42.5E
		13.26	NEUSS	z/W		V = 2.3 Kn		11º20.0S	04º40.3E
		13.57	NEUSS	a/D				11º19.6S	04º41.8E

Station No.	Date	Time	Device	Activity	Length of wire	Speed	Winch	Latitude	Longitude
Wetter: S 4 See 2 c 1013.2hPa L 24.1ø W 25.5ø									
Station # 256									
		18.00	CTD/Ro/WS/ADCP	z/W	SL 995 m	WT 5452 m	W 02	11º20.0S	05º20.0E
		19.02	CTD/Ro/WS/ADCP	a/D				11º20.0S	05º20.0E
		19.08	CTD/Ro/WS	z/W	SL 5403 m	WT 5452 m	W 03	11º20.0S	05º20.0E
		22.10	CTD/Ro/WS	a/D				11º20.0S	05º20.0E
		22.17	Drifter m. Segel	z/W				11º20.1S	05º20.1E
Station # 257									
		02.15	CTD/Ro/WS/ADCP	z/W	SL 995 m	WT 5190 m	W 03	11º20.0S	06º00.0E
		03.11	CTD/Ro/WS/ADCP	a/D				11º20.0S	06º00.0E
		03.14	CTD/Ro/WS	z/W	SL 5137 m	WT 5185 m	W 02	11º20.0S	06º00.0E
		06.28	CTD/Ro/WS	a/D				11º20.0S	06º00.0E
		06.31	MSN	z/W	SL 469 m	V = 2.3 Kn	W 09	11º20.1S	06º00.1E
		07.20	MSN	a/D				11º20.0S	06º02.6E
		06.35	NEUSS	z/W		V = 2.3 Kn		11º20.0S	06º00.3E
		07.06	NEUSS	a/D				11º20.0S	06º01.9E
Station # 258									
		10.55	CTD/Ro/WS	z/W	SL 5228 m	WT 5256 m	W 03	11º20.0S	06º40.0E
		14.08	CTD/Ro/WS	a/D				11º20.0S	06º40.0E
		14.12	CTD/Ro/WS/ADCP	z/W	SL 1014 m	WT 5256 m	W 02	11º20.0S	06º40.0E
		15.14	CTD/Ro/WS/ADCP	a/D				11º20.0S	06º40.0E
		15.19	CTD/Ro/WS	z/W	SL 5217 m	WT 5259 m	W 03	11º20.0S	06º40.0E
		18.34	CTD/Ro/WS	a/D				11º20.0S	06º40.0E
Station # 259									
		22.33	CTD/Ro/WS/ADCP	z/W	SL 995 m	WT 5060 m	W 02	11º20.0S	07º20.0E
		23.32	CTD/Ro/WS/ADCP	a/D				11º20.0S	07º20.0E
		23.36	CTD/Ro/WS	z/W	SL 5029 m	WT 5055 m	W 03	11º20.0S	07º19.9E
	01.05.94	02.37	CTD/Ro/WS	a/D				11º20.0S	07º20.0E
		02.43	MSN	z/W	SL 499 m	V = 2.3 Kn	W 09	11º19.9S	07º20.0E
		03.35	MSN	a/D				11º20.7S	07º22.9E
		02.46	NEUSS	z/W		V = 2.3 Kn		11º20.0S	07º20.3E
		03.18	NEUSS	a/D				11º20.5S	07º22.0E
Station # 260									
		07.12	CTD/Ro/WS/ADCP	z/W	SL 993 m	WT 4864 m	W 02	11º20.0S	08º00.0E
		08.10	CTD/Ro/WS/ADCP	a/D				11º20.0S	08º00.0E
		08.13	CTD/Ro/WS	z/W	SL 4834 m	WT 4860 m	W 03	11º20.0S	08º00.0E

Station No.	Date	Time	Device	Activity	Length of wire	Speed	Winch	Latitude	Longitude
		11.25	CTD/Ro/WS	a/D				11º20.0S	08º00.0E
Wetter: SSE 3 See 1 c 1013.8hPa L 23.9ø W 26.8ø									
Station # 261									
		14.30	CTD/Ro/WS/ADCP	z/W	SL 995 m	WT 4787 m	W 02	11º20.0S	08º30.0E
		15.25	CTD/Ro/WS/ADCP	a/D				11º20.0S	08º30.0E
		15.31	CTD/Ro/WS	z/W	SL 4775 m	WT 4786 m	W 03	11º20.0S	08º30.0E
		18.32	CTD/Ro/WS	a/D				11º20.0S	08º30.0E
		18.37	MSN	z/W	SL 525 m	V = 2.3 Kn	W 09	11º20.0S	08º30.0E
		19.32	MSN	a/D				11º20.6S	08º32.8E
		18.41	NEUSS	z/W		V = 2.3 Kn		11º20.0S	08º30.3E
		19.14	NEUSS	a/D				11º20.4S	08º31.9E
Station # 262									
		22.06	CTD/Ro/WS/ADCP	z/W	SL 997 m	WT 4589 m	W 02	11º20.0S	09º00.0E
		22.56	CTD/Ro/WS/ADCP	a/D				11º20.0S	08º59.9E
		23.00	CTD/Ro/WS	z/W	SL 4578 m	WT 4586 m	W 03	11º20.0S	09º00.0E
	02.05.94	01.41	CTD/Ro/WS	a/D				11º20.0S	09º00.0E
Station # 263									
		04.35	CTD/Ro/WS/ADCP	z/W	SL 995 m	WT 4406 m	W 02	11º20.0S	09º30.0E
		05.38	CTD/Ro/WS/ADCP	a/D				11º20.0S	09º30.0E
		05.47	CTD/Ro/WS	z/W	SL 4380 m	WT 4408 m	W 03	11º20.0S	09º30.0E
		08.30	CTD/Ro/WS	a/D				11º20.0S	09º30.0E
		08.39	MSN	z/W	SL 588 m	V = 2.3 Kn	W 09	11º20.0S	09º30.2E
		09.40	MSN	a/D				11º20.0S	09º33.8E
		08.41	NEUSS	z/W		V = 2.3 Kn		11º20.0S	09º30.0E
		09.13	NEUSS	a/D				11º20.0S	09º32.1E
Station # 264									
		12.00	CTD/Ro/WS/ADCO	z/W	SL 1007 m	WT 4153 m	W 02	11º20.0S	10º00.0E
		12.57	CTD/Ro/WS/ADCP	a/D				11º20.0S	10º00.0E
		12.59	CTD/Ro/WS	z/W	SL 4141 m	WT 4150 m	W 03	11º20.0S	10º00.0E
		15.37	CTD/Ro/WS	a/D				11º20.0S	10º00.0E
		15.44	MSN	z/W	SL 551 m	V = 2.3 Kn	W 09	11º20.1S	09º59.9E
		16.46	MSN	a/D				11º22.4S	10º02.6E
		15.47	NEUSS	z/W		V = 2.3 Kn		11º20.2S	09º59.9E
		16.20	NEUSS	a/D				11º21.5S	10º01.6E
Station # 265									
		18.48	CTD/Ro/WS/ADCP	z/W	SL 999 m	WT 4069 m	W 02	11º20.0S	10º25.0E
		19.54	CTD/Ro/WS/ADCP	a/D				11º20.0S	10º25.0E

Station No.	Date	Time	Device	Activity	Length of wire	Speed	Winch	Latitude	Longitude
		20.00	CTD/Ro/WS	z/W	SL 4039 m	WT 4063 m	W 03	11º20.0S	10º25.0E
		22.25	CTD/Ro/WS	a/D				11º20.0S	10º25.0E
Station # 266									
	03.05.94	00.46	CTD/Ro/WS/ADCP	z/W	SL 996 m	WT 3861 m	W 02	11º20.0S	10º50.0E
		01.45	CTD/Ro/WS/ADCP	a/D				11º20.0S	10º50.0E
		01.48	CTD/Ro/WS	z/W	SL 3844 m	WT 3865 m	W 03	11º20.0S	10º50.0E
		04.25	CTD/Ro/WS	a/D				11º20.0S	10º50.0E
Station # 267									
		06.45	CTD/Ro/WS/ADCP	z/W	SL 995 m	WT 3666 m	W 02	11º20.0S	11º15.0E
		07.43	CTD/Ro/WS/ADCP	a/D				11º20.0S	11º15.0E
		07.50	CTD/Ro/WS	z/W	SL 3678 m	WT 3665 m	W 03	11º20.0S	11º15.0E
		10.15	CTD/Ro/WS	a/D				11º20.0S	11º15.0E
Station # 268									
		12.42	CTD/Ro/WS/ADCP	z/W	SL 1007 m	WT 3345 m	W 02	11º20.0S	11º40.0E
		13.36	CTD/Ro/WS/ADCP	a/D				11º20.0S	11º40.0E
		13.39	CTD/Ro/WS	z/W	SL 3324 m	WT 3335 m	W 03	11º20.0S	11º40.0E
		16.00	CTD/Ro/WS	a/D				11º20.1S	11 º40.0E
Station # 269									
		17.55	CTD/Ro/WS/ADCP	z/W	SL 995 m	WT 2654 m	W 02	11º20.0S	12º00.0E
		18.47	CTD/Ro/WS/ADCP	a/D				11º20.0S	12º00.0E
		18.51	CTD/Ro/WS	z/W	SL 2638 m	WT 2654 m	W 03	11º20.0S	12º00.0E
		20.41	CTD/Ro/Ws	a/D				11º20.0S	12º00.0E
Station # 270									
		22.44	CTD/Ro/WS	z/W	SL 2303 m	WT 2334 m	W 03	11º20.1S	12º20.0E
	04.05.94	00.28	CTD/Ro/WS	a/D				11º20.0S	12º19.9E
		00.42	CTD/Ro/WS/ADCP	z/W	SL 1286 m	WT 2335 m	W 02	11º20.1S	12º20.0E
		01.38	CTD/Ro/WS/ADCP	a/D				11º20.0S	12º20.0E
Station # 271									
		02.46	CTD/Ro/WS/ADCP	z/W	SL 1001 m	WT 1728 m	W 02	11º20.0S	12º30.0E
		03.26	CTD/Ro/WS/ADCP	a/D				11º20.0S	12º30.0E
		03.30	CTD/Ro/WS	z/W	SL 1701 m	WT 1739 m	W 03	11º20.0S	12º30.0E
		05.02	CTD/Ro/WS	a/D				11º20.0S	12º30.0E
Station # 272									
		06.08	CTD/Ro/WS/ADCP	z/W	SL 994 m	WT 1616 m	W 02	11º20.0S	12º40.0E
		07.00	CTD/Ro/WS/ADCP	a/D				11º20.0S	12º40.0E
		07.03	CTD/Ro/WS	z/W	SL 1589 m	WT 1613 m	W 03	11º20.0S	12º40.0E
		08.23	CTD/Ro/WS					11º20.0S	12º40.0E

Station No.	Date	Time	Device	Activity	Length of wire	Speed	Winch	Latitude	Longitude
Station # 273									
		09.37	CTD/Ro/WS/ADCP	z/W	SL 1004 m	WT 1519 m	W 02	11º20.0S	12º50.0E
		10.21	CTD/Ro/WS/ADCP	a/D				11º20.0S	12º50.0E
		10.25	CTD/Ro/WS	z/W	SL 1491 m	WT 1520 m	W 03	11º20.0S	12º50.0E
		11.42	CTD/Ro/WS	a/D				11º20.0S	12º50.0E
Wetter: Umlfd. 1 See 0 c 1014.2hPa L 26.9ø W 28.0ø									
Station # 274									
		12.36	CTD/Ro/WS/ADCP	z/W	SL 994 m	WT 1277 m	W 02	11º20.0S	12º57.0E
		13.19	CTD/Ro/WS/ADCP	a/D				11º20.0S	12º57.0E
		13.22	CTD/Ro/WS	z/W	SL 1249 m	WT 1276 m	W 03	11º20.0S	12º57.0E
		14.27	CTD/Ro/WS	a/D				11º20.0S	12º57.0E
Station # 275									
		16.36	CTD/Ro/WS/ADCP	z/W	SL 993 m	WT 1375 m	W 03	11º00.0S	12º50.0E
		17.36	CTD/Ro/WS7ADCP	a/D				11º00.0S	12º50.0E
Station # 276									
		19.31	CTD/Ro/WS/ADCP	z/W	SL 997 m	WT 1552 m	W 03	11º00.0S	12º30.0E
		20.25	CTD/Ro/WS7ADCP	a/D				11º00.0S	12º30.0E
Station # 277									
		23.25	CTD/Ro/WS/ADCP	z/W	SL 995 m	WT 2476 m	W 03	11º00.0S	12º00.0E
	05.05.94	00.10	CTD/Ro/WS/ADCP	a/D				11º00.1S	12º00.0E
Station # 278									
		03.14	CTD/Ro/WS/ADCP	z/W	SL 994 m	WT 3401 m	W 03	11º00.0S	11º30.0E
		04.00	CTD/Ro/WS/ADCP	a/D				11º00.0S	11º30.0E
Station # 279									
		06.54	CTD/Ro/WS/ADCP	z/W	SL 993 m	WT 3855 m	W 03	11º00.0S	11º00.0E
		07.45	CTD/Ro/WS/ADCP	a/D				11º00.0S	11º00.0E
Station # 280									
		10.47	CTD/Ro/WS/ADCP	z/W	SL 993 m	WT 4057 m	W 03	11º00.0S	10º30.1E
		11.33	CTD/Ro/WS/ADCP	a/D				11º00.0S	10º30.1E
Station # 281									
		15.39	CTD/Ro/WS/ADCP	z/W	SL 993 m	WT 3558 m	W 03	11º40.0S	00º30.0E
		16.23	CTD/Ro/WS7ADCP	a/D				11º40.0S	10º30.0E
Station # 282									
		19.50	CTD/Ro/WS/ADCP	z/W	SL 993 m	WT 3690 m	W 03	11º40.0S	11º00.0E
		20.34	CTD/Ro/WS/ADCP	a/D				11º40.0S	11º59.9E
		20.46	MSN	z/W	SL 599 m	V = 2.3 Kn	W 09	11º40.2S	10º59.9E
		21.42	MSN	a/D				11º42.7S	11º01.7E

Station No.	Date	Time	Device	Activity	Length of wire	Speed	Winch	Latitude	Longitude
		20.49	NEUSS	z/W		V = 2.3 Kn		11º40.3S	11º00.0E
		21.20	NEUSS	a/D				11º41.8S	11º09.0E
Station # 283									
	06.05.94	00.23	CTD/Ro/WS/ADCP	z/W	SL 994 m	WT 3520 m	W 03	11º40.0S	11º30.0E
		01.05	CTD/Ro/WS/ADCP	a/D				11º40.0S	11º30.0E
		01.09	MSN	z/W	SL 564 m	V = 2.3 Kn	W 09	11º40.1S	11º30.1E
		02.00	MSN	a/D				11º42.1S	11º31.5E
		01.12	NEUSS	z/W		V = 2.3 Kn		11º40.2S	11º30.1E
		01.45	NEUSS	a/D				11º41.5S	11º31.0E
Station # 284									
		04.50	CTD/Ro/WS/ADCP	z/W	SL 993 m	WT 2171 m	W 03	11º40.0S	12º00.0E
		05.38	CTD/Ro/WS/ADCP	a/D				11º40.1S	12º00.0E
		05.46	MSN	z/W	SL 521 m	V = 2.3 Kn	W 09	11º40.3S	12º00.2E
		06.43	MSN	a/D				11º41.7S	12º02.7E
		05.49	NEUSS	z/W		V = 2.3 Kn		11º40.4S	12º00.2E
		06.21	NEUSS	a/D				11º41.2S	12º01.7E
Station # 285									
		09.12	CTD/Ro/WS/ADCP	z/W	SL 995 m	WT 1996 m	W 03	11º40.0S	12º30.0E
		09.57	CTD/Ro/WS/ADCP	a/D				11º40.2S	12º29.9E
		10.04	MSN	z/W	SL 480 m	V = 2.3 Kn	W 09	11º40.3S	12º29.9E
		10.57	MSN	a/D				11º42.6S	12º31.1E
		10.06	NEUSS	z/W		V = 2.3 Kn		11º40.5S	12º30.0E
		10.37	NEUSS	a/D				11º41.8S	12º30.7E
Station # 286									
		12.58	CTD/Ro/WS/ADCP	z/W	SL 995 m	WT 1738 m	W 03	11º40.0S	12º50.0E
		13.43	CTD/Ro/WS/ADCP	a/D				11º40.0S	12º50.0E
		13.47	MSN	z/W	SL 499 m	V = 2.3 Kn	W 09	11º40.1S	12º50.1E
		14.39	MSN	a/D				11º42.4S	12º49.1E
		13.50	NEUSS	z/W		V = 2.3 Kn		11º40.2S	12º49.9E
		14.22	NEUSS	a/D				11º41.6S	12º49.4E
Station # 287									
		17.40	CTD/Ro/WS/ADCP	z/W	SL 924 m	WT 1038 m	W 02	11º20.0S	13º05.0E
		18.28	CTD/Ro/WS/ADCP	a/D				11º20.0S	13º05.0E
		18.34	CTD/Ro/WS	z/W	SL 1007 m	WT 1030 m	W 03	11º20.0S	13º05.0E
		19.45	CTD/Ro/WS	a/D				11º20.0S	13º05.0E
		19.50	MSN	z/W	SL 516 m	V = 2.3 Kn	W 09	11º20.1S	13º05.0E
		20.51	MSN	a/D				11º22.6S	13º05.7E

Station No.	Date	Time	Device	Activity	Length of wire	Speed	Winch	Latitude	Longitude
		19.53	NEUSS	z/W		V = 2.3 Kn		11º20.2S	13º05.1E
		20.25	NEUSS	a/D				11º21.6S	13º05.4E
Station # 288									
		21.53	CTD/Ro/WS/ADCP	z/W	SL 800 m	WT 880 m	W 02	11º20.0S	13º15.0E
		22.28	CTD/Ro/WS/ADCP	a/D				11º20.0S	13º15.0E
		22.31	CTD/Ro/WS	z/W	SL 862 m	WT 881 m	W 03	11º20.0S	13º15.0E
		23.31	CTD/Ro/WS	a/D				11º20.0S	13º15.0E
		23.37	MSN	z/W	SL 467 m	V = 2.3 Kn	W 09	11º20.1S	13º15.1E
		00.29	MSN	a/D				11º21.6S	13º16.6E
	07.05.94	23.39	NEUSS	z/W		V = 2.3 Kn		11º20.1S	13º15.2E
		00.10	NEUSS	a/D				11º21.1S	13º16.1E
Station # 289									
		02.50	CTD/Ro/WS/ADCP	z/W	SL 578 m	WT 605 m	W 02	11º20.0S	13º25.0E
		03.22	CTD/Ro/WS/ADCP	a/D				11º20.0S	13º25.0E
		03.25	CTD/Ro/WS	z/W	SL 572 m	WT 601 m	W 03	11º20.0S	13º25.0E
		04.08	CTD/Ro/WS	a/D				11º20.0S	13º25.0E
		04.25	MSN	z/W	SL 522 m	V = 2.3 Kn	W 09	11º20.4S	13º25.4E
		05.20	MSN	a/D				11º20.7S	13º28.2E
		04.28	NEUSS	z/W		V = 2.3 Kn		11º20.4S	13º25.5E
		04.58	NEUSS	a/D				11º20.6S	13º27.0E
Station # 290									
		05.49	CTD/Ro/WS/ADCP	z/W	SL 148 m	WT 156 m	W 02	11º20.0S	13º32.4E
		06.03	CTD/Ro/WS7ADCP	a/D				11º20.0S	13º32.4E
		06.05	CTD/Ro/WS	z/W	SL 138 m	WT 159 m	W 03	11º20.0S	13º32.4E
		06.32	CTD/Ro/WS	a/D				11º20.0S	13º32.4E
		06.58	MSN	z/W	SL 485 m	V = 2.3 Kn	W 09	11º19.9S	13º30.0E
		07.50	MSN	a/D				11º19.3S	13º32.5E
		07.01	NEUSS	z/W		V = 2.3 Kn		11º19.8S	13º30.1E
		07.34	NEUSS	a/D				11º19.4S	13º31.8E

Abbreviations:

z/W device into the water
a/D device onto the deck
SL length of wire

7.1.2 List of XBT Drops

XBT No.	Date	Time		Latitude	Longitude
	31.03.94	22.28	XBT	11º14.1S	34º08.3W
		23.57	XBT	11º08.0S	34º16.5W
	01.04.94	00.47	XBT	11º02.5S	34º24.1W
		01.44	XBT	10º57.0S	34º31.8W
		02.35	XBT	10º51.5S	34º39.3W
		03.29	XBT	10º46.0S	34º46.8W
		04.25	XBT	10º40.0S	34º55.1W
		05.25	XBT	10º34.0S	35º03.3W
		05.58	XCP	10º31.0S	35º07.5W
		06.50	XBT	10º28.0S	35º11.6W
		07.22	XCP	10º26.0S	35º14.4W
		07.58	XBT	10º24.0S	35º17.1W
		08.32	XCP	10º22.0S	35º19.9W
		09.09	XBT	10º20.0S	35º22.6W
		09.44	XCP	10º08.0S	35º25.4W
		10.24	XBT	10º16.0S	35º29.1W
		10.50	XCP	10º14.5S	35º30.3W
		11.20	XBT	10º13.0S	35º32.3W
		11.45	XCP	10º11.5S	35º34.3W
		12.17	XBT	10º10.0S	35º36.4W
		12.41	XCP	10º08.5S	35º38.4W
		13.09	XBT	10º07.0S	35º40.5W
		13.34	XCP	10º05.5S	35º42.6W
		14.01	XBT	10º04.0S	35º44.6W
	06.04.94	16.50	XBT	11º20.0S	31º00.0W
		16.52	XBT	11º20.0S	30º59.6W
	07.04.94	02.05	XBT	11º20.0S	30º20.0W
		11.37	XBT	11º20.0S	29º40.0W
		21.08	XBT	11º20.0S	29º00.0W
		21.14	XBT	11º20.0S	28º59.3W
	08.04.94	07.25	XBT	11º20.0S	28º19.0W
		15.21	XBT	11º20.0S	27º40.0W
	09.04.94	03.40	XBT	11º10.0S	27º00.0W
		12.54	XBT	11º20.0S	26º20.0W
		23.19	XBT	11º20.0S	25º40.0W
		23.21	XBT	11º20.0S	25º39.7W
		23.23	XBT	11º20.0S	25º39.5W
		23.27	XBT	11º20.0S	25º39.2W
	10.04.94	08.35	XBT	11º10.0S	25º00.0W
		17.13	XBT	11º20.0S	24º20.0W
	11.04.94	03.11	XBT	11º20.0S	23º40.0W
		13.18	XBT	11º20.0S	23º00.0W

XBT No.	Date	Time		Latitude	Longitude
		22.37	XBT	11º20.0S	22º20.0W
	12.04.94	08.29	XBT	11º10.0S	21º31.6W
		14.29	XBT	11º17.7S	21º29.5W
		22.40	XBT	11º19.9S	20º59.9W
	13.04.94	10.51	XBT	11º19.9S	20º01.6W
		10.54	XBT	11º20.0S	20º01.0W
		18.30	XBT	11º19.8S	19º59.6W
	14.04.94	05.23	XBT	11º19.9S	19º01.6W
	26.04.94	22.40	XBT	11º20.0S	00º20.0E
	27.04.94	07.01	XBT	11º20.0S	01º00.0E
		08.42	XBT	11º20.0S	01º18.2E
		13.35	XBT	11º20.0S	01º20.0E
		15.36	XBT	11º20.0S	01º40.0E
		19.06	XBT	11º20.0S	01º58.2E
	28.04.94	02.38	XBT	11º20.0S	02º20.0E
		04.24	XBT	11º20.0S	02º38.3E
		11.20	XBT	11º20.0S	03º00.0E
		20.55	XBT	11º20.0S	03º40.0E
	29.04.94	06.55	XBT	11º20.0S	04º20.0E
		08.40	XBT	11º20.0S	04º38.3E
		16.00	XBT	11º20.0S	05º00.0E
	30.04.94	00.12	XBT	11º20.0S	05º40.0E
		08.59	XBT	11º20.0S	06º20.0E
		20.27	XBT	11º20.0S	07º00.0E
	01.05.94	05.13	XBT	11º20.0S	07º40.0E

7.1.3 List of Drifter Launches

Date 1994	Time	Drifter		Latitude	Longitude
13.04.	18.25	Drifter m. Segel	z/W	11º19.8S	19º59.7W
14.04.	09.54	Drifter m. Segel	z/W	11º20.1S	18º59.8W
15.04.	07.08	Drifter m. Segel	z/W	11º20.0S	17º29.8W
16.04.	10.54	Drifter m. Segel	z/W	11º17.2S	15º43.1W
27.04.	13.31	Drifter m. Segel	z/W	11º19.9S	01º20.0E
28.04.	09.24	Drifter m. Segel	z/W	11º20.0S	02º40.0E
29.04.	05.00	Drifter m. Segel	z/W	11º20.2S	04º00.1E
29.04.	22.17	Drifter m. Segel	z/W	11º20.1S	05º20.1E

7.2 Leg M 28/2

7.2.1 CTD Stations

STATION	DATE	TIME	PHI		LAMBDA		DEPTH	
292/1	20-MAY-1994	8:15	21	0.06'S	10	34.44'W	5.0	4300.0
295/2	21-MAY-1994	17:11	21	0.08'S	15	1.05'W	15.0	4000.0
296/3	22-RAY-1994	4:49	22	0.02'S	16	9.01'W	5.0	1565.0
297/4	22-MAY-1994	14:35	22	59.99'S	17	17.04'W	5.0	4310.0
298/5	23-MAY-1994	2:42	23	59.99'S	18	36.03'W	5.0	1495.0
299/6	23-MAY-1994	12: 4	24	59.98'S	19	44.02'W	5.0	4075.0
300/7	23-MAY-1994	23: 6	25	59.99'S	20	56.05'W	5.0	1495.0
301/8	24-MAY-1994	8:33	27	0.06'S	22	10.05'W	5.0	4405.0
302/9	24-MAY-1994	20:21	28	0.06'S	23	24.89'W	5.0	1515.0
303/10	25-MAY-1994	6: 2	29	0.03'S	24	42.04'W	5.0	1505.0
304/11	25-MAY-1994	15:40	30	0.03'S	25	58.63'W	5.0	4440.0
305/12	26-MAY-1994	2:50	30	49.07'S	27	23.04'W	5.0	1505.0
306/13	26-MAY-1994	14:10	31	37.47'S	28	49.09'W	5.0	3780.0
307/14	26-MAY-1994	21:55	32	29.94'S	28	47.98'W	5.0	1495.0
308/15	27-MAY-1994	4: 0	33	22.59'S	28	48.79'W	5.0	1500.0
309/16	27-MAY-1994	13: 6	34	15.52'S	28	52.46'W	5.0	4115.0
310/17	27-MAY-1994	18:30	34	18.91'S	28	29.49'W	5.0	4090.0
313/18	28-MAY-1994	15:45	34	25.15'S	27	52.08'W	5.0	4390.0
316/19	29-MAY-1994	17:55	34	35.19'S	27	3.40'W	5.0	4235.0
318/20	20-MAY-1994	18:41	34	30.82'S	27	19.21'W	5.0	4370.0
320/21	31-MAY-1994	21: 0	35	24.34'S	28	27.39'W	5.0	4855.0
323/22	3-JUN-1994	0:46	34	24.48'S	26	20.05'W	5.0	3935.0
324/23	3-JUN-1994	5:29	34	7.48'S	26	23.05'W	5.0	3800.0
325/24	3-JUN-1994	9:45	33	49.83'S	26	25.97'W	5.0	4530.0
326/25	3-JUN-1994	14:42	33	32.50'S	26	28.95'W	5.0	4290.0
327/26	3-JUN-1994	22:14	33	15.21'S	26	31.66'W	5.0	4665.0
328/27	4-JUN-1994	2:27	33	10.04'S	26	44.85'W	5.0	4570.0
329/28	4-JUN-1994	6:45	33	4.82'S	26	57.85'W	5.0	4505.0
330/29	4-JUN-1994	12: 4	32	59.59'S	27	10.43'W	5.0	3550.0
331130	4-JUN-1994	16:24	32	54.64'S	27	23.58'W	5.0	3825.0
332/31	4-JUN-1994	21:45	32	51.79'S	27	46.94'W	5.0	3195.0
333/32	5-JUN-1994	22:16	35	47.91'S	30	39.96'W	5.0	4130.0
334/33	6-JUN-1994	8: 7	36	42.31'S	31	30.66'W	5.0	1500.0
335/34	6-JUN-1994	15:30	37	36.54'S	32	22.06'W	5.0	4525.0
336/35	7-JUN-1994	0:43	38	31.01'S	33	13.87'W	5.0	1495.0
337/36	7-JUN-1994	8:30	39	25.43'S	34	6.50'W	5.0	1505.0
338137	7-JUN-1994	15:37	39	54.19'S	34	34.79'W	5.0	4865.0
339/38	8-JUN-1994	3:15	38	36.65'S	34	59.05'W	5.0	1495.0
340/39	8-JUN-1994	12:56	37	42.58'S	36	15.65'W	5.0	4985.0
341/40	9-JUN-1994	0: 6	36	48.39'S	37	31.28'W	5.0	1495.0
342/41	9-JUN-1994	9: 4	35	54.14'S	38	46.08'W	5.0	4950.0

STATION	DATE	TIME	PHI	LAMBDA	DEPTH
343/42	9-JUN-1994	20: 5	34 59.97'S	40 0.02'W	5.0 1505.0
344/43	10-JUN-1994	4:50	34 5.93'S	41 13.16'W	20.0 1510.0
345/44	11-JUN-1994	17: 3	34 57.52'S	48 38.97'W	5.0 4540.0

7.2.2 List of XBT Drops

STATION	DATE	TIME	PHI	LAMBDA	DEPTH
1	20-MAY-1994	0: 0	21 4.90'S	8 55.20'W	5.0 895.0
2	20-MAY-1994	1: 0	21 3.90'S	9 8.00'W	5.0 870.0
3	20-MAY-1994	2: 0	21 3.00'S	9 20.60'W	5.0 895.0
4	20-MAY-1994	3: 0	21 2.60'S	9 33.30'W	5.0 870.0
5	20-MAY-1994	4: 0	21 1.10'S	9 46.10'W	5.0 895.0
6	20-MAY-1994	5: 0	21 0.10'S	9 58.60'W	5.0 885.0
7	20-MAY-1994	6: 0	21 0.00'S	10 7.20'W	5.0 880.0
8	20-MAY-1994	7: 0	20 60.00'S	10 19.90'W	5.0 905.0
9	20-MAY-1994	8: 0	21 0.10'S	10 32.80'W	5.0 875.0
10	20-MAY-1994	20: 1	20 59.90'S	10 45.50'W	5.0 905.0
11	20-MAY-1994	21: 0	20 60.00'S	10 57.70'W	5.0 895.0
12	20-MAY-1994	22: 0	21 0.00'S	10 10.30'W	5.0 915.0
13	20-MAY-1994	23: 0	20 60.00'S	11 22.60'W	5.0 910.0
14	21-MAY-1994	0: 0	21 0.00'S	11 34.90'W	5.0 890.0
15	21-MAY-1994	1: 0	21 0.00'S	11 47.00'W	5.0 890.0
16	21-MAY-1994	3: 0	21 0.00'S	12 19.40'W	5.0 865.0
17	21-MAY-1994	5: 0	21 0.00'S	12 32.30'W	5.0 880.0
18	21-MAY-1994	6: 0	21 0.00'S	12 44.40'W	5.0 885.0
19	21-MAY-1994	7: 3	21 0.00'S	12 57.40'W	5.0 880.0
20	21-MAY-1994	8: 0	21 0.00'S	13 9.30'W	5.0 905.0
21	21-MAY-1994	9: 0	21 0.10'S	13 20.90'W	5.0 900.0
22	21-MAY-1994	10: 0	21 0.20'S	13 31.60'W	5.0 905.0
23	21-MAY-1994	11: 0	21 0.00'S	13 44.10'W	5.0 880.0
24	21-MAY-1994	12: 0	21 0.00'S	13 56.80'W	5.0 885.0
25	21-MAY-1994	13: 0	21 0.20'S	14 9.40'W	5.0 855.0
26	21-MAY-1994	14: 0	21 0.10'S	14 22.40'W	5.0 895.0
27	21-MAY-1994	15: 0	21 0.10'S	14 35.30'W	5.0 925.0
28	21-MAY-1994	16: 0	21 0.10'S	14 48.00'W	5.0 900.0
29	21-MAY-1994	17: 0	20 59.80'S	15 0.50'W	5.0 865.0
30	21-MAY-1994	22: 0	21 6.10'S	15 8.30'W	5.0 870.0
31	21-MAY-1994	23: 0	21 14.20'S	15 17.00'W	5.0 890.0
32	22-MAY-1994	0: 0	21 22.00'S	15 25.90'W	5.0 890.0
33	22-MAY-1994	1: 0	21 30.20'S	15 35.20'W	5.0 900.0
34	22-MAY-1994	2: 0	21 38.80'S	15 44.80'W	5.0 885.0
35	22-MAY-1994	3: 0	21 45.80'S	15 52.10'W	5.0 885.0
36	22-MAY-1994	4: 0	21 54.00'S	16 2.20'W	5.0 890.0
37	22-MAY-1994	8: 0	22 7.30'S	16 17.30'W	5.0 905.0
38	22-MAY-1994	9: 0	22 15.80'S	16 26.80'W	5.0 875.0

STATION	DATE	TIME	PHI	LAMBDA	DEPTH
39	22-MAY-1994	10: 0	22 24.10'S	16 36.20'W	5.0 885.0
40	22-MAY-1994	11: 0	22 32.20'S	16 45.40'W	5.0 910.0
41	22-MAY-1994	12: 0	22 40.30'S	16 54.60'W	5.0 885.0
42	22-MAY-1994	13: 0	22 48.40'S	17 3.80'W	5.0 885.0
43	22-MAY-1994	14: 0	22 55.80'S	17 12.40'W	5.0 900.0
44	22-MAY-1994	19: 0	23 1.40'S	17 19.30'W	5.0 905.0
45	22-MAY-1994	20: 0	23 8.70'S	17 28.60'W	5.0 895.0
46	22-MAY-1994	21: 0	23 16.70'S	17 38.90'W	5.0 900.0
47	22-MAY-1994	22: 0	23 24.90'S	17 49.70'W	5.0 890.0
48	22-MAY-1994	23: 0	23 32.70'S	17 59.90'W	5.0 865.0
49	23-MAY-1994	0: 0	23 40.50'S	18 10.20'W	5.0 900.0
50	23-MAY-1994	1: 0	23 48.20'S	18 20.40'W	5.0 910.0
51	23-MAY-1994	2: 0	23 55.90'S	18 30.60'W	5.0 900.0
52	23-MAY-1994	5: 0	24 4.90'S	18 41.50'W	5.0 885.0
53	23-MAY-1994	6: 0	24 12.40'S	18 49.90'W	5.0 890.0
54	23-MAY-1994	7: 0	24 21.00'S	18 59.70'W	5.0 890.0
55	23-MAY-1994	8: 0	24 29.00'S	19 9.00'W	5.0 875.0
56	23-MAY-1994	8:58	24 36.50'S	19 17.30'W	5.0 890.0
57	23-MAY-1994	10: 0	24 44.80'S	19 26.80'W	5.0 875.0
58	23-MAY-1994	11: 0	24 53.00'S	19 35.90'W	5.0 885.0
59	23-MAY-1994	17: 0	25 11.30'S	19 57.40'W	5.0 880.0
60	23-MAY-1994	18: 0	25 19.90'S	20 7.90'W	5.0 895.0
61	23-MAY-1994	19: 1	25 28.10'S	20 17.70'W	5.0 895.0
62	23-MAY-1994	20: 3	25 36.70'S	20 27.90'W	5.0 900.0
63	23-MAY-1994	20:58	25 44.00'S	20 36.70'W	5.0 900.0
64	23-MAY-1994	22: 0	25 52.20'S	20 46.70'W	5.0 895.0
65	24-MAY-1994	1:56	26 8.50'S	21 6.40'W	5.0 895.0
66	24-MAY-1994	3: 0	26 16.50'S	21 16.40'W	5.0 895.0
67	24-MAY-1994	4: 0	26 24.50'S	21 26.10'W	5.0 880.0
68	24-MAY-1994	4:48	26 32.90'S	21 36.60'W	5.0 905.0
69	24-MAY-1994	5:59	26 41.00'S	21 46.50'W	5.0 900.0
70	24-MAY-1994	6:59	26 49.10'S	21 56.40'W	5.0 910.0
71	24-MAY-1994	8: 2	26 57.20'S	22 6.50'W	5.0 900.0
72	24-MAY-1994	13: 0	27 3.80'S	22 14.80'W	5.0 890.0
73	24-MAY-1994	14: 0	27 11.50'S	22 24.50'W	5.0 900.0
74	24-MAY-1994	15: 0	27 19.40'S	22 34.40'W	5.0 890.0
75	24-MAY-1994	16: 0	27 27.20'S	22 44.00'W	5.0 900.0
76	24-MAY-1994	16:58	27 35.10'S	22 53.80'W	5.0 875.0
77	24-MAY-1994	17:58	27 43.00'S	23 3.80'W	5.0 895.0
78	24-MAY-1994	18:58	27 50.80'S	23 13.60'W	5.0 890.0
79	24-MAY-1994	20: 3	27 59.10'S	23 24.00'W	5.0 895.0
80	24-MAY-1994	23: 0	28 7.60'S	23 34.60'W	5.0 895.0
81	25-MAY-1994	0: 0	28 15.10'S	23 44.10'W	5.0 880.0
82	25-MAY-1994	0:58	28 22.20'S	23 53.40'W	5.0 895.0
83	25-MAY-1994	2: 0	28 30.30'S	24 3.50'W	5.0 905.0

STATION	DATE	TIME	PHI	LAMBDA	DEPTH
84	25-MAY-1994	3: 0	28 37.80'S	24 13.00'W	5.0 900.0
85	25-MAY-1994	4: 0	28 45.40'S	24 23.00'W	5.0 900.0
86	25-MAY-1994	5: 0	28 53.00'S	24 33.00'W	5.0 890.0
87	25-MAY-1994	8:59	29 8.60'S	24 53.90'W	5.0 885.0
88	25-MAY-1994	10: 0	29 16.90'S	25 3.30'W	5.0 895.0
89	25-MAY-1994	11: 0	29 25.00'S	25 13.40'W	5.0 870.0

7.2.3 List of Drifter Launches

Sta. No.	Drifter (ARGOS)	Date 1994	Time UTC	Latitude South	Longitude West	Temp (ºC)	Drogue (m)	Remarks
291	00652	20/5	5:20	21º00.0	10º00.1	23.6	100	Drift Sta. only
292	00665	20/5	19:00	20º59.9	10º34.5	23.8	100	Test Sta.
293	00671	21/5	2:15	20º59.8	12º00.0	24.0	100	Drift Sta. only
294	00650	21/5	9:50	21º00.1	13º30.1	24.3	100	Drift Sta. only
295	00626	21/5	21:04	20º59.1	15º01.1	24.5	100	w2 Float Depl.
297	00670	22/5	18:34	22º59.9	17º17.0	24.2	100	w Float Depl.
299	00630	23/5	15:23	25º00.0	19º43.9	24.1	100	w Float Depl.
301	00654	24/5	12:22	26º59.2	22º09.9	22.2	100	w Float Depl.
303	00639	25/5	7:49	28º59.9	24º42.0	21.2	100	w Float Depl.
305	00668	26/5	4:26	30º48.8	27º22.9	21.4	100	w Float Depl.
307	00672	26/5	22:40	32º29.9	28º48.0	20.6	100	w Float Depl.
309	00673	27/5	21:48	34º19.2	28º29.8	19.2	100	H1 w Fl Dep.
313	00653	28/5	19:07	34º25.4	27º52.4	17.4	100	H2º Hunter Ch.
321	00669	1/6	13:59	35º29.8	28º21.4	17.7	100	search for K0
327	00628	3/6	00:46	33º15.4	26º31.9	18.6	100	Hunter Ch East
334	00663	6/6	5:05	36º42.3	31º30.6	16.7	100	SR im Subtr. Gyre
336	00624	7/6	1:46	38º31.0	33º14.0	16.2	100	SR im Subtr. Gyre
338	00647	7/6	19:17	39º54.2	34º34.8	11.5	100	Subtropr. Front
341	00649	8/6	1:20	36º48.1	37º31.3	17.0	100	towards Vema Ch.
343	00635	9/6	21:16	35º00.2	40º00.1	18.9	100	outer Vema Ch.

7.2.4 Mooring Activities

Sta. No.	Ext No.	Int No.	Date dd/mm/yy	Latitude South	Longitude West	Depth (m)	Instrum. Type	Remarks
Current Meter Moorings								
*612	R	363	16/12/92	31º37.1	28º48.6	3719	2ACM	DWBC at Rio G Rise
306			26/05/94				CB	100% recvd
*602	H1	353	11/12/92	34º15.5	28º52.3	4112	6ACM, CB	Hunter West
309			27/5/94				IMAFOS	100% recvd
*605	H3	355	12-14/12/92	approximately 34º23.5	1 27º42.7	(4436)	5ACM	launch interrup, dual release, no CB

Sta. No.	Ext No.	Int No.	Date dd/mm/yy	Latitude South	Longitude West	Depth (m)	Instrum. Type	Remarks
312			29/5/94					100% recvd
*604	H2	354	12/12/92	34º25.5	27º51.6	4292	2ACM, CB	Hunter Cent
313			29/5/92					100% recvd
*609	H6	358	15/12/92	34º32.6	26º58.5	4303	ADCP, CB 5ACM,	Hunter East WD(#5506)
315			29/5/94					dual rel 100% recvd
*607	H5	357	14/12/92	34º35.1	27º03.4	(4836)	2ACM 200m ThCh	Hunter Ch CB lost
316			29/5/94					98% recovd
*606	H4	356	14/12/92	34º30.8	27º19.2	4336	2ACM, CB	Hunter Ch 200mThCh
			30/5/94					100% recovd
Sound Source Moorings								
*603	K0	352	11/12/92	34º18.9	28º30.0	4054	SoSo71	Window 1:30UTC WD alarm on 14-15/01/94
310			27/5/94					no resp. at mooring site
NB: SoSo71 was located at ~35º20 28º30 on ?/5/94, however it was inaccessible for METEOR								
322	K02	3522	2/6/94	34º13.36	28º38.37	4335	SoSo86	Window 1:35UTC
							MAFOS	WD 9243 launched
338	K4	365	7/6/94	39º51.61	34º32.93	4707	SoSo89	Window 1:00UTC
							MAFOS	WD 5513 launched

ADCP	Acoustic Doppler Current Profiler
ACM	Aanderaa Current Meter
CB	Bouy Radio Transmitter (CB Radio)
ThCh	Thermistor Chain
WD	Watch Dog (ARGOS Bouy Transmitter with dimmer)
SoSo	Sound Source, Part of RAFOS System

Station occupied during METEOR Cruise No.22, for details see G. Siedler et al. (1993)

7.2.5 List of RAFOS Float Launches and MAFOS Deployments

Sta. No.	Float IfM	Date 1994	Time UTC	Latitude South	Longitude West	ARGOS (DecNr)	Duration (month)	Remarks
RAFOS Floats								
295	37	21/5	20:56	20º59.5	15º01.1	4986	11	with #43 DBE
295	43	21/5	21:03	20º59.5	15º01.1	5462	18	with #37 DBE
296	47	22/5	6:55	21º59.9	16º09.0	5466	15	W Mid. Ad. RDBE
297	51	22/5	18:33	23º00.0	17º17.0	7462	10	Braz Bas DBE
298	57	23/5	4:16	24º00.0	18º36.0	5479	11	Braz Bas DBE
299	58	23/5	15:10	25º00.0	19º44.0	5480	13	Braz Bas DBE
300	62	24/5	00:49	26º00.0	20º56.1	12622	10	Braz Bas DBE
301	78	24/5	12:20	27º00.0	22º09.9	12612	11	Braz Bas DBE
302	85	24/5	21:52	28º00.0	23º24.9	7469	18	Braz Bas DBE
303	95	25/5	7:45	28º59.8	24º41.9	4984	10	Braz Bas DBE
304	96	25/5	19:08	29º59.9	25º59.1	12624	11	Braz Bas DBE
305	97	26/5	4:26	30º48.9	27º23.0	12613	15	Rio G Rise N
306	99	26/5	17:14	31º37.4	28º49.2	7467	10	R, RioGRise
307	103	26/5	23:00	32º30.1	28º48.1	7468	11	outer HunterCh
308	69	27/5	5:24	33º22.5	28º48.8	6843	13	outer HunterCh
310	100!	27/5	21:47	34º19.1	28º29.7	12616	10	K0, Hunter Ch.
320	98	1/6	2:14	35º25.2	28º27.1	5466	11	South of HCh
333	101	6/6	1:41	35º47.0	30º39.5	12617	18	South of HCh
334	102	6/6	9:00	36º42.2	31º30.5	12618	10	NE Arg Basin
335	104S	6/6	18:27	37º36.6	32º22.0	7466	11	NE Arg Basin
336	105	7/6	1:44	38º31.0	33º14.0	5461	15	NE Arg Basin
337	107	7/6	9:39	39º25.9	34º06.6	6835	10	NE Arg Basin
338	106	7/6	19:15	39º54.2	34º34.8	7465	11	southern comer
339	108	8/6	4:17	38º36.6	34º58.7			
340	109	8/6	15:52	37º42.8	36º15.5			
341	30	9/6	1:18	36º48.4	37º31.3	5463	11	towards Vema
342	110	9/6	12:37	35º54.3	38º46.1	5487	15	towards Vema
343	111	9/6	21:16	35º00.2	40º00.1	5488	10	towards Vema
344	112	10/6	5:53	34º05.7	41º13.3	5489	13	outer Vema Ch

DBE - Deep Basin Experiment
- Float

Sta. No.	Float IfM	Date 1994	Time UTC	Latitude South	Longitude West	ARGOS (DecNr)	Duration (month)	Remarks
MAFOS Monitors								
[K02]	M5	1/6*	21:30*	34º13.7	28º38.4	N/A	21	SoSo86, 4335m
[K4]	M7	6/6*	16:44*	39º51.6	34º32.9	N/A	22	SoSo89, 4707m

*Start Date/Time

7.2.6 List of Plankton Stations during M 28 and Respective Haul Numbers

Station #	NEU #	MCN-OK #	Date YYYYMMDD	Latitude	Longitude	Light	Sorted
165	1		19940330	8º16.2'S	33º27.3'W	N	NEU o
166	2		19940330	8º19.2'S	32º29.8'W	T	NEU o
167	3	1 *	19940331	9º13.3'S	32º59.8'W	N	NEU o
168	4	2 *	19940331	10º14.7'S	33º29.3'W	T	NEU o
169	5	3 +	19940401	10º03.2'S	35º44.8'W	T	NEU o, MCN
170	6	4 *	19940401	10º04.7'S	35º41.8'W	N	NEU o, MCN
171	7	5 +	19940401	10º12.7'S	35º38.2'W	N	NEU o
172	8	6 *	19940402	10º15.4'S	35º33.4'W	N	NEU o, MCN
173	9	7 +	19940402	10º19.5'S	35º27.0'W	T	NEU o
174	10	8 +	19940402	10º24.2'S	35º21.5'W	T	NEU o, MCN
175	11		19940403	10º26.5'S	35º11.7'W	N	NEU o
176	12		19940403	10º33.1'S	35º03.5'W	T	NEU o
177	13	9 -	19940403	10º38.5'S	34º55.9'W	T	NEU o
178	14	10 *	19940403	10º46.1'S	34º44.9'W	N	NEU o, MCN
179	15	11 *	19940404	10º55.5'S	34º30.5'W	N	NEU o
180	16	12 *	19940404	11º06.2'S	34º10.8'W	T	NEU o, MCN
181	17	13 -	19940404	11º18.4'S	34º00.1'W	T	NEU o
182	18	14 *	19940405	11º19.5'S	33º29.7'W	T	NEU o
183	19	15 *	19940405	11º19.5'S	33º00.0'W	T	NEU o, MCN
184	20	16 *	19940405	11º18.7'S	32º30.2'W	N	NEU o
185	21	17 *	19940406	11º19.8'S	31º59.5'W	DT	NEU o, MCN
186	22	18 *	19940406	11º18.9'S	31º19.9'W	T	NEU o
187	23	19 +	19940406	11º19.7'S	30º39.8'W	N	NEU o, MCN
188	24	20 *	19940407	11º19.6'S	30º00.0'W	T	NEU o
189	25	21 *	19940407	11º19.5'S	29º19.7'W	N	NEU o, MCN
190	26	22 *	19940408	11º19.6'S	28º39.7'W	N	
192	27	23 *	19940409	11º19.7'S	27º20.0'W	N	
194	28	24 *	19940409	11º19.7'S	25º59.5'W	N	
197	29	25 *	19940411	11º19.5'S	23º59.8'W	N	
198	30	26 *	19940411	11º19.7'S	23º19.8'W	T	
201	31	27 *	19940412	11º19.9'S	21º30.0'W	T	
203	32	28 *	19940413	11º19.9'S	20º29.8'W	T	
205	33	29 *	19940414	11º19.7'S	19º29.9'W	N	
208	34	30 -	19940414	11º19.8'S	17º57.3'W	N	
210	35	31 -	19940415	11º19.6'S	16º59.7'W	T	
211		32 *	19940415	11º19.8'S	16º34.9'W	N	
213	36	33 *	19940416	11º19.7'S	15º44.8'W	T	
215	37	34 *	19940416	11º19.7'S	14º54.8'W	N	
218	38	35 *	19940417	11º19.8'S	13º39.7'W	T	
221	39	36 *	19940418	11º19.9'S	12º24.9'W	T	
224	40	37 *	19940419	11º19.7'S	10º59.8'W	T	
227	41	38 *	19940420	11º19.7'S	9º29.7'W	DT	

Station #	NEU #	MCN-OK #	Date YYYYMMDD	Latitude	Longitude	Light	Sorted
230	42	39 *	19940421	11º19.6'S	7º59.6'W	T	
232	43	40 -	19940421	11º19.6'S	6º59.8'W	N	
235	44	41 *	19940422	11º19.7'S	5º29.6'W	N	
238	45	42 *	19940423	11º19.8'S	3º59.9'W	N	
240	46	43 *	19940424	11º19.9'S	2º59.6'W	T	
242	47	44 *	19940425	11º19.8'S	1º59.5'W	N	
245	48	4S *	19940426	11º20.0'S	0º44.5'W	N	
246	49	46 *	19940426	11º19.8'S	0º29.6'W	T	
247	so	47 *	19940426	11º20.1'S	0º14.7'W	T	
249	S1	48 *	19940427	11º19.9'S	0º40.3'E	N	
251	52	49 *	19940428	11º19.8'S	2º00.2'E	N	
253	53	so *	19940428	11º19.8'S	3º20.3'E	N	
255	54	51 *	19940429	11º20.0'S	4º40.4'E	T	
257	55	52 *	19940430	11º20.0'S	6º00.4'E	DT	
259	56	53 *	19940501	11º20.0'S	7º20.2'E	N	
261	57	54 *	19940501	11º20.0'S	8º30.2'E	DN	
263	58	55 *	19940502	11º20.0'S	9º30.3'W	T	
264	59	56 *	19940502	11º20.2'S	10º00.0'E	T	
282	60	57 *	19940505	11º40.2'S	10º59.9'E	N	
283	61	58 *	19940506	11º40.2'S	11º30.1'E	N	
284	62	59 *	19940506	11º40.3'S	12º00.1'E	DT	
285	63	60 *	19940506	11º40.4'S	12º30.0'E	T	
286	64	61 *	19940506	11º40.2'S	12º50.0'E	T	
287	65	62 *	19940506	11º20.2'S	13º05.1'E	N	
288	66	63 *	19940506	11º20.1'S	13º15.1'E	N	
289	67	64 *	19940507	11º20.4'S	13º25.4'E	N	
290	68	65 *	19940507	11º19.8'S	13º30.1'E	T	

Explanation of symbols:
OK: * haul OK; + depth failure of individual net; - no quantitative catch.
Light: T Tag (daylight), D Dämmerung (dusk & dawn), N Nacht (night).

7.2.7 Sample List of Sediment- and Water Samples for Geological Investigations

GeoB No.	METEOR No.	Date 1994	Equipment	Bottom contact (UTC)	Latitude	Longitude	Water depth (m)	Core recovery (cm)	Remarks (sample depths in dbar)
ANGOLA BASIN (near MARTIN VAZ FRACTURE ZONE)									
2601-1	292	20.05.	MIC	9:54	21º00,1'S	10º34,4'W	4220	7	TEST LOKATION core recovery 1/4, 3 tubes washed out, 1 sample damaged
2601-2		20.05.	ROS+CTD		21º00,1'S	10º34,4'W	4276		sample depths (4276, 4196,3593,3001,2496, 2001,1801,

GeoB No.	METEOR No.	Date 1994	Equipment	Bottom contact (UTC)	Latitude	Longitude	Water depth (m)	Core recovery (cm)	Remarks (sample depths in dbar)
2602-1	295	21.05.	MIC	18:38	21º00,1'S	15º01,1'W	3978	3	core recovery 2/4, foraminifere ooze, light yellowish brown
2602-2		21.05.	ROS+CTD		21'00,1'S	15º01,1'W	3986		sample depths (3986,3909,3600,3000, 2500,2000,1800,1500, 1300,1200,1100,1000,900, 750,600,500,400,
BRASIL BASIN									
2603-1	296	22.05.	ROS+CTD		22º00,0'S	16º09,0'W	4908		CTD-profile up to 1500 m, sample depths (1500, 1300,1200,1100,1000,900, 710,600,500,400,200,150, 100,80,70, 50, 30, 20, surface (10))
2604-1	297	22.05.	MIC	16:00	23º00,0'S	17º17,1'W	4333	15	core recovery 3/4, foraminifere ooze, light yellowish brown
2604-2		22.05.	ROS+CTD		23º00,0'S	17º17,1'W			sample depths (4295,4196,3600,3000, 2500,2000,1800,1500, 1300,1200,1100,1000,900, 782,600,500,400,200 100,50,30,surface (10))
2605-1	299	23-05.	MIC	13:24	24º59,9'S	19º44,0'W	4047	-	core recovery 0/4, MIC damaged
2605-2		23.05.	ROS+CTD		24º59,9'S	19º44,0'W			sample depths (4061,3949,3600,3000, 2500,2000,1800,1500, 1300,1200,1100,1000,850, 750,600,500,400,200,100, 50,30)
2606-1	301	24.05.	MIC	10:00	27º00,0'S	22º10,1'W	4374	-	core recovery 0/4, MIC damaged
2606-2		24.05.	ROS+CTD		27º00,0'S	22'10,1'W			TEST LOKATION sample depths; (4377,4277,4200,3600, 3000,2500,2000,1800, 1500,1300,1200,1100, 1000,900,830,600,500,400 200,100,50,30,10), He- and Tritium-samples
2607-1	304	25.05.	MIC	18:38	29º59,9'S	25º58,0'W	4372	19	core recovery 3/4, pelagic clay, light brown
2607-2		25.05.	ROS+CTD		29º59,9'S	25º58,0'W			sample depths (4413,4200,3600,3000, 2500,2000,1800,1500, 1300,1200,1100,1000,980, 900,800,600,500,400,200, 100,50,30,10)

GeoB No.	METEOR No.	Date 1994	Equipment	Bottom contact (UTC)	Latitude	Longitude	Water depth (m)	Core recovery (cm)	Remarks (sample depths in dbar)
HUNTER CHANNEL									
2608-1	306	26.05.	MIC	15:30	31°37,5'S	28°49,1'W	3750	-	core recovery 0/4,
2608-2		26.05.	ROS+CTD		31°37,5'S	28°49,1'W			sample depths (3751, 3650,3000,2500,2000, 1800,1500,1300,1200, 1100,1000,980,900, 800,600,500,400,200, 100,50, 50,30,10)
2609-1	310	27.05.	MIC	18:30	34°12,1'S	28°29,46'W	4057	19	core recovery 3/4, pelagic clay, pale brown
2609-2		27.05.	ROS+CTD		34°12,1'S	28°29,46'W			Sample depths (4059,3600,3000,2500, 2000,1800,1500,1300, 1200,1100,960,900, 800,600,500,400,200, 100, 50,30,10)
2610-1	313	28.05.	MIC	17:04	34°25,2'S	27°52,2'W	4357	21	core recovery 4/4, pelagic clay, grayish brown
2610-2		28.05.	ROS+CTD		34°25,2'S	27°52,2'W			sample depths (4374,4200,3600,3000, 2500,2000,1800,1500, 1300,1200,1100,1000, 880,800,600,500,400, 200,100,50,30,10)
2611-1	316	29.05.	MIC	19:08	34°35,1'S	27°03,4'W	4177	-	core recovery 0/4
2612-1	318	30.05.	MIC	19:48	34°30,8'S	27°19,2'W	4332	27	core recovery 4/4, pelagic clay, brown
2613-1	320	31.05.	MIC	20:23	35°24,5'S	28°27,3'W	4770	28	core recovery 4/4, pelagic clay, olive brown
2613-2		31.05.	ROS+CTD		35°24,5'S	28°27,3'W			TEST LOKATION sample depths (4812,4699,4200,3600, 3000,2500,2000,1800, 1500,1300,1200,1100, 1000,875,800,600,500, 400,200,50,30,10),He- and Tritium-samples
2614-1	323	03.06.	MIC	2:07	34°24,6'S	26°19,9'W	3881	11	core recovery 2/4, foram-rich fine-sandy silt, light grey(10YR7/2)
2614-2		03.06.	ROS+CTD		34°24,6'S	26°19,9'W			sample depths (3911, 3820,3599,2998,2501, 2000,1800,1498,1300, 1199,1099,1000,900, 800,600,499,399,200, 95,48,29,10)
2615-1	324	03.06.	MIC	6:31	34°07,1'S	26°23,0'W	3795	10	core recovery 1/4, foram-rich fine-sandy silt, light grey(10YR7/2)

GeoB No.	METEOR No.	Date 1994	Equipment	Bottom contact (UTC)	Latitude	Longitude	Water depth (m)	Core recovery (cm)	Remarks (sample depths in dbar)
2616-1	325	03.06.	MIC	10:58	33º49,9'S	26º25,9'W	4454	10	core recovery 2/4, pelagic clay, brown-very pale brown(10YR513-10YR7/4)
2616-2		03.06.	ROS+CTD		33º49,9'S	26º25,91W			sample depths (4488, 4400,4200,3600,3000, 2500,2000,1800,1500, 1300,1200,1100,1000, 875,800,600,500,400, 200,50,30,10)
2617-1	326	03.06.	MIC	16:09	33º32,6'S	26º28,9'W	4216	24	core recovery 4/4, pelagic clay with forams, brown (10YR5/3), pale brown (10YR6/3), light grey (10YR7/2)
2618-1	332	04.06.	MIC	22:47	32º51,8'S	27º46,9'W	3170	-	core recovery 0/4
ARGENTINE BASIN									
2619-1	333	05.06.	MIC	23:31	35º47,9'S	30º39,9'W	4157	18	core recovery 3/4, pelagic clay, brown, 1 tube lost
2619-2		05.06.	ROS+CTD		35º47,9'S	30º39,9'W			TEST LOKATION sample depths (4076, 4000,3600,3000,2500, 2000,1800,1500,1300, 1200,1100,1000,900, 800,600,500, 400, 200, 50, 30, 10)
2620-1	335	06.06.	MIC	16:45	37º36,5'S	32º22,0'W	4480	22	
2620-2		06.06.	ROS+CTD		37º36,5'S	32º22,0'W			sample depths (4500, 4399,4200,3600,3000, 2500,2000,1800,1500, 1300,1200,1100,998, 900,800,600,500,400, 200,50,30,10)
2621-1	338	07.06.	MIC	17:02	39º54,1'S	34º34,8'W	4808	25	
2621-2		07.06.	ROS+CTD		39º54,1'S	34º34,8'W			sample depths (4839, 4699,4200,3600,3000, 2560,2000,1800,1500, 1300,1200,1100,1000, 900,700,600,500,400, 200,50,30,10) He- and Tritium-samples
2622-1	340	08.06.	MIC	14:21	37º42,6'S	36º15,7'W	4906		
2623-1	342	09.06.	MIC	10:26	39º54,2'S	38º46,1'W	4873		
2623-2		09.06.	ROS+CTD		39º54,2'S	38º46,1'W			

7.2.8 List of Surface Seawater Samples (sampled on XAD-2)

Sample Code	Date 1994	Time (UTC)	Latitude	Longitude	Volume [l]
M28RW1	05/16	09:00	22º25'S	08º48'E	500
		19:00	22º15'S	06º44'E	
M28RW2	05/17	08:33	22º02'S	03º45'W	500
		18:20	21º55'S	01º57'E	
M28RW3	05/18	08:33	21º42'S	00º43'W	300
		22:45	21º29'S	03º37'W	
M28RW4	05/19	10:07	21º18'S	06º00'W	555
	05/20	00:45	21º04'S	09º05'W	
M28RW5	05/21	09:10	21º00'S	13º22'W	550
		10:30	22º28'S	16º40'W	
M28RW6	05/23	09:30	24º40'S	19º22'W	500
	05/24	19:15	27º53'S	23º16'W	
M28RW7	05/25	09:25	29º11'S	24º57'W	316
	05/26	00:45	30º37'S	27º02'W	
M28RW8	05/26	17:30	31º39'S	28º49'W	404
	05/27	17:30	34º18'S	28º28'W	
M28RW9	06/05	10:30	34º01'S	28º54'W	387
		22:35	35º35'S	30º27'W	
M28RW10	06/07	18:20	39º54'S	34º35'W	400
	06/08	15:20	37º40'S	36º18'W	
M28RW11	06/09	13:20	35º49'S	38º46'W	458
	06/10	11:45	34º15'S	42º53'W	
M28RW12	06/11	11:30	34º49'S	46º48'W	400
		18:00	34º57'S	48º40'W	

7.2.9 List of Surface Seawater Samples (sampled on Y.AD-7)

Sample Code	Date 1994	Time (bord time)	Latitude	Longitude	Volume (l)
WP1	05/16	10:46	22º26'S	09º15'E	250
		21:00	22º04'S	04º17'E	
WP2	05/17	10:00	22º04'S	04º17'E	350
		20:00	21º53'S	01º50'E	
WP3	05/18-19	08:30	21º42'S	00º37'W	518
		08:10	21º19'S	05º36'W	
WP4	05/19	08:40	21º19'S	05º44'W	450
		22:15	21º06'S	08º34'W	
WP5	05/22	08:45	22º17S	16º28'W	757
	05/23	20:10	25º45'S	20º38'W	
WP6	05/24	12:50	27º05'S	22º17'W	635
	05/25	11:20	29º34'S	25º26'W	

Sample Code	Date 1994	Time (bord time)	Latitude	Longitude	Volume (l)
WP7	05/26	18:50	31º58'S	28º48'W	500
	05/28	08:00	34º34'S	26º42'W	
WP8	06/05	09:15	34º19'S	29º12'W	530
	06/06	12:00	37º39'S	32º24'W	
WP9	06/09	12:40	35º34'S	39º12'W	460
	06/10	08:00	34º14'S	42º21'W	
WP10	06/11	08:15	34º48'S	47º17'W	280
	06/12	10:00	35º05'S	52º02'W	

7.2.10 List of Micro Layer Samples

Sample Code	Date 1994	Station No.	Latitude	Longitude	Volume [l]
M28MF1	05/20	292	21º00'S	10º34'W	2 x 4
M28MF2	05/21	295	21º00'S	15º01'W	2 x 4
M28MF3	05/22	297	23º00'S	17º17'W	2 x 4
M28MF4	05/23	299	25º00'S	19º44'W	2 x 4
M28MF5	05/24	301	27º00'S	22º10'W	2 x 4
M28MF6	05/25	304	30º00'S	25º58'W	2 x 4
M28MF7	05/26	306	31º37'S	28º49'W	2 x 4
M28MF8	05/28	313	34º25'S	27º52'W	2 x 4
M28MF9	06/02	322	34º10'S	28º36'W	2 x 4
M28MF10	06/06	335	37º37'S	32º23'W	2 x 4
M28MF11	06/06	342	35º54'S	38º46'W	2 x 4

7.2.11 List of High Volume Air Samples

Sample Code	Date 1994	Time (UTC)	Latitude	Longitude	Volume [m^{-3}]
M28RL2P	05/16	07:50	22º26'S	09º14'E	1010
	05/17	07:00	22º04'S	04º28'E	
M28RL3P	05/17	07:40	22º04'S	04º20'E	1075
	05/18	07:00	21º43'S	00º22'W	
M28RL4P	05/18	09:40	21º38'S	00º56'W	1034
	05/19	08:00	21º20'S	05º33'W	
M28RL5P	05/19	09:25	21º18'S	05º52'W	1000
	05/20	06:45	21º00'S	10º17'W	
M28RL6P	05/20	07:15	21º00'S	10º23'W	1320
	05/21	11:00	21º00'S	13º43'W	
M28RL7P	05/21	12:15	21º00'S	14º13'W	2520
	05/23	16:40	25º09'S	19º55'W	
M28RL8P	05/23	17:13	25º13'S	20º00'W	1012
	05/24	17:35	27º40'S	23º00'W	

Sample Code	Date 1994	Time (UTC)	Latitude	Longitude	Volume [m^{-3}]
M28RL9P	05/24	18:10	27º44'S	23º05'W	1008
	05/25	19:00	29º60'S	25º60'W	
M28RL10P	05/26	09:20	31º20'S	28º18'W	420
	05/27	09:30	34º00'S	28º50'W	
M28RL11P	05/27	09:45	34º08'S	28º52'W	952
	05/28	09:05	34º20'S	27º56'W	
M28RL12P	05/28	15820	34º25'S	27º52'W	1012
	05/29	12300	34º32'S	26º59'W	
M28RL13P	05/29	13:35	43º32'S	26º59'W	799
	05/30	09:05	34º25'S	27º18'W	
M28RL14P	05/31	12:25	35º19'S	28º26'W	1007
	06/01	11:50	35º31'S	28º19'W	
M28RI15P	06/01	15:00	35º22'S	28º30'W	1210
	06/02	24:00	34º32'S	26º20'W	
M28RL16P	06/03	00:30	34º25'S	26º20'W	1257
	06/04	10:00	33º04'S	26º57'W	
M28RL17P	06/05	10:45	34º19'S	29º12'W	1050
	06/06	10:30	37º07'S	31º54'W	
M28RL18P	06/06	11:35	37º14'S	32º00'W	1022
	06/07	17:30	39º54'S	34º35'W	
M28RL19P	06/08	11:10	37º53'S	36º01'W	1015
	06/09	15:00	35º37'S	39º09'W	
M28RL20P	06/09	15:55	35º30'S	39º19'W	970
	06/10	15:40	34º20'S	43º17'W	
M28RL21	06/10	16:10	34º21'S	43º23'W	1010
	06/11	18:00	34º57'S	48º40'W	
Lp1	03/15	14:35	22º26'S	13º03'E	267
		19:50	22º26'S	11º20'E	
Lp2	05/16	09:00	22º26'S	09º15'E	975
	05/17	09:00	22º04'S	04º17'E	
Lp3	05/17	09:00	22º04'S	04º17'E	325
		18:30	21º55'S	02º21'E	
Lp4	05/18	09:00	22º04'S	01º05'W	1082
	05/19	18:30	21º55'S	05º48'W	
Lp5	05/19	10:20-18:00	06º00'W	07º41'W	307
			21º10'S	21º10'S	
Lp6	05/20	08:40	21º00'S	10º34'W	1447
	05/21	08:40	20º59'S	13º29'W	
Lp7	05/21	11:15	21º00'S	13º59'W	324
		18:15	20º59'S	15º01'W	
Lp8	05/22	09:30	22º26'S	16º39'W	886
	05/23	09:05	24º44'S	19º26'W	
Lp9	05/23	12:50	25º00'S	19º44'W	134
		16:45	25º17'S	20º05'W	

Sample Code	Date 1994	Time (UTC)	Latitude	Longitude	Volume [m^{-3}]
Lp10	05/24	09:35	27º00'S	22º10'W	915
	05/25	08:20	29º11'S	24º56'W	
Lp11A	05/25	10:00	29º18'S	25º05'W	77
		12:00	29º40'S	25º33'W	
Lp11B	05/25	12:20	29º42'S	25º35'W	70
		14:15	29º58'S	25º56'W	
Lp11C	05/25	14:35	29º59'S	25º57'W	76
		17:00	29º59'S	25º58'W	
Lp12	05/26	09:20	31º24'S	28º26'W	1054
	05/27	10:40	34º15'S	28º51'W	
Lp13	05/28	11:00	34º22'S	27º42'W	298
		19:40	34º30'S	27º54'W	
Lp14	05/29	10:15	34º32'S	26º58'W	886
	05/30	08:10	34º25'S	27º18'W	
Lp15	05/31	08:40	35º23'S	28º39'W	315
		19:00	35º24'S	28º27'W	
Lp16	06/01	09:15	35º24'S	28º23'W	842
	06/02	10:00	34º17'S	27º48'W	
Lp17A	06/03	08:30	33º49'S	26º25'W	73
		11:00	33º47'S	26º26'W	
Lp17B	06/03	11:15	33º47'S	26º26'W	77
		14:40	33º32'S	26º28'W	
Lp17C	06/03	14:50	33º32'S	26º28'W	141
		19:30	33º18'S	26º31'W	
Lp18	06/05	08:20	34º13'S	29º06'W	931
	06/06	08:30	37º17'S	32º04'W	
Lp19	06/06	10:20	37º17'S	32º04'W	304
		18:05	37º58'S	32º43'W	
Lp20	06/07	08:40	39º42'S	34º23'W	855
	06/08	09:00	37º49'S	36º06'W	
Lp21	06/08	09:15	37º47'S	36º08'W	305
		18:15	37º47'S	37º03'W	
Lp22	06/09	09:50	35º54'S	38º46'W	869
	06/10	08:45	34º14'S	42º26'W	
Lp23	06/10	09:05	34º14'S	42º28'W	521
		23:20	34º35'S	45º30'W	
Lp24	06/11	09:30	34º50'S	47º35'W	108
		12:30	34º54'S	48º16'W	

7.2.12 List of Low Volume Air Samples

Sample Code	Date 1994	Time (bord time)	Latitude	Longitude	Volume (l)
LOW1	05/16	13:35	22º21’S	08º17’E	37
		18:40	22º18’S	07º28'E	
LOW2	05/17	08:00	22º04’S	04º28'E	40
		13:50	21º59’S	03º17’E	
LOW3	05/17	14:00	21º59’S	03º17’E	35
		21:00	21º53’S	01º50'E	
LOW4	05/18	10:15	21º38’S	00º50’W	40
		18:20	21º32’S	02º43’W	
Blind 4	05/18	18:30	21º38’S	00º50’W	0
		18:40	21º32’S	02º43’W	
LOW5	05/19	10:30	21º17’S	06º04’W	65,8
		20:50	21º18’S	07º25’W	
LOW6	05/20	08:20	21º00’S	10º34’W	47
		15:45	21º00’S	10º34’W	
LOW7	05/21	12:35	21º00’S	14º16’W	31,5
		18:35	20º59’S	15º00’W	
LOW8	05/23	09:00	24º44’S	19º26’W	40
		16:00	25º07’S	20º04’W	
LOW9	05/24	09:20	26º59’S	22º10’W	121
	05/25	08:50	29º10’S	24º55’W	
LOW10	05/25	11:10	29º33’S	25º24’W	35
		18:10	30º00’S	25º59’W	
LOW11	05/26	09:35	31º27’S	28º31’W	34,5
		16:05	31º37’S	28º49’W	
LOW12	05/29	09:55	34º22’S	26º58’W	49,9
		18:20	34º35’S	27003’W	
LOW13	05/31	08:50	35º23’S	28º39’W	37,5
		18:50	35º24’S	28º27’W	
LOW14	06/01	09:00	35º24’S	28º23’W	47,9
		18:50	34º35’S	27º54’W	
LOW15	06/03	08:45	33º49’S	26º25’W	52,2
		19:30	33º18’S	26º31’W	
LOW16	06/05	08:35	34º16’S	29º09’W	48,7
		19:15	35º40’S	30º32’W	
BLIND16	06/05.	8:40	34º16’S	29º09’W	0
LOW17	06/06	10:10	37º16’S	32º03’W	44,8
		18:05	37º58’S	32º43’W	
LOW18	06/08	09:20	37º45’S	36º11’W	42,4
		18:30	37º06’S	37º05’W	
LOW19	06/10	08:40	34º14’S	42º23’W	20
		23:30	34º35’S	45º30’W	

Sample Code	Date 1994	Time (bord time)	Latitude	Longitude	Volume (l)
LOW20	06/11	09:55	34º50'S	47º41'W	70
		19:55	34º58'S	49º16'W	
LOW21	06/12	09:10	35º13'S	52º02'W	36,5
		16:30	35º15'S	55º23'W	

8 Concluding Remarks

Foremost we thank the captains and the crew of RV METEOR for their skilled work. Special thanks go to Mrs. S. Drews. She run the coordinator's office in Kiel with great competence and patience. We all appreciate the professional travel services provided by Mrs. I. Weigert of Contiways Reisen, Hamburg. Not forgotten are the excellent co-operations with the staff of the German diplomatic representatives in Brasilia, Luanda, Walfish Bay, and Buenos Aires.

Financial support for the cruise and the scientific data analysis come from the 'Deutsche Forschungsgemeinschaft' (DFG) (Ze 145/7-1) and the 'Bundesministerium Bir Bildung, Wissenschaft, Forschung und Technologie' (BMBF) (FKZ 03F0121A).

9 References

AHLSTROM, E. and H.G. MOSER (1981): Systematic's and development of early life history stages of marine fishes: Achievements during the past century, present status and suggestions for the future. Rapp. P.-v. Réun. Cons. CIEM 178, 541 - 546.

ANDRES, H.G., H.-Ch. JOHN and C. ZELCK (1992): Biologische Ozeanographie und marine Taxonornie. In: SIEDLER, G. and W. ZENK (1992): WOCE Sildatlantik 1991, Reise Nr. 15, 30. Dezember 1990 - 23. März 1991. METEOR -Berichte, Universität Hamburg 92-1, 74 - 85.

BENNEKOM, A.J. and G.W. BERGER (1984): Hydrography and silica budget of the Angola Basin. Netherl. Journ. Sea Res. 17, 149-200.

BLACHE, J. (1964): Le genre Bathylagus dans l'Atlantique tropical oriental sud (Teleostei, Clupeiformi, Opistoproctoidei, Bathylagidae). Cah. ORSTOM (océanogr.) 2 (1), 7-16.

BROWN, N. and G.K. MORRISON (1978): WHOI/Brown Conductivity, temperature, and depth profiler. Woods Hole Oceanographic Inst. Techn. Rep. No. WHOI-78-23.

CULBERSON, C.H. (1991): 15 pp in the WOCE Operations Manual (WHP Operations and Methods) WMPO 91/1, Woods Hole.

CULBERSON, C.H. and S. HUANG (1987): An automated amperometric oxygen titration. Deep Sea Research, 34, 875-880.

De MADRON, X.D. and G. WHEATHERLY (1994): Circulation, transport and bottom boundary layers of the deep currents in the Brazil Basin. Journ. Mar. Res. 52, 583-638.

EHRICH, S., H.-Ch. JOHN and P. WESTHAUS-EKAU (1987): Southward extension of the reproductive range of Macroramphosus scolopax in the up-welling area off North-West Africa. S. Afr. J. Mar. Sci. 5, 95 - 105.

FISCHER, J. and M. VISBEK (1993): Deep Profiling with Self-contained ADCPs. Journ. Atmos. Oean. Techn., 10, 5, 764-773.

GARRETT, W.D. (1965): Surface chemistry of the sea. Limnol. and Oceanogr., 10, 602-610.

GRASSHOFF, K. (1976): Methods of seawater analysis. Verlag Chemie, Weinheim, 305pp

HAMAN, I., H.-Ch. JOHN and E. MITTELSTAEDT (1981): Hydrography and its effect on fish larvae in the Mauritanian up-welling area. Deep-Sea Res. 28 A(6), 561 - 575.

HEMPEL, G. and H. WEIKERT (1972): The neuston of the subtropical and boreal Northeastern Atlantic Ocean. A review. Mar. Biol. 13 (1), 70 - 88.

HERMES, R. and M.P. OLIVAR (1987): Larval development of Bathylagus argyrogaster Norman 1930 (Teleostei, Bathylagidae). Pesq. 51 (4), 483 - 489.

HYDES, D.J. (1984): A manual of methods for the continuous flow determination of ammonia, nitrate-nitrite, phosphate and silicate in seawater. Institute of oceanographic Sciences Report No. 177, 40pp.

HYDES, D.J. and N.C. HILL. (1985): Use of Copper Cadmium Alloy in the determination of dissolved nitrate. Est. Coastal Shelf Sci. 21, 27-31.

Hydrographic Department of the Admirality (1945): Quarterly Surface Current Charts of the Atlantic Ocean. Prepared in the Marine Branch of the Meteorological Office and published by the authority of the Meteorological Committee, 25.

JAENICKE, R. (1987): Aerosol physics and chemistry. In: G. FISCHER (ed.): Landolt Bbrnstein, Volume 4 'Meteorology', 391-457, Springer Verlag, Berlin.

JOHN, H.-Ch. (1976/77): Die Hdufigkeit des Ichthyoplanktons an der Oberfldche des mittleren und südlichen Atlantischen Ozeans. Meeresforsch. 25 (1-2), 23 - 36.

JOHN, H-Ch. (1979): Regional and seasonal differences in ichthyoneuston off Northwest Africa. "METEOR" Forsch.-Ergebn. D 29, 30 - 47.

JOHN, H.-Ch. (1984): Drift of larval fishes in the ocean: Results and problems from previous studies and a proposed field experiment. P. 39-60 in: MCCLEAVE, J.D.; G.P. ARNOLD, J.J. DODSON and W.H. NEILL (eds): Mechanisms of migration in fishes. Plenum Publ. Corp., New York, 574 pp.

JOHN, H.-Ch. (1985): Horizontal and vertical distribution patterns of fish larvae off NW Africa in relation to the environment. P. 489-512 in: BAS, C., R. MARGALEF and P. RUBIES (eds.): Simposio internacional sobre las areas de afloramiento mas importantes del oeste africano (Cabo Blanco y Benguela). Vol. 1. Inst. In. Pesqueras, Barcelona.

JOYCE, T.M. (1989): On in situ "calibration" of shipboard ADCP. Journ. Atmos. and Ocean. Techn. 6, 169-172.

JOYCE, T., C. CORRY and M. STALCUP (1991): Requirements for WOCE hydrographic programme data reporting, WHPO 90-1, 71pp.

KLOPPMANN, M. (1990): The sampling efficiency of a horizontally towed BE multiple-opening-closing-net. ICES 1990, C.M. 1990/L, 97, 11 pp.

KOBYLYANSKIY, S.G. (1985): Material for the revision of the genus Bathylagus Giinther (Bathylagidae): The group of "light" deep sea smelts. J. Ichthyol. 25 (1), 1 - 17.

KRÄMER, W. and K. BALLSCHMITER (1987): Detection of a new class of organochlorine compounds in the marine environment: The chlorinated paraffins. Fresenius z. Anal. Chem., 327, 47-48.

LASKER, R. (1981): Marine fish larvae. Washington Sea Grant Program, Seattle, 131 pp.

LOPES, P.C. and H.-Ch. JOHN (1986): Ichthyoplankton at the surface of the Equatorial Atlantic. Bol. Soc. Port. Cienc. Nat. 23, 83 - 111.

MOLLER, T. (1981): Current and temperature measurements in the North-East Atlantic during NEADS. Ber. Inst. Meereskunde, Nr. 90, 98 pp.

MOLLER et al. (1994): Improving MKIII measurements. In: WOCE Operations Manual, Part 3.1.3: WFIP Operations and methods. WOCE Hydrographic Programme Office, Woods Hole Oceanographic Institution (update July 1993 in press).

MURPHY J. and J.P. RILEY (1962): A modified single solution method for the determination of phosphate in natural waters. Anal. Chim. Acta, 27, 31-36.

NGCD (1993): Global relief data, CD-ROM, National Geophysical Data Center.

NORMAN, J.R. (1930): Oceanic fishes and flatfishes collected in 1925 - 27. Discovery Rep. 2, 261 - 370.

OWENS, B. and R. MILLARD (1985): A new algorithm for CTD Oxygen calibration. Journ. Phys. Oceanogr. 15, 621-631.

PETERSON, R.G. and T. WHITWORTH 111 (1989): The Subantarctic and Polar Fronts in relation to deep water masses through the Southwestern Atlantic. Journ. Geophys. Res. 94, 10817-10838.

POLLARD, R. and J. READ (1989): A method for calibrating ship-mounted acoustic Doppler profilers and the limitations of gyro compasses. Journ. Atmos. Ocean. Techn., 6, 6, 859-865.

ROBINSON, I.S., N.S. WELLS and H. CHARNOCK (1984): The sea surface thermal boundary layer and its relevance to the measurement of sea surface temperature by airborne and space-borne radiometers. International Journal of Remote Sensing, 5, (n1), 19-45.

SAUNDERS, P.M., K.-H. MAHRT and R.T. WILLIAMS (1991): Standards and laboratory calibrations. In: WOCE Operations Manual, Part 3.1.3: WHP Operations and methods. WOCE Hydrographic Programme Office, Woods Hole Oceanographic Institution (update July 1993 in press).

SCHLUESSEL, P., W.J. EMERY, H. GRASSL, and T. MAMMEN (1990): On the bulk-skin temperature difference and its impact on satellite remote sensing of sea surface temperature. Journal of Geophysical Research, 95(C8), 13341-13356.

SIEDLER, G., A. KUHL and W. ZENK (1987): The Madeira Mode Water. J. Phys. Oceanogr., 17 (10), 1561-1570.

SIEDLER, G. and W. Zenk (1992): WOCE Sddatlantik 1991, Reise Nr. 15, 30. Dezember - 23. März 1991. METEOR -Berichte, Universität Hamburg, 92-1, 126 S.

SIEDLER, G., W. BALZER, T.J. MOLLER, R. ONKEN, M. RHEIN and W. ZENK (1993): WOCE South Atlantic 1992, Cruise No. 22, 22 September 1992 - 31 January 1993. METEOR - Berichte, Universität Hamburg, 93-5, 131pp.

SPEER, K.G., W. ZENK, G. SIEDLER, J. PATZOLD and C. HEIDLAND (1992): First resolution of flow through the Hunter Channel in the South Atlantic. Earth and Planeary Science Letters, 113, 287-292.

SPEER, K.G. and W. ZENK (1993): The flow of Antarctic Bottom Water into the Brazil Basin. J. Phys. Oceanogr. 23, 2667-2682.

STRAMMA, L. and R.G. PETERSON (1990): The South Atlantic Current, J. Phys. Oc., 20, 846-859.

TARBELL, S., R. MEYER, N. HOGG and W. ZENK (1994): A moored array along the southern boundary of the Brazil Basin for the Deep Basin Experiment - Report on a joint experiment 1991-1992. Ber. Inst. f. Meereskunde Kiel, Nr. 243.

UNITED STATES NAVAL OCEANOGRAPHIC OFFICE, 1955: Atlas of Pilot Charts Central American Waters and South Atlantic Ocean. Published by the Defense Mapping Agency Hydrographic Center, Washington D.C.

VIESBEK, M. and J. FISCHER (1995): Sea surface conditions remotely sensored by upwardlooking ADCPs. J. Atmos. a. Oceanic Techn., in press.

WARREN, B.A. and K.G. SPEER (1991): Deep circulation in the eastern South Atlantic. Deep-Sea Res. 38 (Suppl. 1), 5281-5322.

WICK, G.A., W.J. EMERY and P. SCHLUSSEL (1992): A comprehensive comparison between skin and multi-channel sea surface temperature. Journal of Geophysical Research, 97(C4), 5569-5595.

ZELCK, C. (1993): Biological oceanography and marine taxonomy. In: SIEDLER, G., W. BALZER, T.J. MÜLLER, R. ONKEN, M. RHEIN and W. ZENK (1993): WOCE South Atlantic 1992. Cruise No. 22, 22 September 1992 - 31 January 1993. METEOR-Berichte, Universitdt Hamburg 93-5, 73 - 76.

ZENK, W. and N.G. HOGG (1994): Climate changes of Antarctic Bottom Water flowing into the Brazil Basin? Deep-Sea Res. (submitted).

ZENK, W., K.G. SPEER and N.G. HOGG (1993): Bathymetry at the Vema Sill. Deep-Sea Res. 40(9), 1925-2933.

Tritium HELIUM ISOTOPE DATA DOCUMENTATION

CRUISE METEOR 28 WHP A8

The data was aquired by

Prof. Dr. Wolfgang Roether
Tracer-Ozeanographie
FB1
Universitaet Bremen
PO.Box. 330 440
28334 Bremen
Tel.: 0421/218-3511 / 4221
Fax: 0421/218-7018
email: wroether@physik.uni.bremen.de

for questions about measurement and data processing please contact

Birgit Klein
Tel: 0421/210-2931
email: bklein@physik.uni-bremen.de

In the data file we enclose final (tritium corrected delhe3 data) and final tritium data.

Final delhe3 data:

Two different sets of helium samples have been taken during the cruise:

1. Most samples were taken in the usual manner with pinched- off copper tubes. After the gas extraction in Bremen they were measured in the Laboratory with a dedicated Helium - Neon Isotope Mass Spectrometer.

2. Another set was sampled into glass-pipettes and extracted at sea. The glass ampoules with the extracted gas were then transported back to Bremen for measurement.

All samples were calibrated using an air standard (regular air) in the Bremen laboratory. The Copper tube samples are now corrected for tritium decay during storage time! Because of the very low tritium concentrations in the South Atlantic the tritium correction was very small. For samples from the upper layer, the maximum reduction in delta ^{3}He of about 0.24% and on average 0.05%. The samples which had been extracted at sea did not need a correction for delhe3 because their storage time was zero.

Tritium data:
Tritium was sampled in 1l glass bottles which were analyzed after the cruise in the laboratory at bremen. Tritium was measured through in-growth of helium3 from radioactive decay. For this procedure the water samples are degassed and transferred into special

glass containers which are sealed off and placed into freezers. After a storage time of 6 month to about a year to allow for sufficient in-growth of helium3 the samples are measured with a special noble gas spectrometer.

Tritium concentrations are scaled to 1 April 1994 and individual errors have been assigned. The quality flags follow WOCE standard.

Cruise: M28/1 Expocode 06MT28_1
The cruise covers the sections A08.

CFCs:

CFC11, CFC12, CFC113 and CCL4 have been measured on the cruise. A capillary column (mega bore) has been used. CFC measurements have been calibrated against the SIO93 scale. CFC measurements have been assigned individual errors. Error flags follow Woce standards. The overall performance is decribed below:

Reproducibility:
F-11: 0.3 % or 0.004 pmol/kg (whichever is greater)
F-12: 0.7 % or 0.003 pmol/kg (whichever is greater)
F-113: 7.4 % or 0.006 pmol/kg (whichever is greater)
CCl4: 0.8 % or 0.006 pmol/kg (whichever is greater)

Precision:
F11: 0.004 pmol/kg corresponding to 0.3% relative error
F12: 0.003 pmol/kg corresponding to 0.3% relative error
F-113: 0.004 pmol/kg corresponding to 3% relative error
CCl4: 0.002 pmol/kg corresponding to 0.1% relative error

Mean water blank, detection limit:
F-11: 0.004 pmol/kg ± 0.004
F-12: 0.004 pmol/kg ± 0.004
F-113: 0.005 pmol/kg ± 0.004
CCl4: 0.004 pmol/kg ± 0.004

Air measurements:
ALE/GAGE values for 1994 (southern hemisphere) (SIO-1993 Scale):

F-11	F-12	F-113	CCl4
261.0	511	81.0	100

Mean of air measurements (SIO93) performed during the cruise:

F-11	F-12	F-113	CCl4
pptv	pptv	pptv	ptpv
259.0(±2.0)	501.(±4.5)	80.8(±13.5)	108.0(±4.5)

Evaluation of CTD and bottle salinity data from Woce section A08.

The WOCE A08 section was collected South in the South Atlantic along latitude 11 degrees 30 minutes on METEOR Cruise 28, Leg 1 during April and May of 1994 and consists of stations numbers 165 to 290. A map of beginning station position, created from data in the summary file, is displayed in the upper panel of figure 1 with a plot of bottom depth versus station number shown in the lower panel. The rise in topography ending at station 219 is associated with the mid-Atlantic ridge and has a minimum bottom depth of less than 3000 meters which blocks (except for flow through deep channels) most of the AABW from reaching the Eastern Basin. The CTD data of A08 has no oxygen and only roughly one quarter of the observations in the bottle file have either water sample salinity or oxygen observations. The water sample salinity data comparisons are sparse compared to most WOCE cruises previously examined but the lack of bottle salinities does not appear to limiting the CTD salinity (conductivity) calibration.

A salinity versus potential temperature plot (figure 2) shows all water sample file salinities (Water sample and CTD up cast) along with the 2 decibar down-profile CTD data from section A08. The salinities are well matched to the bottle salinities at the scales resolved by the plot. There are a number of stations with fresh surface salinities compare to most of the surface layer (one stations surface salinity (270) is less than 28 psu while most mixed layer salts of the station are over 35.0 psu). Attention is called to stations with fresh surface salinities later. As indicated in the lower part of figure 1, below 3000 meters the mid-Atlantic ridge separates the deep waters into two basins with different water mass characteristics as indicated by comparing salinity versus potential temperature at depth for the Western part of the 11 South section in figure 3 (stations 165 to 219) with the Eastern part shown in figure 4 containing stations 220 through 290. At least one station in the western basin of figure 3 appears to be slightly salty compared to neighboring profiles. The deep water range of salinity is much narrower in the Eastern Basin shown in figure 4 since most of the cold and fresh Antarctic Bottom Water (AABW) is cut off by the Mid-Atlantic Ridge. The expanded salinity scale of figure 4 reveals that the down-profile 2-dbar CTD salinities appear to be fresher than corresponding water sample salinities (o). This discrepancy is examined further. Another odd feature seen in figure 4 is the salinity freshing of roughly 0.003 psu at the bottom of each profile as can be seen by examining salinities around 1.9 C and 34.88 psu. Each profile shows a tailing off of salinity towards fresher values by 0.003 psu at the bottom for every cast examined. This ubiquitous salinity anomaly at the bottom of each cast seems an artifact of either the instrument or the data processing methodology.

A comparison of the up-profile CTD and water sample salinity data in the water sample file (A08.hyd) is shown in figure 5. The up-cast CTD salinities are very well matched to the water sample salinities both overall (upper panel) and

below 1000 dbars (center panel) with a standard deviation for the salt differences of 0.00178 psu. No variation in the vertical can be seen in the plot of differences versus pressure in the bottom panel of figure 5.

The down-profile CTD salinity interpolated at the pressure of the up-profile water sample bottle positions (figure 6 a, b, & c), on the other hand, shows systematic differences between the CTD salinity and water sample salinity values at all depths including the bottom of the cast. The CTD salinity is underestimated with a mean difference (CTD-WS) of -0.003 psu for all depths. The differences below 2000 dbars (center figure 6) middle panel) show a fairly uniform deep salinity offset across all deep stations while the salinity differences versus pressure (bottom figure 6) indicates that the differences with depth are larger near the surface. The deepest values of the down-profile CTD salinity are fresh compared to the up profile which seems odd since the down and up cast should match at the bottom but as noted before the salinity of the lowest 15 meters of the down profile tails off towards lower values of salinity. Figure 7 is histograms of interpolated down-profile CTD salinity minus bottle salt broken up into 1500 dbar pressure intervals below 1500 dbars and 500 dbar intervals above 1500 dbars. Below 1500 dbars, this summary shows a reasonably small scatter of from 0.002 to 0.0033 psu but a mean differences that progressively increases from -0.0018 to -0.0046 psu between the bottom and 1500 dbars. In the interval between 500 and 1500, the mean salt differences have grown to -0.0084 psu.

Some surface salinities of the CTD 2 decibar down profiles look suspect as they are fresh by .5 to 8 psu compared with the salinity at 2 decibars or subsequent depths in an otherwise nearly homogeneous upper layers down to 30 to 70 meters. Some of these anomalous surface salinities may be the result of CTD stations taken during a rainy intervals or coastal stations near rivers but others are probably associated with surface observations that have conductivity values biased low due to air trapped in conductivity cell in the first pressure interval. It would be useful to identify those stations with a fresh upper layer from rain or river discharge. The following 20 stations have surface salinities where the salinity of the first interval is greater than 0.25 psu/dbars with the first interval salinity gradient also ten times that of the third pressure interval. The vertical profiles of stations 179, 187*, 189, 190, 194, 197*, and 203 are shown in figure 8. Stations with an (*) also have an a surface salinity less than 34.9 psu. Other than the near surface fresh layer, the salinity profiles are nearly homogeneous to 50 dbars or deeper. The vertical profiles of stations 212*, 221, 233, 249*, 252, 255, and 263 are given in figure 9. Again except for upper few meter, the salinity is well mixed down to nearly 50 dbars except for 263. The vertical profiles of stations 265, 266, 267, 269*, 270*, and 290* are plotted in figure 10. Some of the West African coastal stations may see river discharge.

As noted earlier in figure 4, the lowest portion of every profile examined shows anomalous low salinities. They run lower by about -0.002 to -0.003 psu than salinity values immediately above. The extent of this data artifact is between 14 to 16 decibars from the bottom of the profile as can be seen in the near bottom vertical profiles of salinity shown in figures 11 for stations 194 to 202 and figure 12 for stations 247 to 254.

WOCE line A15 intersects A08 at 19°30 W and 11°30 S. A potential temperature versus salinity plot in figure 13 shows station 68 of A15 (black line with squares) along with stations 205 to 207 from A08. There is good agreement between stations 205 & 206 and A15 station 68 at the 0.002 psu level but station 207 appears to be +0.004 psu saltier than neighboring stations. Another salinity versus potential temperature plot (Figure 14) shows station 204 to have a high salinity similar to station 207. The high deep water salinity for both of these stations is noted in the earlier salinity versus potential temperature plot of figure 3 for data West of the mid-Atlantic ridge.

Stability

The stability of the CTD data is checked by looking at the first differences of the potential density anomaly values of the 2 decibar data within a station. Unstable density anomaly differences (i.e. denser above lighter) that exceed -0.0075 kg/dbar and a more stringent -0.005 kg/dbar are plotted in figure 15. The table below indicating stations with observations failing the -0.0075 kg/dbar criteria with additional values failing -0.005 kg/dbars following. All of the density unstable observations are in the upper 4 decibars except for one 10 meter observation. Most seem to be associated with slightly colder temperatures (perhaps associated with a temperature lag from readings on deck ???). A salinity versus potential temperature plot (see figure 16) of the upper waters shows the surface value colder (which produces salty for a given conductivity) for stations 272 and 273 but not found in the up cast CTD and water sample salinities.

Station	Dsg/dp	Pres.	Salt	Dt/dp	dsg/dp < -0.0075 kg/dbar
170	-0.03629	2.0	37.0360	0.12320	
171	-0.02821	2.0	37.0730	0.05430	
171	-0.00893	4.0	37.0628	0.01540	
172	-0.05794	2.0	37.0655	0.19270	
172	-0.01649	4.0	37.0689	0.05320	
174	-0.01208	2.0	36.9688	0.02605	
177	-0.03260	2.0	37.1166	0.08810	
177	-0.00985	4.0	37.1142	0.02695	
180	-0.07184	2.0	37.1375	0.10445	
180	-0.02533	4.0	37.1028	0.03695	
184	-0.01956	2.0	37.0712	0.13935	
184	-0.00803	4.0	37.0906	0.04565	

195	-0.02482	2.0	36.9019	0.05975
198	-0.04874	2.0	36.9977	0.14355
202	-0.25224	2.0	36.8708	0.39230
202	-0.03987	4.0	36.8189	0.06255
206	-0.07383	2.0	36.7953	0.46225
206	-0.03339	4.0	36.8793	0.20250
208	-0.12524	2.0	36.7671	0.26340
208	-0.02346	4.0	36.7489	0.05140
209	-0.05500	2.0	36.7277	0.16895
209	-0.00866	4.0	36.7296	0.02915
210	-0.03844	2.0	36.7094	0.11920
210	-0.00996	4.0	36.7090	0.03065
216	-0.01100	2.0	36.8047	0.08445
217	-0.05139	2.0	36.7909	0.12430
217	-0.01413	4.0	36.7809	0.03255
226	-0.17850	2.0	36.7325	0.25360
226	-0.04088	4.0	36.6737	0.05905
239	-0.02082	2.0	36.4632	0.21400
239	-0.00772	4.0	36.4974	0.06580
240	-0.07849	2.0	36.4817	0.11485
240	-0.01570	4.0	36.4594	0.02325
241	-0.03716	2.0	36.5250	0.09210
241	-0.00805	4.0	36.5193	0.01880
243	-0.20325	2.0	36.6036	0.34510
243	-0.05331	4.0	36.5428	0.09700
246	-0.30014	2.0	36.8635	0.50015
246	-0.08295	4.0	36.7579	0.13830
247	-0.17031	2.0	36.7966	0.31570
247	-0.04303	4.0	36.7492	0.08065
253	-0.01081	2.0	36.4233	0.02170
254	-0.01719	2.0	36.4392	0.18220
254	-0.01117	4.0	36.5115	0.12425
257	-0.13990	2.0	36.7304	0.36680
257	-0.03223	4.0	36.7132	0.08400
258	-0.00920	2.0	36.7128	0.02050
261	-0.01449	2.0	35.7359	0.05175
262	-0.04595	2.0	35.7187	0.11445
262	-0.01129	4.0	35.7088	0.02390
272	-0.29981	2.0	36.0977	0.55450
272	-0.06197	4.0	36.0367	0.12040
273	-0.26208	2.0	35.9994	0.38260
273	-0.05137	4.0	35.9276	0.07470

Station	Dsg/dp	Pres.	Salt	Dt/dp	observations in additional to above. with dsg/dp< -0.005
170	-0.00720	4.0	37.0373	0.02310	
212	-0.00553	8.0	36.7923	0.00100	
212	-0.00742	10.0	36.7725	0.00010	
219	-0.00548	2.0	36.7635	0.05165	

Figure number with file names (_.jpg) and figure caption

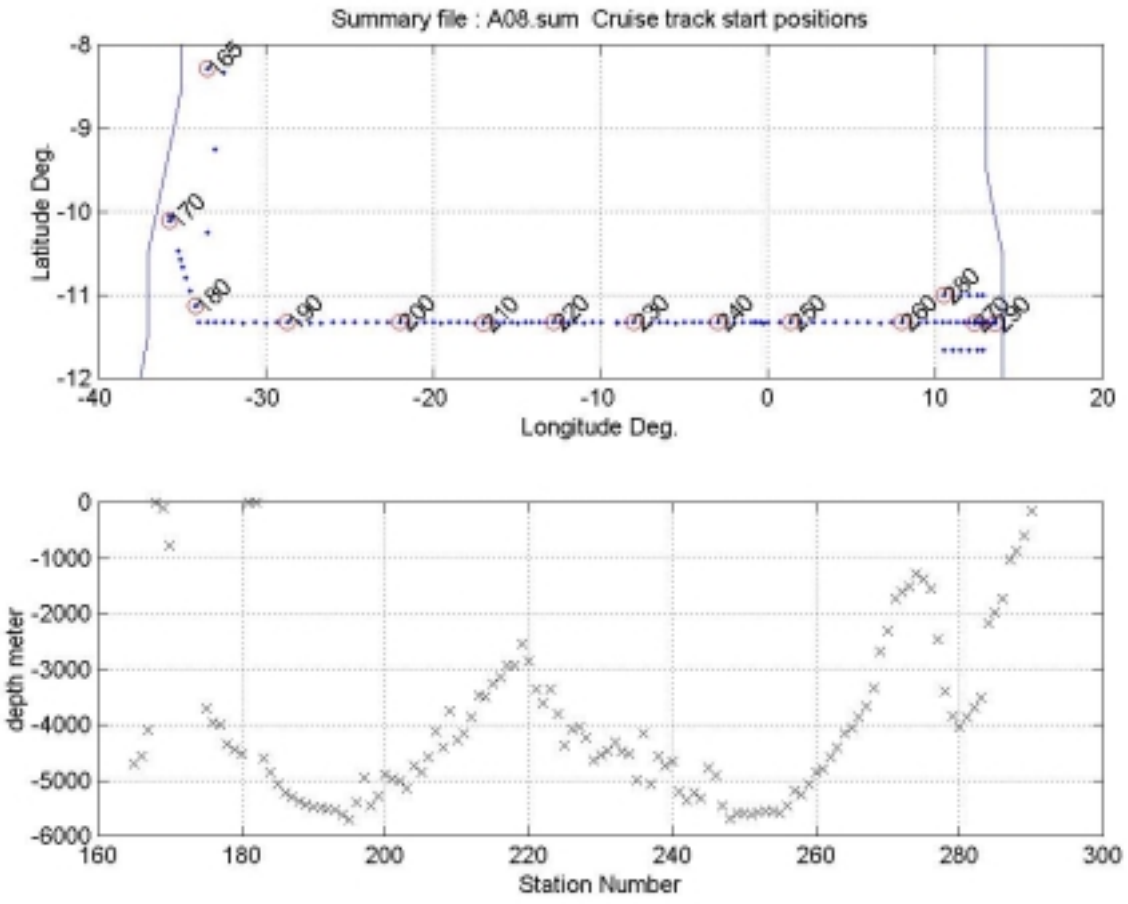

1) fig1_a8.jpg
Plot of annotated beginning station positions with bottom topography plotted versus station number in lower panel.

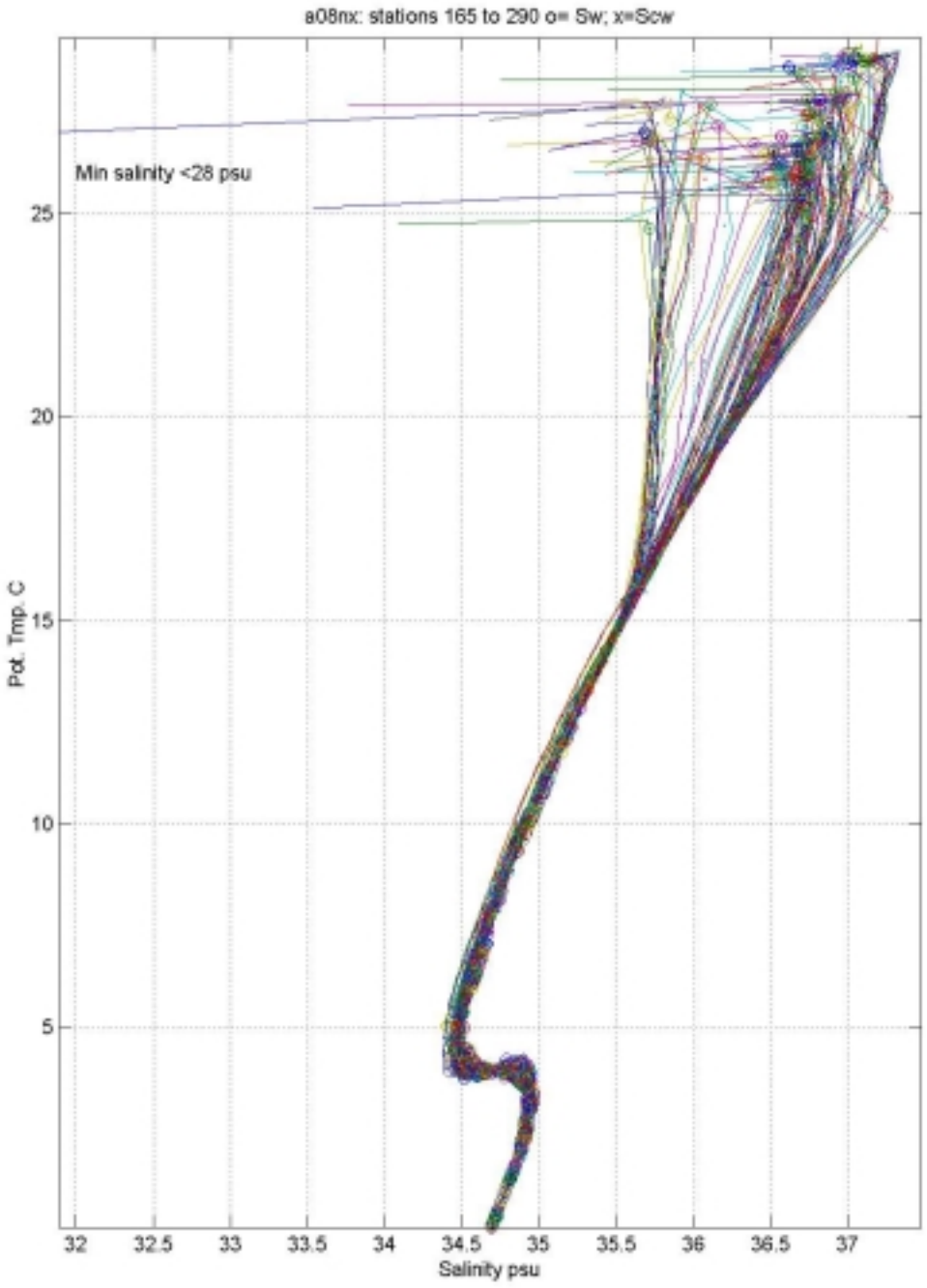

2) fig2_a8.jpg
Overall plot of Salinity versus Potential temperature for all down profile 2-decibar CTD salinities plus QUAL1 "good bottle file water sample (o) and CTD (x).

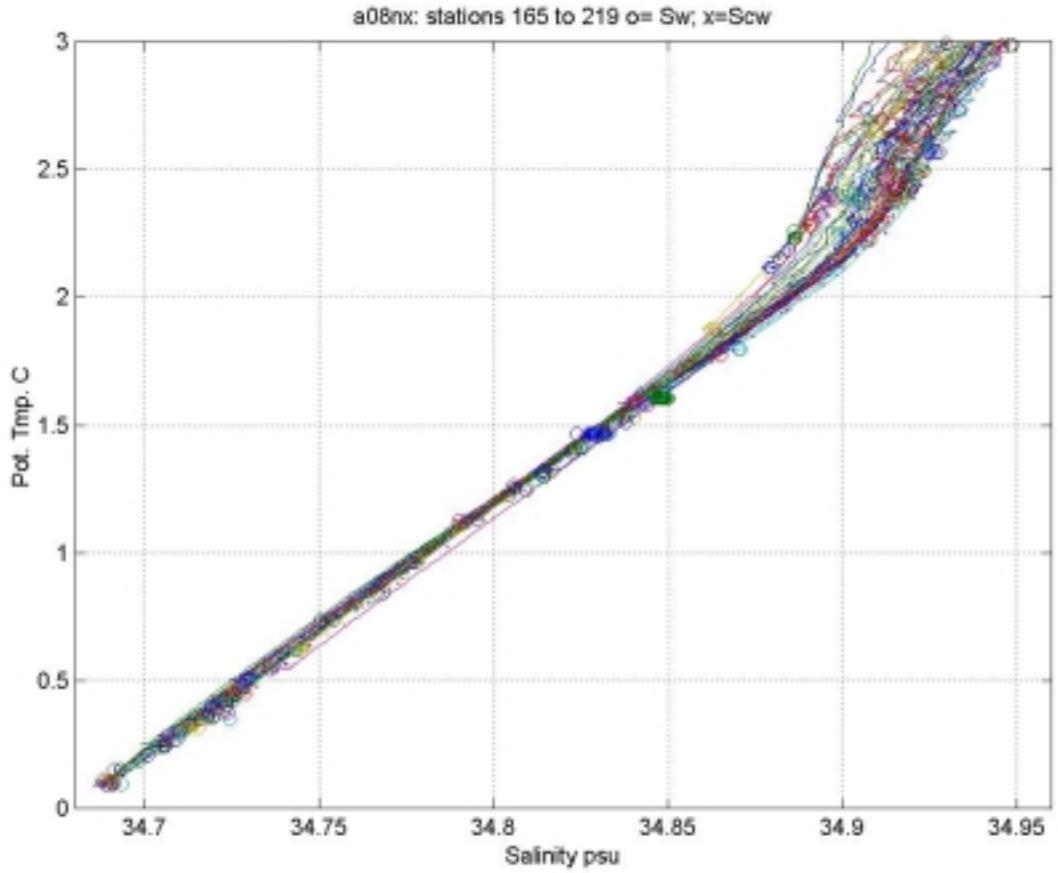

3) fig3_a8.jpg
Deep water plot of Salinity versus Potential temperature West of the mid-Atlantic ridge for all down profile 2-decibar CTD salinities plus QUAL1 "good bottle file water sample (o) and CTD (x).

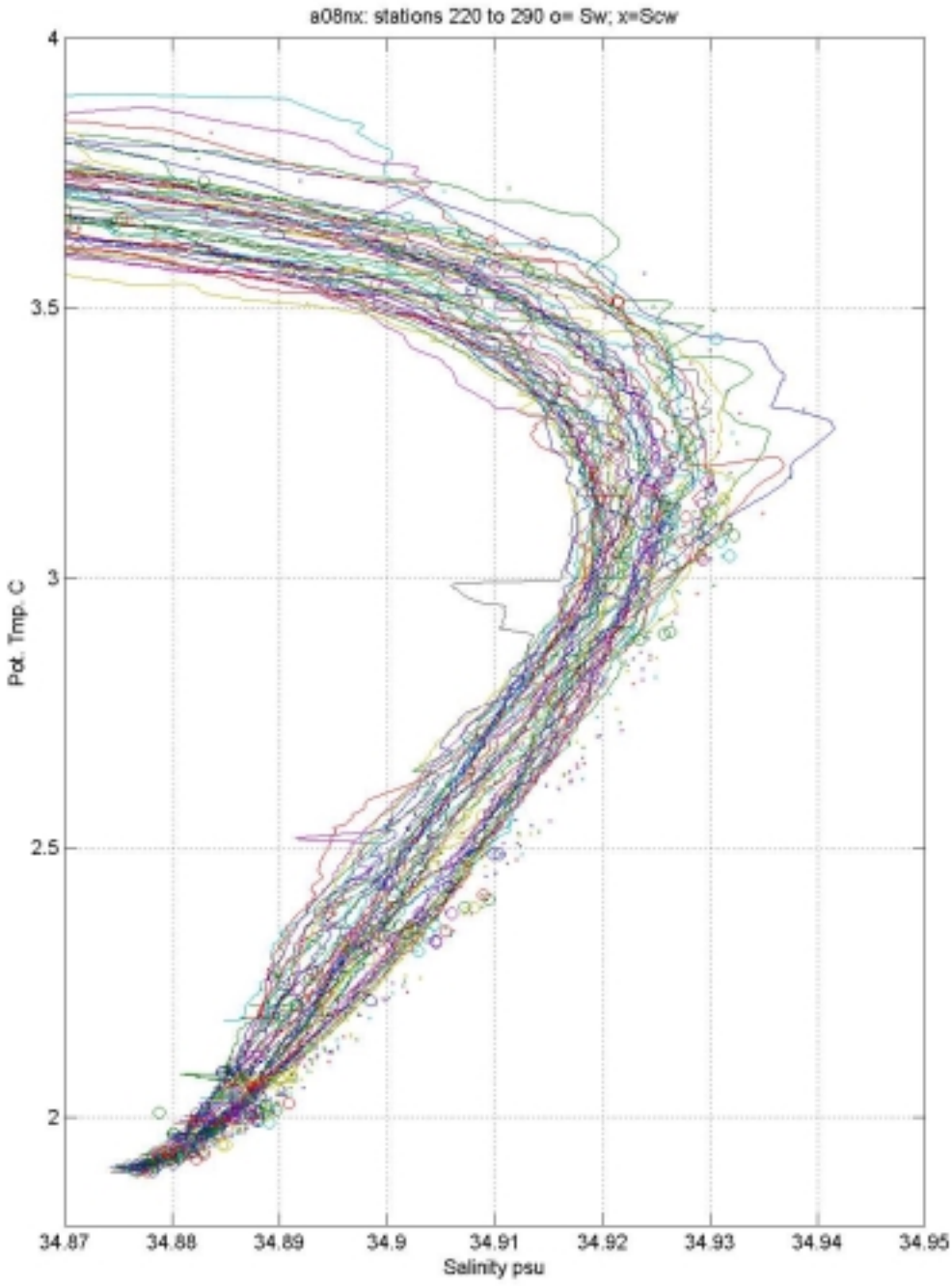

4) fig4_a8.jpg
Deep water plot of Salinity versus Potential temperature East of the mid-Atlantic ridge for all down profile 2-decibar CTD salinities plus QUAL1 "good bottle file water sample (o) and CTD (x).

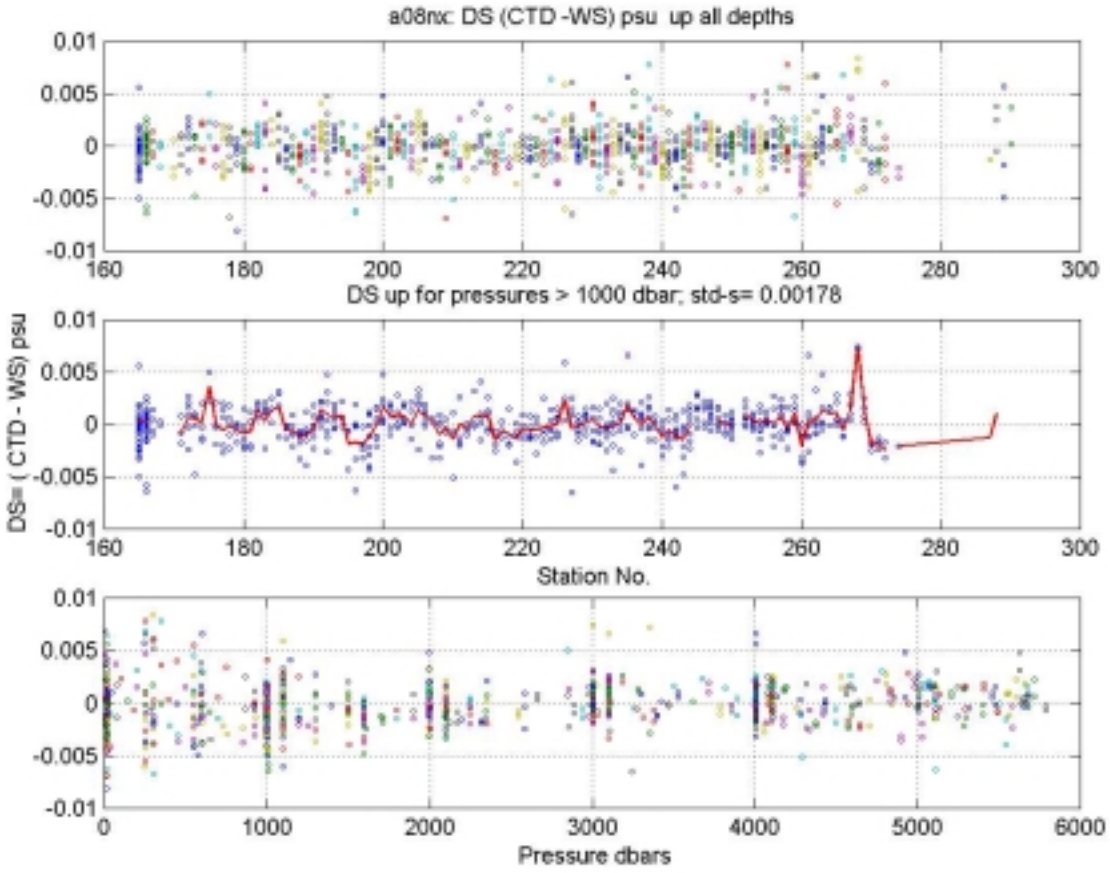

5) fig5_a8.jpg
3 Plot panels of up cast salinity differences Ds=(CTD-WS) psu versus station number (a) all pressures (b) below 1000 dbars and (c) versus pressure.

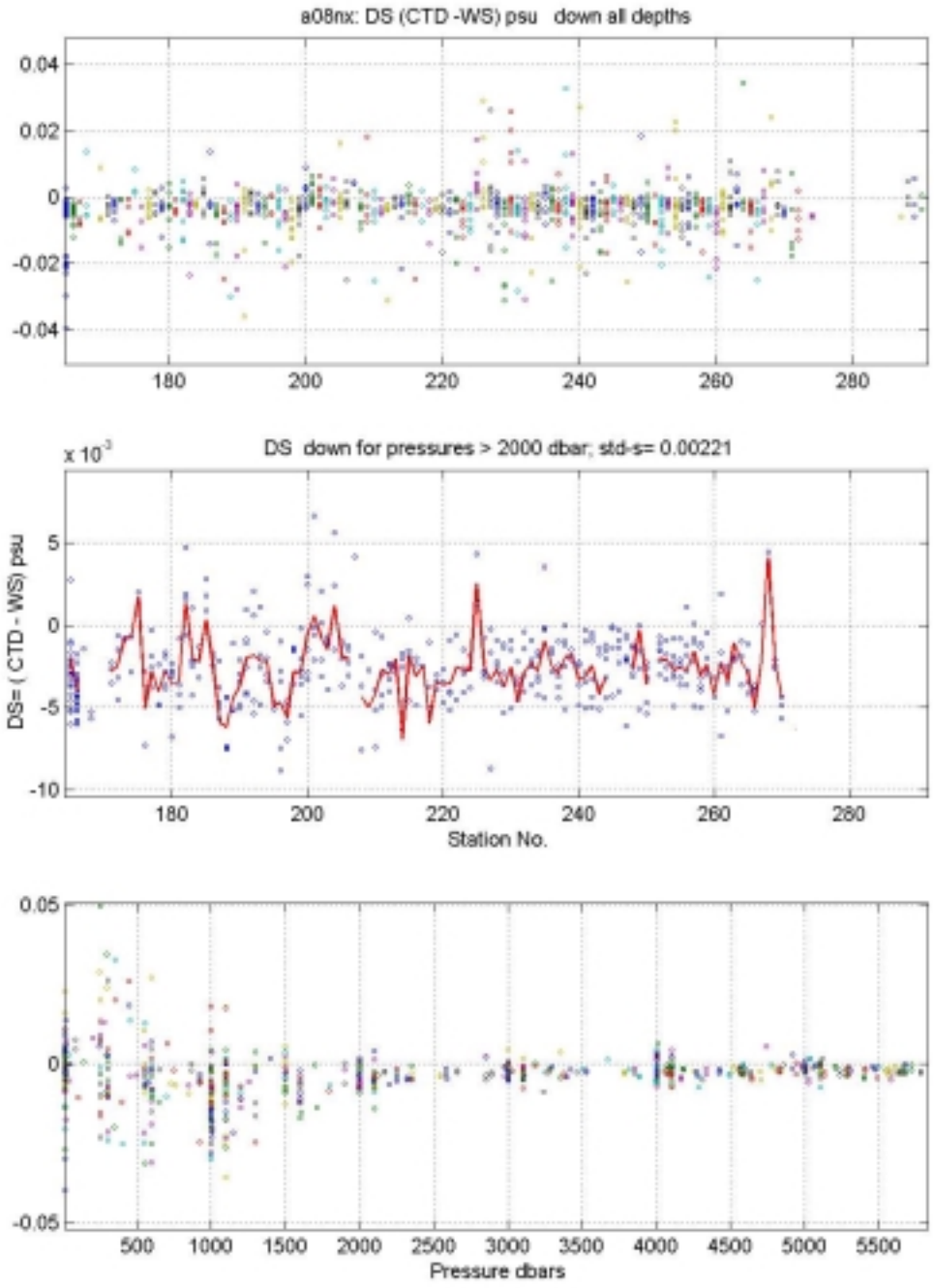

6) fig6_a8.jpg
3 Plot panels of downcast salinity differences Ds=(CTD-WS) psu versus station number (a) all pressures (b) below 1000 dbars and (c) versus pressure.

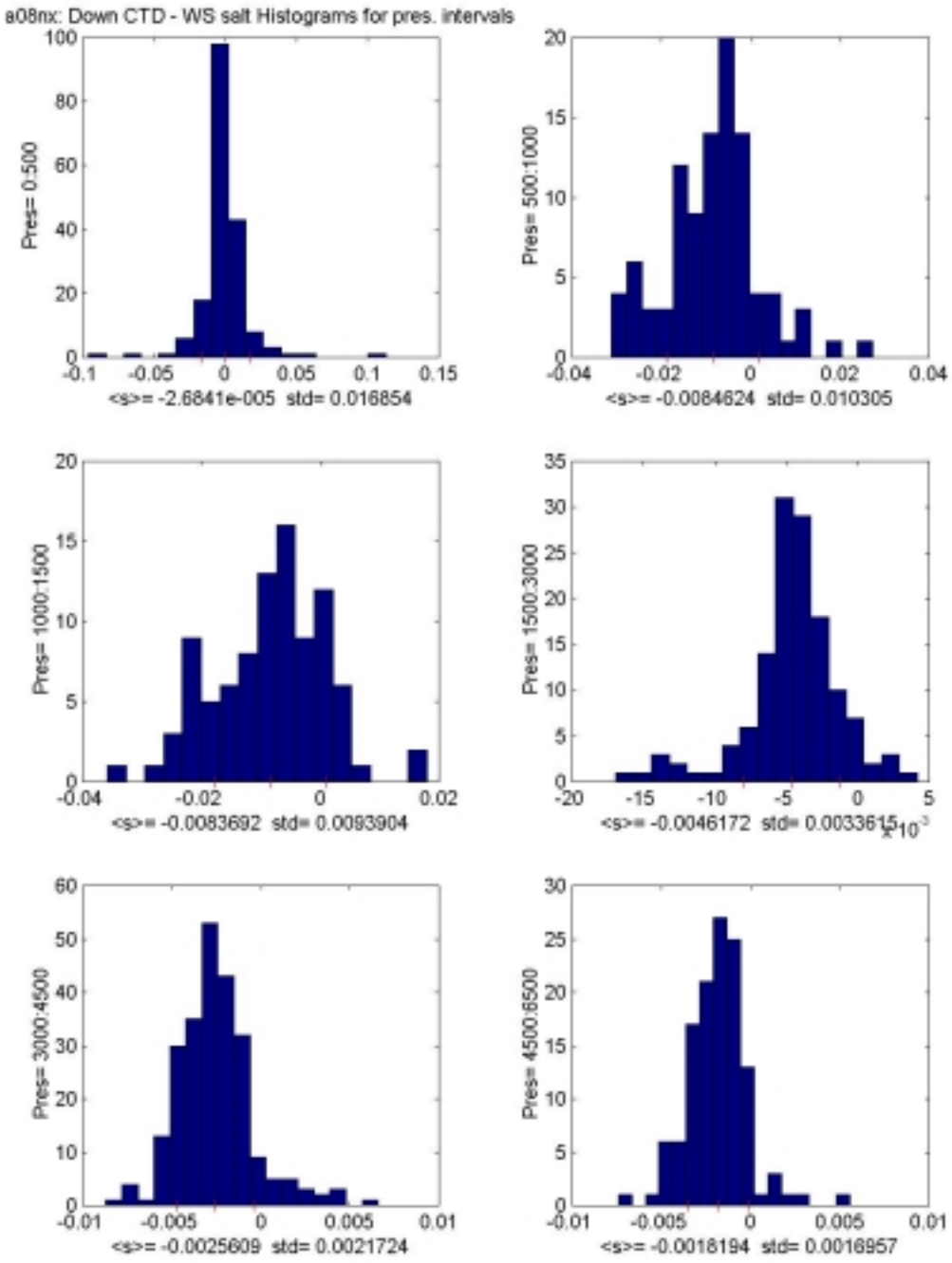

7) fig7_a8.jpg
6 histogram panels of downcast salinity differences Ds=(CTD-WS) psu for various pressure intervals as labeled.

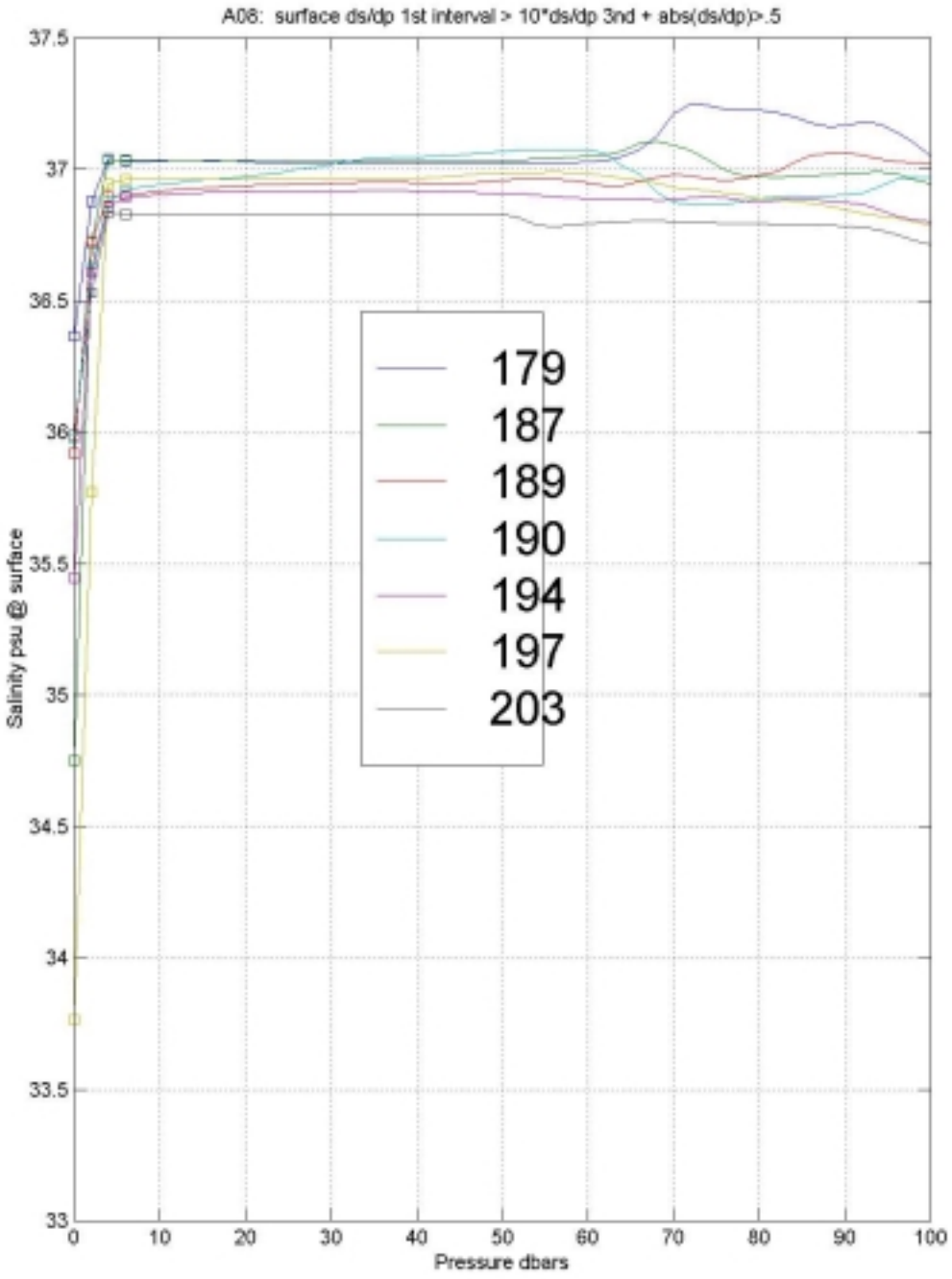

8) fig8_a8.jpg
Plot of salinity versus pressure for stations 179, 187, 189, 190, 194, 197, & 203 in upper 100 decibars for stations with low salt at surface.

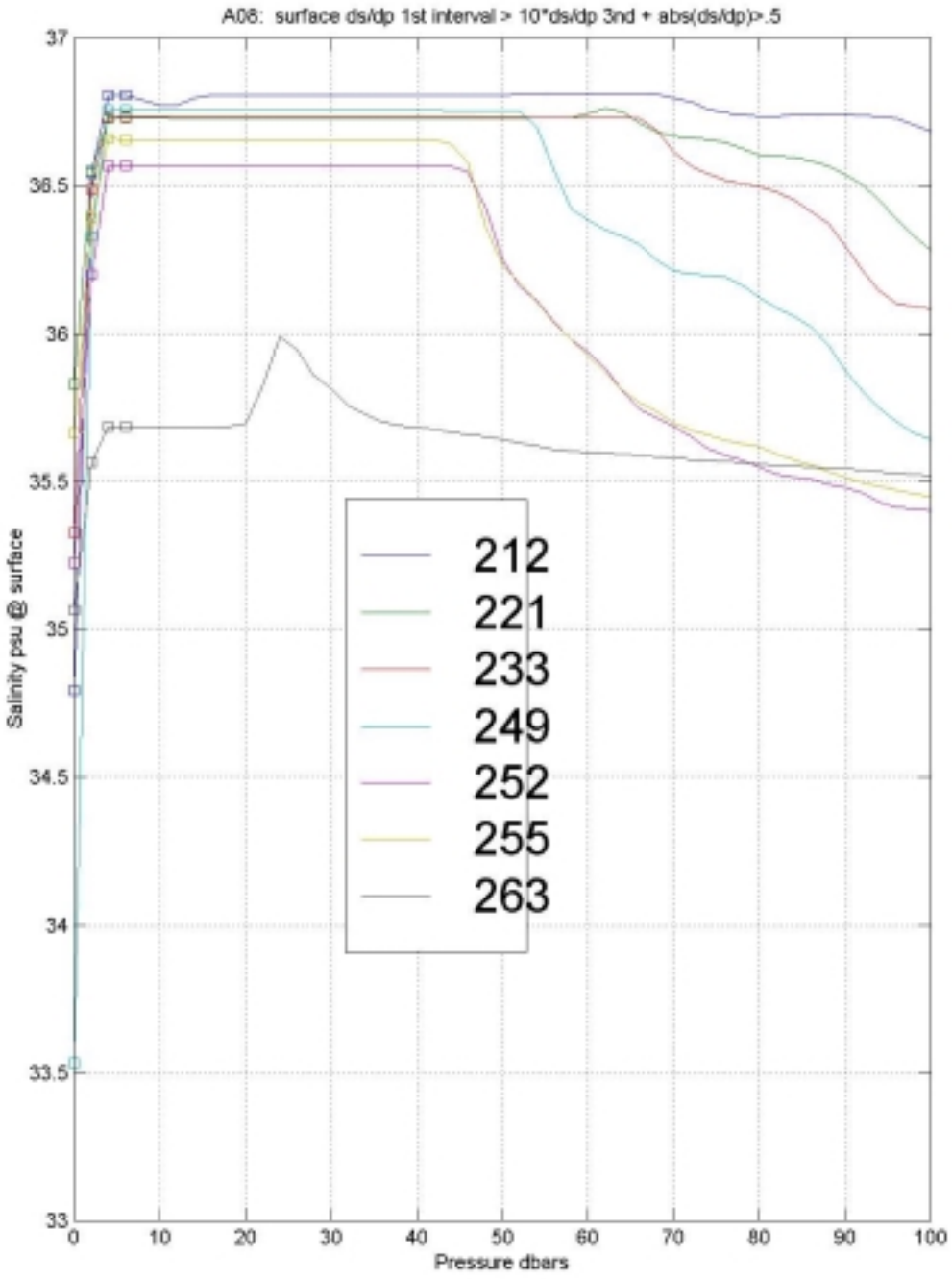

9) fig9_a8.jpg
Plot of salinity versus pressure for stations 212, 221, 233, 249, 252, 255, & 263 in upper 100 decibars for stations with low salt at surface.

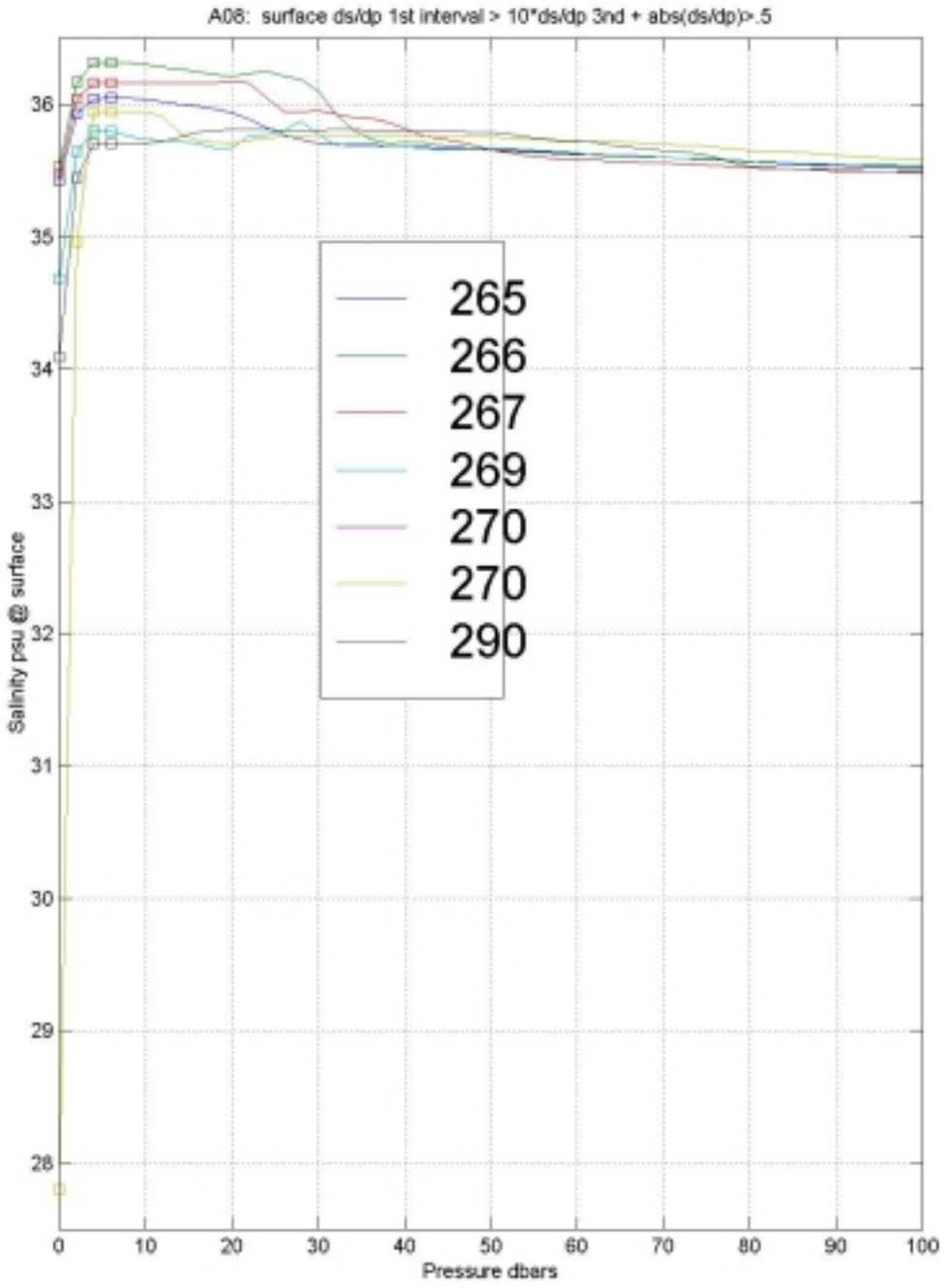

10) fig10_a8.jpg
Plot of salinity versus pressure for stations 265, 266 267, 269, 270 & 290 in upper 100 decibars for stations with low salt at surface.

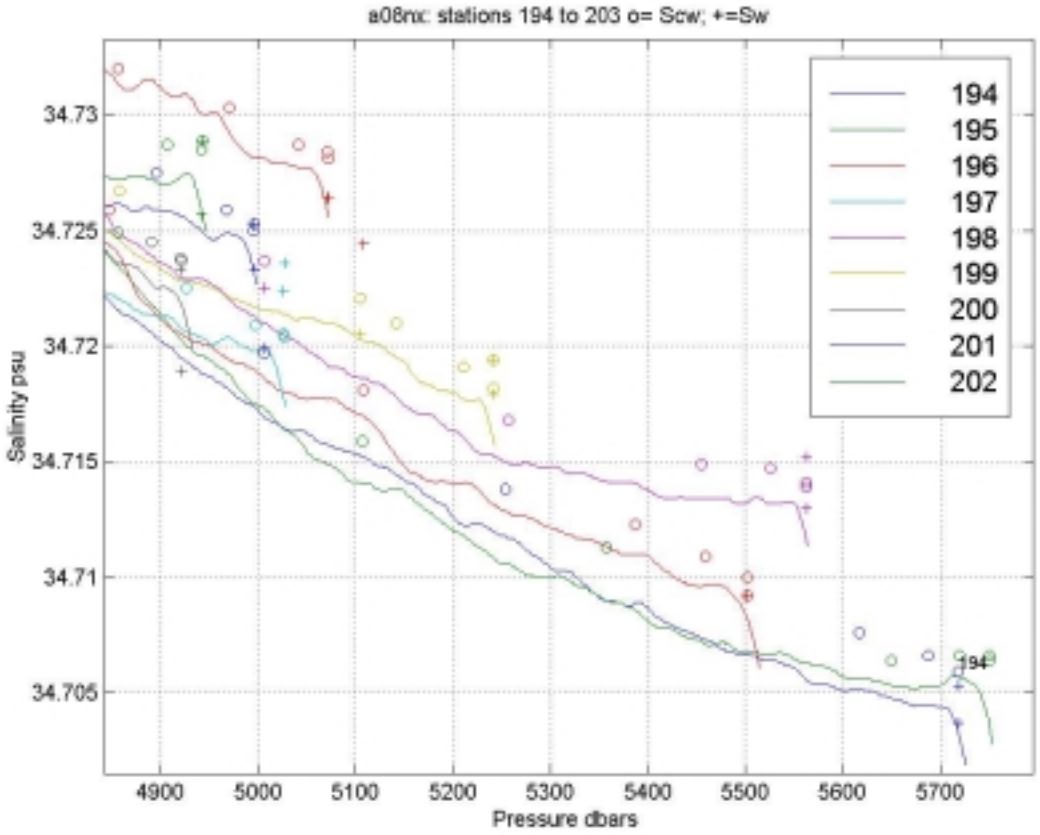

11) fig11_a8.jpg
Plot of salinity versus pressure near the bottom for stations 194 to 202 showing odd low salinity characteristic in lower 15 dbars.

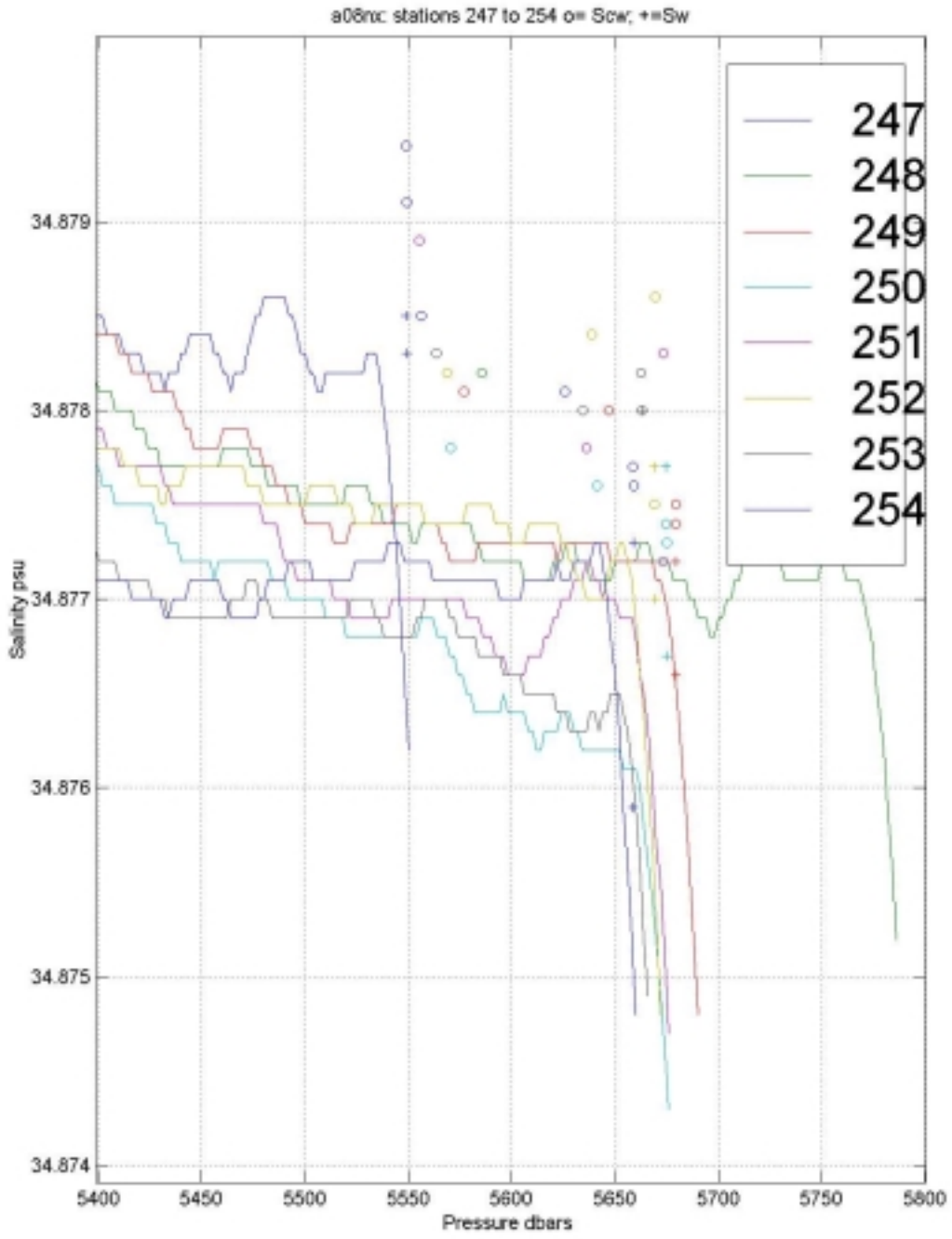

12) fig12_a8.jpg
Plot of salinity versus pressure near the bottom for stations 247 to 254 showing odd low salinity characteristic in lower 15 dbars.

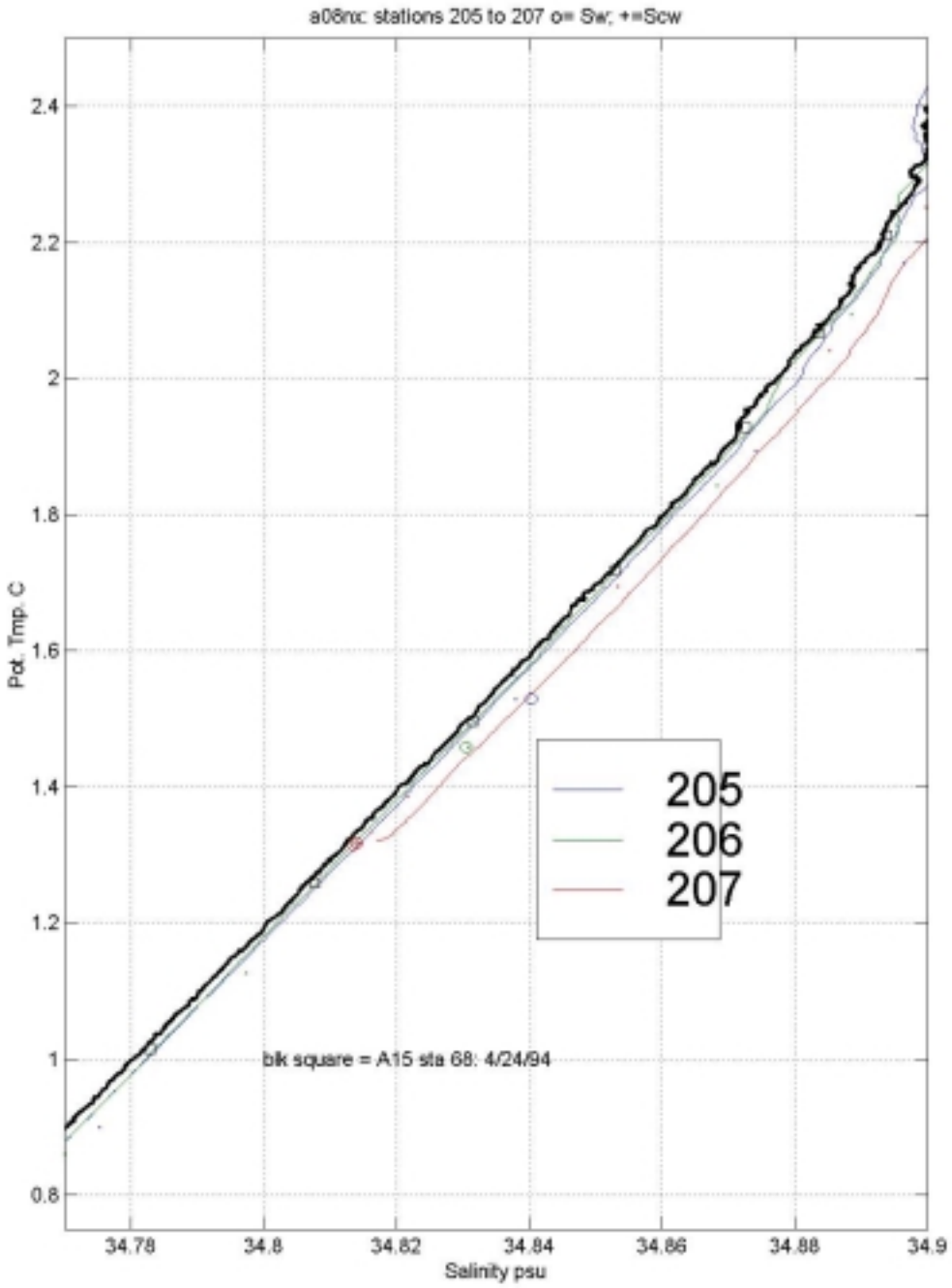

13) fig13_a8.jpg

A comparison of salinity on potential temperature at 11.3S and 19W of A15 stations 68 versus WOCE line A8 stations 205 to 207. Salinity of A8 is approximately 0.002 psu saltier than A15. Station 207 is 0.004 psu saltier than other neighboring A08 deep stations.

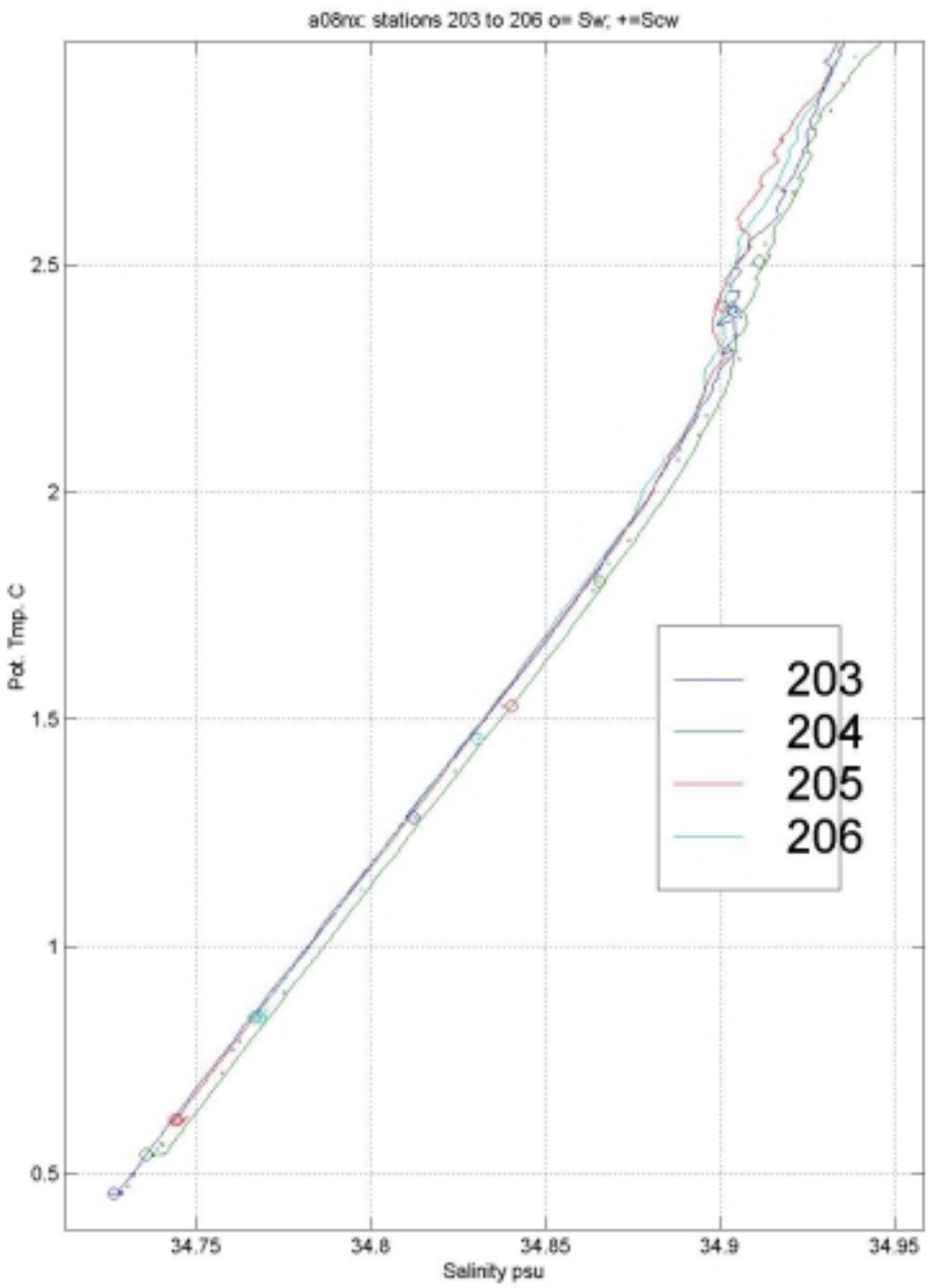

14) fig14_a8.jpg
salinity versus potential temperature shows station 204 to be saltier than neighboring stations by 0.004 psu as is station 207.

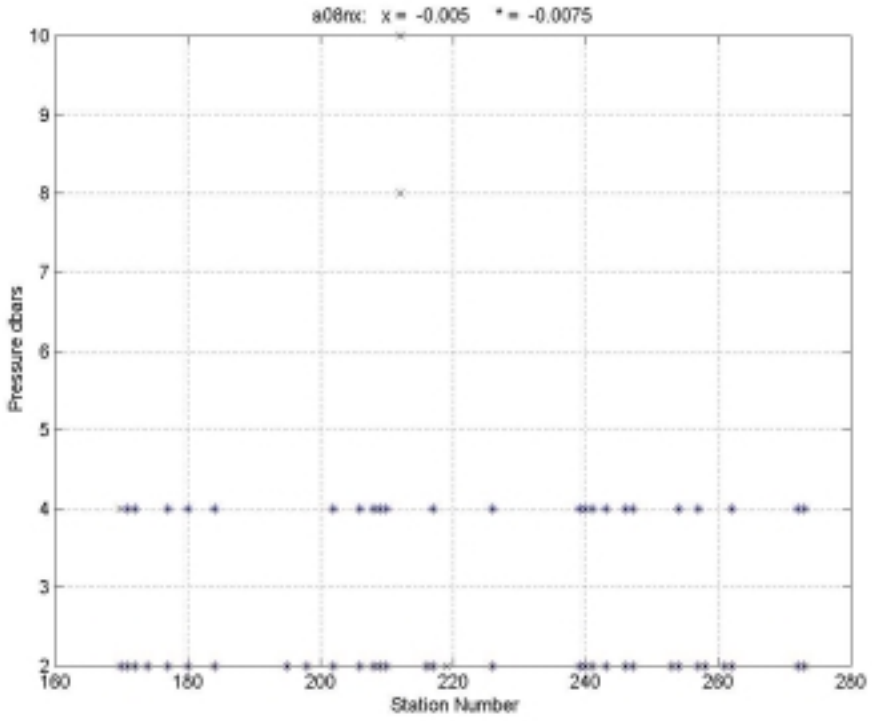

15) fig15_a8.jpg
A plot of pressure versus station indicating unstable values of density change with pressure: b) x exceeding -0.005 kg/M3/dbar a) * exceeding -0.0075 kg/M3/dbar

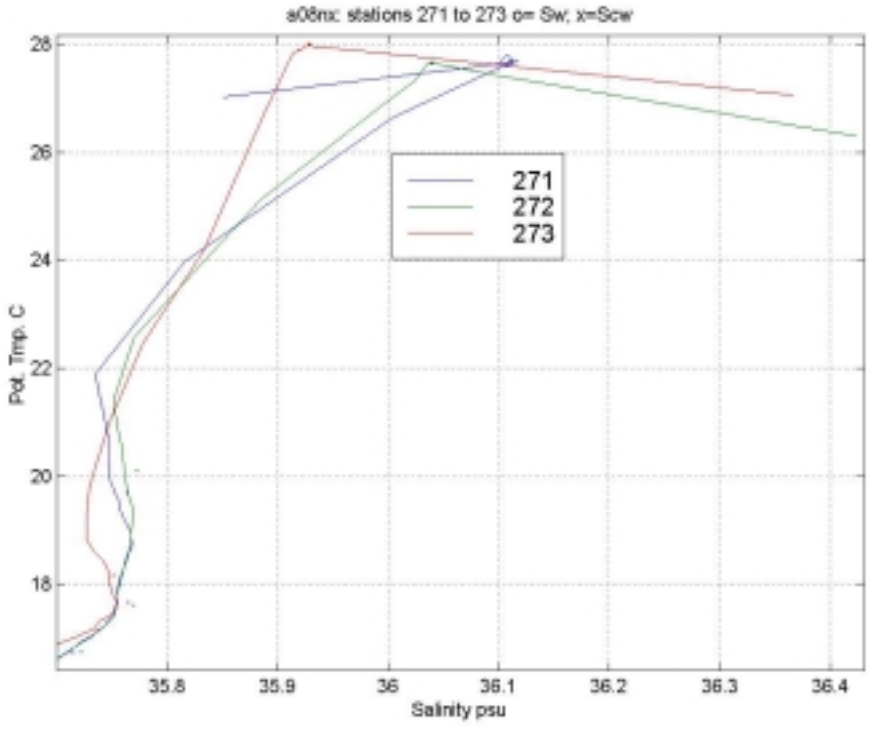

16) fig16_a8.jpg

A08 DQE notes: Nutrients and dissolved oxygen

Joe C. Jennings, Jr. and Louis I. Gordon

The WOCE A08 section is a South Atlantic transect along the nominal latitude of 11°30' South. The data was collected in April/May 1994 during METEOR Cruise 28, Leg 1, and consists of stations numbered 169 – 290. There is no nutrient or oxygen data for stations 165 – 168 or stations 271 – 290. Dissolved oxygen, silicate, and nitrate plus nitrite were reported, but phosphate, nitrite and CTD oxygen were not reported.

Overall, the data quality appears to be very high. There is a number of obvious bottle and/or sampling problems, particularly with the dissolved oxygen; and a number of what are probably typographic errors (typos). These latter are all oxygen concentrations reported as < 5 μM/Kg when the water column should be ca 200 μM/Kg. Many of these should be correctable by the data originator.

At several stations, a number of the oxygen values appear to have been assigned to incorrect pressures. These series of oxygen concentrations appear either too high or too low as reported, but would fit well if they were shifted by one bottle. The data originator may be able to check and possibly correct these stations. Comments on specific stations are listed below and a complete list of questionable data points is appended.

Station 172: Sample 257 @ 1700.4 db looks like a double trip with sample 258 except for the salinity. Possible sampling error?

Station 175: The oxygen values from 1089.2 db to 1698.8 db all look high. These may have been assigned to the wrong depths.

Station 176: Sample 382 @ 10.6 db appears to be out of order in the data file. It is listed between samples 430 and 431 rather than between samples 381 and 383.

Station 183: Sample 843 @ 3838.7 db looks like a double trip with sample 842.

Station 186: Sample 995 @ 1598 db looks like a possible double trip with sample 996 @ 1394.9 db.

Station 192: Nutrient and oxygen values for samples 1375 (3858.2 db) and 1374 (4107.8 db) look as though they've been reversed.

Station 200-106: There is a substantial decrease in deep-water oxygen concentrations between station 202 and 203. These stations are close to the western rise of the Mid-Atlantic Ridge and the changes are probably real. Several high oxygen values at station 203-206 have not been flagged because they lie within the oxygen/theta envelope of stations 200-202.

Station 212: Samples 2380 (2599 db) and 2381 (2599.1 db) are very poor replicates and I expect that the pressure of one of these samples has been incorrectly assigned. Sample

2380 also has an oxygen value so low it must be a typo. The value of 2.30 should probably be ca. 223 uM/Kg.

Station 214: Sample 2450 (130.3 db) has oxygen so low that it may be a typo. The value of 1.80 should probably be 180 uM/Kg.

Station 218: Oxygen values for samples 2675 (49 db) and 2714 (2951 db) are both so low that they are probably typos.

Station 220: Oxygen values for samples 2808 (1296.3 db) and 2800 (2850.4 db) are both so low they are probably typos.

Station 242: Silicate values for samples 268 (3101 db) and 269 (2856.3 db) may have been reversed. As assigned, 268 looks low and 269 looks high.

Station 256: Sample 1624 (1598 db) has an oxygen value of –0.7. This must be a typo.

Station 262: Oxygen values from 921 db to 2098.3 db (samples 2398, 2400 – 2405) all look as though they have been mis-assigned pressures by one bottle. If shifted up, they would fit well.

Station 263: Oxygen values from 496.8 db to 996 db all look low. If shifted up by one bottle they would fit well. Could be a sampling error or a data entry error.

Cruise A08									
METEOR Cruise 28 / Leg 1									**Comments**
Sta.	**Samp.**	**Press.**	**O_2**	**O_2**	**Si**	**Si**	**N+N**	**N+N**	**No Phosphate or nitrite data**
				Flag		**Flag**		**Flag**	
172	257	1700.4	Low	y	High	y	High	y	Looks like double trip except for salt.
	253	2480	High	y					
175	384	3707.5	V Low	y					
	342	1089.2	High	y					
	335	1298	High	y					
	397	1497.3	High	y					
	398	1698.8	High	y					
176	382	10.6							Looks like surface sample but doesn't fit tripping sequence.
	434	452.9	High	y					
178	490	397.6	High	y					
179	575/576	650.8		y					Poor replicates of O_2, flagged both
180	650	2351.6	Low	y					
	599/600	650.8	High	y	Low	y	Low	y	Poor replicate.

Cruise A08									
METEOR Cruise 28 / Leg 1									Comments
Sta.	Samp.	Press.	O_2	O_2 Flag	Si	Si Flag	N+N	N+N Flag	No Phosphate or nitrite data
181	676	199.6	Low	y	High	y	High	y	
	675	2249.5	Low	y	High	y	High	y	
	685	600.4	Low	y					Poor replicate of O_2
182	711	696.7	High	y					
	712	698.6	Low	y					Compare with 711, poor replicates.
	766	1997.7	High	y					752 - 766: O_2 looks high vs Z and theta.
	765	2250	High	y					O_2 looks high vs Z and theta.
	764	2500.2	High	y					" " " " "
	763	2749.5	High	y					" " " " "
	762	3001.5	High	y					" " " " "
	761	3252.6	High	y					" " " " "
	760	3550.2	High	y					" " " " "
	759	3754.6	High	y					" " " " "
	758	4005.5	High	y					" " " " "
	757	4254.2	High	y					" " " " "
	756	4504.8	High	y					" " " " "
	755	4754.5	High	y					" " " " "
	754	4936	High	y					" " " " "
	753	5005.9	High	y					" " " " "
	752	5038.6	High	y					
183	843	3838.7	Low	y	High	y	High	y	Looks like double trip with sample 842, except for salinity.
184	875	2600.7	Low	y					
185	905	1997.7	Low	y					
186	991	2499.1			High	y			
	995	1598	Low	y		y	High	y	Looks like dbl-trip with 996 @1394.9, except for salinity.
188	1099	3101.6	Low	y					No nutrient shift
	1106	1496.7	High	y					
	1110	924.1	Low	y					
	1157	4605.9	Low	y					No nutrient shift
189	1140	398.5	High	y	Ok	y	Low	y	Sil flagged due to O_2 & N+N
190	1227	500.7					Low	y	
	1225	699	High	y					
	1224	847.7	High	y					
	1222	1003.8	High	y					
192	1375	3858.2			High	y	High	y	Looks like nutrients reversed
	1374	4107.8			Low	y	Low	y	Looks like nutrients reversed

Cruise A08									
METEOR Cruise 28 / Leg 1									Comments
Sta.	Samp.	Press.	O_2	O_2	Si	Si	N+N	N+N	No Phosphate or nitrite data
				Flag		Flag		Flag	
195	1545	4606.6	Low	y					
196	1561	4607.2	High	y					
198	1674	1003.6	Low	y					
202	1871	600	High	y					Offset between Stns 200-202 and 203-205.
203	1930	2603	Low	y					
205	2027	1997.5	Low	y					Could be real.
	2024	2247.9	Low	y					
206	2101	3754.3	Low	y	High	y	High	y	
209	2233	3762.5			Low	y	Low	y	
	2245	1797.2					High	y	
211	2361	1698.4	Low	y			High	y	
212	2380	2599	Low	y	High	y	Low	y	Poor Duplicate.
	2381	2599.1			Low	y	Low	y	Poor Duplicate.
213	2462	3371.4	High	y					
214	2450	130.3	Low	y					
216	2611	920.5	High	y					
218	2675	49	Low	y					Typo?
	2714	2951	Low	y					Typo?
220	2808	1296.3	Low	y					Probably decimal place errors
	2800	2850.4	Low	y					
224	2956	497.1			Low	y			More obvious vs theta than z
	2959	201.1	High	y					
	2960	199	Low	y	High	y	High	y	
231	3346	40.5	Low	y	High	y	High	y	Salt too low. Looks like a pre-trip
232	3417	400.4	Low	y					
235	3594	696	High	y					Differs from replicate by 15 μM/Kg
237	3657	2599.6	Low	y					
	3656	2850.5	High	y					
238	3678	349.5	High	y					
	3707	2349.3	High	y					
239	3713	2500.9	High	y					
240	3807	2500.3	High	y					
242	269	2856.3			High	y			Possibly reversed with 268
	268	3101			Low	y			Possibly reversed with 269
244	481	995.8	High	y					Possibly reversed with 478
	478	1196.2	Low	y					Possibly reversed with 481
251	1091	4756.1	Low	y					

Cruise A08									
METEOR Cruise 28 / Leg 1									Comments
Sta.	Samp.	Press.	O_2	O_2 Flag	Si	Si Flag	N+N	N+N Flag	No Phosphate or nitrite data
255	1493	1002	Low	y	Low	y	Low	y	
256	1624	1598	Low	y					Typo?
	1628	1000.5	Low	y	Low	y	High	y	Poor replicate of 1629.
261	2326	3102.1	High	y					
262	2405	921	Low	y					2512 - 2516 all look one depth too low.
	2404	1095.6	Low	y					If shifted up by one depth they look good.
	2403	1296.1	Low	y					
	2402	1496.2	Low	y					
	2401	1697.8	Low	y					
	2400	1899.1	Low	y					
	2398	2098.3	Low	y					
263	2468	397.5	High	y					
	2516	496.8	Low	y					12512 - 2516 all look one depth too low.
	2515	597.2	Low	y					If shifted up by one depth they look good.
	2514	696.5	Low	y					
	2513	846.1	Low	y					
	2512	996	Low	y					
	2506	1997.8	High	y					
	2557	2248.7	Low	y					
	2542	3252.6	High	y					
	2549	3753	High	y					
269	3051	1095.2	Low	y	High	y	High	y	
	3060	248.1	High	y					

WHP A08
Data Status Notes
Remarks on the status
Status: 1996.10.02
This file: A08.TXT
Cruise: WHP section A08 at 11 S 30'
METEOR cruise 28/1, 29-MAR-1994 to 12-MAY1994, Recife, Brazil to Walvisbay, Namibia

Bottle data filename: A08.sea, WHP format

Files on:
WHPSUN: /whp/a/home/cruhsam/a08

1. General remarks

The bottle data file has STNNBR, CASTNO, SAMPNO, BTLNBR, CTDRAW, CTDPRS, CTDTMP, CTDSAL, THETA0, SALNTY, OXYGEN SILCAT, NITRAT, CFC-11, CFC-12, CFC113, CCL4. Units are as requested by the WHP (dbar, ITS90, ISS78 and mass units.
****
The CFC-11, CFC-12, CFC113 and CCL4 still need qualification by the PI (A. Putzka, Bremen) and are not public.
****
The carbonate system data are still with the PI's (K. Johnson & D. Wallace, BNL).

The -SUM file is pending. W. Erasmi <werasmi@ifm.uni-kiel.de> has been asked to prepare it for the WHP-O soon; Jane is aware of this.

The CTD-files are pending. The calibration coefficients are ready. W. Erasmi will be asked to prepare the files.

See also the blue cover cruise report: METEOR-Berichte 95-1, 1995.

2. The bottle data

2.1 Non WHP stations included in bottle file:
Stat. 164 - 168: Test stations
165, 166 : multiple bottle closing at large depths
245, 247 : extra CTD's for biological measurements; no bottles
275 - 286 : CTD/LADCP only; no bottles; waiting for clearance for Angola
2.2 About STNNBR, CASTNO, SAMPNO, BTLNBR
The data cycles are organized to increasing STNNBR. CASTNO's are counted consecutively (1, 2, 3, 4, 5,...) regardless which CTD was used; one station may have several casts (mostly two). BTLNBR's are within 301 and 324 for the rosette with the main (deep) CTD NB3, and within 201 and 224 for the shallow CTD NB2.

Within a STNNBR, cycles are organized to increasing CTDPRS. Therefore, the CASTNO needs not to be a monotonically increasing function in the file.
The SAMPNO is counted with time for each CTD separately (with an offset which makes them unique).

2.3 Oxygen
Conversion from Umol/l to Umol/Kg using potential temperature at depth where bottles were closed.
2.4 Nutrients
Phosphate not measured due to problems with standardization (see report above).Conversion of units from Umol/l to Umol/Kg with mean laboratory temperature (20˚C) to calculate density.
T.J. Mueller

1999.02.19
A08 (Mueller: 06MT28_1) now has Helium and Neon (and associated parameters)in the bottle data file. Since we have no word on these data, they are masked out of the on-line file pending approval from the Chief Scientist.
Steve Diggs

1999.05.11
a08hy_merged_all_values.19990219.txt
Changed the cast numbers from consecutive throughout the file to conform with the cast numbers in the .sum file and reordered the file into station and cast order. Used information given by the PI in the .doc file. See below.
Ran over wocecvt with no errors, but I don't guarantee that there are no errors.
Sarilee